BULGARIAN CHEMICAL COMMUNICATIONS

2009 Volume 41 / Number 1

Journal of the Chemical Institutes
of the Bulgarian Academy of Sciences
and of the Union of Chemists in Bulgaria

Bulgarian Chemical Communications, Volume 41, Number 1 (pp. 3–11) 2009

Flow injection analysis coupled with atomic spectrometry

B. D. Koleva[1], E. H. Ivanova[2]*

[1] *Directorate General, National Center of Metrology, Bulgarian Institute of Metrology, G. M. Dimitrov Blvd., 52 B, 1040 Sofia, Bulgaria*
[2] *Institute of General and Inorganic Chemistry, Bulgarian Academy of Sciences, Acad. G. Bonchev St., Block 11, 1113 Sofia, Bulgaria*

Received June 23, 2008; Revised September 24, 2008

The basic concepts of flow injection analysis, the components of the flow injection manifold as well as the main applications of flow injection analysis are presented. Special emphasis is put on the use of knotted reactors for flow injection separation and preconcentration of trace elements. The coupling of flow injection analysis with detection devices based on atomic spectrometry – flame atomic absorption spectrometry, electrothermal atomic absorption spectrometry and inductively coupled plasma mass spectrometry – is discussed. Examples are given for the on-line flow injection separation/preconcentration – atomic spectrometric determination of a large number of elements on trace- and ultra-trace levels in samples of complex matrix composition.

Key words: flow injection analysis, atomic spectrometric detection, knotted reactor.

INTRODUCTION

The progress in trace element analysis of environmental and biological matrices is driven forward by three major factors: (i) the demand for quantification of an increasing number of elements on lower concentration levels; (ii) the interest in elemental speciation in view of bioavailability and toxicity and (iii) the need of minimizing contamination and sample manipulation.

Attempts to extend modern analytical methods to significantly lower detection limits are often fraught with problems of sampling and storage, on the one hand, and contamination originating from handling and reagents, on the other. There is a close link between the advances in instrumental detection capabilities and the methodology of sample pretreatment, which has encouraged the minimization and miniaturization of sample handling and its on-line implementation to the detection instrument. Complex chemical processing accomplished on-line alleviates the need for extensive and costly clean room facilities, while permitting information to be obtained using small-size samples.

FLOW INJECTION ANALYSIS

The flow injection analysis (FIA) has now reached a well-established position in modern chemical analysis. It is recognized that FIA may serve as an interface between solution chemistry and analytical instruments. This is evident from the numerous (more than 15000) monographs and papers [1] published since the first paper on FIA by Ruzicka and Hansen, which appeared in 1975 [2]. Three key attributes of FIA ensured its rapid development and wide acceptance: (i) the fundamental principles are easy to understand and implement; (ii) the instrumentation can be readily assembled from simple, inexpensive and accessible components and (iii) it provides simple means of automating many manual chemical analytical procedures [3]. Practically, FIA can be coupled with all methods of detection that are used in modern chemical analysis.

Basic concepts of FIA

It is very difficult to give a precise definition of what flow injection analysis really is. Some authors, e.g., Fang [4], explain this by its high versatility, so that definitions are rapidly outdated by new developments. One of the early definitions for FIA, given by Ruzicka and Hansen in their monograph published in 1988 [5] is: "*A technique for information-gathering from a concentration gradient formed from an injected, well-defined zone of a fluid, dispersed into a continuous unsegmented stream of a carrier*". According to Ruzicka and Hansen, FIA is based on three main principles: (i) sample injection; (ii) controlled dispersion of the injected sample zone and (iii) reproducible timing of the movement of the injected zone from the injection point to the detector.

* To whom all correspondence should be sent:
E-mail: eliva@svr.igic.bas.bg

© 2009 Bulgarian Academy of Sciences, Union of Chemists in Bulgaria

In 1995 Fang [4] emphasized on another characteristic feature of FIA, namely the thermodynamically non-equilibrium conditions, under which the processes are performed. According to Fang: "*FIA is a flow analysis technique performed by reproducibly manipulating sample and reagent zones in a flow stream under thermodynamically non-equilibrated conditions.*"

The simplest flow injection (FI) manifold, the single-line manifold, is represented in Fig. 1. It consists of pump, sample injector, reaction coil and detector. The pump is used to propel the carrier stream through a narrow tube. The role of the injector is to inject reproducibly a defined volume of sample into the carrier stream. The main function of the reaction coil is to promote reproducible radial mixing of two or more merged components through generation of secondary flows. The resulting species is sensed by the detector as a transient peak. The height and area of the peak are proportional to the analyte concentration.

Fig. 1. Schematic diagram of a single-line FI manifold. P – pump, C – carrier stream, S – sample injector, RC – reaction coil, D – detector, W – waste.

The flow injection manifold has become considerably complicated to fulfill the new requirements due to the expanded applications of FIA. Thus, the basic principles of FIA should be understood in much broader sense, for example, "*sample injection should be understood as introduction of any liquid zone or series of zones into a flow by any reproducible means*" [4].

Dispersion during the transportation of a sample injected in a unsegmented stream of a carrier, is the most important physical phenomenon in all flow injection systems. The specific features of dispersion processes in FIA are that they are reproducible and controllable through the manipulation of flow parameters and geometrical dimensions of the flow conduits.

The dispersion process typical of FIA systems is shown in Fig. 2. The driving forces active in dispersion of the injected zone into the carrier stream are convection and molecular diffusion. The convection occurs as a result of (i) linear flow rate differences of fluid elements located at different points along the radial axis of the conduit and (ii) secondary flows created by centrifugal forces perpendicular to the flow direction in non-straight conduits. Convex parabolic front of the injected zone and concave parabolic tailing edge are developed upon penetration into the carrier stream, the extent increasing with the distance traveled. The main experimental parameters influencing the dispersion of an injected zone are: sample volume, geometrical dimensions of transport conduits (internal diameter and length), configuration (straight, coiled, knotted) and flow rates of carrier and merging fluid streams. The dispersion of the injected zones increases with the use of small sample volume, straight long transport conduit with large inner diameter and high flow rates. Thus, under the specific conditions applied in FIA and with a fixed conduit, the acting forces are well under control, so that no random turbulence occurs. As a result perfectly reproducible concentration–time relationships may be obtained, which provide the basis for obtaining reproducible readouts under the physically and chemically non-equilibrium conditions specific for FIA.

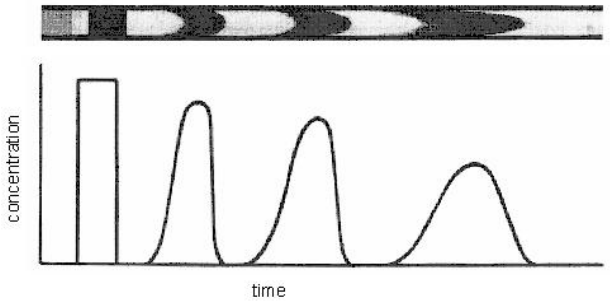

Fig. 2. Dispersion process of an injected fluid zone in an FI system.

Components of the FI manifold

Propulsion devices. Considering the versatility and precise timing features of FI systems, the

and small dead volume. The most common valves are: the six-port rotary valve, the multifunctional eight-channel valve and the commutator valve.

Transport conduits. The transport conduits provide connections between the various components of the FI manifold. To this purpose, PTFE tubings of 0.35–1.0 mm i.d. are mostly used.

Mixing reactors. Mixing reactors of various geometries can be used in a FI manifold. They can be classified into coiled reactors, knotted reactors and stirred chambers. The main function of coiled or knotted reactors is the promotion of reproducible radial mixing of two or more merged components through generation of secondary flows. Knotted reactors are widely used in the separation and preconcentration of trace elements. Mixing chambers are mainly used for FI titration and dilution.

Applications of FIA

The main applications of FIA are for sample digestion, sample dilution, separation and preconcentration of trace elements.

Sample digestion. Sample digestion constitutes an important part of sample pretreatment prior to AS detection of the species of interest and it is often the rate-limiting factor on sample throughput. Digestion procedures almost always involve operations at elevated temperatures, which cause operational difficulties in closed flow systems such as evolution of gases during digestion, high pressure build-up, and incomplete mineralization of the sample owing to the short reaction times and large percentage of non-absorbed power. This appears to be the reason for the rather late development of on-line digestion procedures [4]. Examples of FI on-line digestion can be found in ref. [6, 7].

Sample dilution. Dilution is a stage of the sample preparation process. It is necessary, for example, when AAS is used for detection because of its relatively narrow dynamic range – usually not more than three orders of magnitude. Although the different FI methods for sample dilution are based on different principles, there are some general features: (i) no volumetric glassware is involved in the dilution process; (ii) no precisely defined dilution factors are pursued but actual dilution factors can be evaluated when required; (iii) standard solutions for calibration are prepared to cover the concentration range of the undiluted samples since the calibration standards undergo the same dilution process as the sample; (iv) dilutions are performed on-line with the dilution system directly connected to the spectrometer [4]. A method involving FI on-line dilution is described in [8].

Separation and preconcentration of trace elements. Developments in analytical instrumentation allow trace and ultra-trace analyses in diverse kinds of samples. Despite these advances it is still often necessary to use separation and preconcentration procedures prior to detection. Upon on-line operation using FI techniques the drawbacks of batch-wise operation can be overcome to a great extent and currently on-line preconcentration may be achieved almost as efficiently as a simple AS determination, both in terms of sample throughput

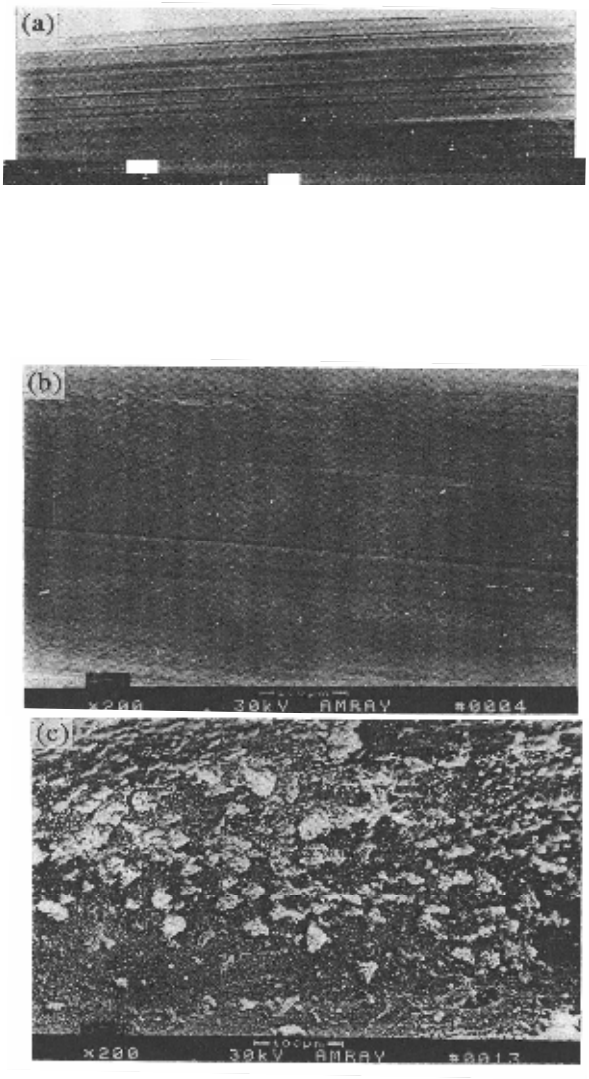

Fig. 4. Scanning electron micrograph of the inner walls of a PTFE KR (200-fold magnification).
(a) Untreated walls; (b) Cd-DDC sorbed on the walls for 50 s; (c) Cd-DDC - Fe(II)-HMDC coprecipitate collected on the walls [58].

The scheme of the FI manifold, used for separation and preconcentration of trace elements by sorption of their complexes onto the inner walls of a KR, has undergone essential further development since its first use. Initially, the flow injection scheme consisted of two steps only: (i) on-line formation of a neutral analyte complex and its subsequent sorption on the inner walls of the KR and (ii) on-line elution of the sorbed analyte complex for FAAS detection [58]. Later on, Chen *et al*. [61] modified the system by sandwiching the eluted sample zone with air segments, thereby avoiding mixing of the neighboring phases of eluate and eluent at fast elution rates. Further, other developments in the FI manifold were introduced such as rinsing with a suitable liquid [62, 63] or blowing air through the KR and connecting tubing before elution [64].

An improvement in the scheme of FI on-line separation and preconcentration using a KR was proposed in 1999 by Ivanova *et al*. [68]. The authors divided the preconcentration stage of the procedure into two separate stages – (i) immobilization of the reagent onto the inner walls of the KR and (ii) formation of an analyte complex with the immobilized reagent. The new scheme offers several advantages in comparison with the conventional preconcentration scheme of on-line merging of sample and reagent solution: (i) higher sensitivity owing to more favorable conditions of analyte complexation with the immobilized reagent; (ii) better optimization of the separate processes of reagent sorption on the KR and analyte preconcentration, (iii) no analyte losses due to adsorption of complexes outside the KR, (iv) no need of a pre-filling step between samples of different analyte concentrations [68].

FI on-line sorption onto a KR was successfully applied as a separation/preconcentration procedure for a number of elements in various matrices using reagents such as NaDDC (Cd [58], Cu [61, 69], Pb [65], Pb [70]), APDC (Pb [64], Sb [66], As [67], Co [71], Tl [72], Cr [73,74], Pt [75], Fe [76], Cu, Ni [77], Co [78], Ag, Cd, Co, Cu, In, Mo, Ni, Pb, Sb [79]), DDPA (Pb [60], Bi [80], Cd, Pb [81]), HQ (Cu, Mn, Ni [77], Co [78], Co [84]), 1-phenyl-3-methyl-4-benzoylpyrazol-5-one (PMBP) (Co [78], Cu, Mn [68], rare earth elements [83]), 2-nitroso-1-naphthol-4-sulphonic acid (Co [78]), nitroso-R-salt/ tetrabutyl ammonium bromide (Co [84]) and dithione (Cd, Co, Cu, Zn [62]). Methods for speciation of Sb [66], As [67], Tl [72], Fe [76], and Cr [73, 74, 85] were also developed.

FLOW INJECTION ANALYSIS WITH ATOMIC SPECTROMETRIC DETECTION

Flow injection analysis was successfully coupled to detection devices based on different principles, mainly atomic spectrometry (FAAS, ETAAS, ICP AES, ICP MS). The combination of FI methodologies with AS has attracted considerable interest in the past 25 years owing to the great potential in enhancing the relative sensitivity and selectivity of these analytical techniques using combined systems. Additionally, the analytical procedures can be automated and considerably simplified for samples with complicated matrices owing to the separation and preconcentration of the analytes achieved.

FIA coupled with FAAS and ETAAS

Coupling a flame atomic absorption spectrometer to a flow injection system is not technically problematic, as both systems operate in continuous mode. The coupling is accomplished by connecting

the sample introduction capillary of the spectrometer to the capillary coming from the FI system. Specific feature of the FI separation and preconcentration - FAAS detection system is the possibility of improving the nebulization efficiency through optimization of the sample introduction flow rate. Additional enhancement in sensitivity can be achieved by introducing organic solvents often used as eluents [4].

The specific features of ETAAS operation impose special requirements on the design and operation of FI separation and preconcentration systems, which differ from those of FAAS and are due to the discontinuous operation of ETAAS and the small volume of the graphite tube. The continuous flow techniques are now successfully combined with ETAAS by synchronization by parallel computerized systems. For introducing the concentrate, obtained by FI pretreatment into the graphite tube, various approaches have been proposed, e.g., eluate zone sampling, use of a preheated graphite tube, multiple injection of eluate with intermediate drying, and others [128–133]. As the introduction of a sample with a complex matrix into the graphite tube would cause serious interferences, rinsing of the KR and connecting tubing were introduced before elution [66]. This step aims at removing non-adsorbed or weakly adsorbed concomitant elements.

There are many scientific papers in the literature dealing with the FI-FAAS and FI-ETAAS analysis of clinical samples [86–88], foods [87, 89–92], medicines [41, 61, 93, 94], environmental samples, such as water [63, 86, 95–102], soils and sediments [86, 97, 103, 104] and plants [64, 69, 104]. Two reviews on FI-ETAAS appeared recently [105, 106].

FIA coupled with ICP MS

Like FAAS, ICP MS operates in continuous mode. This is the reason for its easy coupling to the continuously operating FI system – the sample introduction capillary of the ICP MS instrument is connected to that coming from the FI manifold. However, there are some special features of ICP MS, which an analyst must take into account and modify the FI manifold according to them. To avoid blocking of the sampling cone, drift of sensitivity, high interferences and poor precision, when solutions with high content of dissolved solids (over 0.2%) are introduced into the plasma, a rinsing step of the FI system is introduced before the elution. To reduce or eliminate the effect of organic solvents, which lead to instability or even extinction of the plasma, as well as to carbide polyatomic ion interferences [134], microlitre volumes of organic solvent [32], cooling spray chamber [135] or ultrasonic nebulizer with membrane desolvation [79, 136] are used.

FI-ICP MS has been widely used for trace and ultra-trace analysis of clinical samples [87, 110–117], foods and beverages [87, 114, 118–120], plants [121–123], soils and sediments [122–126], medicines [94, 127], biological samples [137, 138], waters [19, 107–109, 139], *etc*.

It may hence be concluded that FIA is a technique offering wide possibilities covering all areas of sample preparation – digestion, dilution, trace element separation and preconcentration. It has been successfully adapted to various AS methods of detection. As a result, precise and reliable FI-AS methods for trace and ultra-trace analysis in a variety of sample types have been developed.

REFERENCES

1. www.flowinjection.com.
2. J. Ruzicka, E. H. Hansen, *Anal. Chim. Acta*, **78**, 145 (1975).
3. www.globalfia.com.
4. Z. Fang, Flow Injection Atomic Absorption Spectrometry, Jonh Wiley & Sons, Chichester, 1995.
5. J. Ruzicka, E. H. Hansen, Flow Injection Analysis, 2nd ed., Jonh Wiley & Sons, New York, 1988.
6. S. N. Willie, J. W. H. Lam, L. Yang, G. Tao, *Anal. Chim. Acta*, **447**, 143 (2001).
7. J. L. Burguera, M. Burguera, C. Rondon, *Talanta*, **58**, 1167 (2002).
8. E. C. Silva, M. C. U. Araújo, R. S. Honorato, J. L. F. C. Lima, E. A. G. Zagatto, S. M. B. Brienza, *Anal. Chim. Acta*, **319**, 153 (1996).
9. B. Welz, *Microchem. J*., **45**, 163 (1992).
10. M. G. Pereira, M. A. Z. Arruda, *Microchim. Acta*, 141, 115 (2003).
11. L. Nord, B. Karlberg, *Anal. Chim. Acta*, **125**, 199 (1981).
12. G. Tao, Z. Fang, *Spectrochim. Acta Part B*, **50**, 1747 (1995).
13. S. C. Nielsen, S. Stürup, H. Spliid, E. H. Hansen, *Talanta*, **49**, 1027 (1999).
14. P. Martinez-Jiménez, M. Gallego, M. Valcárcel, *Anal. Chem*., **59**, 69 (1987).
15. Z. Fang, M. Sperling, B. J. Welz, *Anal. At. Spectrom*., **6**, 301 (1991).
16. X.-P. Yan, R. Kerrich, M. J. J. Hendry, *Anal. At. Spectrom*., **14**, 215 (1999).
17. J. L. Burguera, M. Burguera, C. Rondón, P. Carrero, M. R. Brunetto, Y. Petit de Peña, *Talanta*, **52**, 27 (2000).
18. O. D. Sant'Ana, A. L. R. Wagener, R. E. Santelli, R. J. Cassella, M. Gallego, M. Valcárcel, *Talanta*, **56**, 673 (2002).
19. H. H. Chen, D. J. Beauchemin, *Anal. At. Spectrom*., **16**, 1356 (2001).
20. P. Martinez-Jiménez, M. Gallego, M. Valcárcel, *Analyst*, **112**, 1233 (1987).

21. H. Chen, S. Xu, Z. J. Fang, *Anal. At. Spectrom*., **10**, 533 (1995).
22. S. Nielsen, J. J. Sloth, E. H. Hansen, *Talanta*, **43**, 867 (1996).
23. S. Nielsen, J. J. Sloth, E. H. Hansen, *Analyst*, **121**, 31 (1996).
24. B. Welz, S. Xu, M. Sperling, *Appl. Spectrosc*., **45**, 1433 (1991).
25. H. Chen, J. Jin, Y. Wang, *Anal. Chim. Acta*, **353**, 181 (1997).
26. J. Liu, H. Chen, X. Mao, X. Jin, *Intern. J. Environ. Anal. Chem*., **76**, 267 (2000).
27. Z. Zhuang, X. Wang, P. Yang, C. Yang, B. Huang, *J. Anal. At. Spectrom*., **9**, 779 (1994).
28. J. Wang, E. H. Hansen, *Trends Anal. Chem*., **22**, 836 (2003).
29. H. Karami, M. F. Mousavi, Y. Yamini, M. Shamsipur, *Anal. Chim. Acta*, **509**, 89 (2004).
30. K. A. Tony, S. Kartikeyan, B. Vijayalakshmy, T. P. Rao, C. S. P. Iyer, *Analyst*, **124**, 191 (1999).
31. A. Ali, Y. Ye, G. Xu, X. Yin, *Fresenius J. Anal. Chem*., **365**, 642 (1999).
32. D. Pozebon, V. L. Dressler, A. J. Curtius, *Anal. Chim. Acta*, **438**, 215 (2001).
33. V. L. Dressler, D. Pozebon, A. J. Curtius, *Spectrochim. Acta, Part B*, **53**, 1527 (1998).
34. V. L. Dressler, D. Pozebon, A. J. Curtius, *Anal. Chim. Acta*, **438**, 235 (2001).
35. M. Moldovan, M. M. Gómez, M. A. Palacios, *Anal. Chim. Acta*, **478**, 209 (2003).
36. A. M. Haji Shabani, S. Dadfarnia, K. Dehghan, *Talanta*, **59**, 719(2003).
37. S. Dadfarnia, A. M. Haji Shabani, M. Gohari, *Talanta*, **64**, 682 (2004).
38. J. R. Baena, M. Gallego, M. Valcarcel, *Trends Anal. Chem*., **21**, 187 (2002).
39. Y. Petit de Peña, M. Gallego, M. Valcárcel, *J. Anal. At. Spectrom*., **12**, 453 (1997).
40. J. Muñoz, J. R. Baena, M. Gallego, M. Valcárcel, *J. Anal. At. Spectrom*., **17**, 716 (2002).
41. A. Lásztity, Á. Kelkó-Lévai, K. Zih-Perényi, I. Varga, *Talanta*, **59**, 393 (2003).
42. K. Zih-Perenyi, A. Lasztity, Z. Horvath, A. Levai, *Talanta*, **47**, 673 (1998).
43. A. N. Anthemidis, G. A. Zachariadis, J. A. Stratis, *Talanta*, **54**, 935 (2001).
44. L. Yang, B. Hu, Z. Jiang, H. Pan, *Microchim. Acta*, **144**, 227 (2004).
45. R. J. Cassella, D. T. Bitencourt, A. G. Branco, S. L. C. Ferreira, D. S. De Jesus, M. S. De Carvalho, R. E. Santelli, *J. Anal. At. Spectrom*., **14**, 1749 (1999).
46. A. N. Anthemidis, G. A. Zachariadis, J. A. Stratis, *Talanta*, **58**, 831 (2002).
47. V. A. Lemos, M. de la Guardia, S. L. C. Ferreira, *Talanta*, **58**, 475 (2002).
48. D. B. Taylor, H. M. Kingston, D. J. Nogay, D. Koller, K. Hutton, *J. Anal. At. Spectrom*., **11**, 187 (1996).
49. S. Hirata, Y. Ishida, M. Aihara, K. Honda, O. Shikino, *Anal. Chim. Acta*, **438**, 205 (2001).
50. E. Vassileva, N. Furuta, *Spectrochim Acta, Part B*, **58**, 1541 (2003).
51. L. A. Ellis, D. J. Roberts, *J. Anal. At. Spectrom*., **13**, 631 (1998).
52. F. M. Fernández, M. B. Tudino, O. E. Troccoli, *J. Anal. At. Spectrom*., **15**, 687 (2000).
53. S. N. Willie, R. E. Sturgeon, *Spectrochim. Acta, Part B*, **56**, 1707 (2001).
54. X. Su, M. Wang, Y. Zhang, J. Zhang, H. Zhang, Q. Jin, *J. Anal. At. Spectrom*., **16**, 1341 (2001).
55. A. P. Packer, M. F. Gine, C. E. S. Miranda, B. F. Dos Reis, *J. Anal. At. Spectrom*., **12**, 563.(1997).
56. 56. Yang L, Sturgeon R E, (2002) J Anal At Spectrom, 17: 88.
57. J. A. Sweileh, E. M. El-Nemma, *Anal. Chim. Acta*, **523**, 287 (2004).
58. Z. L. Fang, S. K. Xu, L. P. Dong, W. Q. Li, *Talanta*, **41**, 2165 (1994).
59. X. P. Yan, Y. Jiang, *Trends. Anal. Chem*., **20**, 552 2001).
60. X. P. Yan, F. Adams, *J. Anal. At. Spectrom*., **12**, 459 (1997).
61. H. W. Chen, S. K. Xu, Z. L. Fang, *Anal. Chim. Acta*, **298**, 167 (1994).
62. S. Y. Chen, Z. F. Zhang, H. M. Yu, *Anal. Chim. Acta*, **451**, 305 (2002).
63. Y. Li, Y. Jiang, X. P. Yan, *Talanta*, **64**, 758 (2004).
64. Y. Li, Y. Jiang, X. P. Yan, W. J. Peng, Y. Y. Wu, *Anal. Chem*., **74**, 1075 (2002).
65. M. Sperling, X. P. Yan, B. Welz, *Spectrochim. Acta, Part B*, **51**, 1891 (1996).
66. X. P. Yan, W. Van Mol, F. Adams, *Analyst*, **121**, 1061 (1996).
67. X. P. Yan, R. Kerrich, M. J. Hendry, *Anal. Chem*., **70**, 4736 (1998).
68. K. Benkhedda, E. Ivanova, F. Adams*, J. Anal. At. Spectrom*., **14**, 957 (1999).
69. X. P. Yan, Y. Li, Y. Jiang, *J. Anal. At. Spectrom*., **17**, 610 (2002).
70. J. A. Salonia, R. G. Wuilloud, J. A. Gasquez, R. A. Olsina, L. D. Martinez, *J. Anal. At. Spectrom*., **14**, 1239 (1999).
71. X. P. Yan, W. Van Mol, F. Adams, *Lab. Rob. Autom*., **9**, 191 (1997).
72. E. Ivanova, X. P. Yan, W. Van Mol, F. Adams, *Analyst*, **122**, 667 (1997).
73. S. C. Nielsen, E. H. Hansen, *Anal. Chim. Acta*, **422**, 47 (2000).
74. W. Som-Aum, S. Liawruangrath, E. H. Hansen, *Anal. Chim. Acta*, **463**, 99 (2002).
75. E. Ivanova, F. Adams, *Fresenius J. Anal. Chem*., **361**, 445 (1998).
76. X. P. Yan, M. J. Hendry, R. Kerrich, *Anal. Chem*., **72**, 1879 (2000).
77. E. Ivanova, K. Benkhedda, F. Adams, *J. Anal. At. Spectrom*., **13**, 527 (1998).
78. K. Benkhedda, H. G. Infante, E. Ivanova, F. Adams, *J. Anal. At. Spectrom*., **15**, 429 (2000).
79. K. Benkhedda, H. G. Infante, E. Ivanova, F. Adams, *J. Anal. At. Spectrom*., **15**, 1349 (2000).

80. E. Ivanova, X. P. Yan, F. Adams, *Anal. Chim. Acta*, **354**, 7 (1997).
81. E. Ivanova, W. Van Mol, F. Adams, *Spectrochim. Acta, Part B*, **53**, 1041 (1998).
82. S. Tsakovski, K. Benkhedda, E. Ivanova, F. Adams, *Anal. Chim. Acta*, **453**, 143 (2002).
83. K. Benkhedda, H. G. Infante, E. Ivanova, F. Adams, *J. Anal. At. Spectrom*., **16**, 995 (2001).
84. K. Benkhedda, H. G. Infante, E. Ivanova, F. Adams, *Fresenius J. Anal. Chem*., **368**, 288 (2000).
85. S. Nielsen, E. H. Hansen, *Anal. Chim. Acta*, **366**, 163 (1998).
86. M. Soylak, S. Saracoglu, U. Divrikli, L. Elci, *Talanta*, **66**, 1098 (2005).
87. A. Taylor, S. Branch, D. Halls, M. Patriarca, M. White, *J. Anal. At. Spectrom*., **19**, 505 (2004).
88. M. M. Tibben, J. M. Rademaker-Lakhai, J. R. Rice, D. R. Stewart, J. H. M. Schellens, J. H. Beijnen, *Anal. Bioanal. Chem*., **373**, 233 (2002).
89. V. A. Lemos, E. M. Gama, A. S. Lima, *Microchim. Acta*, **153**, 179 (2006).
90. V. A. Lemos, D. R. Vieira, C. G. Novaes, M. E. Rocha, M. S. Santos, R. T. Yamaki, *Microchim. Acta*, **153**, 193 (2006).
91. R. F. Orsi, R. G. Wuilloud, J. C. A. de Wuilloud, R. A. Olsina, L. D. Martinez, *J. AOAC Int*., **85**, 1410 (2002).
92. K. Ndung'u, S. Hibdon, A. R. Flegal, *Talanta*, **64**, 258 (2004).
93. A. Lévai, A. Lásztity, K. Zih-Perényi, Zs. Horváth, *Microchem. J*., **58**, 272 (1998).
94. A. Lásztity, Á. Kelkó-Lévai, I. Varga, K. Zih-Perényi, É. Bertalan, *Microchem. J*., **73**, 59 (2002).
95. A. C. Ferreira, M. G. A. Korn, S. L. C. Ferreira, *Microchim. Acta*, **146**, 271 (2004).
96. M. A. A. Akl, I. M. Kenawy, R. R. Lasheen, *Microchem. J*., **78**, 143 (2004).
97. I. Narin, M. Soylak, *Talanta*, **60**, 215 (2003).
98. M. Grotti, M. L. Abelmoschi, F. Soggia, R. Frache, *Anal. Bioanal. Chem*., **375**, 242 (2003).
99. M. Grotti, M. L. Abelmoschi, F. Soggia, R. Frache, *J. Anal. At. Spectrom*., **17**, 46 (2002).
100. A. Ceccarini, I. Cecchini, R. Fuoco, *Microchem. J*., **79**, 21 (2005).
101. F. Shemirani, M. Baghdadi, K. Ramezani, M. R. Jamali, *Anal. Chim. Acta*, **534**, 163 (2005).
102. H. Matsumiya, T. Kageyama, M. Hiraide, *Anal. Chim. Acta*, **507**, 205 (2004).
103. T. Myohanen, V. Mantylahti, K. Koivunen, R. Matilainen, *Spectrochim. Acta, Part B*, **57**, 1681 (2002).
104. M. Tuzen, *Microchem. J*., **74**, 289 (2003).
105. Y. Wang, M. L. Chen, J. H. Wang, *Appl. Spectrosc. Reviews*, **42**, 103 (2007).
106. M. Burguera, J. L. Burguera, *Spectrochim. Acta, Part B*, **62**, 884 (2007).
107. M. S. Jiménez, R. Velarte, J. R. Castillo, *Spectrochim. Acta, Part B*, **57**, 391 (2002).
108. G. J. Batterham, N. C. Munksgaard, D. L. Parry, *J. Anal. At. Spectrom*., **12**, 1277 (1997).
109. P. Jitaru, K. Tirez, N. De Brucker, *At. Spectrosc*., **24**, 1 (2003).
110. M. Krachler, A. Alimonti, F. Petrucci, K. J. Irgolic, F. Forastiere, S. Caroli, *Anal. Chim. Acta*, **363**, 1 (1998).
111. P. Schramel, I. Wendler, J. Angerer, *Int. Arch. Occup. Environ. Health*, **69**, 219 (1997).
112. B. Gammelgaard, O. Jons, L. Bendahl, *J. Anal. At. Spectrom*., **16**, 339 (2001).
113. J. Begerow, M. Turfeld, L. Dunemann, *J. Anal. At. Spectrom*., **12**, 1095 (1997).
114. A. Taylor, S. Branch, A. Fisher, D. Halls, M. White, *J. Anal. At. Spectrom*., **16**, 421 (2001).
115. S. Hann, G. Koellensperger, K. Kanitsar, G. Stingeder, M. Brunner, B. Erovic, M. Müller, C. Reiter, *Anal. Bioanal. Chem*., **376**, 198 (2003).
116. V. Vacchina, L. Torti, C. Allievi, R. Lobinski, *J. Anal. At. Spectrom*., **18**, 884 (2003).
117. M. Bettinelli, *Microchem. J*., **79**, 357 (2005).
118. M. M. Castiñeira, R. Brandt, A. Von Bohlen, N. Jakubowski, *Fresenius J. Anal. Chem*., **370**, 553 (2001).
119. C. M. R. Almeida, M. T. S. D. Vasconcelos, M. Barbaste, B. Medina, *Anal. Bioanal. Chem*., **374**, 314 (2002).
120. F. Cubadda, A. Raggi, *Microchem. J*., **79**, 91 (2005).
121. M. Krachler, C. Mohl, H. Emons, W. Shotyk, *J. Anal. At. Spectrom*., **17**, 844 (2002).
122. R. Djingova, H. Heidenreich, P. Kovacheva, B. Markert, *Anal. Chim. Acta*, **489**, 245 (2003).
123. B. A. Leśniewska, B. Godlewska-Zylkiewicz, B. Bocca, S. Caimi, S. Caroli, A. Hulanicki, *Sci. Total Environ*., **321**, 93 (2004).
124. C. A. Ponce de León, K. De Nicola, M. M. Bayón, J. A. Caruso, *J. Environ. Monit*., **5**, 435 (2003).
125. D. Malinovsky, A. Stenberg, I. Rodushkin, H. Andren, J. Ingri, B. Öhlander, D. C. Baxter, *J. Anal. At. Spectrom*., **18**, 687 (2003).
126. D. Cicchella, B. De Vivo, A. Lima, *Sci. Total Environ.*, **308**, 121 (2003).
127. N. Lewen, M. Schenkenberger, T. Larkin, S. Conder, H. G. Brittain, *J. Pharm. Biomed. Anal*., **13**, 879 (1995).
128. R. Ma, W. Van Mol, F. Adams, *Anal. Chim. Acta*, **293**, 251 (1994).
129. M. Sperling, X. Yin, B. Welz, *Analyst*, **117**, 629 (1992).
130. M. Sperling, X. Yin, B. Welz, *Anal. At. Spectrom*., **6**, 295 (1991).
131. B. Welz, M. Sperling, X. Sun, *Fresenius J. Anal. Chem*., **346**, 550 (1993).
132. Z. Grobenski, R. Lehmann, B. Radziuk, U. Voellkopf, *At. Spectrosc*., **5**, 87 (1984).
133. M. S. Jiménez, J. R. Castillo, *J. Anal. At. Spectrom*., **12**, 1397 (1997).
134. U-5000AT$^+$ Ultrasonic Nebulizer/Membrane Desolvator Operator's Manual, CETAC Technologies Inc., 1997.
135. R. Thomas, *Spectroscopy*, **16**, 56 (2001).
136. B. Brenner, A. Zander, M. Plantz, J. Zhu, *J. Anal. At. Spectrom*., **12**, 273 (1997).

137. F. Zheng, B. Hu, *Anal. Chim. Acta*, **605**, 1 (2007).
138. C. M. P. V. Lopes, A. A. Almeida, M. L. Saraiva, J. L. Lima, *Anal. Chim. Acta*, **600**, 226 (2007).
139. B. Dimitrova-Koleva, K. Benkhedda, E. Ivanova, F. Adams, *Talanta*, **71**, 44 (2007).

ПОТОЧНО-ИНЖЕКЦИОНЕН АНАЛИЗ СЪЧЕТАН С АТОМНА СПЕКТРОМЕТРИЯ

Б. Д. Колева[1], Ел. Хр. Иванова[2]*

[1] Главна дирекция „Национален център по метрология“, Български институт по метрология, бул. „Г. М. Димитров“ № 52 Б, София 1040
[2] Институт по обща и неорганична химия, Българска академия на науките, ул. „Акад. Г. Бончев“, бл. 11, София 1113

Постъпила на 23 юни 2008 г.; Преработена на 24 септември 2008 г.

(Резюме)

Представени са основите на поточно-инжекционния анализ и компонентите на поточно-инжекционното устройство. Специално внимание е отделено на използването на плетен реактор. Описани са поточно-инжекционни методи за подготовка на пробите за анализ (разтваряне, разделяне и концентриране), съчетани с последваща атомно спектрометрична детекция – пламъков и електротермичен атомноабсорбционен анализ и масспектрометрия с индуктивно свързана плазма. Дадени са примери за определяне на голям брой елементи-примеси в обекти със сложен матричен състав.

Bulgarian Chemical Communications, Volume 41, Number 1 (pp. 12– 18) 2009

5,6,7,8-Tetrahydrobenzo[b]thieno[2,3-d]pyrimidine-4(3*H*)one as a synthon of heterocyclic systems

H. M. F. Madkour*, M. E. Azab, M. A. E. Ibraheem

Synthetic Organic Chemistry Laboratory, Chemistry Department, Faculty of Science, Ain Shams University, Abbassiya, Cairo, Egypt

Received November 12, 2007; Revised March 7, 2008

Reaction of 5,6,7,8-tetrahydrobenzo[b]thieno[2,3-*d*]pyrimidine-4(3*H*)-one with ethyl chloroacetate afforded an ester**,** which upon treatment with *p*-chlorobenzaldehyde under various conditions and with benzylamine gave new compounds. Chlorothienopyrimidine reacted with thiourea, benzoylhydrazine, thiosemicarbazide, semicarbazide, sodium azide and glycine, to give pyrimidinethione, 1,2,4-triazole, thioxo-1,2,4-triazole, oxo-1,2,4-triazole, tetrazole**,** and imidazole, respectively. The reaction of pyrimidinthione with β-aroylacrylic acid produced γ-ketoacid**,** which reacted with acetic anhydride and hydrazine hydrate to afford furanone and pyridazinone**,** respectively. Ethyl 2-amino-4,5,6,7-tetrahydrobenzo[b]thiophene-3-carboxylate was utilized to synthesize the 3-aminothienopyrimidinone derivative *via* reaction with benzoyl chloride followed by hydrazine hydrate. An interesting condensation product was obtained by reaction of ethyl 2-amino-4,5,6,7-tetrahydrobenzo[b]thiophene-3-carboxylate with ethyl cyanoacetate in DMF.

Key words: thieno[2,3-*d*]pyrimidin-4(3*H*)-one, triazole, tetrazole, imidazole, furanone and pyridazinone.

INTRODUCTION

In the last few decades thieno[2,3-*d*]pyrimidines have attracted attention due to their wide-scope applications and biological activity, which consists in their functioning as acaricida [1], aldose reductase inhibitory [2], angiotensin II receptor blocking [3], antiallergic [4], antibacterial [5], antibiotic [6], antidepressant [7], antihypertensive [8, 9], antimicrobial [10, 11], analgesic and antiinflammatory [12, 13], bactericidal [14], blood platelet aggregation inhibitory [15], fungicidal [16], hyper-sensitivity inhibitory [17] and insecticidal [18] activity.

The therapeutic importance of thieno[2,3-*d*]-pyrimidine derivatives directed us to synthesize several analogues by combination of other groups and active moieties. We, hereby, report the synthesis of polycyclic heterocycles containing different nuclei fused with, or attached to thieno[2,3-*d*]pyrimidines. The key intermediate for the target heterocyclic systems is 5,6,7,8-tetrahydrobenzo[*b*]thieno[2,3-*d*]-pyrimidin-4(3*H*)-one (**1**), which was prepared according to the previously reported method [19].

RESULTS AND DISCUSSION

In our ongoing heterocyclic chemistry research [20–25], and continuing our synthetic study on thienopyrimidines [26], pyrimidinone **1** was allowed to react with ethyl chloroacetate in dry acetone, in the presence of anhydrous potassium carbonate, to yield ethyl (5,6,7,8-tetrahydrobenzo[*b*]thieno[2,3-*d*]pyrimidin-4-yloxy)acetate (**2**) [26–28]. The ester **2** contains an active methylene group that can condense with aromatic aldehydes under different basic conditions, which strongly affect the reaction products. Thus, when ester **2** was allowed to react with 4-chlorobenzaldehyde in ethanolic sodium ethoxide solution, it afforded ethyl [3-(4-chlorophenyl)-2-(5,6,7,8-tetrahydrobenzo[*b*]-thieno[2,3-*d*] pyrimidin-4-yloxy)]propenoate (**3**) and a small amount of 3-(4-chlorophenyl)-2-(5,6,7,8-tetrahydrobenzo[*b*]thieno[2,3-*d*]pyrimidin-4-yloxy) propenoic acid (**4**) (16%). On the other hand, the ester **2** reacted with 4-chlorobenzaldehyde in *tert*-butanol in the presence of potassium tert-butoxide as a stronger basic catalyst, yielding the cinnamic ester derivative **3** together with a relatively large amount of the cinnamic acid derivative **4** (25%). However, when even stronger basic catalyst, namely sodium hydride in dry benzene, was used, the product **4** was isolated as a sole product (see Scheme 1).

The reaction of ester **2** with benzylamine upon refluxing ethanol gave N-benzyl-2-(5,6,7,8-tetrahydrobenzo[b]thieno[2,3-d]pyrimidin-4-yloxy)acetamide (**5**) in good yield (Scheme 1).

The present work was extended aiming at introducing fused five-membered heterocyclic systems to the thienopyrimidine moiety, *via* nucleophilic substitution, followed by cyclo-condensation. Thus,

* To whom all correspondence should be sent:
Present address: Institute of Biochemistry,
University of Balochistan, Quetta-Pakistan
E-mail: hmfmadkour@yahoo.com

© 2009 Bulgarian Academy of Sciences, Union of Chemists in Bulgaria

compound **1** reacted with phosphorus oxychloride to afford 4-chloro-5,6,7,8-tetrahydrobenzo[b]thieno [2,3-d]pyrimidine (**6**), which was utilized to achieve our goal. The m.p. of the pyrimidine derivative **6** is in accordance with the preceding value [12].

Chloropyrimidine derivative **6** reacted with thiourea in refluxing ethanol and the chlorine atom was replaced by SH [29] to afford 5,6,7,8-tetrahydrobenzo[b]thieno[2,3-d]pyrimidine-4(3H)-thione (**7**) and not the thiourea derivative **8** (Scheme 1).

On the other hand, when the 4-chloropyrimidine derivative **6** was allowed to react with benzoyl hydrazine in refluxing DMF, thiosemicarbazide or semicarbazide hydrochloride in ethanol, it produced 3-phenyl[1]benzothieno[3,2-e][1,2,4]triazolo[4,3-c] pyrimidine (**9**), 3-thioxo[1]benzothieno[3,2-e][1,2,4] triazolo[4,3-c]pyrimidine (**10**), and 3-oxo[1]benzothieno[3,2-e][1,2,4]triazolo[4,3-c]pyrimidine (**11**), respectively. Compound **9** was synthesized by an alternative method from 4-hydrazino-5,6,7,8-tetrahydrobenzo[b]thienopyrimidine *via* reaction with benzaldehyde followed by treatment with bromine/acetic acid [19].

Compound **6** was also treated with sodium azide in ethanol or glycine in pyridine to produce [1]benzothieno[3,2-e]tetrazolo[1,5-c]pyrimidine (**12**) [30] and 3-oxo-[1]benzothieno-[3,2-e]pyrazolo[1,2-c]pyrimidine (**13**), respectively (Scheme 2).

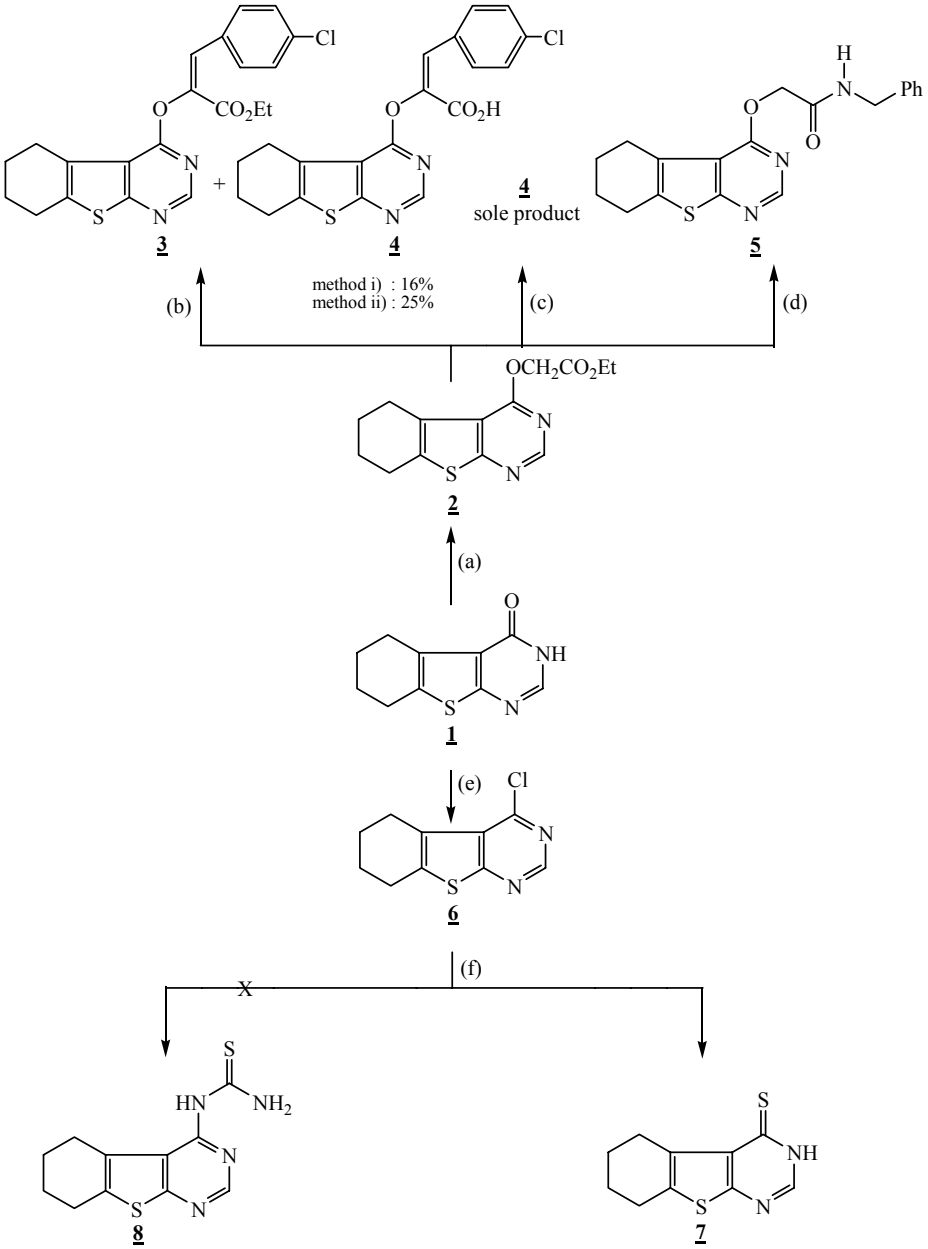

Sheme 1: Reagents and conditions: a. $ClCH_2CO_2Et/K_2CO_3$; b. *p*-Chlorobenzaldehyde, i – NaOEt/EtOH or ii – ButOK/ButOH; c. *p*-Chlorobenzaldehyde, NaH/dry benzene; d. $PhCH_2NH_2$/EtOH; e. $POCl_3$; f. thiourea/EtOH.

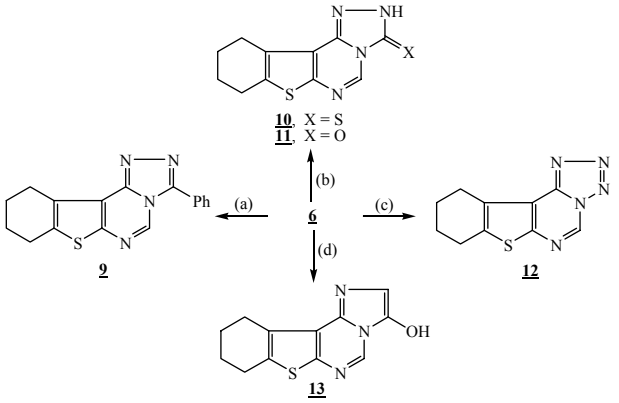

Sheme 2. Reagents and conditions:
a. $PhCONHNH_2$/DMF; b. $NH_2NHCSNH_2$ or $NH_2NHCONH_2$/EtOH/reflux; c. NaN_3/EtOH; d. NH_2CH_2COOH/pyridine.

It was interesting to investigate the behaviour of the pyrimidinethione derivative **7** towards β-aroylacrylic acid. Thus, refluxing **7** with 3-(4-chloro-3-methylbenzoyl)-2-propenoic acid in benzene produces the adduct 3-(4-chloro-3-methylbenzoyl)-2-(5,6,7,8-tetrahydrobenzo-[*b*]thieno[2,3-*d*]pyrimidin-4-ylthio)propanoic acid (**14**) (Scheme 3).

Heating under reflux the γ-ketoacid **14** with freshly distilled acetic anhydride resulted in cyclodehydration reaction with the formation of 5-(4-chloro-3-methylphenyl)-3-(5,6,7,8-tetrahydrobenzo-[*b*]thieno[2,3-*d*]pyrimidin-4-ylthio)furan-2(3*H*)-one (**15**).

Compound **14** reacted with hydrazine hydrate in refluxing ethanol to afford 6-(4-chloro-3-methylphenyl)-4-(5,6,7,8-tetrahydrobenzo[*b*]thieno[2,3-*b*] pyrimidin-4-ylthio)-1,4-dihydropyridazin-3(2*H*)-one (**16**) (Scheme 3).

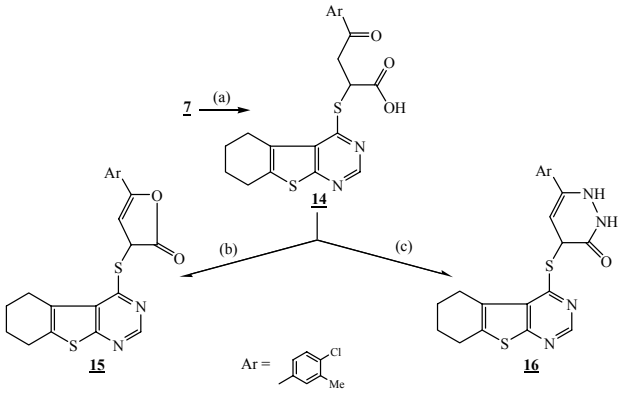

Sheme 3. Reagents and conditions:
a. Ar–COCH=CH–COOH/Dry benzene/Δ; b. Ac_2O/Δ; c. N_2H_4/EtOH/Δ.

Moreover, ethyl 2-amino-4,5,6,7-tetrahydrobenzo[*b*]thiophene-3-carboxylate (**17**) [31–33] reacted with benzoyl chloride in pyridine in the cold to produce ethyl 2-benzoylamino-4,5,6,7-tetrahydrobenzo[*b*]thiophene-3-carboxylate (**18**), which reacted with hydrazine hydrate in refluxing DMF to afford 3-amino-2-phenyl-5,6,7,8-tetrahydrobenzo[*b*]thieno [2,3-*d*]-pyrimidin-4(3*H*)-one (**19**) [34] (Scheme 4).

An interesting condensation product was obtained from ester **17** *via* its reaction with ethyl cyanoacetate in DMF, during passing a current of hydrogen chloride gas in the reaction mixture. The product was identified as ethyl 3-amino-3-(3-ethoxycarbonyl-4,5,6,7-tetrahydrobenzo[*b*]thieno-2-ylimino)propanoate (**20**) (Scheme 4).

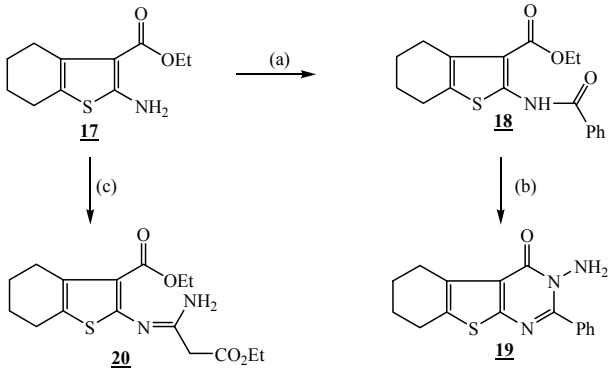

Sheme 4. Reagents and conditions:
a. PhCOCl/pyridine; b. NH_2NH_2/DMF; c. $NCCH_2CO_2Et$/DMF/HCl.

EXPERIMENTAL

All reported melting points are uncorrected and were determined on a Stuart electric melting point apparatus. The IR spectra were measured on a Unicam 200 Spectrometer or Mattson infinity series FT-IR using KBr wafer technique. The ^{1}H-NMR spectra were recorded in $CDCl_3$ or DMSO-d_6 solutions on Varian Gemini 200 MHz instrument using TMS as internal standard with chemical shifts (δ expressed in ppm form down to up field). The mass spectrum was recorded on Shimadzu GC-MS-QP 1000 EX instrument operating at 70 eV. TLC was preformed on ready-to-use silica gel plates Merck 60 to monitor the reactions and ascertain the purity of the newly synthesized compounds. The microanalytical data were measured in microanalytical unit of the Faculty of Science, Cairo University. The title compound **1** as well as ethyl(5,6,7,8-tetrahydrobenzo[b]thieno[2,3-d]pyrimidin-4-yloxy) acetate (**2**) have been synthesized in our laboratory [26].

Ethyl [3-(4-chlorophenyl)-2-(5,6,7,8-tetrahydrobenzo[b]thieno[2,3-d]pyrimidin-4-yloxy)]-propenoate (**3**) *and 3-(4-chlorophenyl)-2-(5,6,7,8-tetrahydrobenzo[b]thieno[2,3-d]-pyrimidin-4-yloxy)propenoic acid* (**4**)**.** *Method A*: A mixture of 4-chlorobenzaldehyde (10 mmol, 1.4 g) and ester **2** (10 mmol, 2.92 g) was added to a solution of NaOEt (prepared

from 0.5 g Na metal and 60 ml absolute ethanol) or *tert*-KOBu (1.68 g) in *tert*-BuOH (80 ml). The mixture was refluxed for 4 h. Most of the solvent was removed under reduced pressure. The cold residue was poured into water and extracted with diethyl ether. The aqueous layer was acidified with diluted hydrochloric acid. The ethereal layer was poured over dry anhydrous $MgSO_4$, evaporated to dryness to obtain oil, which on trituration afforded solid product. This product on crystallization from benzene yielded **3** as yellow crystals: m.p. 207–209°C; yield [10.5% (ethoxide), 8.56% (butoxide)]. IR: ν 3050 (CH_{ar}), 2946 (CH_{al}), 1729 (C=O ester) and 1672 cm^{-1} (C=N); ^{1}H-NMR (DMSO-d_6): δ 1.12 (t, 3H, –$COOCH_2C\underline{H}_3$), 1.96 (br.s, 4H, C-6H and C-7H of tetrahydrobenzothienopyrimidine nucleus), 2.63 (br. s, 2H, C-5H), 2.75 (br. s, 2H, C-8H), 4.1 (q, 2H, $COOC\underline{H}_2CH_3$), 7.20 (m, 5H, Ar–H and olefinic H), 7.91 (s, 1H, C-2H); Anal. Calcd. for $C_{21}H_{19}ClN_2O_3S$ (414.5): C, 60.79; H, 4.62 ; Cl, 8.54; N, 6.75; Found: C, 60.67; H, 4.59; Cl, 8.46; N, 6.69.

On the other hand, the solid obtained from acidification of the aqueous layer was crystallized from benzene affording **4** as yellow crystals; m.p: 178–182°C yield (16% (ethoxide), 25% (butoxide)). IR: ν 3422 (OH acid), 3056 (CH_{ar}), 2933 (CH_{al}) and 1669 cm^{-1} (C=O of α,β-unsaturated acid); ^{1}H-NMR (DMSO-d_6): δ 1.81 (br.s, 4H, C-6H and C-7H), 2.61 (br.s, 2H, C-5H), 2.70 (br.s, 2H, C-8H), 7.35–7.47 (m, 5H, Ar–H and olefinic H) and 8.12 (s, 1H, C-2H); Anal. Calcd. for $C_{19}H_{15}ClN_2O_3S$ (386.5): C, 58.99 ; H, 3.91 ; Cl, 9.16; N, 7.24; Found: C, 58.89; H, 3.79; Cl, 9.07; N, 7.18.

Method B: An equimolar amount of 4-chlorobenzaldehyde (10 mmol, 1.4 g) and ester **2** (10 mmol, 2.92 g) was refluxed in 50 ml dry benzene for 4h in the presence of (0.4 g) sodium hydride. The reaction mixture was left to cool down after evaporating most of the solvent to give solid, which was dissolved in water and acidified by diluted hydrochloric acid. The crude solid was crystallized from benzene to give **4** as yellow crystals; m.p. 178–181°C; yield 56.6%.

n-Benzyl-2-(5,6,7,8-tetrahydrobenzo[b]thieno [2,3-d]pyrimidin-4-yloxy)acetamide (**5**) A mixture of thienopyrimidine **2** (10 mmol; 2.92 g) and benzyl amine (10 mmol; 1.1 ml) in ethanol (40 ml) was refluxed for 10 h. Most of the solvent was evaporated and the rest was left to cool down. The solid product that separated out was filtered off, dried and then recrystallised from ethanol to give **5** as white solid; m.p. 202–205°C; yield 33.99%. IR: ν 3298 (NH), 3057 (CH_{ar}), 2938 (CH_{al}), 1687 (C=O acyclic amide), 1653 cm^{-1} (C=N); ^{1}H-NMR (DMSO-d_6): δ 1.79 (br.s, 4H, C-6 and C-7 H), 2.51 (br.s, 2H, C-5H), 2.88 (br.s, 2H, C-8H), 4.35 (d, 2H, OCH_2CO), 4.69 (s, 2H, benzylic proton of –$C\underline{H}_2$Ph), 7.26–7.35 (m, 5H, Ph–H), 8.28 (s, 1H, C-2H) and 8.79 (s, 1H, NH, D_2O exchangable); Anal. Calcd. for $C_{19}H_{19}N_3O_2S$ (353): C, 64.59; H, 5.38; N, 11.89; Found: C, 64.47; H, 5.19; N, 11.76.

4-Chloro-5,6,7,8-tetrahydrobenzo[b]thieno[2,3-d]pyrimidine (**6**). The solution of pyrimidinone **2** (10 mmol; 2.92 g) in phosphorus oxychloride (5 ml) was heated under reflux on water bath for 1 h, left to cool down and poured onto ice water forming a solid product. Filtration and crystallization of the crude product from light petroleum (40–60°C) afforded the title product **6** as pale yellow crystals; m.p. 106–108°C; yield 89.7%. The m.p. is in satisfactory agreement with preceding value [12].

5,6,7,8-Tetrahydrobenzo[b]thieno[2,3-d]pyrimidin-4(3H)thione (**7**). An equimolar mixture of chloropyrimidine **6** (10 mmol; 2.24 g) and thiourea (10 mmol; 0.8 g) in dry methanol (30 ml) was refluxed for 5 h. Most of solvent was evaporated and the reaction mixture was left to cool down, the solid product that separated out was filtered off. Crystallization from benzene to yield the thiol **7** as orange crystals; m.p. 247–250°C; yield 85.5%. IR: ν 3132 (NH), 3045 (CH_{ar}), 2983($CH_{al.}$), 1661 (C=N), 1569 (C=C) and 1367 cm^{-1} (C=S); ^{1}H-NMR ($CDCl_3$): δ 1.87 (m, 4H, C-6H and C-7H), 2.61 (br.s, 2H, C-5H), 2.76 (br.s, 2H, C-8H), 7.85 (s, 1H, C-2H), 11.83 (br.s, 1H, NH); Anal. Calcd. for $C_{10}H_{10}N_2S_2$ (222): C, 54.05; H, 4.50; N, 12.61. Found: C, 53.89; H, 4.35; N, 12.49.

3-phenyl[1]benzothieno[3,2-e][1,2,4]triazolo [4,3-c]pyrimidine (**9**). A mixture of chloropyrimidine **6** (10 mmol; 2.24 g) and benzoylhydrazine (10 mmol; 1.36 g) in 50 ml of dimethylformamide was refluxed for 5 h. Most of solvent was evaporated and the reaction mixture was left to cool down, the solid product that separated out was filtered off. Crystallization of the crude product from dimethyl formamide yielded product **9** as orange crystals; m.p: 215–218°C; yield: 37.1%. IR: ν 3054 (CH_{ar}), 2935 (CH_{al}), 1621 cm^{-1} (C=N), with the disappearance of C=O; ^{1}H-NMR (DMSO-d_6): δ 1.82 (br.s, 4H, C-9 and C-10H), 2.60 (br.s, 2H, C-11H), 2.82 (br.s, 2H, C-8H), 7.57–7.54 (m, 5H, Ph–H), 8.22 (s, 1H, pyrimidine proton); Anal. Calcd. for $C_{17}H_{14}N_4S$ (306): C, 66.67; H, 4.57; N, 18.30; Found: C, 66.49; H, 4.51; N, 18.12.

3-(2H)-Thioxo[1]benzothieno[3,2-e][1,2,4]triazolo[4,3-c]pyrimidine (**10**). To a solution of chloropyrimidine **6** (10 mmol; 2.24 g) in 30 ml of dimethylformamide, thiosemicarbazide (12 mmol; 1.58 g) was added and the reaction mixture was refluxed for 6 h, concentrated and left to cool down.

An oily substance was formed, which solidified upon trituration with ethanol gave a solid product. The solid product was collected by filtration, dried and then recrystallised from ethanol to give **10** as orange solid; m.p. 284–286°C; yield 41.6%. IR: ν 3120 (NH), 3050 (CH_{ar}), 2930 (CH_{al}), 1635 cm^{-1} (C=N) ;^{1}H-NMR (DMSO-d_6): δ 1.86 (br.s, 4H, C-9 and C-10H, 2.65 (br.s, 2H, C-4H), 2.74 (br.s, 2H, C-8H), 8.40 (s, 1H, C-5H) and 9.14 and 9.57 (two s, 1H, HN–C=S ⇆ N=CSH). Anal. Calcd. for $C_{11}H_{10}N_4S_2$ (262): C, 50.38; H, 3.82; N, 21.37; Found: C, 50.18; H, 3.79; N, 21.27.

3-(2H)-Oxo[1]benzothieno[3,2-e][1,2,4]triazolo [4,3-c]pyrimidine **(11)** A mixture of chloropyrimidine **6** (10 mmol; 2.24 g) and semicarbazide hydrochloride (12 mmol; 1.34 g) in dimethyl formamide (30 ml) was heated under reflux for 6 h. Most of the solvent was evaporated, the residual was left to cool down. The solid product that separated out was filtered off, dried and then recrystallised from benzene to give **11** as orange solid; m.p. 230°C (*d*); yield 48.3%. IR: ν 3115 (NH), 3073 (CH_{ar}), 2936 (CH_{al}), 1753 (C=O) and 1616 cm^{-1} (C=N); ^{1}H-NMR (DMSO-d_6): δ 1.88 (br.s, 4H, C-9 and C-10H), 2.67 (br.s, 2H, C-11H), 2.77 (br.s, 2H, C-8H), 8.43 (s, 1H, C-5H) and 9.28 and 9.62 (two s, 1H, NH–C=O ⇆ N=C–OH); Anal. Calcd. for $C_{11}H_{10}N_4OS$ (246): C, 53.66; H, 4.07; N, 22.76; Found: C, 53.57; H, 3.99; N, 22.45.

[1]benzothieno[3,2-e]tetrazolo[1,5-c]pyrimidine **(12).** To a solution of chloropyrimidine **6** (10 mmol; 2.24 g) in 30 ml of ethanol, sodium azide (10 mmol; 0.65 g) was added and the reaction mixture was stirred for 1 h and left to cool down. The solid product that precipitated down was filtered off by suction, dried and then recrystallised from ethanol to give **12** as white solid; m.p. 141–143°C; yield 49.13%. IR: ν 3069 (CH_{ar}), 2935 (CH_{al}), 1641 (C=N), 1605 cm^{-1} (C=C); ^{1}H-NMR (DMSO-d_6): δ 1.83 (br.s, 4H, C-9H and C-10H), 2.70 (br.s, 2H, C-11H), 2.82 (br.s, 2H, C-8H), 8.12 (s, 1H, C-2H); Anal. Calcd. for $C_{10}H_9N_5S$ (231): C, 51.95; H, 3.90; N, 30.30, Found: C, 52.12; H, 4.09; N, 30.49.

3-hydroxy[1]benzothieno[3,2-e]pyrazolo[1,2-c] pyrimidine **(13).** A mixture of chloropyrimidine **6** (10 mmol; 2.24 g) and glycine (10 mmol; 0.75 g) was fused for 2 h at temperature not higher than 140°C, left to cool down and treated by light petroleum (60–80°C). The solid product that separated out was filtered off, dried and then recrystallised from benzene to give **13** as violet solid; m.p. 188–190°C; yield 48.3%. IR: ν 3425 (OH), 3060 (CH_{ar}), 2937 cm^{-1} (CH_{al}); ^{1}H-NMR (DMSO-d_6): δ 1.86 (br.s, 4H, C-6H and C-7H), 2.64 (br.s, 2H, C-5H), 2.86 (br.s, 2H, C-8H), 5.79 (s, 1H, pyrazole), 8.21 (s, 1H, C-2H), 9.43 (br.s, 1H, OH, D_2O exchangeable); MS: m/e: 245 (M^+, 42.9), 228 (3.2), 226 (19.0), 224 (61.9), 196 (100), 169 (14.1), 134 (16.2); Anal. Calcd. for $C_{12}H_{11}N_3OS$ (245): C, 58.77; H, 4.49; N, 17.14; Found: C, 58.64; H, 4.41; N, 16.99.

3-(4-Chloro-3-methylphenyl)carboxy-2-(5,6,7,8-tetrahydro[b]benzothieno[2,3-d]pyrimidin-4-ylthio) propanoic acid **(14)**. A mixture of pyrimidine **7** (10 mmol; 2.22 g) and β-aroylacrylic acid namely 3-(4-chloro-3-methylbenzoyl)-2-propenoic acid (10 mmol; 2.24 g) in 40 ml of benzene was heated under reflux for 5 h. Most of the solvent was evaporated and left to cool down. The solid product that separated out was filtered off, dried and then recrystallised from benzene affording **14** as yellow solid; m.p. 168–170°C; yield: 94.1%. IR: ν 3037 (CH_{ar}), 2934 (ν_{CHal}), 1736 (CO acid) and 1684 cm^{-1} (CO ketone); ^{1}H-NMR (DMSO-d_6): δ 1.77 (br.s, 4H, C-6 and C-7H), 2.41 (s, 3H, CH_3), 2.59 (br.s, 2H, C-5H), 2.78 (br.s, 2H, C-8H), 2.98 (d, 2H, Ar–CO–CH_2–), 4.14 (d, 1H, –S–CH–), 7.82–7.91 (m, 3H, Ar–H), 8.17 (s, 1H, C-2H pyrimidine), 13.69 (br.s, 1H, CO_2H, D_2O exchangeable); Anal. Calcd. for $C_{21}H_{19}ClN_2O_3S_2$ (446.5): C, 56.44; H, 4.26; Cl, 7.95; N, 6.27; Found: C, 56.08; H, 4.09; Cl, 7.76; N, 6.14.

5-(4-Chloro-3-methylphenyl)-3-(5,6,7,8-tetrahydro[b]benzothieno[2,3-d]pyrimidin-4-ylthio)furan-2(3H)-one **(15).** To a gently warmed solution of acetic anhydride (5 ml), the acid **14** (10 mmol; 2.4 g) was added and the mixture heated under reflux for 0.5 h and then left to cool down. The solid that separated out was filtered off and washed by light petroleum (60–80°C), dried and then recrystal-lised from benzene to give **15** as violet solid; m.p. 223–225°C; yield 46.5%. IR: ν 3089 and 3057 (CH_{ar}), 2929 (CH_{al}), 1787 (C=O furanone), 1641 cm^{-1} (C=N); δ 1.80 (br.s, 4H, C-6 and C-7H), 2.44 (s, 3H, CH_3), 2.63 (br.s, 2H, C-5H), 2.81 (br.s, 2H, C-8H), 4.25 (d, 1H, –S–CH–), 6.12 (d, 1H, CH=), 7.77–7.92 (m, 3H, Ar–H), 8.21 (s, 1H, C-2H pyrimidine); MS: m/z: 428 (M^+, 90.3), 222 (100), 207 (78.7), 153 (89.9), 125 (53.2), 89 (45), 53 (25); Anal. Calcd. for $C_{21}H_{17}ClN_2O_2S_2$ (428.5): C, 58.81; H, 3.97; Cl, 8.28; N, 6.53; Found: C, 58.68; H, 3.77; Cl, 8.04; N, 6.67.

6-(4-Chloro-3-methylphenyl)-4-(5,6,7,8-tetrahydro[b]benzothieno[2,3-d]pyrimidin-4-ylthio)-1,4-dihydropyridazin-3(2H)-one **(16)**. A mixture of **14** (10 mmol; 2.4g) and hydrazine hydrate (10 mmol; 0.5 ml) in ethanol (40 ml) was refluxed for 12 hrs, left to cool down, then filtered off, dried and then recrystallised from benzene to afford **16** as yellow crystals; m.p. 202–204°C; yield 54.5%. IR: ν 3145 (NH), 3056 (CH_{ar}), 2932 (CH_{al}), 1672 cm^{-1} (C=O); ^{1}H-NMR ($CDCl_3$): δ 1.85 (br s, 4H, C-6 and C-7H),

2.42 (s, 3H, CH_3), 2.57 (br s, 2H, C-5H), 2.83 (br s, 2H, C-8H), 4.23 (d, 1H, –S–CH–, 6.18 (d, 1H, CH=), 7.59–7.84 (m, 3H, Ar–H), 8.27 (s, 1H, C-2H), 12.98 and 13.31 (two s, 2H, 2NH, D_2O exchangeable); Anal. Calcd. for $C_{21}H_{19}ClN_4OS_2$ (442.5): C, 56.95; H, 4.29; Cl, 8.02; N, 12.66; Found: C, 56.78; H, 4.11; Cl, 7.81; N, 12.47.

Ethyl 2-(benzoylamino)-4,5,6,7-tetrahydrobenzo[b]thiophene-3-carboxylate (**18**)**.** To a solution of thiophene ester **17** (10 mmol; 2.25 g) in 30 ml of pyridine, benzoyl chloride (10 mmol; 1.4 ml) was added and the reaction mixture was stirred at room temperature for 2 h, poured onto ice water, acidified with cold diluted HCl to give a solid product, which was filtered off, dried and then recrystallised from benzene to give **18** as yellow solid; m.p. 178–180°C; yield: 68.19%. IR: ν 3238 (NH), 3071 and 3033 (CH_{ar}), 2932 (CH_{al}), 1658 cm^{-1} (CO); ^{1}H-NMR ($CDCl_3$): δ 1.39 (t, J = 7.08 Hz, 3H, $CH_2C\underline{H}_3$), 1.80 (br s, 4H, C-5 and C-6H), 2.68 (br s, 2H, C-4H), 2.80 (br s, 2H, C-7H), 4.36 (q, J = 7.18 Hz, 2H, $C\underline{H}_2CH_3$), 7.48-8.03 (m, 5H, Ar-H), 12.33 (s, 1H, NH); Anal. Calcd. for $C_{18}H_{19}NO_3S$ (329): C, 65.65; H, 5.78; N, 4.26; Found: C, 65.57; H, 5.74; N, 4.07.

3-Amino-2-phenyl-5,6,7,8-tetrahydro[b]benzothieno[2,3-d]pyrimidin-4(3H)-one (**19**)**.** Compound **18** (10 mmol; 3.33 g) and hydrazine hydrate (10 mmol; 0.5 ml) were dissolved in dimethylformamide (30 ml) and refluxed for 5 h. It was left to cool down, poured onto ice water, filtered off, dried and then recrystallised from ethanol to afford **19** as yellow crystals; m.p. 145–146°C; yield 60.14%. IR: ν 3289 and 3213 (NH_2), 3055 and 3028 (CH_{ar}), 2951 (CH_{al}) and 1658 cm^{-1} (CO); ^{1}H-NMR ($CDCl_3$): δ 1.88 (br.s, 4H, C-6 and C-7H), 2.59 (br s, 2H, C-5H), 2.73 (br.s, 2H, C-8H), 5.02 (s, 2H, NH_2, D_2O exchangeable), 7.47–7.88 (m, 5H, Ar-H), Anal. Calcd. for $C_{16}H_{15}N_3OS$ (297): C, 64.64; H, 5.05; N, 14.14; Found: C, 64.57; H, 4.89; N, 14.07.

Ethyl 2-ethoxycarbonylmethylaminomethylideneamino-4,5-tetrahydrobenzo[b]thiophene-3-carboxylate (**20**)**.** To a solution of thiophene ester **17** (40 mmol; 9 g) in 30 ml dimethylformamide, ethyl cyanoacetate (40 mmol; 5 ml) was added and HCl gas was passed through the reaction mixture at room temperature for 2 h. The reaction mixture was poured onto ice water, the solid product that precipitated was filtered off, dried and recrystallised from light petroleum (60–80°C) giving **20** as yellow solid; m.p. 98–101°C; yield 59.19%. IR: ν 3406 and 3300 (NH_2), 3077 (CH_{ar}), 2984 and 2937 (CH_{al}), 1744 (CO ester), 1647 cm^{-1} ($\nu_{C=N}$) in addition to the disappearance of $\nu_{C\equiv N}$; ^{1}H-NMR ($CDCl_3$): δ 1.29 (t, 3H, CH_2–$COOCH_2C\underline{H}_3$), 1.39 (t, 3H, C3–$COOCH_2C\underline{H}_3$), 1.79 (m, 4H, C-5 and C-6H), 2.48 (br.s, 2H, C-4H), 2.72 (br.s, 2H, C-7H), 3.21 (s, 2H, $C\underline{H}_2$–COOEt), 4.05 (q, 2H, –CH_2–$COOC\underline{H}_2CH_3$), 4.25 (q, 2H, C3–$COOC\underline{H}_2CH_3$), 5.93 (br.s, 2H, NH_2, D_2O exchangeable); Anal. Calcd. for $C_{16}H_{22}N_2O_4S$ (338): C, 56.80; H, 6.51; N, 8.28; Found: C, 56.67; H, 6.34; N, 8.17.

REFERENCES

1. J. J. Marr, R. L. Berens, N. K. Cohn, D. J. Nelson, R. S. Kelin, *Antimicrob. Agents Chemother.*, **25**, 292 (1984) [Chem. Abstr., **100**, 150632 (1984)].
2. K. Ogawa, I. Yamawaki, Y. Matsushita, N. Nomura, *Jpn. Kokai,* **225**, 485 (1990) [Chem. Abstr., **114**, 102035 (1991)].
3. M. Taguchi, T. Ota, K. Hatayama; PTC Int. Pat. 03,040 (1993) [Chem. Abstr., **119**, 160309 (1993)].
4. A. W. Gomol, D. L. Temple, *Drug Dev. Res*., **10**, 579 (1987).
5. Z. A. Hozien, A. A. Abdel-Wahab, K. M. Hassan, F. M.Atta, S. A. Ahmad, *Pharmazie*, **52**, 753 (1997).
6. V. I. Shvedov, V. M. Aryuzina, M. D. Mashkovski, A. J. Polezhaeva, L. F. Roshchina, USSR Pat. 745,160 (1983) [Chem. Abstr., **99**, 82509 (1983)].
7. K. Ninomiya, K. Nitsuta, A. Tobe, M. Egawa, R. Kikumoto; *Jpn. Kokai*, **16**, 557 (1990) [Chem. Abstr., **114**, 102035 (1991)].
8. J. B. Press, R. K. Russell, U.S. Pat. 835,157 (1989) [Chem. Abstr., **111**, 174121 (1989)].
9. V. P. Litvinov, L. A. Rodinovskaya, Yu. A. Sharanin, A. M. Shestopalov, A. Senning, *Sulfur Reports*, **13**, 1 (1992).
10. A. E. Abdel-Rahman, E. A. Bakhite, E. A. Al-Taifi, *J. Chin. Chem. Soc.*, **49**, 233 (2002) [Chem. Abstr., **137**, 294919 (2002)].
11. Y. A. Ammar, M. M. Ismail, M. S. A. El-Gaby, M. A. Zahran, *Indian J. Chem.*, **41**, 1486 (2002) [Chem. Abstr., **138** (2003)].
12. A. Santagati, G. Granata, M. Santagati, V. Gutuli, N. G. Mangano, A. Caruso, *Arzneim. Forsch.,* **52**, 448 (2002).
13. A. K. El-Ansary, A. H. Omar, *Bull. Fac. Pharm. (Cairo Univ.)*, **39**, 17 (2001) [Chem. Abstr., **136**, 216712 (2002)].
14. K. Fujii, T. Tanaka, Y. Fukuda, Eur. Pat. 370,704 (1990) [Chem. Abstr., **113**, 212005 (1990)].
15. H. Fukumi, F. Saitoh, H. Hovikoshi, S. Kobayashi; Eur.Pat. 82,023 (1983) [Chem. Abstr., **99**, 158453 (1983)].
16. S. El-Bahaie, A. El-Deeb, M. G. Assy; *Pharmazie*, **46**, 26 (1991).
17. A. A. Larsen, D. A. Owens, Ger.Pat. 231,103 (1983) [Chem. Abstr., **98**, 204410 (1983).
18. T. Obata, K. Fujii, I. Narita; Eur.Pat. 356,158 (1990) [Chem. Abstr., **113**, 59210 (1990).
19. V. J. Ram, H. K. Pandey, A. Vlietinck, *J. Heterocycl. Chem*., **18**, 1277 (1981).
20. H. M. F. Madkour, M. A. I. Salem, T. M. Abdel-Rahman, M. E. Azab, *Heterocycles*, **38**, 57 (1994).

21. A. S. Hamad, M. E. Azab, *Phosphorus, Sulfur, Silicon*, **173**, 105 (2001).
22. M. E. Azab, G. A. M. El-Hag Ali, A. F. Abdel-Wahab, *Acta Chem. Pharm.*, **53**, 213 (2003).
23. M. A. I. Salem, E. A. Soliman, M. B. Smith, M. R. Mahmoud, M. E. Azab, *Phosphorus, Sulfur, Silicon*, **179**, 61 (2004).
24. H. M. F. Madkour, *ARKIVOC*, 36 (2004).
25. H. M. F. Madkour, *Chem. Pap*., **56**, 314 (2002).
26. M. E. Azab, M. A. E. Ibraheem, H. M. F. Madkour, *Phosphorus, Sulfur, Silicon,* **181**, 1299 (2006).
27. M. A. El-Hashash, M. A. Hassan, M. A. Sayed, *Pak. J. Sci. Ind. Res.*, **20**, 336 (1977).
28. F. M. Soliman, M. A. El-Hashash, L. Souka, A. S. Soliman, *Rev. Roum. Chim.,* **41**, 109 (1996) [Chem. Abstr., **125**, 244743 (1996)].
29. Z. A. Hozien, F. M. Atta, Kh. M. Hassan, A. A. Abdel-Wahab, A. A. Ahmad, *Synth. Commun*., **26**, 3733 (1996).
30. V. J. Ram, *Arch. Pharm.*, **312**, 19 (1979).
31. K. Gewald, *Chimia,* **34**, 101 (1980) [Chem. Abstr., **92**, 215303 (1980)].
32. K. Gewald, *Lect. Heterocycl. Chem.*, **6**, 121 (1981).
33. K. Gewald, E. Schinke, H. Böttcher; *Chem. Ber*., **99**, 94 (1966).
34. F. Sauter, P. Stanetty, H. Potuzak, *Arch. Pharm.*, **309**, 914 (1976).

5,6,7,8-ТЕТРАХИДРОБЕНЗО[B]ТИЕНО[2,3-D]ПИРИМИДИН-4(3H)-ОН КАТО СИНТОН ЗА ХЕТЕРОЦИКЛЕНИ СИСТЕМИ

Х. М. Ф. Мадкур*, М. Е. Азаб, М. А. Е. Ибрахим

Лаборатория по синтетична органична химия, Департамент по химия, Факултет по науки, Университет Аин Шамс, Абасия, Кайро, Египет

Постъпила на 12 ноември 2007 г.; Преработена на 7 март 2008 г.

(Резюме)

При реакцията на тетрахидробензо[b]тиено[2,3-d]пиримидин-4(3*H*)-он с етилхлорацетат е получен естер, който при взаимодействие с *p*-хлоробензалдехид в различни условия и с бензиламин дава нови съединения. При реакцията на хлоротиенопиримидин с тиокарбамид, бензоилхидразин, тиосемикарбазид, семикарбазид, натриев азид и глицин са получени съответно пиримидинтион, 1,2,3-триазол, тиооксо-1,2,4-триазол, оксо-1,2,4-триазол, тетразол и имидазол. При реакцията на пиримидинтион с β-арилакрилова киселина е получена γ-кетокиселина, която при реакция с оцетен анхидрид и хидразинхидрат дава съответно фуранон и пиридазинон. Етил-2-амино-4,5,6,7-тетрахидробензо[b]тиофен-3-карбоксилат е използван при синтеза на производно на 3-аминотиено-пиримидинон чрез реакция с бензоилхлорид и хидразинхидрат. Получен е интересен продукт на кондензация при реакцията на етил-2-амино-4,5,6,7-тетрахидро[b]тиофен-3-карбоксилат с етилцианоацетат в диметил-формамид.

Bulgarian Chemical Communications, Volume 41, Number 1 (pp. 19–22) 2009

Use of newly synthesized guar based chelating ion exchange resin in chromatographic separation of copper from nickel ions

S. Loonker[1], J. K. Sethia[2]*

Department of Chemistry, Jai Narain Vyas University, Jodhpur – 342 001 (Rajasthan), India

Received November 10, 2007; Revised May 10, 2008

Crosslinked guar functionalized with β-amino-α-methylphenethyl alcohol (AMPA) is found to be very efficient for separation of copper from nickel ions in a mixture using column chromatography. The IR spectra of the resin and the nitrogen content data support the successful incorporation of chelating agent in the guar matrix. The moisture content, bulk density, bulk volume and ion exchange capacity were determined by standard methods. Distribution coefficient data, determined at various pH for both metal ions, reveal an effective separation of Cu(II) from Ni(II) ions using the newly synthesized guar epoxy ether of β-amino-α-methylphenethyl alcohol (GEE-AMPA)

Key words: functionalized guar resin, Cu(II) and Ni(II) ions separation.

INTRODUCTION

The determination of low concentration levels of heavy metal ions in water samples from different sources received considerable attention in recent years [1–3]. In general, certain metal ions and a number of toxic elements have traditionally been determined by several atomic spectrometric methods [4–6]. A great need still exists to investigate fast, accurate, and sensitive analytical methods for separation and subsequent determination of different metal ions especially at trace levels in a wide spectrum of test samples.

Ion-exchangers and chelating resins are very often used in the removal, preconcentration and determination of various metal ions in aqueous solutions. Ion-exchange fibers are also used as drug reservoir materials for storage and controlled drug delivery [7]. The specific applications include the use of such resins in hydrometallurgical processes [8]. This area receives more attention since many metals are recovered from secondary sources, wastes and rinsing water. Resins are particularly useful in metal recovery, when the concentration of targeted ion in the solution is low and thus the treatment of large volumes of solution is inevitable.

Nine heavy metal ions were simultaneously determined at μg/L levels by Cardellicchio *et al*. [9] in 22 minutes, using column chromatography in ground water samples. Santoyo *et al*. [10] determined lead, copper, cadmium, cobalt, zinc and nickel ions in ground water using three ionic separation column systems including HPIC-CS2 of Dionex as a cationic column, HPIC-AS4 of Dionex as an anionic column and IonPac CS5 of Dionex as a bifunctional ion-exchange column.

In our work we have attempted the separation of Cu and Ni ions on GEE-AMPA resin synthesized in our laboratory. We have used the guar-based resin because of its abundance in the region, low cost, hydrophilic nature and flocculent action. Both ion-exchanging and chelating abilities are shown by AMPA thus giving better results in comparison to other chelating agents. AMPA is found to give good results for copper in comparison to other functionalizing agents like imino diacetic acid, anthranilic acid, *p*-amino benzene sulphonic acid, *etc*., reported by us, using various polymeric supports. Though the resin can also separate other ions on the basis of distribution coefficient values, this paper focuses on the separation of Cu and Ni only.

EXPERIMENTAL

Guar is procured from local industries and other AR purity grade chemicals are procured from Sarabhai M. Chemicals, Baroda.

Physical Parameters

The IR spectra of resin, recorded on Schimadzu IR 400 spectrophotometer using KBr pellets, revealed the appearance of a band at 3657 cm^{-1} (1 spike), that

[1] Present address: Dr. Sangeeta Loonker, "Neil", 70, Jwala Vihar, Behind Jeevan Jyoti Hospital, Jodhpur, Rajasthan, India
[2] Present address: Dr. Jinendra Sethia, Solvay Specialities India Pvt. Ltd., Plot No. 3526-27, GIDC Estate, Panoli – 394116, Dist. Bharuch, Gujarat, India

* To whom all correspondence should be sent:
E-mail: jinen140579@gmail.com

© 2009 Bulgarian Academy of Sciences, Union of Chemists in Bulgaria

is assigned to ν(N–H) of R–NH–R group. Another band at 3585 cm^{-1} is ascribed to ν(–OH) of alcohol. The disappearance of peak at 3565 cm^{-1} (2 spike) shows that AMPA has been successfully incurporated into epoxy ether of guar.

Flame atomic absorption spectrophotometer (FAAS) model Schimadzu AA-630-12 was used for analysis of metal ions in test sample.

The resin characteristics i.e., bulk density; moisture content, nitrogen content estimation and ion exchange capacity were determined by the standard methods. The results are summarized in Table 1.

Table 1. Resin characteristics.

Resin	Moisture content, %	Bulk density, g/cm^3	Specific bulk volume, cm^3/g	Nitrogen content, %	Ion exchange capacity, meq/g
GEE-AMPA	1.6	0.721	2.75	1.68	0.991

The pH titration or neutralization curve (in Fig. 1**)** of chelating ion exchanger is carried out to establish the character of the exchanging group. The results reveal that it is a weakly basic chelating anion exchange resin.

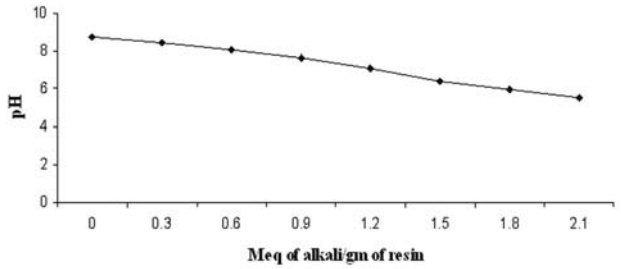

Fig. 1. pH titration curve.

Synthesis of epoxy ether of guar

Guar was first subjected to reaction with epichlorohydrin. The obtained epoxy ether is then used to synthesize GEE-AMPA. One mole of guar (486 g) was suspended in dioxane in a round bottom flask. The reaction mixture was rendered alkaline by adding 20 mL of 50% aqueous sodium hydroxide solution. The contents were magnetically stirred and refluxed at 45ºC for an hour. 1 mole (92.53 g) of epichlorohydrin was added and pH was adjusted between 9 to 10. The contents were refluxed upon constant stirring for another 4–5 hours at 45ºC. The product was filtered on a vacuum pump and washed with 80% aqueous CH_3OH + HNO_3 solution, to remove inorganic impurities and excess of alkali. The complete removal of chloride by the washing was ensured using $AgNO_3$ solution and removal of alkali was ensured using litmus solution. The washed product was dried in an oven at 50ºC and used for further derivatization.

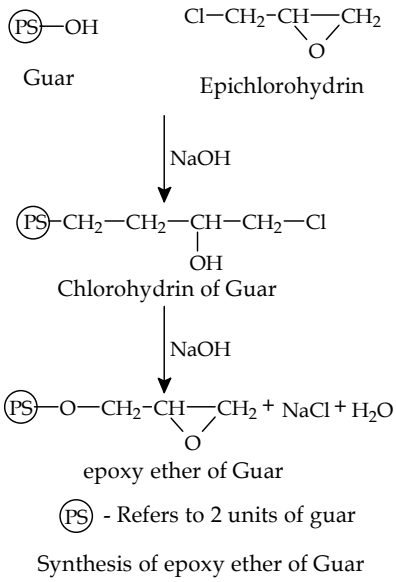

Synthesis of epoxy ether of Guar

Synthesis of guar epoxy ether of β-amino-α-methyl-phenethyl alcohol (GEE-AMPA)

0.01 moles of guar epoxy ether was suspended in 70% aqueous isopropyl alcohol. 10 mL of 50% aqueous sodium hydroxide solution was added to the reaction mixture under reflux upon constant stirring at 50 ± 5ºC.

0.02 moles of AMPA were added to the reaction mixture. The contents were refluxed and stirred for 5–6 hours at 55ºC on a water bath. The product was filtered off under vacuum and washed with 50% aqueous CH_3OH + HNO_3 solution to remove the inorganic impurities. The dried product was suspended in 0.1N HCl and filtered immediately. The successive washings with 0.1N NaOH and 0.1N HCl were carried out, the contents were finally washed with absolute alcohol and dried under vacuum.

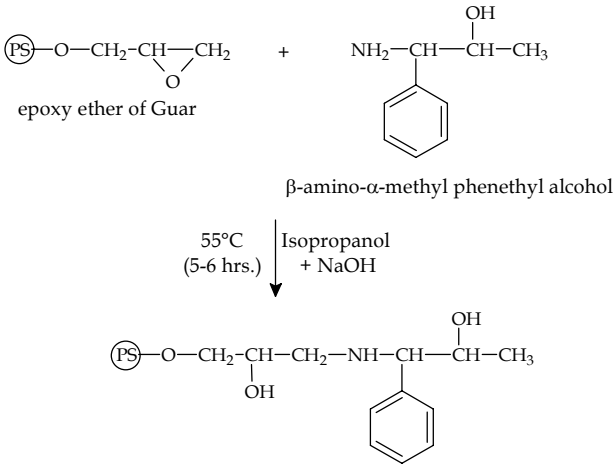

Guar epoxy ether of β-amino-α-methyl phenethyl alcohol

Analysis of metal uptake

Batch equilibrium technique was employed for measuring the metal uptake by the resin. In a set of six glass stoppered flasks, 0.084g of dried resin was taken and 40 mL of buffer (prepared by mixing different volumes of 0.2 M acetic acid and 0.2 M sodium acetate) was added to each flask for adjusting the pH value to 3.5, 4.0, 4.5, 5.0, 5.5 and 6.0, respectively. 1 mL of 1000-ppm metal ion solution was added to each flask and the contents were agitated for an hour. The two phases were separated after reaching equilibrium, using batch method and the metal content was determined in an aliquot of the filtrate by flame atomic absorption spectrometry (FAAS). Analyzing the eluates for the copper and nickel concentration in each set of experiments using FAAS we checked the achievement of equilibrium.

It was found that copper shows maximum chelation at pH 6.0, whereas nickel shows maximum chelation at pH 5.0 as inferred from their Distribution coefficient (D_f) values in Table 2. The resin was found to be highly selective for Cu at pH 6.0. The metal uptake is much higher in comparison to the theoretical uptake, calculated based on its nitrogen content data. This can be well explained by the fact that guar derivatives also act as very good adsorbents.

Table 2. Distribution coefficients.

pH	Distribution coefficient (D_f), mL/g	
	Cu	Ni
3.5	342	126
4.0	–	202
4.5	717	468
5.0	880	859
5.5	1835	619
6.0	2098	543
6.5	1017	–

Column separation

An ion exchange column of 20 cm height was packed with a slurry of GEE-AMPA prepared in dioxane. The buffer of 6.0 pH was allowed to flow through the column. An aliquot of sample solution containing standard amount of Cu(II) and Ni(II) ions was passed though the column at a flow rate of 1–2 mL/min. Loaded metal ions were eluted using 0.1 N HCl. In the first 10 mL fraction Ni(II) ions were eluted completely. The second fraction obtained had neither Ni(II) nor Cu(II) ions. Elution of Cu(II) was complete by addition of another 40 mL portion of eluate, which was collected as third fraction. Metal concentration in the eluate for each set of experiments was analyzed using FAAS.

RESULTS AND DISCUSSION

The theoretical ion exchange capacity of GEE-AMPA resin was calculated and found out to be 0.991 meq/g. The metal capacity versus pH contours of GEE-AMPA resin with Cu(II) and Ni (II) ions are shown in Fig 2.

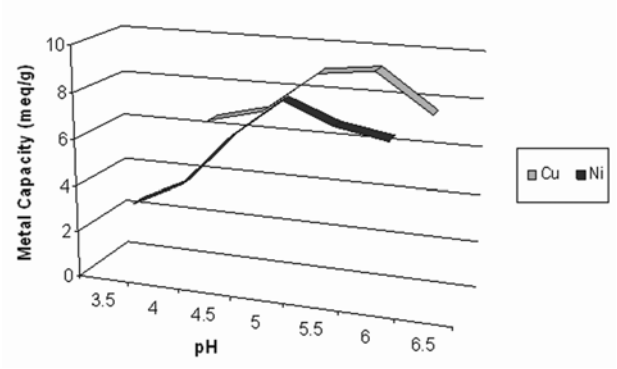

Fig. 2. Metal capacities *versus* pH for GEE-AMPA resin.

The perusal of the results reveals that the metal uptake by the resin increases at first and then decreases with increasing pH. The resin exhibited maximum metal uptake capacity for Cu (II) at pH 6.0, which is found to be four times higher than that shown for Ni (II). The distribution of metal ions in the resin also followed the above order. Maximum value for distribution coefficient for Cu was 2098 mL/g, while for Ni it was just 543 mL/g. Studies were also carried out for Fe(II), Zn(II) and Co(II). The comparison of their D_f values at pH 6.0 revealed that the resin is highly specific for Cu(II) at this pH and can be successfully used for separation of Cu from a sample containing Cu and Ni. Their D_f values decrease in the order

Cu II (2098) > Zn II (908) > Fe II (874) > Co II (858) > Ni II (543).

D_f values for Cu and Ni at various pH are summarized in Table 2. Analysis of Table 2 data reveals that effective separation of Cu and Ni can be carried successfully using column chromatography at pH 6 due to their appreciably high difference in D_f values. The results are reported in Table 3 and they are the average of four determinations.

Table 3. Separation of Cu(II)ions from Ni(II)ions.

Sam-ple	Amount of Cu(II) and Ni(II) in mixture on column		Amount of Cu(II) and Ni(II) ions in eluate					
No.	Cu(II) mg	Ni(II) mg	Cu(II) mg	SD	RSD, %	Ni(II) mg	SD	RSD %
1	3.0	7.0	2.91	0.09	3.00	6.92	0.08	1.14
2	4.0	5.0	3.89	0.11	2.75	4.92	0.08	1.60

Note: Average of four determinations for each set is reported.

REFERENCES

1. Y. F. Lasheen, A. F. Seliman, A. A. Abdel-Rassoul, *J. Chromatogr. A,* **1136**, 202 (2006).
2. V. K. Singh, K. P. Singh, D. Mohan, *Environ. Monit. Assess.,* **105**, 43 (2005).
3. H. Karami, M. F. Mousavi, Y. Yamini, M. Shamsipur, *Anal. Chim. Acta,* **509**, 89 (2004).
4. G. Doner, A. Ege, *Anal. Chim. Acta,* **547**, 14 (2005).
5. M. A. A. Akl, I. M. M. Kenawy, R. R. Lasheen, *Microchem. J.,* **78**, 143 (2004).
6. M. Soylak, S. Saracoglu, U. Divrikli, L. Elci, *Talanta,* **66,** 1098 (2005).
7. T. Jaskari, M. Vuorio, K. Kontturi, A. Urtti, J. A. Manzanares, J. Hirvonen, *J. Control. Release,* **67**, 179 (2000).
8. A. W. Trochimczuk, S. Czerwińska, *React. Func. Polym.*, **63**, 215 (2005).
9. N. Cardellicchio, S. Cavalli, P. Ragone, J. M. Riviello, *J. Chromatogr. A,* **847**, 251 (1999).
10. E. Santoyo, S. Santoyo-Gutierrez, P. V. Surendra, *J. Chromatogr. A,* **884**, 229 (2000).

ИЗПОЛЗВАНЕ НА НОВОСИНТЕЗИРАНА ХЕЛАТНА ЙОНООБМЕННА СМОЛА НА ОСНОВАТА НА ГУМА ГУАР ЗА ХРОМАТОГРАФСКО РАЗДЕЛЯНЕ НА МЕДНИ ОТ НИКЕЛОВИ ЙОНИ

С. Луункер, Дж. К. Сетия*

Департамент по химия, Университет Джай Нараин Виас, Джодпур 342 001 (Раджастан), Индия

Постъпила на 10 ноември 2007 г.; Преработена на 10 май 2008 г.

(Резюме)

Установено е, че омрежена гума гуар, функционализирана с β-амино-α-метилфенилетилов алкохол (АМФА) е много ефективна за разделяне на медни от никелови йони в смеси при използване на колонна хроматография. ИЧ спектри на смолата и данните за съдържанието на азот са в подкрепа на успешното въвеждане на хелатния агент в матрицата на гумата гуар. Съдържанието на влага, насипната плътност, насипният обем и йонообменният капацитет са определени със стандартни методи. Данните за коефициентите на разпределение, определени при различни pH за двата метални йони показват ефективно разделяне на йоните Cu(II) от Ni(II) с помощта на новосинтезирания епокси етер на β-амино-α-метилфенилетил алкохол и гума гуар.

Bulgarian Chemical Communications, Volume 41, Number 1 (pp. 23–30) 2009

Atomic force microscopy for the characterization of human platelets before and after interaction with selected anticoagulant drugs

E. Gorodkiewicz[1]*, A. Sankiewicz[1], I. Sveklo[2], Z. A. Figaszewski[1,3]

[1] *Department of Electrochemistry, Institute of Chemistry, University of Bialystok, Al. J. Pilsudskiego 11/4, 15-443 Bialystok, Poland*
[2] *Institute of Experimental Physics, University of Bialystok, Lipowa 41, 15-333 Bialystok, Poland*
[3] *Laboratory of Electrochemical Power Sources, Faculty of Chemistry, University of Warsaw, Pasteur St. 1, 02-093 Warsaw, Poland*

Received January 16, 2008; Revised May 19, 2008

Human platelets, i.e thrombocytes are the smallest non-nucleated blood cells, which are highly reactive components of the circulatory system and play a key role in many pathophysiologic processes, such as thrombosis, hemostasis, inflammation, host defense, tumor biology, as well as in maintenance and regulation of vascular tone. The platelets aggregation process and the formation of platelet plugs are a fundamental part of the blood clotting process and prevent bleeding from capillaries, small arterioles and venules. However, thrombosis disorders are one of the reasons for complications in surgical procedures. Abciximab and Eptifibatide are efficient antiplatelet drugs used during and after coronary artery treatments, such as angioplasty, in order to prevent platelets from sticking together and causing thrombus formation inside the coronary artery.

The aim of this work was the comparison of different methods for preparation and immobilization of blood platelets on a glass or mica bedding in terms of suitability for the investigation of Abciximab or Eptifibatide interaction with platelets by Atomic Force Microscopy (AFM). AFM is a very useful tool for the observation of the topography of biological structures. The investigation was performed on dry mica, dry glass and in a buffer solution.

On mica, changes in the shape and size of inactive and activated platelets can be observed, as well as their aggregation with fibrinogen. Abciximab and Eptifibatide, deposited onto the mica sheet, form 'twig-crystal' structures. Surprisingly, the smaller Eptifibatide molecules form a bigger structure than that of Abciximab. This is probably caused by Eptifibatide molecular aggregation.

Platelet-inhibitor complex adhesion on mica or glass sheets was observed. The low number of activated platelets was observed after incubation of a sample with both drugs. These drugs surrounded the platelets as a result of interaction with glycoprotein GP IIb/IIIa. Frequently, whole platelets were surrounded with drugs. Each image shows the aggregation process in a different phase with a characteristic platelet filopodia. Each procedure can be used for the observation of platelets and their changes under the influence of different agents, for example drugs.

Key words: Atomic force microscopy (AFM), human blood platelets, abciximab, eptifibatide.

INTRODUCTION

Human blood platelets (PLT), i.e thrombocytes are the smallest non-nucleated blood cells. They are tiny and discoid in shape, with dimensions of approximately 2.0–4.0 μm. Platelets are produced in the bone marrow and arise from megakaryocyte. The circulating life time of a platelet is 7–10 days [1]. A normal platelet count in a healthy person is 150 000–450 000 cells/mm^3 of blood (www.lab-testsonline.org). They are highly reactive components of the circulatory system and play a key role in many pathophysiologic processes, such as thrombosis, hemostasis, inflammation, host defense, tumor biology, maintenance and regulation of vascular tone [2].

Human blood platelets contain granules (alpha, dense, lysosomes), mitochondria and an endoplasmmatic reticulum [3]. Alpha and dense granules contribute to the very important function of platelets in hemostasis. The alpha granules play a primary role in hemostatis, while dense granules in the aggregation [1]. The aggregation process and the formation of a platelet plug are a fundamental part of the blood clotting process and they prevent bleeding from capillaries, small arterioles, and venules. This is a two-phase process. At first, single platelets bind to the site of the wound – this is the adhesion process. Next, the platelets are activated. During activation, the platelets are drastically changing shape. They undergo change from a discoid form to a flat spread form, 7–10 μm in diameter [4]. Activation can be stimulated by substances released by these cells (for example: adenosine diphosphate,

* To whom all correspondence should be sent:
E-mail: ewka@uwb.edu.pl

© 2009 Bulgarian Academy of Sciences, Union of Chemists in Bulgaria

serotonin and thromboxane) and by components, which circulate in the blood (for example the Von Willebrand Factor, thrombine). The result of these two processes is the aggregation of platelets.

Platelets play an increasing role in vascular and endovascular procedures. Thrombosis disorders are one reason for complications in surgical procedures. Many agents, for example specific drugs, foods, spices and vitamins could impair platelet function [5]. Today, there is a number of drugs that inhibit platelet function [6]. The classic inhibitor of platelet function is aspirin (acetylsalicylic acid). Aspirin prevents blood from clotting by blocking the production of thromboxane A–2.

Thromboxane A-2 is produced in platelets and causes them to clump. Aspirin inhibits the enzyme cyclo-oxygenase-1 (COX-1) that produces thromboxane A-2 [1, 5, 6]. Clopidogrel is a potent oral antiplatelet agent often used in the medical treatment of coronary artery disease, peripheral vascular disease, and cerebrovascular disease. The mechanism of action of clopidogrel is the irreversible blockade of the adenosine diphosphate (ADP) receptor on platelet cell membranes [7]. A number of new drugs, inhibitors of fibrinogen, preventing platelet aggregation by binding to glycoprotein IIb/IIIa, has been recently studied. Three of them: abciximab (ReoPro), eptifibatide (Integrilin) and tirofiban (Aggrasrat) have been registered as efficient antiplatelet drugs [8, 9]. Abciximab is a human-murine chimeric Fab fragment of the monoclonal antibody c7E3 directed against the glycoprotein IIb/IIIa [10]. Eptifibatide is a cyclic heptapeptide containing six amino acids and one mercaptopropionyl (des-amino cysteinyl) residue [11]. Tirofiban is a synthetic, nonpeptide inhibitor acting on glycoprotein (GP) receptors, type IIb/IIIa, in human thrombocytes. These inhibitors are mainly used during and after coronary artery procedures, such as angioplasty to prevent platelets from sticking together and causing thrombus (blood clot) formation inside the coronary artery [12].

There are many methods for studying platelet properties. Platelet functions are studied by the measurement of key biochemical markers that can show changes in platelet activation. There are two principal assay systems: ELISA and flow cytometry [13–15]. Markosyan *et al*. [16] used a laser photometer to study platelet shape and aggregation. The elastic properties of cells have been measured using a mechanical indenter called a cell poker [17], optical tweezers [18], scanning acoustic microscopy [19] or fine glass needles [20]. Electron microscopy and an Atomic Force Microscope have been used [4, 21] to study the architecture of the cytoskeleton and changes in the platelet during activation [22], as well as to diagnose platelet disorders [23]. The interaction between platelet receptor and ligand (for example fibrinogen) in the presence of platelet inhibitors (abciximab, tirofiban, eptifibatide) has been studied using fluorescence laser-scan microscopy [24], confocal microscopy [25], laser tweezers [26], electron microscopy [27], fluorescence and differential interference contrast microscopy [28].

The aim of this work was the comparison of different methods for the preparation and immobilization of blood platelets on a different bedding**,** in terms of the suitability for investigation of the interactions between anticoagulant drugs (abciximab or eptifibatide) and platelets by the Atomic Force Microscopy (AFM). More precisely, the aim was the observation of changes in platelet topography on dry mica bedding and on a glass bedding, both dry and from an aqueous buffer solution.

EXPERIMENTAL

AFM measurements

The AFM measurements were performed with a commercial Ntegra Prima scanning probe microscope (NT-MDT, Russia) using a "Tapping mode" for "in air imaging" and a contact mode for in "liquid and air imaging". A scanning head for measurements in liquid and air (100 mkm scanner) was equipped with capacitive position sensors, which allow the removal of the hysteresis of piezodrivers. CSG01 probes with a force constant of 0.01–0.08 N/m were used for the contact mode and NSG03 probes with resonance frequency 90–116 kHz were used for the tapping mode. All measurements were done at room temperature.

Chemicals

Acetone, sodium hydrogen carbonate $NaHCO_3$, sodium dihydrogen phosphate NaH_2PO_4, sodium chloride NaCl, potassium chloride KCl, magnesium chloride $MgCl_2$ (all analytical purity grade, POCH, Gliwice, Poland), Tyrode buffer (12 mM, 4 mM, 137 mM, 2.6 mM, 1 mM, pH = 7,3), abciximab (REOPRO, Centocor B.V. Holland), eptifibatide (INTEGRILIN, Glaxo Group Ltd, Great Britain). Water was deionized with a MilliQ (Millipore) apparatus.

Platelet preparation

Blood samples, taken from healthy adult subjects were supplied by the Blood Donor Centre in Bialystok. The blood was treated with sodium citrate as an anticoagulant.

Next, the platelet rich plasma was separated by centrifuging the blood amount 130 g for 8 min at room temperature. This platelet rich plasma was then centrifuged at 2200 g for 10 min to obtain a platelet bottom. The supernatant was removed. The platelet bottoms were washed twice with isotonic saline.

Sample preparation for AFM measurement

a). On the mica sheet. After the last washing, the platelets were resuspended in acetone to a solid concentration of ~10^{-5} g/l. 100 µl of platelet suspension in acetone was dropped onto a freshly cleaved mica sheet. The mica sheet was dried in air for at least 4 h.

b). On the glass cover slip. Platelets were also prepared from the freshly drawn blood of one of the team. 100 µl of blood were deposited onto a glass cover slip. After 30 s, the sample was vigorously rinsed with Tyrode buffer to separate all blood cells from the activated platelets that had adhered strongly to the glass. The glass cover slip with platelets was left in air to dry.

For AFM measurements in the buffer solution, the glass slides with platelets were deposited in a special cell.

c). With abciximab and eptifibatide. The drugs were dissolved in acetone and immobilized on the mica in accordance with the procedure described in *a*) or were dissolved in aqueous buffer in accordance with the procedure described in *b*).

The interaction between drugs in therapeutic concentration (abciximab – 3.57 µg/ml of blood and or eptifibatide – 2.57 µg/ml of blood) and platelets was studied after incubation of blood or isolated platelets for 1 hour at 37ºC. The procedure of platelet preparation was the same as before (see *Platelet preparation*). 100 µl platelet solution was deposited onto a glass cover slip or mica sheet. After vigorous rinsing, the samples were observed by AFM.

RESULTS AND DISCUSSION

In order to investigate the opportunity to observe immobilized human platelets by the AFM technique, platelets were immobilized on the mica sheet. This was performed by putting a suspension of platelets in acetone on the mica surface and drying. The sample contains both inactive platelets and those at different stages of activation. Both inactive and activated platelets, immobilized on mica can be observed by the AFM. Fig. 1 shows AFM images of human platelets in different activation phases. Changes in the shape and size of inactive and activated platelets can be observed (compare Fig. 1A–C). The glycoprotein receptors located on the platelets surface change their 3D configuration under the influence of activating factors, causing them to lose their granular structure. This involved a change in platelet shape. Before these changes, platelets exhibit a regular shape and dimensions [4]. Their diameter is 2.25 µm and their thickness is 170 nm (Plot Fig. 1A). The activated platelet's shape becomes irregular. Figure 1b shows the platelet having a diameter of 4.5 µm and a thickness of 250 nm (Plot Fig. 1B), while Fig. 1c shows the platelet having a diameter of 4.25 µm and a thickness of only 30 nm (Plot Fig. 1C). The next stage of change is filopodia formation (see Fig.1C). The filopodia formation is the morphological effect of platelet activation. Simultaneously, a release reaction occurs i.e. the platelet releases substances activating the next platelets and their GPIIb/IIIa receptors. The glycoprotein (GPIIb/IIIa) fibrinogen receptor is composed of two subunits, αII_b and β_3, which form a complex. GPIIb/IIIa is specific for platelet surfaces and binds to adsorbed protein ligands, including fibrinogen, the von Willebrand factor and fibronectin. The fibrinogen plays a fundamental role in forming bridges between platelets and causes aggregation. Due to receptor activation, platelets join together with fibrinogen. Fibrinogen bridges are formed between platelets (see Fig. 2A). This process is responsible for platelet aggregation. The deposition procedure, of platelets from the acetone suspension on the mica sheet enables good and fast adhesion in different activation platelet phases.

Fig. 2 shows AFM pictures obtained after applying three different ways of platelet deposition: i) on the mica sheet from the acetone suspension (shown in picture A), ii) on the glass slide from the fresh unprocessed blood, after washing and drying (shown in picture B), iii) on the glass slide from an aqueous buffer solution (shown in picture C). The first two were dry probes and the third one was measured from an aqueous solution.

Each image shows the aggregation process in a different phase with a characteristic platelet filopodia. Each procedure can be used for the observation of platelets and their changes under the influence of different agents, for example drugs.

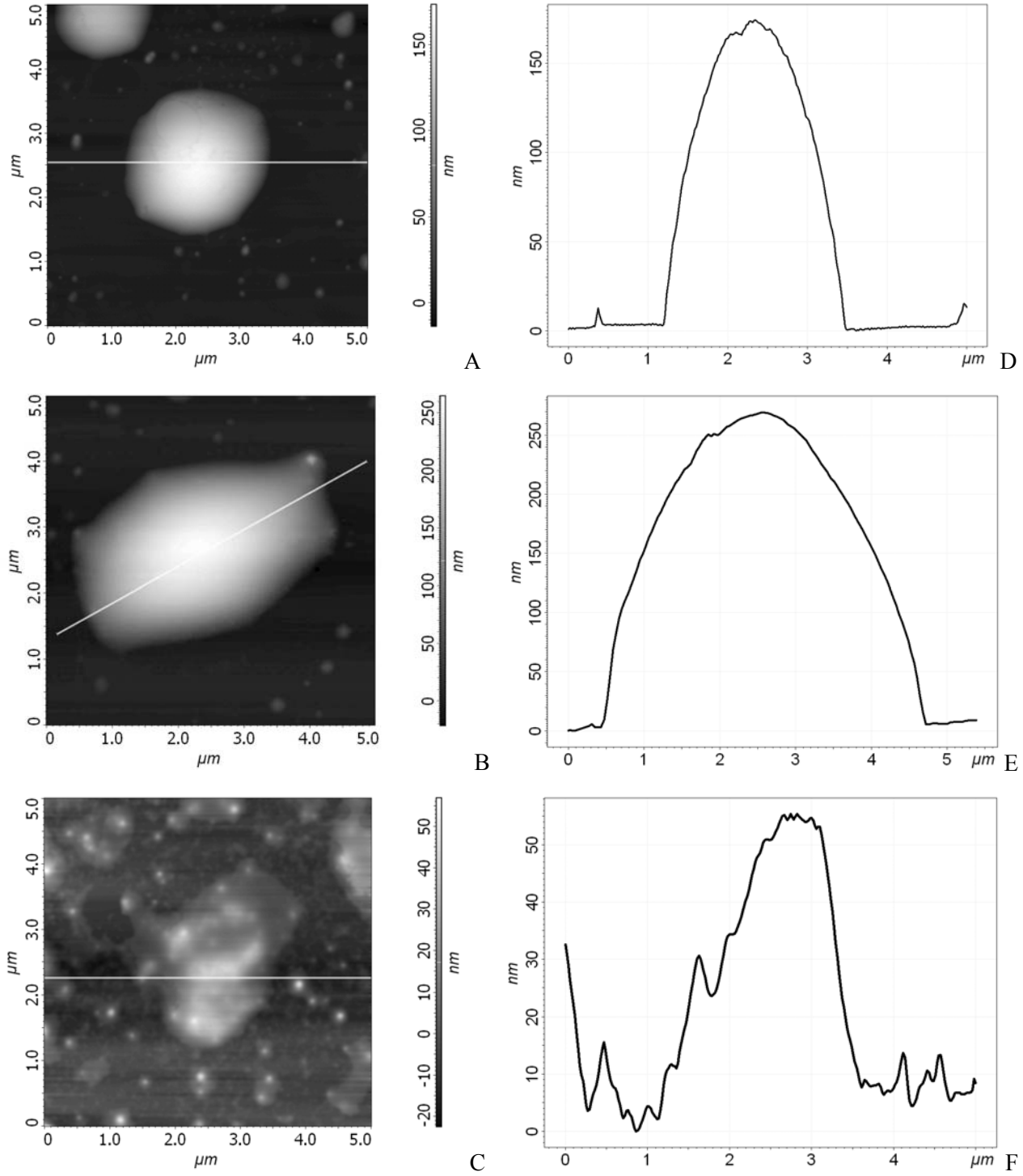

Fig. 1. Human platelets on the mica sheet imaged with the AFM and cross-sectional plots showing along the lines shown in images respectively (A, D) inactivity platelet; (B, E) activation process; (C, F) activated platelet.

In Fig. 3, two anticoagulant drugs, deposited onto the mica sheet, can be observed (A for abciximab and B for eptifibatide). A 'twig-crystal' structure is observed in both cases. Similar effects were observed with samples immobilized on a glass bedding. Abciximab is a bigger molecule and its special structure is more apparent. In the case of eptifibatide, larger structures are apparent in the pictures than in the case of abciximab, despite the fact that eptifibatide is a smaller molecule. The formation of these larger structures is probably caused by the eptifibatide molecule aggregation. Both drugs are platelet aggregation inhibitors due to fibrinogen receptor blocking. Abciximab (molecular weight of 48 kD [29]) is a human-murine chimeric Fab fragment of the monoclonal antibody c7E3. Moreover, abciximab shows a very high affinity to platelets. This molecule joins to the receptor αIIbβ3

with an antibody fragment, hindering the joining of fibrinogen, and in this manner inhibits platelet aggregation due to steric hindrance. Two amino acids sequences: RGD and KQAGDV are responsible for bonding of abciximab to this receptor [30].

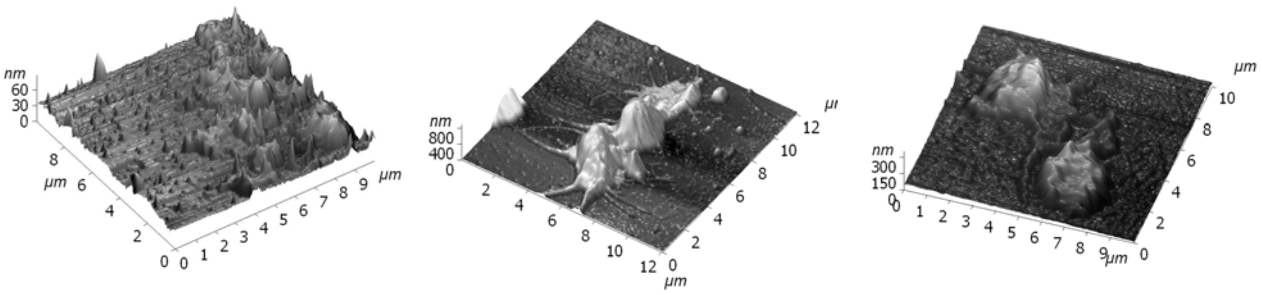

A B C

Fig. 2. AFM image of human platelets deposited onto mica-cluster of aggregate platelets (A), glass sheet-separate platelet (B), glass sheet in buffer solution-separate platelets (C).

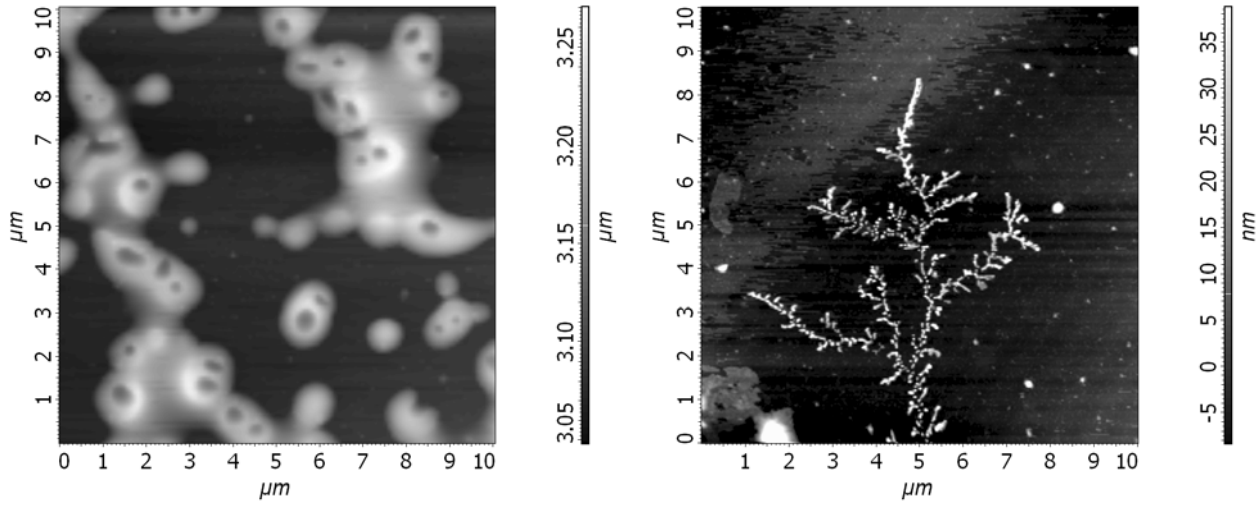

A B

Fig. 3. AFM images of anticoagulant drugs deposited onto mica sheet: A - eptifibatide; B - abciximab.

Eptifibatide (molecular weight of < 1 kD [29] is a cyclic heptapeptide containing six amino acids with a characteristic amino acids sequence Lys-Gly-Asp (KGD). It is a specific blocker of receptor $\alpha II_b\beta_3$, due to the recognition of a specific amino acid sequence (KGD) [11]. In this manner, eptifibatide blocks the fibrinogen junction to the platelet receptor. It is likely that eptifibatide forms the same steric structure as N-terminal region γ-fibrinogen chains and in this way inhibits ligand binding. On the mica sheet these drugs form "twig-crystal" structures.

These inhibitors do not influence the adhesion of platelets, as this process is caused by another platelet receptor. This is why it is possible to observe platelet-inhibitor complex adhesion on the mica or glass sheets by AFM (see Fig. 4, picture A and B, respectively). The low number of aggregated platelets is observed after incubation period of a sample with both drugs. These drugs surround the platelets as a result of interaction with glycoprotein (Fig. 4).

Frequently, whole platelets are surrounded by the drug. On the surface of each platelet there are approximately 50000 GPIIb/IIIa receptors [31]. Abciximab also binds to other platelet receptors, such as the vintronectin receptor $\alpha_V\beta_3$. The platelet shapes are deformed, especially those adsorbed on glass. This effect may be caused both by the interaction with the drug, as well as by interaction with the glass surface. Abciximab and eptifibatide block the active centre in glycoprotein GPIIb/IIIa. Therefore, the interaction of the platelet with fibrinogen is impossible.

The described experiments show that the fastest method for sample preparation prior to AFM measurements is the immobilization of platelets by just putting a blood drop on the glass. In spite of

visible biological pollution, the best images were observed for samples immobilized on mica. On the other hand, the observation of interactions from the aqueous buffer solution, although technically difficult, enables kinetic measurements.

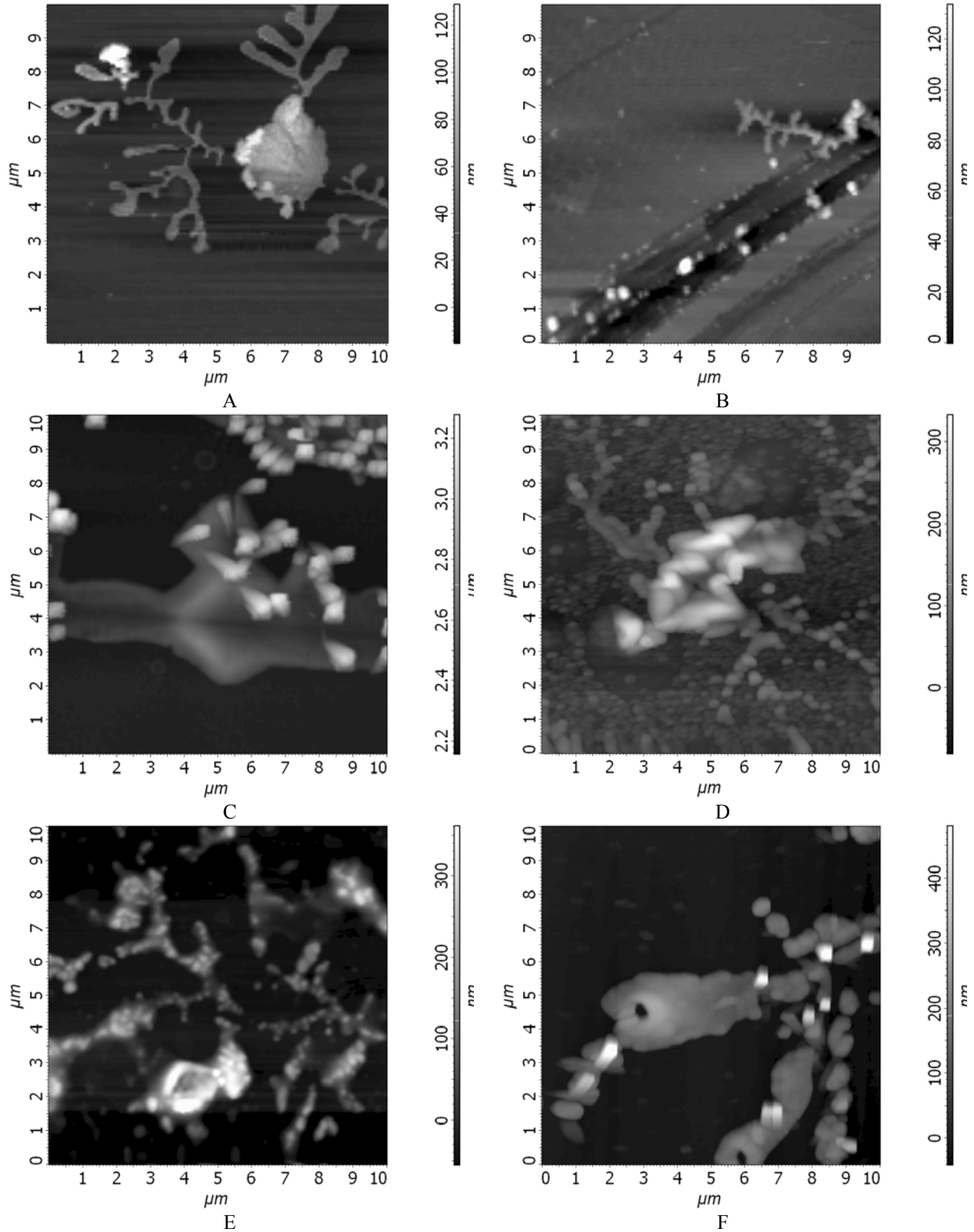

Fig. 4. AFM images of human platelets in absence anticoagulant drugs: after blood incubation with abciximab on mica and glass (A, C); after platelets incubation with abciximab on mica (B); after blood incubation with eptifibatide on mica and glass (D, F); after platelets incubation with eptifibatide on mica (E).

Acknowledgements: *This research was supported by the Marie Curie European Reintegration Grant (ERG) "Study of the interaction of bioactive compounds by the SPR imaging system" (MERG-6-CT-2005-516800) and by the Polish Ministry of National Education (Contract 19/6.PR UE/2006/7). The authors are indepted Prof. A. Maziewski for his interest in and support of the present work.*

REFERENCES

1. R. A. Chaer, J. A. Graham, L. Mureebe, *Vasc. Endovasc. Surgery,* **40**, 261 (2006).
2. P. Harrison, *Blood Reviews,* **19**, 111 (2005).
3. A. D. Michelson, *J. Thromb. Thrombolysis,* **6**, 7 (2003).
4. M. Fritz, M. Radmacher, H. E. Gaub, *Biophys. J.,* **6**, 1328 (1994).
5. J. N. George, *The Lancet,* **355,** 1531 (2000).
6. J. S. Bennet, *Annu. Rev. Med.,* **52,** 161 (2001).
7. R. Izaguirre-Avila, A. De La Pena-Diaz, F. Barina-garrementeria-Aldatz, H. Gonzalez-Pacheco, A. E. Ramirez-Gutierrez, J. L. Ruiz-Sandoval, A. Quiroz-Martinez, C. Cantu-Brito, *Clin. Appl. Thromb. Hemost*., **8,** 169 (2002).
8. E. J. Topol, T. V. Byzova, E. F. Plow, *Lancet,* **353,** 227 (1999).
9. G. Proimos, *J. Thromb. Thrombolysis,* **11**, 99 (2001).
10. N. Chronos, A. Vahanian, A. Betriu, H. Emanuelsson, S.Goldberg, D. Gluba, B. A. van Hout, *Am. Heart J.*, **135,** 67 (1998).
11. R. D. Phillips, M. R. Scarborough, *Am. J. Cardiol.,* **80,** 11B (1997).
12. S. Vickers, A. D. Theoharides, B. Arison, S. K. Balani, Dan Cui, C. A. Duncan, J. D. Ellis, L. M. Gorham, S. L. Polsky, T. Prueksaritanont, H. G. Ramjit, D. E. Slaughter, K. P. Vyas, *Drug Metab. Dispos.,* **27,** 1360 (1999).
13. D. Cox , *Am. Heart J.* **135**, 160 (1998).
14. E. Tanning, *Dan. Med. Bull.*, **39,** 343 (1992).
15. D. H. Hickerson, A. P. Bode, *Hematol. Oncol. Clin. North Am*., **16**, 421 (2002).
16. R. A. Markosyan, E. G. Popov, A. Y. Radin. *Bull. Exp. Biol. Med.*, **87,** 73 (1979).
17. N. O. Peterson, W. B. McConnaughey, E. L. Elson, *Proc. Natl. Acad. Sci. U. S. A.,* **79,** 5327 (1982).
18. A. Askin, J. M. Dziedzic, *Proc. Natl. Acad. Sci. U. S. A.,* **86,** 7914 (1989).
19. J. A. Hildebrand, D. Rugar, *J. Microsc.,* **134,** 245 (1984).
20. D. S. Adams, *J. Cell Biol.,* **117**, 83 (1992).
21. M. Radmacher, M. Fritz, C. M. Kacher, J. P. Cleveland, P. K. Hansma, *Biophys. J.*, **70,** 556 (1996).
22. J. H. Hartwing, *J. Cell. Biol.,* **118,** 1421 (1992).
23. J. G. White, *Semin. Thromb. Hemos.,* **24,** 163 (1998).
24. R. Loncar, U. Kalina, V. Stoldt, V. Thomas, R. E. Scharf, A. Vodovnik, *Thromb. J.,* **4,** 1 (2006).
25. J. P. Collet, G. Montalescot, C. Lesty, J. Soria, Z. Mishal, D. Thomas, C. Soria, *Arterioscler. Thromb. Vasc. Biol.*, **2,** 142 (2000).
26. R. I. Litvinov, H. Shuman, J. S. Bennet, J. W. Weisel, *Proc. Natl. Acad. Sci. U. S. A,* **99,** 7426 (2002).
27. J. Kawaski, N. Katori, M. Kodaka, H. Miyao, K. A. Tanaka, *Anesth. Analg.,* **99,** 1440 (2004).
28. C. L. Yap, S. C. Hughan, S. L. Cranmer, W. S. Nesbitt, M. M. Rooney, S. Gouliano, S. Kulkarni, S. M. Dopheide, Y. Yuan, H. H. Salem, S. P. Jackson, *J. Biol. Chem.,* **275,** 41377 (2000).
29. C. M. Dyke, *Am. Heart J.,* **138,** 307 **(**1999).
30. K. Kawecka-Jaszcz, A. Olszanecka, M. Loster, *Choroby Serca i Naczyń,* **3,** 91 (2006).
31. M. A. Hussain, C. A. Siedlecki, *Micron*, **35,** 565 (2004).

АТОМНО СИЛОВА МИКРОСКОПИЯ ЗА ОХАРАКТЕРИЗИРАНЕ НА ЧОВЕШКИ ТРОМБОЦИТИ ПРЕДИ И СЛЕД ВЗАИМОДЕЙСТВИЕ С ОПРЕДЕЛЕНИ АНТИКОАГУЛИРАЩИ ЛЕКАРСТВА

Е. Городкиевич[1]*, А. Санкиевич[1], И. Свекло[2], З. А. Фигашевски[1,3]

[1] Департамент по електрохимия, Институт по химия, Университет на Бялисток, ал. „Й. Пилсудски“ 11/4, Бялисток 15-443, Полша

[2] Институт по експериментална физика, Университет на Бялисток, Липова 41, Бялисток 15-333, Полша

[3] Лаборатория по електрохимични източници на ток, Химически факултет, Варшавски университет, ул. „Пастьор“ № 1, Варшава 02-093, Полша

Постъпила на 16 януари 2008 г.; Преработена на 19 май 2008 г.

(Резюме)

Тромбоцитите са най-малките безядрени кръвни клетки, които са силно реактивоспособни компоненти на системата на кръвообращението и взимат участие в много патофизиологични процеси като тромбоза, хемостаза, възпаление, защита, биология на туморите, в поддържането и регулирането на тонуса на кръвоносната система. Процесът на агрегиране на тромбоцитите и образуването на тромбоцитни запушалки са основна част от процеса на съсирване на кръвта и предовратяват течението от капилярите, малките артериоли и венулите. Нарушения в съсирването на кръвта обаче, са една от причините за усложнения при хирургичните процедури. Абсиксимаб и Ептифибатид са ефикасни антитромбоцитни лекарства, използвани по време или след процедури върху коронарни артерии, като ангиопластия, с цел да се предоврати събирането на тромбоцити и образуването на тромби в коронарната артерия.

Целта на настоящата работа е сравнение на различни методи за подготовка и имобилизиране на кръвни тромбоцити върху стъкло или слюда с оглед изследване на взаимодействието на тромбоцитите с Абсиксимаб и Ептифибатид чрез атомно силова микроскопия (АСМ). АСМ е много полезен инструмент за наблюдение на топографията на биологични структури. Изследването е проведено върху суха слюда, сухо стъкло и в разтвор на буфер.

Върху слюда могат да се наблюдават промени във формата и размера на неактивните и активираните тромбоцити, както и тяхното агрегиране с фибриноген. Абсиксимаб и Ептифибатид, поставени върху слюда, образуват структури “клонест кристал”. Изненадващо, по-малките молекули Ептифибатид образува по-големи структури околкото Абсиксимаб. Това, вероятно, се дължи на молекулно агрегиране на Ептифибатид.

Наблюдавана е адхезия на комплекса тромбоцит-инхибитор върху слюда или стъкло. Наблюдаван е малък брой от активирани тромбоцити след инкубация на пробата и с двата медикамента. Тези медикаменти заобикалят тромбоцитите като резултат от взаимодействие с гликопротеин GP IIb/IIIa. Често целите тромбоцити са заобиколени с медикамента. Отделните снимки показват процеса на агрегиране в различна фаза с характеристична филоподия на тромбоцита. Всяка процедура може да се използва за наблюдение на тромбоцитите и техните изменения под влияние на различни агенти, напр. лекарства.

Bulgarian Chemical Communications, Volume 41, Number 1 (pp. 31–38) 2009

Study of the copolymerization of *n*-(dichlorophenyl) maleimides with methyl methacrylate

V. B. Konsulov*, Z. S. Grozeva, J. I. Tacheva, K. D. Tachev

Faculty of Natural Sciences, Konstantin Preslavsky University of Shumen, 115 Universitetska st., 9712 Shumen, Bulgaria

Received November 27, 2007; Revised May 22, 2008

N-(2,3-dichlorophenyl)maleimide (2,3-DCMI), N-(2,4-dichlorophenyl)maleimide (2,4-DCMI) and N-(2,6-dichlorophenyl)maleimide (2,6-DCMI) were synthesized by the reaction of maleic anhydride with 2,3-, 2,4- or 2,6-dichloroaniline in two steps. The copolymerization of 2,3-, 2,4- and 2,6-DCMI (M_1) with methylmethacrylate (MMA – M_2) was performed in 1,4-dioxane (DO) in the presence of α,α′-azobisisobutironitrile (AIBN) as an initiator at 60°C. The monomer reactivity ratios in the copolymerization of DCMI with MMA (M_2) and Alfrey-Price *Q*-*e* values were determined as follows: $r_1 = 0.16$, $r_2 = 1.97$, $Q = 0.58$, $e = 1.47$ for 2,3-DCMI-MMA; $r_1 = 0.09$, $r_2 = 2.23$, $Q = 0.55$, $e = 1.65$ for 2,4-DCMI-MMA; $r_1 = 0.04$, $r_2 = 4.19$, $Q = 0.30$, $e = 1.75$ for 2,6-DCMI-MMA. The thermostability of the resulting maleimide copolymers was investigated by thermogravimetric analysis. Effects of molecular structure of the 2,3-, 2,4- and 2,6-DCMI compounds on their copolymerization with MMA and the properties of the copolymers have been discussed.

Key words: copolymerization, N-(dichlorophenyl)maleimides, methyl methacrylate, reactivity ratios, molecular structure, thermostability.

INTRODUCTION

New functional polymers and thermostable polymeric materials, such as resistors, nonlinear optics polymer materials, membranes, sorbents, biocatalysts and other materials with medical application [1–3], have been obtained by copolymerization of N-substituted maleimides (RMI) with vinyl or methacrylic monomers. For example, poly(maleimide-co-2-ethylacrylic acid) shows curative effect on Lewis lung carcinoma [3].

There is a great interest in the investigation of copolymerization and obtaining maleimide copolymers of MMA with halogen-containing RMI [1, 2, 5–14]. It is known that on the basis of polymethylmethacrylate, the first industrial positive electron beam resistor was obtained. The sensitivity of the resistor depends on the type of the halogen atom and on the glass transition temperature (T_g) [1, 4].

Radical copolymerization of N-(4-bromophenyl) maleimide (BPMI) with MMA or 2-hydroxyethylmethacrylate (HEMA) in dioxane was investigated in [5, 6]. The structure of the methacrylate monomers affects the reactivity ratios of BPMI-MMA ($r_1 = 0.098$ and $r_2 = 1.610$) and BPMI-HEMA ($r_1 = 0.124$ and $r_2 = 1.823$). As it is shown in [5], there is a linear dependence of T_g with the increase of the number of maleimide links in the poly(N-4-bromophenylmaleimide-co-methylmethacrylate). A linear correlation was found between the T_g values and BPMI content of the copolymers.

Janovič reported results [7] of a study of the copolymerization of N-(2,4,6-tribromophenyl)maleimide (TBMI) with methylacrylate (MA) and MMA in toluene solution. The reactivity ratios were found to be $r_1 = 0.095$ and $r_2 = 2.17$ for the system TBMI-MA and $r_1 = 0.037$ and $r_2 = 4.32$ for the system TBMI-MMA. The copolymers show a considerable enhancement of the thermal stability and a raise in the glass transition temperature upon increasing TBMI content.

The copolymerization of MMA with N-chlorophenyl maleimide (CPMI) was investigated in a number of articles [8–10]. The results show higher reactivity ratio of MMA compared to maleimide comonomers and indicate a random copolymerization. Mishra *et al*. [10] evaluated the effect of incorporation of varying molar fraction of N-(2-, 3- or 4-chlorophenyl)maleimides in the poly(methyl methacrylate) backbone on the optical, physicomechanical and thermal properties of cast acrylic sheets.

Copolymers of N-(3- or 4-halogenophenyl)maleimides with ethyl and butyl methacrylates were synthesized by free-radical bulk polymerization [11–13]. The influence of UV radiation on the structure and on the thermal stability, chemical

* To whom all correspondence should be sent:
E-mail: konsulov@shu-bg.net

© 2009 Bulgarian Academy of Sciences, Union of Chemists in Bulgaria

resistance and on some physico-mechanical properties of the copolymers was studied [11].

In a number of articles [5–14] the effect of the type of halogen atom (Cl or Br) and its position (*o*-, *m*- or *p*-) in the phenyl ring of RMI on the values of reactivity ratios (r_1 and r_2) and on the properties of maleimide copolymers was discussed. This paper reports the influence of the structure of N-dichlorophenyl maleimides (2,3-, 2,4- and 2,6-Cl substituents in the phenyl ring) on the copolymerization with methyl methacrylate, the reactivity ratios and the properties of the random copolymers.

EXPERIMENTAL

Materials

The monomer methyl methacrylate (Fluka AG) was distilled at a temperature of 99–100ºC (MM = 100.12, ρ = 0.943 g/cm^3). The maleic anhydride (Merck) was purified from maleic acid by sublimation. The 2,3-, 2,4- and 2,6-dichloroanilines (Fluka AG) were purified by vacuum distillation. The 2,2′-azobisisobutyronitrile (AIBN) was recrystallized from ethanol (m.p. 103–104ºC). 1,4-dioxane (Fluka AG) was distilled over potassium hydroxide. All other reagents and solvents were of analytical purity grade (p.a.).

Synthesis and characterization of N-(dichlorophenyl)maleimides

N-Dichlorophenylmaleimides were prepared by reaction of maleic anhydride (MA) with 2,3-, 2,4-, and 2,6- chloroaniline, followed by cyclodehydration of the resulting maleamic acid.

Procedure for synthesis of N-(2,6-dichlorophenyl)maleimide. The maleimide monomer N-(2,6-dichlorophenyl)maleimide (2,6DCMI) was obtained from maleic anhydride (MA) and 2,6-dichloroaniline (DCA) according to the following two-step reaction procedure: 32.404 g (0.2 mol) DCA were dissolved in 40 ml of dry chloroform. The prepared solution was added to 19.612 g (0.2 mol) MA dissolved in 31 ml chloroform upon stirring continuously for 2 h in a glass reactor.

The obtained precipitate of N-(2,6-dichlorophenyl)maleamic acid was filtered, washed with chloroform, and dried. 26.4 g (0.1 mol) of the resulting product and 2.9 g of sodium acetate were dissolved in 40 ml of acetic anhydride and the mixture was heated at 90ºC for 1 hour. The cooled down reaction mixture was poured onto 800 ml of ice water. The precipitate was filtered and the product was purified by recrystallization in ethanol-water mixture. The obtained yield was 23.5 g (89.0%). The N-(2,6-dichlorophenyl)maleimide is a crystalline substance with melting point of 130–131ºC.

Analysis: Calculated for $C_{10}H_5O_2NCl_2$ (242.06): C, 49.61; H, 2.08; N, 5.79; Cl, 29.29 %. Found: C, 49.55; H, 2.06; N, 5.72; Cl, 29.15%.

The molecular structure and the molecular diagram of N-(2,6-dichlorophenyl)maleimide are presented in the scheme:

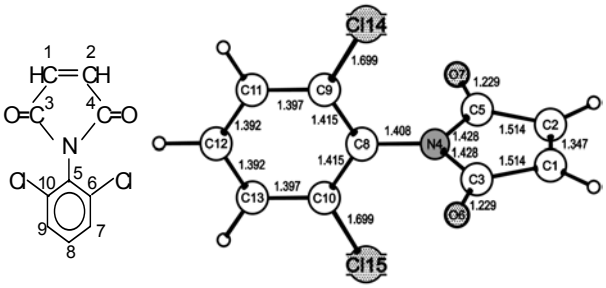

FT-IR: (cm^{-1}), 3097 and 3067 ($\nu_{=C-H}$), 1776, 1715 ($\nu^{s}_{C=O}$, $\nu^{as}_{C=O}$), 1642 ($\nu_{CH=CH}$), 1584, 1488, 1433 ($\nu_{C=C}$ Ar), 1392 (ν_{C-N} Ar), 1217 (ν_{C-O}),1155 (ν_{C-N-C} MI), 1055 (ν_{C-Cl}), 832($\gamma_{=C-H}$, *cis*-MI), 804 and 715 (1,2,3-substituted phenyl), 686 (carbonyl ring deformation).

^{1}H NMR ($CDCl_3$, TMS) δ, ppm: 7.43–7.28 (3H, Ar =C–H), 6.89 (2H, CH=CH).

^{13}C NMR($CDCl_3$) δ, ppm: 168.30 (C3, C4), 134.4 (C1, C2), Aromatic carbons:135.39 (C5), 131.16 (C6, C10), 128.51 (C7, C9) and 127.29 (C8).

The N-(2,3-dichlorophenyl)maleimide and N-(2,4-dichlorophenyl)maleimide were synthesized by a similar method.

Copolymerization

The copolymerization was performed as follows: a solution of DCMI, comonomer MMA and initiator AIBN in 1,4-dioxane as solvent were poured into a glass ampoule. The solution was degassed using dry nitrogen and the ampoule was immediately sealed and thermostated in an ultra-thermostat at 60 ± 0.1ºC. After the polymerization for a given time interval the glass ampoule was reopened and the viscous mixture was poured into ethanol. The obtained copolymers were purified twice by reprecipitation from acetone solution into ethanol. The polymers were filtered and dried in vacuum at 50ºC. The composition of the obtained copolymers was calculated by elemental analysis data of nitrogen or chlorine and by ^{1}H NMR spectra [9, 15].

Instrumental analysis

The IR spectra were recorded on a BOMEM Michelson 100 FTIR spectrometer using KBr pellets or on Specord 75 IR instrument using suspension in nujol or polymer films. The ^{1}H and ^{13}C NMR

spectra were recorded on a Bruker DRX-250 spectrometer in solution of $CDCl_3$ or DMSO-d_6. The thermogravimetric analysis (TGA) was carried out in air atmosphere at a heating rate of 10ºC/min by means of a Derivatograph OD-102/MOM. The viscosity was measured in DO (or DMF) at 25ºC by means of an Ubbellode viscosimeter VPG (d = 0.54 mm). The elemental analysis was carried out on a Carlo Erba analyzer. The melting points of the crystalline products (maleimides) were determined by the Kofler microscope.

RESULTS AND DISSCUSSION

Synthesis and characterization of N-dichlorophenyl maleimides

N-(Dichlorophenyl)maleimides were obtained from maleic anhydride and 2,3-, 2,4- or 2,6-dichloroaniline (DCA) *via* two-step reaction:

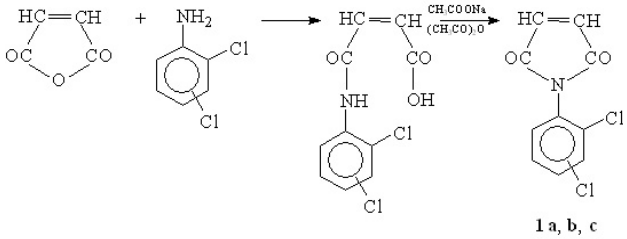

1 a, b, c

During the first stage in chloroform solution at 25ºC a reaction of N-acylation is taking place and the corresponding maleamic acid (MAA) is obtained. The MAA is light yellow sediment.

The reaction mixture of the obtained MAA with acetic anhydride was then treated with anhydrous sodium acetate and was heated up to 85–95ºC. The amount of sodium acetate (catalyst) affected the reaction rate. The optimal result was obtained in the presence of about 10% sodium acetate [16]. Under the above mentioned conditions, the MAA underwent cyclodehydration and the maleimide monomers **1a, b, c** were obtained as a result.

The obtained DCMI are white crystalline substances, soluble in chloroform, acetone, dioxane, dimethylformamide. The experimental results are summarized in Table 1.

Table 1. Yield and characteristics of N-dichlorophenyl maleimides (2,3-, 2,4- and 2,6-DCMI).

Sample	DCMI	Yield, %	Elemental analysis*, %				m.p., ºC
			C	H	N	Cl	
1a	2,3-DCMI	87.6	49.52	2.03	5.69	29.10	94–95
1b	2,4-DCMI	90.4	49.53	2.04	5.70	29.12	106–107
1c	2,6-DCMI	89.0	49.55	2.06	5.72	29.15	130–131
*Theoretical for $C_{10}H_5O_2NCl_2$			49.61	2.08	5.79	29.29	

Synthesis and characterization of copolymers of N-dichlorophenyl maleimides with methyl methacrylate

The copolymerization of N-dichlorophenyl maleimides (**1a, b, c**) with methyl methacrylate was carried out at 60ºC in dioxane in the presence of 0.75% AIBN as initiator according to the following scheme:

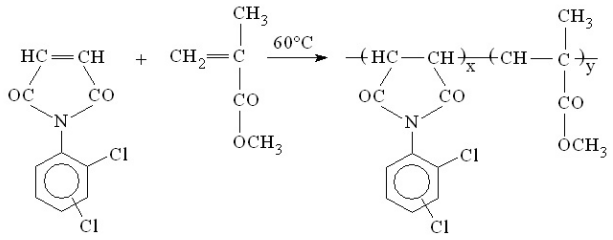

1 a, b, c **2 a, b, c**

Under these conditions the polymerization proceeded *via* chain-radical mechanism in homogeneous medium. The copolymers were isolated through precipitation of the polymer solution in ethanol and were purified by double precipitation from acetone in ethanol/water or diethyl ether. The obtained maleimide copolymers of MMA are white powder-like substances, soluble in organic solvents such as dioxane, acetone, chloroform, dichloroethane, etc. The experimental results are shown in Table 2.

Table 2. Copolymerization of N-dichlorophenyl maleimides (M_1) with methyl methacrylate (M_2) at monomer ratio of 50:50 mol.% (C_m = 1.1 mol/l, 60ºC, 5 h).

Copolymer sample	M_1	Yield, %	Elemental analysis, %		Copolymer composition, mol.%		[η]*, dl/g
			N	Cl	M_1	M_2	
2 a	2,3-DCMI	71.6	2.65	13.25	25.9	74.1	0.45
2 b	2,4-DCMI	69.8	2.38	12.04	22.4	77.6	0.48
2 c	2,6-DCMI	77.5	1.74	8.72	15.1	84.9	0.42

* η determined in DMF at 25ºC (d_k = 0.54 mm, Ubbelode).

The structure of the copolymers was proved by ^1H and ^{13}C NMR as well as by IR-spectroscopy. In the IR-spectrum of poly(N-2,3-dichlorophenylmaleimide-co-methyl methacrylate) film the maleimide units were identified by the bands at 1782, 1705 (broad, intensive), 1580, 1430, 980, 830, and 740 cm^{-1}. Characteristic of MMA monomer units are the IR bands at 2960 cm^{-1} ($–CH_2–$) and at 1460 and 1380 cm^{-1} due to asymmetric and symmetric bending vibrations of the $–CH_3$ and $–OCH_3$ bonds. The broad and intensive band at 1280–1120 cm^{-1} is assigned to the stretching vibrations ($\nu_{C–O}$) of MMA units.

In the ^1H NMR spectrum of poly(N-2,4-dichlorophenylmaleimide-co-methyl methacrylate) the

presence of maleimide monomeric units was proved by the resonance signals at 7.76, 7.51, and 7.32 ppm for the aromatic protons. The signals between 3.64–3.72 ppm were assigned to the protons of the $–OCH_3$ group in MMA units, while the triplet centered at 1.21 ppm was attributed to the protons of the $–CH_3$ groups. To the protons of $–CH_2–$ were assigned signals at 1.71–2.15 ppm, and the signals of methyne protons –CH– appeared at 2.86 and 2.94 ppm.

The ^{13}C NMR spectrum of the poly(N-2,6-dichlorophenylmaleimide-co-metyl methacrylate) containing 39.5 mol% maleimide units is shown in Fig. 1. The signals at 175.3–177.8 ppm characterize the maleimide carbonyl groups, these at 173.2–174.2 ppm – the ester carbonyl groups. The carbon atoms in the aromatic ring give resonance signals at 127.9, 128.6, 131.3, 134.1, 134.3, and 134.6 ppm. The MMA-units are characterized by: 15.0–19.1 ppm α-methyl groups; 51.8–55.7 ppm $–OCH_3$ ester groups.

The copolymer compositions were determined by elemental analysis (Table 2) and by ^1H NMR [9, 15], based on the intensity of the aromatic protons signals (3H, at about 7.32–7.76 ppm) from maleimides and the intensity of MMA proton signal (3H, at about 3.64–3.72 ppm). The mole fraction of DCMI (m_1) in the copolymers was calculated according to the following equation:

$$m_1 = \frac{I_1}{(I_1 + I_2)}, \qquad (1)$$

where I_1 and I_2 represent the integrated area intensities of the aromatic protons in DCMI and of the methoxy protons in MMA respectively. These results were correlated with experimental data for the copolymer composition, obtained by elemental analysis (Table 3).

Reactivity ratios. Effect of the molecular structure of N-dichlorophenylmaleimides

To determine the reactivity ratios of the monomers r_1 (2,3-, 2,4-, or 2,6-DCPMI) and r_2 (MMA) the copolymerization of the comonomers with a conversion degree up to 15–20 % has been studied. Some of the obtained results are represented in Table 3.

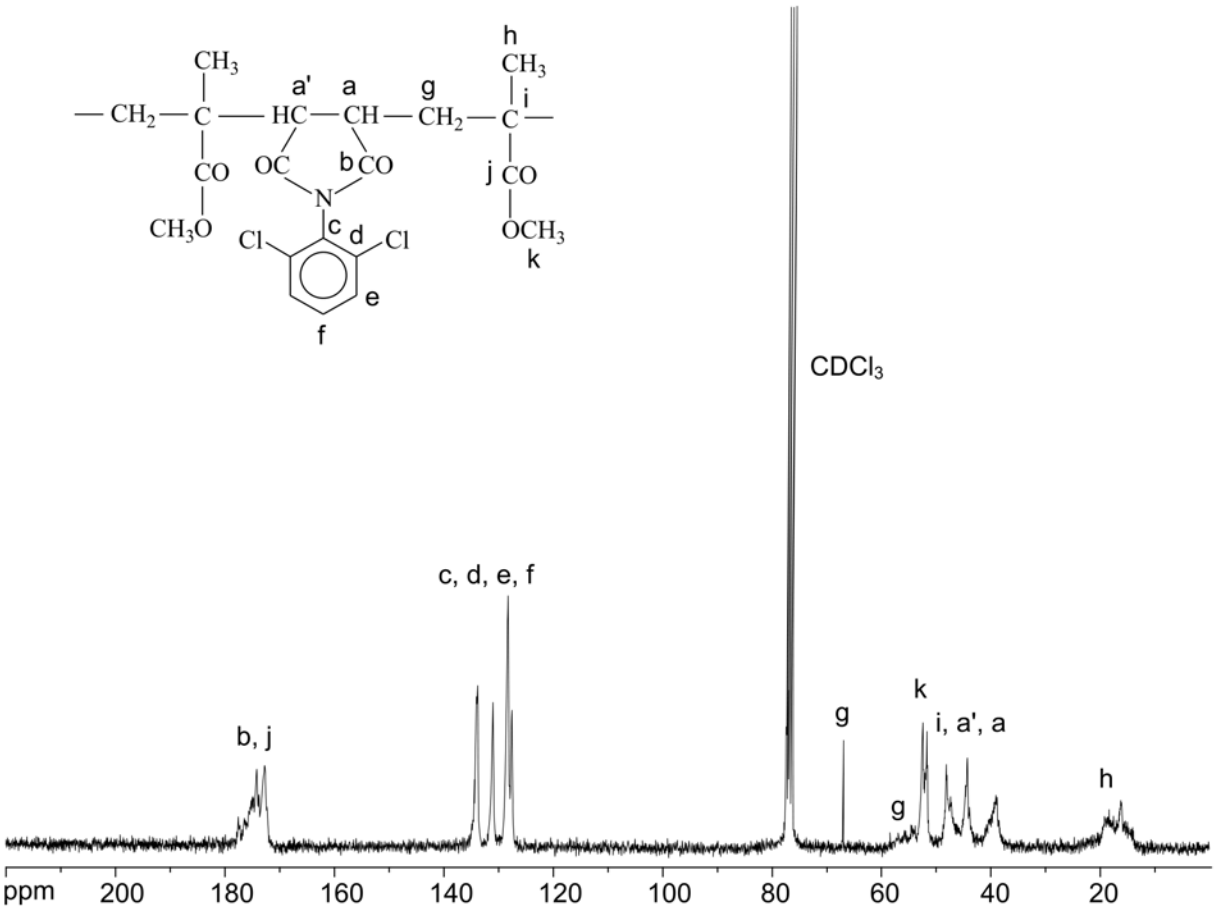

Fig. 1. ^{13}C NMR spectrum of poly[(N-2,6-dichlorophenyl) maleimide-co-methyl methacrylate] containing 39.5 mol.% N-(2,6-dichlorophenyl)maleimide.

Table 3. Copolymerization of N-dichlorophenylmaleimides (M_1) with methyl methacrylate (M_2) in dioxane solution at different monomer feed ratios (C_M = 1.0 mol/l, T = 60ºC).

Sample number	DCMI (M_1) in monomer feed		Conversion, %	Polymerization rate, R_p %/min	Fraction of DCMI (M_1) in copolymer (mol.%)		[η]*
		mol. %			N	^{1}H NMR	dl/g
1	2,3-DCMI	20.0	15.4	0.15	9.9	9.6	0.32
2		50.0	17.5	0.18	27.4	27.9	0.23
3		79.8	15.7	0.14	54.1	54.6	0.18
4	2,4-DCMI	20.5	17.1	0.12	9.5	9.3	0.29
5		50.0	18.0	0.13	26.5	26.6	0.24
6		79.8	16.8	0.11	48.5	48.9	0.11
7	2,6-DCMI	20.0	16.5	0.13	9.3	9.2	0.25
8		48.7	18.9	0.23	14.7	14.8	0.21
9		79.8	15.4	0.10	39.5	40.0	0.20

*η determined in 1,4-Dioxane at 25ºC (d_k = 0.54 mm, Ubbelode).

The experimental data showed that the copolymerization rate (R_p) depends only slightly on the content of DCMI in the monomer feed. A weak kinetic maximum, shifted from the equimolar composition, was observed at higher MMA content (66–75 mol.%). This is characteristic of monomer systems with weak electron donor or electron acceptor interactions [1, 7, 16].

The monomer reactivity ratios for the copolymerization of DCMI with MMA were determined based on the monomer feed ratios and the copolymer composition by Kelen-Tüdös (KT) method [17–18]. The dependence of the obtained copolymer composition (m_2) upon monomer feed composition (M_2 = MMA) according to experimental data from three series of experiments is represented in Fig. 2. The dependence curves show that the copolymerization of all the three monomer pairs lead to obtaining random copolymers. In the resulting copolymers the number of MMA units prevails over the maleimide units (see also Table 2).

The r_2 values for MMA are higher ($r_2 > 1$) than the r_1 values for the maleimides ($r_1 << 1$) for the three monomer systems (Table 4). The connection between the structure of the monomer and its reactivity in free-radical reactions is controlled by resonance, polar and steric factors. The Q-e scheme gives a quantitative evaluation of the role of resonance and polar effects. The Q_1 and e_1 values of N-(2,3-, 2,4- and 2,6-dichlorophenyl)maleimides were calculated using the Alfrey-Price Q-e scheme [19, 21] based on the reactivity ratios:

$$e_1 = e_2 \pm (-\ln r_1 . r_2)^{0.5} \quad (2)$$

$$Q_1 = \frac{Q_2}{r_2} \exp[-e_2(e_2 - e_1)] \quad (3)$$

Values of Q_2 = 0.74 and e_2 = 0.40 for MMA were used for this purpose according to the literature data [7, 15].

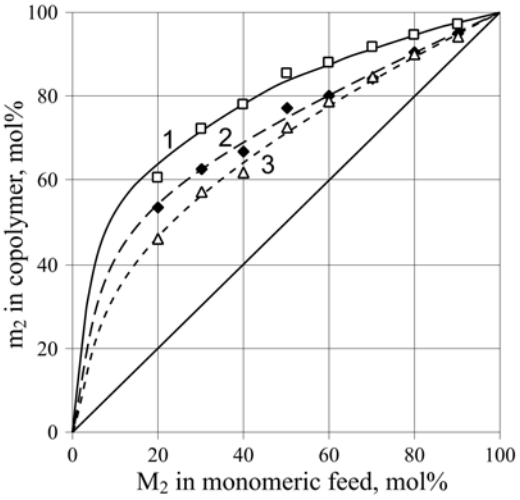

Fig. 2. Monomer-copolymer composition curves for the copolymerization of methyl metacrilate (M_2) with M_1: N-(2,6-dichlorophenyl)maleimide (curve 1), N-(2,4-dichlorophenyl)maleimide (curve 2) or N-(2,3-dichlorophenyl)maleimide (curve 3).

Table 4. Monomer reactivity ratios r_1, r_2 and Q–e values for copolymerization of N-dichlorophenyl maleimides (M_1) with methyl methacrylate (M_2).

M_1	r_1	r_2	$1/r_1$	$1/r_2$	$r_1.r_2$	Q_1	e_1
2,3-DCMI	0.16 ± 0.02	1.97 ± 0.08	6.2	0.51	0.315	0.58	1.47
2,4-DCMI	0.09 ± 0.03	2.23 ± 0.11	11.1	0.45	0.200	0.55	1.65
2,6-DCMI	0.04 ± 0.01	4.19 ± 0.09	25.6	0.24	0.168	0.30	1,75

The resonance effect influences the reactivity of the monomer and its radical. The conjugation in the MMA molecule determines the high reactivity of the monomer, while the activity of its radical is lower. Although MMA is 1,1-disubstituted monomer, the steric factor does not affect its polymerization ability [19]. One can conclude in view of the *r*-values that the reactivity of the N-dichlorophenyl maleimides decreases, when the second Cl-atom is located at a greater distance from the first one (at *ortho*-position in the aromatic ring). The reactivity ratios decrease in the following order: 2,3-DCMI > 2,4-DCMI > 2,6-DCMI. A possible explanation of these observations could be connected with the influence of the induction effect (I-effect > M-effect for Cl-atom) on the electron acceptor properties of the functional –CH=CH– group of the maleimide ring resulting in a decrease of the donor-acceptor interactions with the weak donor monomer MMA [7]. The 2,6-DCMI is about 25 times more active with respect to MMA radical in the reaction

of cross propagation. ($1/r_1 = k_{12}/k_{11} \sim 25$). The ortho steric effect has a weaker influence on 2,3- and 2,4-DCMI as they have asymmetric structure. These monomers are about 6 and 11 times more active to MMA-radical, respectively.

The reactivity ratios show that the two macroradicals in the examined systems have higher activity to methacrylic monomer and the obtained copolymers are enriched in MMA-units. The MMA has high polymerization activity in the reaction of homo and cross propagation [7, 11]. The reaction of homopropagation occurs at higher rate ($k_{22} > k_{21}$) and as a result in the polymer chain the number of consecutive MMA units alternate ($r_1.r_2 < 1$) the maleimide link or diads [5, 6, 11]. Therefore, the distribution of the monomeric links and the design of the macromolecules of the three copolymers of MMA with 2,3-, 2,4-, and 2,6- DCMI would differ. They would depend also on the monomer ratio DCMI/MMA, at which the maleimide copolymer is obtained (see Table 3, Fig. 2).

Copolymer microstructure

The microstructure in the resulting copolymers was determined using the monomer reactivity ratios. The placement probabilities P_{11}, P_{12}, P_{21} and P_{22} and the mean sequences length μ_1 (DCMI) and μ_2 (MMA) were calculated using the equations in references [21, 22]. The values of P_{11}, P_{12}, P_{21}, P_{22}, μ_1 and μ_2 are represented in Table 5.

Table 5. Data for the structure of copolymers of N-dichlorophenylmaleimide (M_1) with metylmethacrylate (M_2).

Type of DCMI	Sample	P_{11}	P_{12}	P_{21}	P_{22}	Mean sequence lenght	
						μ_1	μ_2
2,3-DCMI	1	0.0385	0.9615	0.1126	0.8874	1.04	8.89
	2	0.1379	0.8621	0.3367	0.6633	1.16	2.97
	3	0.3872	0.6128	0.6672	0.3328	1.63	1.50
2,4-DCMI	4	0.0227	0.9773	0.1037	0.8963	1.02	9.65
	5	0.0825	0.9174	0.3300	0.6700	1.09	3.23
	6	0.2627	0.7373	0.6394	0.3606	1.36	1.56
2,6-DCMI	7	0.0099	0.9901	0.0563	0.9437	1.01	17.76
	8	0.0366	0.9634	0.1847	0.8153	1.04	5.19
	9	0.1365	0.8635	0.4853	0.5147	1.16	2.06

The obtained data show that the probability of formation of maleimide diads (P_{11}) is low and it depends on the mole fraction DCMI in the monomer feed. The mean sequence length μ_1 values increase from 1.04 to 1.63 in the 2,3-DCMI/MMA system, from 1.02 to 1.36 in the 2,4-DCMI/MMA system and from 1.01 to 1.16 in the 2,6-DCMI/MMA system. The P_{21} values are higher than P_{11} and increase with the concentration of maleimide monomers. For all studied comonomer ratios the probabilities P_{12} and P_{22} are higher than P_{11} and P_{21}. This implies that in maleimide copolymers, diads, triads and even much longer sequences of MMA units are formed. The μ_2 values increase from 1.50 to 8.9 in the 2,3-DCMI/MMA system; from 1.56 to 9.65 in the 2,4-DCMI/MMA system and from 2.06 to 17.76 in the 2,6-DCMI/MMA system.

Thermostability of the copolymers of DCMI with MMA

The thermal properties of copolymers DCMI with MMA were determined by TGA in static air atmosphere. Data at the temperature of the initial weight loss [5, 7, 12] of a sample (T_I), the temperature at 50% weight loss (T_{50}), the temperature of maximum decomposition rate (T_{max}) and final decomposition temperature (T_f), as well as the percentage of the weight loss of the samples at 350ºC and 500ºC are summarized in Table 6 and shown in Figure 3.

Table 6. Thermal properties of copolymers of N-(dichlorophenyl)maleimides with metylmethacrylate (heating rate 7ºC/min in static air atmosphere).

Copolymer sample	T_I,	T_{50},	T_{max},	T_f,	Percentage weight loss at		Residue at T_f,
	ºC	ºC	ºC	ºC	350ºC	500ºC	%
1	316	373	378	530	28	93	7
4	320	365	370	500	33	99	1
7	325	375	380	520	16	98	2

The copolymer samples were stable up to 316ºC for 2,3-DCMI-MMA, up to 320ºC for 2,4-DCMI-MMA and up to 328ºC for 2,6-DCMI-MMA. All the samples showed a single step decomposition in the temperature region 280–420ºC, which corresponds to random main chain scission of MMA-MMA links (335–427ºC) of PMMA. The maximum values of the weight loss (decomposition) are at about 370–380ºC. In the case of 2,3-DCMI-MMA copolymer, the weight loss up to 350ºC was 28%, that of 2,4-DCMI-MMA – 33%, and that of 2,6-DCMI-MMA – 16%. The percentage of char yield increased upon increasing DCMI content in the maleimide copolymers.

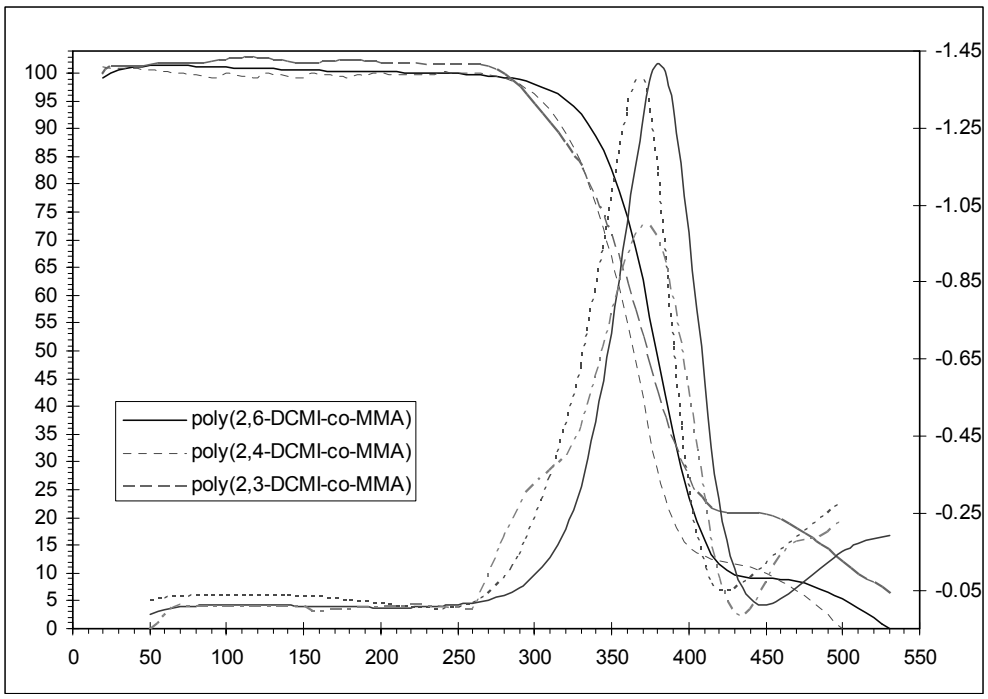

Fig. 3. TG and DTG trace of poly(2,6-DCMI-co-MMA), poly(2,4-DCMI-co-MMA) and poly(2,3-DCMI-co-MMA) in air atmosphere (heating rate 10ºC/min).

CONCLUSIONS

By the radical copolymerization of N-(2,3-dichlorophenyl)maleimide, N-(2,4-dichlorophenyl) maleimide, and N-(2,6-dichlorophenyl)maleimide with methyl methacrylate random maleimide copolymers have been obtained. The monomer reactivity ratios of N-dichlorophenylmaleimides r_1 (0.18, 0.09 and 0.04 for 2,3-, 2,4-, and 2,6- DCMI respectively) revealed the effect of molecular structure of N-substituted maleimides on their copolymerization with methyl methacrylate and on the properties of the obtained maleimide copolymers. The thermostability of the studied maleimide copolymers was about 80–90ºC higher compared to polymethylmethacrylate. The role of the position of Cl-atoms in the phenyl ring of N-dichlorophenylmaleimides for the thermal properties of the copolymers was insignificant. Their thermostability increased with the molar fraction of N-dichlorophenyl maleimide units in the macromolecules.

REFERENCES

1. V. B. Konsulov, in: Polymeric Materials Encyclopedia: Maleimide copolymers (N-substituted), vol. 6, J. C. Salamone (Ed.), CRC Press Boca Raton, New York, 1996, p.3996.
2. Tz. Godjevargova, R. Nenkova, V. Konsulov, *J. Mol. Catal. B: Enzym.*, **38**, 59 (2006).
3. Z. Zhu, L. Shi, J. Huang, *Bioorg. Med. Chem. Lett.,* **12**, 2843 (2002).
4. B. M. Gong, J. C. W. Chien, *J. Polym. Sci. Part A: Polym. Chem.*, **27**, 1149 (1989).
5. J. Borbely, T. Kelen, V. Konsulov, Z. Grozeva, *Polymer Bull.*, **26**, 253 (1991).
6. V. Konsulov, Z. Grozeva, *Bulg. Chem. Commun.*, **31**, 38 (1999).
7. Z. Janovič, T. Matusinovič, F. Ranogajec, *Makromol. Chem.*, **194**, 1915 (1993).
8. A. Kumar, *J. Macromol. Sci.*, **A24**, 711 (1987).
9. V. Choudhary, A. Mishra, *J. Appl. Polym. Sci.*, **62**, 707 (1996).
10. A. Mishra, T. J. M. Sinha, V. Choudhary, *J. Appl. Polym. Sci.*, **68**, 527 (1998).
11. A. Ryttel, *J. Appl. Polym. Sci.*, **74**, 2924 (1999).
12. A. Ryttel, *J. Appl. Polym. Sci.*, **81**, 3244 (2001).
13. H. Naguib, G. Saad, M. Elsabeé, *Polym. Int.*, **52**, 1217 (2003).
14. V. Konsulov, Z. Grozeva, T. Kelen, J. Borbély, *Makromol. Chem.*, **193**, 847 (1992).
15. A. O. Kress, L. J. Mathias, G. Cei, *Macromolecules*, **22**, 537 (1989).
16. C. P. Yang, S. S. Wang, *J. Polym. Sci. Part A: Polym. Chem.*, **27**, 15 (1989).
17. T. Kelen, F. Tűdös, *J. Macromol. Sci.-Chem.*, **A9**, 1 (1975).
18. T. Kelen, F. Tűdös, B.Turcsanyi, *Polym. Bull.*, **2**, 71 (1980).
19. G. E. Ham (ed) in: Copolymerization, Khimia, Moscow, 1971, pp. 65–81.
20. G. S. Georgiev, V. P. Zubov, *Eur. Polym. J.*, **14**, 93 (1978).
21. S. Morariu, C. Hulubei, *High Perform. Polym.*, **18**, 185 (2006).
22. V. Konsulov, D. Dyakova, A. Lyapova, Z. Grozeva, *Bulg. Chem. Commun.*, **39**, 72 (2007).

ИЗСЛЕДВАНЕ НА СЪПОЛИМЕРИЗАЦИЯТА НА N-(ДИХЛОРОФЕНИЛ)МАЛЕИМИДИ С МЕТИЛМЕТАКРИЛАТ

В. Б. Консулов*, З. С. Грозева, Й. И. Тачева, К. Д. Тачев

Факултет по природни науки, Шуменски университет „Епископ Константин Преславски“, Ул. „Университетска“ № 115, 9712 Шумен

Постъпила на 27 ноември 2007 г.; Преработена на 22 май 2008 г.

N-(2,3-дихлорофенил)малеимид (2,3-ДХМИ), N-(2,4-дихлорофенил)малеимид (2,4-ДХМИ), N-(2,6-дихлорофенил)малеимид (2,6-ДХМИ) са синтезирани чрез взаимодействие на малеинов анхидрид с 2,3-, 2,4- или 2,6-дихлороанилин в два стадия. Съполимеризацията на 2,3-, 2,4- и 2,6-ДХМИ (M_1) с метилметакрилат (ММА-M_2) е проведена в 1,4-диоксан (ДО) в присъствие на α,α'-азобисизобутиронитрил като инициатор при 60°C. Определени са константите на съполимеризация и Q–e стойностите: $r_1 = 0.16$, $r_2 = 1.97$, $Q = 0.58$, $e = 1.47$ за 2,3-ДХМИ-ММА; $r_1 = 0.09$, $r_2 = 2.23$, $Q = 0.55$, $e = 1.65$ за 2,4-ДХМИ-ММА; $r_1 = 0.04$, $r_2 = 4.19$, $Q = 0.30$, $e = 1.75$ за 2,6-ДХМИ-ММА. Термостабилността на получените малеимидни съполимери е изследвана чрез термогравиметричен анализ. Дискутира се влиянието на молекулната структура на 2,3-, 2,4- и 2,6-ДХМИ върху съполимеризацията им с ММА и свойствата на получените съполимери.

Bulgarian Chemical Communications, Volume 41, Number 1 (pp. 39–45) 2009

Investigation of the processes and mechanism of electrodeposition of copper from ammonium nitrate electrolyte by the method of cyclic voltamperometry

L. N. Petkov*, K. N. Ignatova

University of Chemical Technology and Metallurgy, 8 Kliment Ohridski Blvd., Sofia 1756, Bulgaria

Received March 21, 2008; Revised April 23, 2008

This article reports results, obtained by the method of cyclic voltamperometry, applied to study the processes and mechanism of deposition of copper from ammonium nitrate electrolyte. The effect of the initial potential has been studied as well as that of the potential sweeping rate and the nature of the cathode substrate (copper or silver) in regard to the course of the voltamperograms. It has been established that the deposition of copper on a copper substrate is proceeding via two-step mechanism, whereupon the elemental copper is obtained by reduction of cuprous ammonium ions. Upon applying the diagnosis criteria of the method it was confirmed that the mechanism corresponds to the Electrochemical-Chemical-Electrochemical (EChE) type i.e. two consecutive reversible electrochemical steps (cupric/cuprous ammonium complexes and cuprous ammonium complexes/elemental copper), with an intermediate chemical step of copper disproportionation. In case of silver substrate, only the mechanism of the anodic process is relatively the same. The ascertained difference in the mechanisms of copper deposition is very important for the combined deposition of copper and silver and for obtaining Ag-Cu alloyed coating, taking into account the fact that silver is the more electropositive metal in the system. The obtained results are an essential part of an extensive study, connected with preparing an alloyed finely dispersed Ag-Cu powder under stationary conditions and in impulse potentiostatic regime.

Keywords: Cu powder, cyclic voltamperometry, ammonium nitrate electrolyte.

INTRODUCTION

The electrolysis is a method, enabling to prepare directly alloyed metal powders of high purity and compositions varying within wide limits [1–3]. The applying of an impulse potentiostatic regime enriches considerably the options in this respect. In this case the investigation of the mechanism of the processes of separate deposition of the metals in detail is extremely important, as upon applying a potentiostatic impulse there is a continuous transition from zero to very high values of the overpotential. All the steps of the mechanism of the occurring processes are reflected on the quality of the final product [2–5].

The alloyed Ag–Cu powders are valuable in view of their electroconductivity and thermal conductivity properties. They are used mainly for improving the electroconductivity of contacts in the electronics and also for components of pastes for depositing on metal surfaces before their soldering [6, 7]. Nevertheless data on the conditions of deposition are scarce. Our preliminary work [8] concerns alloyed Ag-Cu powders.

After studying a series of electrolytes the ammonium electrolyte for copper deposition became of fundamental interest, taking into account the fact that the copper in it is available in two different soluble forms: the cupric Cu^{2+} and cuprous Cu^{+} ammonium complexes. However only a few articles [9 – 12] are devoted to this system. Some of them investigate the influence of pH and that of some anions like Cl^- [9–11] or NO_3^- [10] at very low concentrations of the copper. These are focused on the mechanism of formation of nuclei of copper crystals. It has been shown that the NO_3^- ions can dissolve partially the growing copper crystal nuclei. Another investigation points out that the NO_3^- ions (e.g. originating from NH_4NO_3) not only promote the electroconductivity of the solution but they can also adsorb on the electrode surface thus facilitating the electrodeposition of copper ions. In most of the studies the copper is introduced in the form of $CuSO_4$ [13–19]. The most detailed data on the mechanism of electrodeposition are represented in the article [12], where the application of the method of cyclic chronovoltamperometry is combined with physical methods and a specific mechanism of copper deposition is proposed for the various pH regions (pH = 4, 6 and 8).

The complete analysis of the literature data imposes the conclusion that the ammonium electrolyte with an additive of ammonium nitrate is

* To whom all correspondence should be sent:
E-mail: l.petkovv@abv.bg

© 2009 Bulgarian Academy of Sciences, Union of Chemists in Bulgaria

especially appropriate for the combined deposition of copper and silver in the form of alloyed coating or powder, especially when ammonia is in moderate excess (pH about 8.5–9). In all the other electrolytes: sulfuric acid [12], pyrophosphate [20], fluoroborate [21], trionate [22], alkaline [23], etc. the silver forms hardly soluble compounds and the electrolytes on their basis are unstable.

On the basis of the above arguments a composition of the electrolyte was chosen, in which the copper is in the form of $Cu(NO_3)_2$ and its concentration was varied from 2.5 to 10 g·dm^{-3}, whereupon ammonia is added to obtain pH = 8.5–9. The method of cyclic voltamperometry was applied to electrodes of copper and silver in view of the purpose of this study. The method is especially suitable for complex systems such as those, in which there is a two-step transfer of electrons and ions of changing valence, which form complexes completely different in stability. The elaborated diagnosis criteria of the method [24–26] allow a strict and detailed evaluation of the occurring processes. These criteria originate from the basic equations of the method. They represent the dependences of the deviation of the cathode potential E_p^c, the relationship between the currents, corresponding to the anode and cathode maxima (I_p^a/I_p^c), as well as the ratio of the cathode current in the position of the peak and the square of the rate of sweeping the potential v. It is obvious that depending on the specific mechanism of the process, for which the above parameters have been calculated, the values will be quite different.

EXPERIMENTAL

The electrolyte, in which the studies have been carried out, has the composition: 2.5 g·dm^{-3} Cu (in the form of $Cu(NO_3)_2$); 40 g·dm^{-3} NH_4NO_3 solution and 25% NH_3 solution to obtain pH = 8.5–9. The salts are both added consecutively to the water and as they are both well soluble in water, there are no substantial peculiarities in this step of solution preparation. There follows a gradual addition of ammonia, whereupon the solution becomes dark at pH = 7–8. The addition of ammonia to reach pH = 8.5 and further pH = 9 makes the solution trans-parent, blue-colored, which is an indication of the formation of cupric ammonia complex $[Cu(NH_3)_4]^{2+}$ [27].

The measurements have been carried out in a three-electrode cell with working electrodes, made of copper (99.97%) and silver (96.97%), in the form of disks with working area 1 cm^2. Platinum net was used as anode, while the reference electrode was saturated calomel electrode (SCE).

The cyclic chronovoltamperograms have been recorded by means of potentio-scanner of the type "Wenking" (Germany) in the range of potentials 0.450 V ÷ –0.800 V (*versus* SCE). The polarization was always carried out starting from the chosen initial potential and moving towards more negative potentials. The curves, which are represented in the figures in this article, have been obtained after several cycles (4 to 5 cycles). The sweeping rate of the potential was varied in the range from 10 to 150 mV·s^{-1}. The rate, at which the peculiarities of the mechanism of copper deposition are best demonstrated, was found to be v = 20 mV·s^{-1}.

RESULTS AND DISCUSSION

Values of the potentials of the electrochemical reactions

In order to facilitate the analysis of the results all the basic reactions, which could possibly occur in the working electrolyte, as well as their standard potentials versus NHE, are represented in Table 1. The table lists also the calculated values of the reversible potentials in the reactions with respect to SCE [27].

An assumption has been made, during the calculation of the potentials of the reactions (1) and (3), that the copper disproportionation reaction is occurring according to the following equations:

$$Cu + [Cu(NH_3)_4]^{2+} = 2[Cu(NH_3)]^{+} + 2NH_3 \quad (a)$$

$$2[Cu(NH_3)]^{+} + 2NH_3 = 2[Cu(NH_3)_2]^{+} \quad (b)$$

$$Cu + [Cu(NH_3)_4]^{2+} = 2[Cu(NH_3)_2]^{+} + 2NH_3$$

Another assumption is that the constant of disproportionation, in accordance with the literature data [28], is equal to:

$$K = \frac{\left[Cu(NH_3)_2^{+}\right]^2}{\left[Cu(NH_3)_4\right]^{2+}} = 6.04.10^{-7} \quad (7)$$

During the calculations it has been accepted for the concentration of $[Cu(NH_3)_4]^{2+}$ that the free cupric ions are entirely bonded in an ammonia complex i.e. it is 2.5 g·dm^{-3} (or 0.0393 M).

Cyclic voltamperometry of copper–ammonium nitrate electrolyte

Voltamperograms on copper electrode. Figure 1 represents the voltamperogramme of copper-ammonium nitrate electrolyte in the interval of potentials from E_i = –0.200 V to E_c = –0.750 V.

Table 1: Standard potentials of the basic reactions in ammonium nitrate electrolyte for the deposition of copper (E_0) with respect to SVE, as well as the values of the potential of these reactions (E) in regard to RCE, recalculated on the basis of the equation of Nernst.

No.	Reaction	E°, V [NHE]	E_{calc}, V [SCE]
(1)	$[Cu(NH_3)_4]^{2+} + e^- = [Cu(NH_3)_2]^+ + 2NH_3$	–0.010	–0.115
(2)	$Cu + [Cu(NH_3)_4]^{2+} = 2[Cu(NH_3)_2]^+ + 2NH_3$ Copper disproportionation reaction		
(3)	$[Cu(NH_3)_4]^{2+} + 2e^- = Cu + 4NH_3$	–0.050	–0.334
(4)	$[Cu(NH_3)_2]^+ + e^- = Cu + 2NH_3$	–0.120	–0.586
(5)	$NO_3^- + 5H_2O + 6e^- = NH_2OH + 7\ OH^-$	–0.300	–0.085
(6)	$[Ag(NH_3)_2]+ + e^- = Ag + 2NH_3$ (for $C_{Cu} = 2.5\ g{\cdot}dm^{-3}$ and $C_{Ag} = 2.5\ g{\cdot}dm^{-3}$)	0.373	0.034

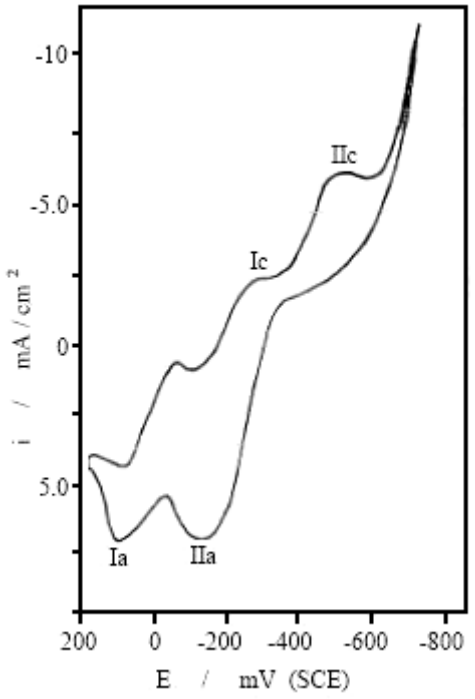

Fig. 1. Voltamperogramme of copper-ammonia nitrate electrolyte on copper electrode; 2.5 $g{\cdot}dm^{-3}$ Cu in the form of $Cu(NO_3)_2$, (40 $g{\cdot}dm^{-3}$ NH_4NO_3 and 25% NH_3 until pH = 9 is reached); E_i = +0.200 V, E_c = –0.750 V, $v = 20\ mV{\cdot}s^{-1}$.

As it can be seen from the figure two consecutive cathode peaks are observed on the voltamperogramme – Ic and IIc and their corresponding anode peaks IIa and Ia. The first cathode peak, as it follows from the data represented in Table 1, is associated with the reduction of cupric ammonium ions $[Cu(NH_3)_4]^{2+}$ into cuprous ammonium ions $[Cu(NH_3)_2]^+$ in accordance with the stoichiometric Eqn. (1):

$$[Cu(NH_3)_4]^{2+} + e^- = [Cu(NH_3)_2]^+ + 2NH_3 \quad (1)$$

As our visual observations in this field of potentials show, no elemental copper has been deposited. When the equilibrium concentration is reached, the obtained cuprous ammonium ions $[Cu(NH_3)_2]^+$ are immediately involved in the reaction of disproportionation (2), which in this case is the following:

$$[Cu(NH_3)_4]^{2+} = 2[Cu(NH_3)_2]^+ + 2NH_3 \quad (2)$$

This reaction does not lead to a peak in the current, but it rather contributes to the preservation of the current intensity value on a certain level. In the region of the second cathode peak IIc the cupric ammonium ions $[Cu(NH_3)_4]^{2+}$ are reduced to elemental copper following the stoichiometric equation (3):

$$[Cu(NH_3)_4]^{2+} + 2e^- = Cu + 4NH_3 \quad (3)$$

It is not probable that the deposition of elemental copper could occur via reduction of cuprous ammonium complexes $[Cu(NH_3)_2]^+$ in the studied electrolyte, containing a sufficient surplus of ammonia, which forms stable complexes with the divalent copper ions. In fact the calculations, which we performed (Table 1), point to the fact that this reaction is possible, but it occurs at higher cathodic potentials, compared to reaction (3).

As it follows from Figure 1 the first anodic peak (in the order of appearance upon returning the curve to the initial potential) IIa appears at about –0.150 V (SCE) and it is weakly dependent on the sweeping rate of the potential. It is connected with oxidation of the deposited copper coating via the reaction:

$$Cu + 4NH_3 = [Cu(NH_3)_4]^{2+} + 2e^- \quad (4)$$

In the next step the cupric ammonia ions $[Cu(NH_3)_4]^{2+}$, located most closely to the electrode, are reduced chemically *via* reaction (2) to cuprous ammonia ions (the reaction of disproportionation).

The second anodic peak Ia appears at about 0.100 V (CE) and it is connected with the soluble forms of the copper in solution, i.e. with the reaction of oxidation of the cuprous ammonia complexes into cupric ammonia complexes, described by the stoichiometric equation:

$$[Cu(NH_3)_2]^+ + 2NH_3 = [Cu(NH_3)_4]^{2+} + e^- \quad (5)$$

Fig. 2 (a–c) shows three cyclic voltamperometric dependences in an electrolyte of composition 2.5 g·dm^{-3} Cu; 40 g·dm^{-3} NH_4NO_3; NH_3 (until pH = 8.5 is reached) on copper electrode at three different values of the initial potential: 0.000, 0.100, 0.200 V. The course of the curves is an indication that the variation of the initial potential in the studied interval does not change substantially the mechanism of the entire process.

Voltamperogrammes on silver electrode. A weak initial cathodic peak is observed in the voltamperogrammes, taken with a silver electrode in an electrolyte, containing in advance cupric ammonia ions $[Cu(NH_3)_4]^{2+}$ (Fig. 3), at more positive potentials and a stretching plateau at the more negative potentials (–0.100 V). In this case, no stepwise deposition of copper is observed, as in the case with copper electrode. It is not possible that the reaction of disproportionation of the copper can occur on a silver electrode and it has been demonstrated above that it is exactly this reaction that lies in the basis of the two-step copper deposition.

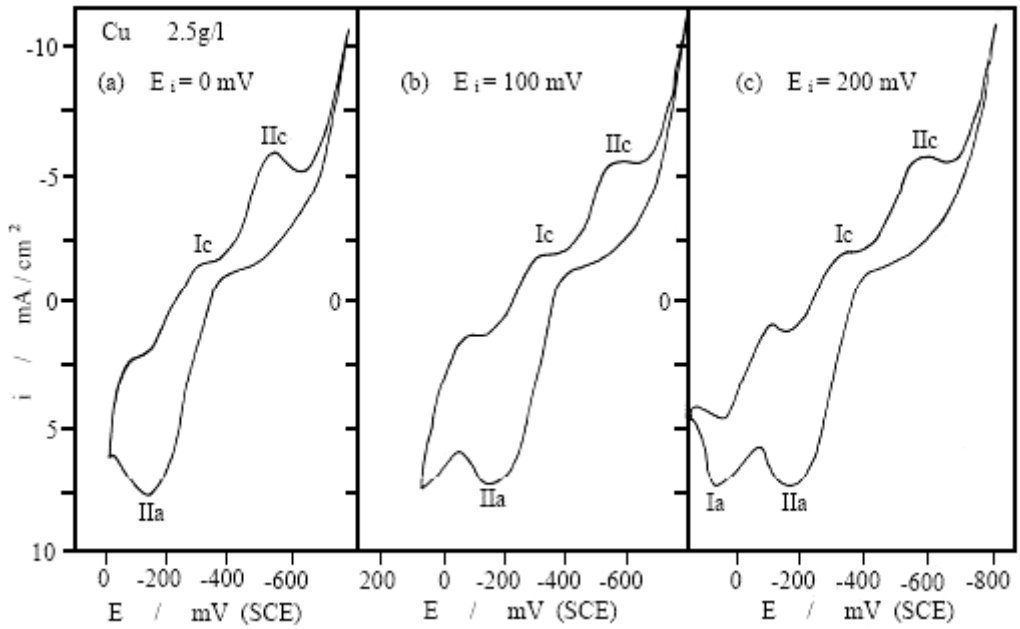

Fig. 2. Voltamperogramme of copper–ammonia nitrate electrolyte at various values of the initial potential E_i: (a) E_i = 0.000 V; (b) E_i = 0.100 V, (c) E_i = 0.200 V; v = 20 mV·s^{-1}.

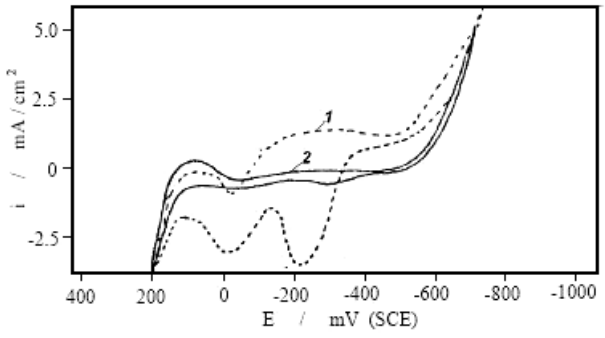

Fig. 3. Voltamperogramme of copper-ammonia nitrate electrolyte on silver electrode; E_i = 0.200 V, final potential E_c = –0.750 V, v = 20 mV·s^{-1} (curve 1). Curve 2 is the basic electrolyte.

In the anodic region the character of the curves is not different from that on a copper electrode – two peaks IIa and Ia are observed. They are associated with the consecutively occurring reactions (4) and (5), i.e. the oxidation of the copper coating, deposited in the cathodic region.

It is obvious that on a silver electrode only the reduction of copper is occurring by a mechanism different from that on a copper substrate, which is due to obstruction of the reaction of disproportionation (6). The fact that the deposition of copper, in this case, is proceeding on a substrate of different nature, is the reason for the registered comparatively lower currents in the process of copper deposition, compared to those on a copper electrode.

Cyclic voltamperometry of a basic electrolyte. The voltamperogrammes of an electrolyte not-containing any copper ions and having a composition 40 g·dm^{-3} NH_4NO_3 and NH_3 (until pH = 9 is reached) represent some interest (Fig. 4). As it can be seen from the comparison with the respective dependence for solutions containing copper ions (curve 1), there exists an analogy between the peaks in the current in intensity, but those in the copper-containing solutions are higher. It can be supposed that their appearance in the basic electrolyte is owing to processes, in which copper ions are parti-

cipating. The same peaks are obtained upon cycling in anodic direction (the represented dependence is recorded after five cycles) or as a result of chemical dissolution of the copper electrode in the ammonia medium at the above-specified values of pH (8.5–9).

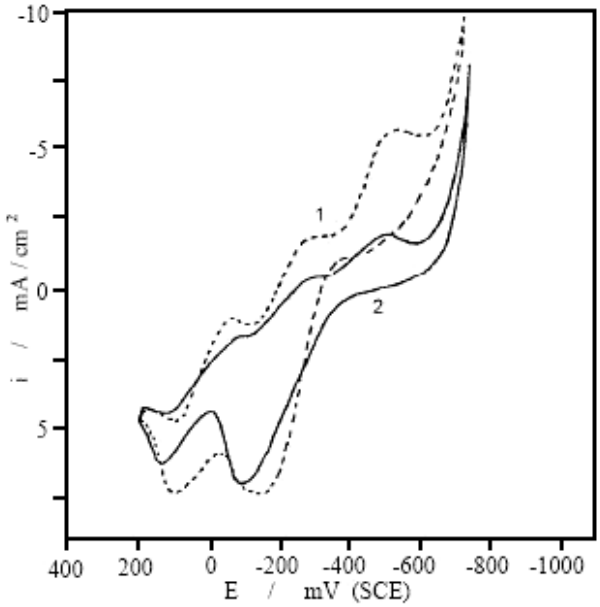

Fig. 4. Voltamperogramme of the basic electrolyte on copper electrode (40 g·dm^{-3} NH_4NO_3 and 25% NH_3 until pH = 9 is reached) on copper electrode (curve 2); Curve 1 is the copper containing electrolyte.

When the initial potential has a value amounting to E_i = –0.295 V the only occurring process is the evolution of hydrogen (Fig. 5) and no maxima in the current intensity are observed.

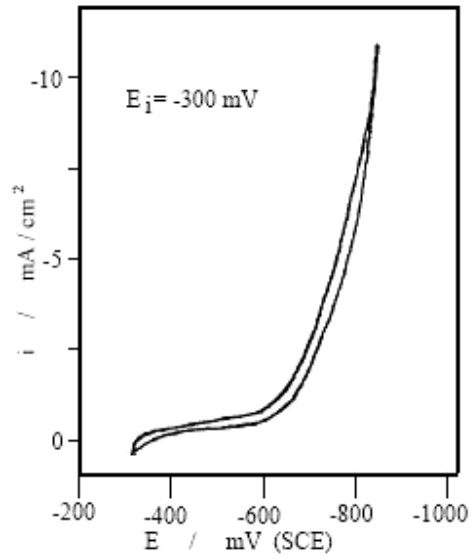

Fig. 5. Voltamperogramme of the basic electrolyte on copper electrode at initial potential E_i = –0.300 V.

The appearance of two consecutive cathodic peaks in the curves and the respective anodic peaks are observable in case of shifting of the initial potential in positive direction (up to 0.300 V).

Evidence in favour of the statement that the current peaks, obtained on copper electrode, are connected with the copper ions, is given by the voltamperogrammes, recorded with a silver electrode in the basic electrolyte (Fig. 6 curve 1). No current maxima are observed in the range of potentials from 0 to –0.800 V i.e. no processes are occurring in this electrolyte. Such peaks/processes are observable both in the cathodic and in the anodic direction but at potentials 0.00 – 0.400 V. These are most probably associated with the processes of formation and reduction of the silver ammonia complexes $[Ag(NH_3)_4]^+$ into Ag^o – reaction (6) from Table 1.

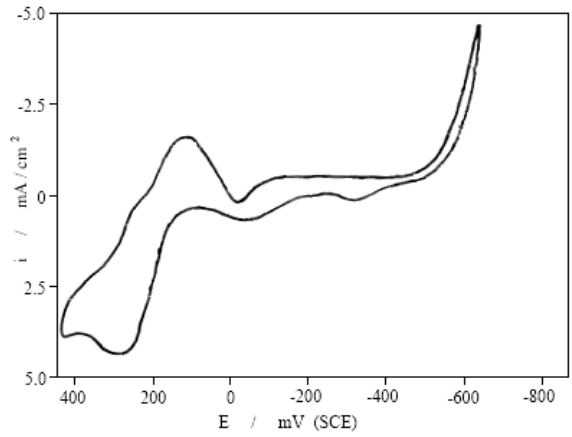

Fig. 6. Voltamperogramme of the basic electrolyte on silver electrode at initial potential E_i = +0.450 V.

Influence of the rate of sweeping of the potential (scan rate)

The voltamperogrammes were recorded in a copper-containing electrolyte with a copper electrode at different rates of sweeping of the potential from 20 to 150 mV·s^{-1} (Fig. 7). Both cathodic peaks and the respective anodic peaks are growing up with the increase of the rate of sweeping of the potential and they have a comparatively symmetrical character, which indicates the fact that they are connected with reversible processes.

The diagnosis criteria of the method of cyclic chronovoltamperometry [17, 18] were applied to each one of the two peaks separately (Table 2). The following was established for the first cathodic peak (Ic) and the respective anodic peak (IIa): A) The potential in the region of the cathodic peak is slightly shifted cathodically with the rate of sweeping the potential; B) The ratio $I^a_p/I^c_p > 1$ (varying from 1.32 to 1.07) and it is decreasing with the increase of the square root of the rate $\sqrt{v}$; C)

The function of the current $I_p^c/\sqrt{v}$ does not change with the increase of $\sqrt{v}$. These dependences point to the occurring of an Electrochemical-Chemical (EC) mechanism, consisting of a reversible electrochemical reaction, followed by a reversible chemical reaction.

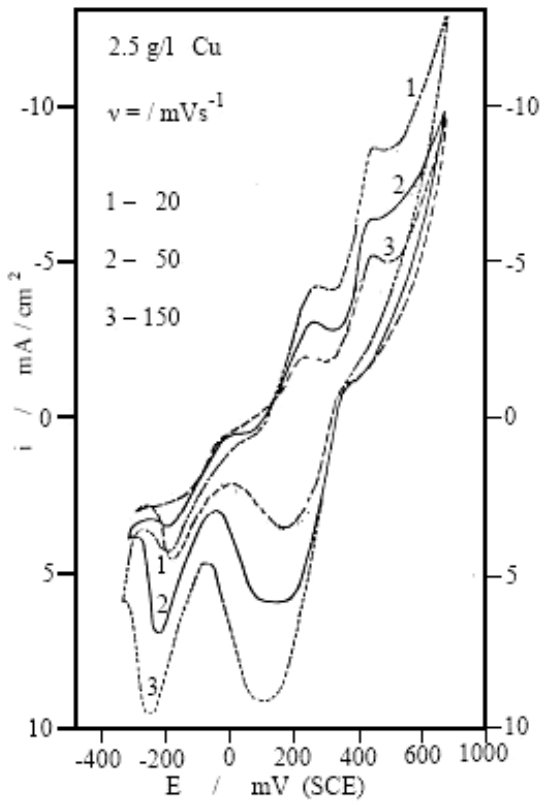

Fig. 7. Influence of the sweeping rate of the potential (v) upon the course of the voltamperogrammes, recorded in copper-containing electrolyte (2.5 g·dm^{-3} Cu in the form of $Cu(NO_3)_2$; 40 g·dm^{-3} NH_4NO_3 and 25% NH_3 until pH = 9 is reached) on copper electrode in the range of potentials from E_i = 0.300 V up to E_{sw} = –0.700 V, 1 – v = 20 mV·s^{-1}; 2 – v = 50 mV·s^{-1}; 3 – v = 150 mV·s^{-1}.

The calculations, performed in this way in regard to the second cathodic peak (IIc) and the respective anodic peak (IIa) (Table 2) showed the following. A) The potential in the region of the cathodic peak is slightly shifted anodically with the sweeping rate of the potential. B) The ratio $I^a_p/I^c_p > 1$ (varying from 1.13 to 2.05) and it is growing up with the square root of the rate $\sqrt{v}$ (Fig. 7); The function of the current $I^c_p/\sqrt{v} < 1$ (from 0.69 to 0.36) and it is decreasing with the increase of $\sqrt{v}$. These dependencies indicate that this is a CE mechanism, consisting of a reversible electrochemical reaction, preceded by a reversible chemical reaction.

The calculations carried out are an indication that the entire mechanism of deposition of copper from ammonium nitrate electrolyte can be denoted as Electrochemical-Chemical-Electrochemical (EChE) type, i.e. occurring of two consecutive reversible electrochemical reactions (1) and (3) and an intermediate reversible chemical reaction of disproportionation of the copper (2).

CONCLUSIONS

The process of copper deposition from ammonium nitrate electrolyte has been studied at pH = 8.5–9 by the method of cyclic voltamperometry. On the basis of the criteria of this method it has been ascertained that the deposition of copper is proceeding in accordance with an ECE type of mechanism i.e. a mechanism comprising two consecutive reversible electrochemical reactions and an intermediate chemical reaction – disproportionation of the copper.

The experiments carried out form an early stage of the investigation, associated with the process of preparation of alloyed Ag-Cu powders from the above-specified electrolyte.

Table 2. Values of the diagnosis parameters of the cyclic chronovoltamperometry: value (deviation) of the cathodic potential E^c_p, the ratio I^a_p/I^c_p and the function of the current $I^a_p/\sqrt{v}$ on the square root of sweeping of the potential $\sqrt{v}$ for the two cathodic peaks (Ic and IIc) and the respective anodic peaks (Ia and IIa).

UV, (mV·s^{-1})$^{1/2}$	Ic (Ia)			IIc (IIa)		
	E^c_p, mV	I^a_p/I^c_p	I^c_p / UV	E^c_p, mV	I^a_p/I^c_p	I^c_p / UV
4.47	–220	1.32	0.43	–465	1.13	0.69
7.07	–270	1.21	0.46	–440	1.64	0.52
12.25	–289	1.07	0.44	–435	2.05	0.36

REFERENCES

1. K.I. Popov, M.G. Pavlovic, in: Electrodeposition of Metal Powders with Controlled Particles Grains Size and Morphology (Modern Aspects of Electrochemistry, vol. 24**)**, B. E. Conway, J. O'M. Bockris, R. E. White, (Eds.), Plenum, New York (1993), pp. 299–391.
2. K. J. Popov, M. G. Pavlovic, J. N. Jovicevic, *Hydrometallurgy*, **23**, 127 (1989).
3. H. M. A. Solimen, H. H. Abdel-Rahman, *J. Braz. Chem. Soc.*, **17**, 705 (2006).
4. K. J. Popov, N. D. Nikolic, M. G. Pavlovic, *J. Serbian Chem. Soc.*, **74**, 397 (2006).
5. K. J. Popov, M. G. Pavlovic, G. Z. Removic, *J. Appl. Electrochem.*, **2**, 742 (1991).
6. M. Seniquchi, K. Nakahara, K. Omal, H. Shimamara, *JP* 169,051 (Cl B22 F 1/00) 17 Jun 2002.
7. A. Tsurkoka, K. Sayama, E. Kazuhiro, *JP* 2000, 290,701 (Cl C B22 F 1/00) 11 Oct 2000.
8. K. Jgnatova, L. Nikolova, E. Kashchieva, *Bull. Electrochem*., **14**, 315 (1998).
9. C. Nila, J. Gonzales, *J. Electroanal. Chem.*, **401**, 171 (1996).
10. A. Rames, M. M. Hernandes, J. Gonzales, *J. Electrochem. Soc*., 149, 2002, p. 390.
11. U. J. Larin, E. B. Khobotova, J. D. Gorobets , V. N. Baumer, V. V. Datschenko, *Electrokhimiya*, **26**, 165 (1990).
12. D. Gryjicic, B. Pesic, *Electrochim. Acta*, **50**, 4426 (2005).
13. A. U. Danilov, E. B. Molodhina, Iu. M. Polukarov, *Russ. J. Electrochem*., **36**, 987 (2000).
14. A. Milchev, T. Zapryanova, *Electrochim. Acta*, **1**, 2926 (2006).
15. D. Stoychev, St. Rashkov, *Compt. Rend. Acad. Bulg. Sci.*, **26**, 243 (1973); *ibid.*, **32**, 1515 (1979); *ibid.*, **50**, 71 (1997).
16. D. Stoychev, St. Rashkov, *Bulg. Chem. Commun.*, **9**, 618; 633; 653 (1976); *ibid.*, **18**, 157 (1985); *ibid.*, **35**, 65 (2003).
17. D. Stoychev, St. Rashkov, *Surf. Technol.*, **7**, 155; 427; 433 (1978); *ibid.*, **10**, 209 (1980).
18. D. Stoychev, I. Tomov, I. Vitanova, *J. Appl. Electrochem.*, **15**, 878 (1985); *ibid.*, **22**, 978 (1992).
19. D. Stoychev, *Trans*. *Inst. Met. Finishing (England)*, **76** (26); 73 (1998).
20. A. Radisic, G. J. Lany, P. M. Hoffman, P. C. Searson, *J. Electrochem. Soc.*, **148**, 41 (2000).
21. G. Oskam, P. M. Veresken, P. C. Learcon, *J. Electrochem. Soc.*, **146**, 1436 (1999).
22. M. S. Zakharov, O. V. Devyatkova, O. U. Zakharova, *JVUZ Khimiya i Khim. Tekhnol* , **47**, 44 (2004).
23. P. Borthen, J. B. Hwang, H. H. Strechblow, D. M. Koev, *J. Phys. Chem.*, **104,** 5078 (2000).
24. A. J. Bard, L. R. Faulkner, Electrochemical Methods. Fundamentals and Applications, J. Wiley & Sons, New York, 1980, p. 213.
25. Z. Galus, Teoretical Bases of the Electrochemical Analysis, Mir, Moscow, 1974, p. 421 (in Russian).
26. E. R. Brown, R. F. Large, in: Cyclic Voltametry, A Weisberger (Ed.), Wiley Interscience, 1994, Part II A.
27. A. M. Suhotina (Ed.), Handbook in Electrochemistry, Khimia, Leningrad, 1981, p. 133 (in Russian).
28. A. P. Tomilov (Ed.), Industrial Electrochemistry, Khimia, Moscow, 1984, p. 420 (in Russian).

ИЗСЛЕДВАНЕ НА ПРОЦЕСИТЕ И МЕХАНИЗМА НА ЕЛЕКТРООТЛАГАНЕ НА МЕД ОТ АМОНИЕВОНИТРАТЕН ЕЛЕКТРОЛИТ С МЕТОДА НА ЦИКЛИЧНАТА ВОЛТАМПЕРОМЕТРИЯ

Л. Петков*, К. Игнатова

Химико-технологичен и металургичен университет, бул. „Климент Охридски" № 8, 1756 София

Постъпила на 21 март 2008; Преработена на 23 април 2008

В статията са докладвани резултатите от прилагането на метода на цикличната волтамперометрия за изследване на процесите и механизма на отлагане на мед от амониевонитратен електролит. Изследвано е влиянието на началния потенциал, на скоростта на разгъване на потенциала, както и на природата на катодния материал (мед и сребро) върху хода на волтамперограмите. Установено беше, че отлагането на мед върху меден електрод протича по двустадиен механизъм, като чрез редукция на купроамнячните йони. Чрез прилагане на диагностичните критерии на метода беше потвърдено, че механизмът съответствува на ЕСЕ, тоест два последователни обратими електрохимични стадия (купри-/купроамонячни комплекси и купроамонячни комплекси/елементарна мед), с междинен химичен стадий на диспропорциониране на медта. Върху сребърен електрод само механизмът на анодния процес е относително същия. Установеното различие в механизма на отлагане на мед е много важно за съвместното отлагане на мед и сребро и получаване на сплавно Ag-Cu покритие, като се има предвид че среброто е по-електроположителният метал в системата.

Получените резултати са важна част от по-обширно изследване, свързано с получаване на сплавен финодисперсен Ag-Cu прах в условията на стационерен и импулсен потенциостатичен режим.

Bulgarian Chemical Communications, Volume 41, Number 1 (pp. 46–49) 2009

Synthesis, characterization and some properties of lanthanum complex of N,N'-bis-(2-butyl-5-chloro-3H-imidazol-4-ylmethylene)-ethane-1,2-diamine, a salen type ligand

K. Jailakshmi, K. M. Lokanatha Rai∗, H. D. Revanasiddappa

Department of Studies in Chemistry, University of Mysore, Manasagangotri, Mysore, Karnataka, India

Received July 17, 2007; Revised April 22, 2008

Diamagnetic lanthanum complex was prepared with a salen type ligand "imidozalen", bis(2-*n*-butyl-4-chloro-imidazole)-5-iminoethane and the complex was characterized by elemental analyses, magnetic studies, UV-Vis and IR, spectroscopy, NMR, thermal and conductance studies. Antifungal and antibacterial properties were also studied. The complex has a potential as an epoxidation catalyst.

Key words: lanthanum, imidozalen, salen-type complex, epoxidation, antifungal, antibacterial activity.

INTRODUCTION

Salen ligands form a variety of complexes with almost all kinds of metals [1–4]. Lanthanum complexes of salen and its derivatives have also been studied [5–7]. Lanthanum complexes are generally noted to have higher coordination number and the reported crystalline structure of such complexes helps in understanding the mode of coordination in these complexes [8–10]. The most common coordination numbers of lanthanum are 8 and 9. A coordination number of 8 is probably the most characteristic of lanthanum with square antiprism being the preferred stereochemistry. Many previously accepted examples of coordination number 6 are actually invalid because some coordinated solvent molecules are present and they raise the true coordination number to 7, 8 or 9.

Remarkably high asymmetric amplifications (positive nonlinear effects) were realized in some chiral lanthanide complex-catalyzed organic reactions [11] such as the asymmetric hetero-Diels–Alder reaction, Michael's addition reaction, epoxidation, *etc*. These phenomena may be explained by the autogenetic formation of the enantio-pure lanthanide complexes as the most active catalysts. The high coordination numbers of the lanthanides seem to play an important role through the formation of aggregates of the heterochiral complexes as less active catalysts. Chiral lanthanum complexes [12] have been used in the asymmetric catalysis and highly enantio-selective epoxidation has been achieved *via* this mode. It is found that imidazole and its derivatives are biologically active molecules [13], which emphasizes that antibacterial, antifungal and antimitotic studies of metal complexes are also an interesting area of research.

Inspired by the applicability of salen complexes and biological activity of imidazole derivatives, we studied a new salen type of Schiff base "imidozalen" and its complex. Imidozalen, the salen type of Schiff base was derived from 2-*n*-butyl-4-chloro-5-formyl imidazole with ethylene diamine and the structure of the ligand was studied by X-ray diffraction crystal studies [14]. We further studied the activity of the prepared imidazolen and its complex against a set of fungi by using potato dextrose agar medium and we also checked its antibacterial activity. We report in this paper the synthesis, application and the probable structure of imidozalen lanthanum complex, based on spectral and analytical studies.

MATERIALS AND METHOD

All reagents were of AR grade of purity and used without any further purification. Imidozalen was derived from 2-*n*-butyl-4-chloro-5-formyl imidazole and ethylene diamine [14]. Elemental analysis for C, H, and N was performed on an Elementar Vario EL III device. Electronic absorption spectra were recorded on an Analytik Jena, Specord-50 spectrometer. IR spectra were obtained on a Jasco FTIR-4100 instrument. Magnetic moment was measured in the solid state using a Guoy Balance with mercury tetrathiocyanatocobaltate(II) as standard at room temperature. The molar conductivity was measured using an Elico CM-180, conductivity meter. ^{1}H NMR spectra were recorded on Bruker AMX-400 NMR spectrometer.

* To whom all correspondence should be sent:
E-mail: kmlrai@yahoo.com

© 2009 Bulgarian Academy of Sciences, Union of Chemists in Bulgaria

The antibacterial activity was studied by well known method. 20 ml of nutrient agar was poured into 9 cm Petri plates. The medium was allowed to cool down and kept overnight. These plates were swabbed with the test bacteria. The concentration of bacterial cells in the inoculums was maintained at a minimum of 1×10^4 cells/ml in 0.5% of peptone solution. Using a flame cork borer, 5 mm diameter wells were made in the nutrient agar plates at a distance of 2 cm from the periphery of the plates. These wells were filled with 50 µl suspension of the complex and the ligand in DMF**.** Sterile distilled water and DMF served as control. These plates were incubated at 28°C in an upright position in a BOD incubator for 24 h. After a period of incubation, the plates were inspected for inhibition zone, if any, and measured using an mm scale.

Antifungal activity was studied by disc diffusion method. Fungal cultures were prepared for anti-fungal activity one day prior to the experiment. Fungal culture was prepared by mixing mycelium and spores with water; the suspension was properly mixed by using cyclomixer. The final concentration of fungi spores was determined and adjusted at the required concentration. The complex and the ligand were made up to a concentration of 5 mg/100 µl (5%) in DMSO and studied in regard to antifungal activity. DMSO was also used as a negative control. A systematic fungicide Bavistin (Carbendenzim) of 2 mg/ml concentration was prepared in distilled water and used as positive control in antifungal assay. All the fungal cultures were obtained from the Department of Applied Botany and Biotechnology, University of Mysore, Mysore.

EXPERIMENTAL

Preparation of the complex

An ethanolic solution of lanthanum(III) nitrate hexahydrate (0.433 g, 0.01 mol) in 100 ml ethanol was added slowly to an ethanolic solution of imidozalen ligand (0.397 g, 0.01 mol) in 100 ml ethanol at room temperature, stirred continuously for about 30 min. During the addition, the colour changed from pale yellow to bright yellow with immediate formation of a turbid solution, which disappears after stirring and refluxing on a water bath for 3 h yielding an orange-yellow solution. The solution was concentrated to yield a deep orange-yellow precipitate, which was separated, washed with ether and dried over fused $CaCl_2$.

The yield was 0.612 g (77%); m.p. 140–143°C, IRS (nujol) ν cm^{-1}: 3550–3332 (br), 3185 (m), 1631 (w), 1511 (m), 1458 (m), 1431 (w), 1326 (m), 1255 (s), 1182 (w), 1032 (s), 1097 (m), 1007 (w), 940 (w), 816 (s), 740 (w), 555 (m), 482 (w), 427 (w), 407 (m). UV-Vis λ_{max} nm, (ν cm^{-1}): 305 (32786), 401 (24937), 470 (21276), 704 (14204). ^{1}H NMR ($CDCl_3$): 0.8 (t, 6H, CH_3), 1.30 (m, 4H, CH_2), 1.62 (m, 4H, CH_2), 2.59 (t, 4H, CH_2), 3.78 (s, 4H, N–CH_2), 13.10 (b, 2H, –CH=N–). Anal. calcd. for C_{24} $H_{42}Cl_2N_8O_9La$: C, 36.18; H, 5.27; N, 14.07. Found: C, 36.23; H, 5.32; N, 14.19.

Asymmetric epoxidation using the prepared complex as a catalyst

Styrene (0.9 g, 8.64 mmol) was treated with sodium hypochlorite solution, 5 ml, in the presence of 4 mg of lanthanum imidozalen catalyst in 10 ml ethanol, under ice cold conditions. The reaction time was 20 min with continuous stirring. The yield was 0.415 g, 40%, b.p. 192–195°C (Lit. 193–196°C), IRS (neat): 1600, 1010 cm^{-1}. ^{1}H NMR ($CDCl_3$) δ: 2.84 (b, 2H, OCH_2), 3.80 (t, 1H, OCH), 7.15 (bs, 5H, ArH). Anal. calcd. for C_8H_8O: C, 79.97; H, 6.71. Found: C, 79.15; H, 6.58. Further studies on catalytic activity of this complex are in progress.

RESULTS AND DISCUSSION

The lanthanum complex was formed as shown in Scheme 1.

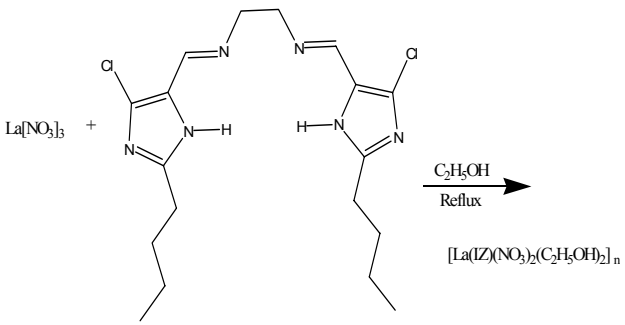

Scheme 1: Synthetic routefor lanthanum imidozalen complex.

The electrical conductance measurements were made using chloroform and the values obtained for the blank, ligand and the lanthanum complexes were 0.94×10^{-6} S, 1.35×10^{-6} S and 1.4×10^{-6} S, respectively. The order being the same, the values indicate that the complex can be termed a non-electrolyte. Elemental analyses agree with the empirical formula assigned, *viz*., $[La(IZ)(NO_3)_2(C_2H_5OH)_3]_n$ (Fig. 1), where IZ = $C_{18}H_{24}Cl_2N_6$.

The very broad peak appearing in the region 3550–3332 cm^{-1} indicates the presence of the ethanol molecule. This band can be attributed to the –OH stretching frequency of the ethanol molecule. Moreover, the assignment of this peak to the –OH of water molecules does not fit well with the analytical data and it is also confirmed by thermogravimetric

studies, which indicate that the first step weight loss takes place in the temperature range 85–100°C, which can account for the loss of ethanol molecules. Also, the appearance of an additional band at 1032 cm^{-1} in case of spectra of nitrate complexes suggests the presence of ethanol in the system [15]. The band in the region 1640–1620 cm^{-1} is attributed to C=N stretching vibrations. The free ligand exhibits a peak at 1635 cm^{-1} and its complex shows a band at 1631 cm^{-1}, which suggests that –C=N group may not be involved in the bonding [8].

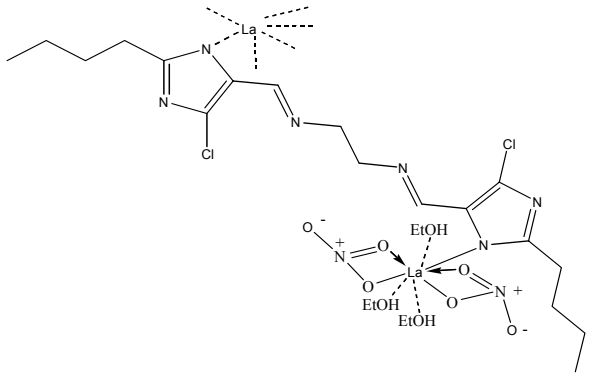

Fig. 1: Possible structure of lanthanum imidozalen complex.

The –NH group of the imidazole ring of the free ligand shows a peak at 3400–3350 cm^{-1}, which is difficult to distinguish in the complex as it overlaps with broad peak of –OH in the region 3550–3332 cm^{-1}, although appearance of another broad peak of medium intensity at 3185 cm^{-1} can be assigned to the shift due to the bonding of –NH. The deprotonation of –NH group may take place and the complex is supposed to have a polymeric form as in the case of salen lanthanum complex [8].

The ν_{M-N} and the ν_{M-O} vibrations are found at 427 cm^{-1} and at 407 cm^{-1}, respectively, in the titled complex. The nitrate ligand acts as a bidentate ligand and the peaks at 1511 cm^{-1} and 1326 cm^{-1} can be assigned to ν_4 and ν_1 vibrations of nitrate ligand, respectively, as the difference, $\Delta\nu$, is 185 cm^{-1}, which agrees with the literature reports [16, 17]. The absence of a band at 1380 cm^{-1} rules out the possibility of presence of ionic nitrate.

The ^1H NMR spectrum of the complex shows a strong peak at δ 3.5 attributed to $–CH_2$ of ethanol, which supports the IR spectral data. The UV-Vis spectra of the ligand showed absorption maximum at 32786 cm^{-1}, which is also present in the complex. But the appearance of new bands at 24937 cm^{-1} and at 14204 cm^{-1} can be attributed to electron transfer between the metal center and the coordinated ligand. The magnetic moments showed that the complex has diamagnetic nature, as it is expected for any closed shell complex.

The catalytic activity of the complex was checked with styrene as a substrate in the presence of sodium hypochlorite. The control experiment was run without the lanthanum catalyst. However, the yield was low and the percentage of enantiomeric excess obtained was also low. The boiling point of the formed product was checked individually and also as a mixture of the pure readily available product from Aldrich to check the mixed boiling point. The NMR peak at 2.84 δ proved the epoxide formation in case of the sample with the catalyst. The sample without the catalyst took a longer time, compared to the sample with catalyst, to form the expected product.

Lanthanum imidozalen complex and the imidozalen ligand were studied in regard to their toxicity. The ligand, imidozalen and the lanthanum complex were screened against the following bacterial strains: *S. aureus*, *E. coli*, *S. typhi*, *S. typhimurium*, *Salmonella paratyphi. A, Salmonella paratyphi. B, Shigella boydii*, *Klebsiella*, *Citrobacter,* and *Pseudomonas*. Sterile distilled water and DMF served as control. The ligand did not show any activity. The lanthanum imidozalen complex exhibited very mild activity against *S. aureus* and *E. coli*.

The lanthanum imidozalen complex did not show any antifungal activity. Surprisingly, the ligand showed very mild antifungal activity only for *Fusarium solani*. The tested organisms are *Curvularia Lunata, Alternaria alternata, Aspergillus niger, Aspergillus flavus, Fusarium solani, Aspergillus ochraceous*. DMSO was used as a negative control. A systematic fungicide Bavistin (Carbendenzim) of 2 mg/ml concentration was prepared in distilled water and used as positive control in antifungal assay.

The complex contains –C=N group and a masked –NH groups, which generally, if present, imply activity. A possible explanation of the toxicity of the complexes has been postulated in the light of chelation theory [18]. The importance of toxicity in the compounds containing nitrogen and sulphur has been well established in many fungicides [19]. It was suggested that the chelation reduces considerably the charge of the metal ion mainly because of partial sharing of its positive charge with the donor groups and possible n-electron delocalization over the whole chelate ring. This increases the lipophilic character of metal chelate, which favours its permeation through lipoid layers of fungus membranes. Furthermore, the mode of action of the compounds may involve the formation of the chelate or the ligand with the active centers of the fungal cell constituents resulting in interference with the normal cell process.

CONCLUSION

The imidozalen was expected to act as a quadridentate ligand [20] but it unexpectedly mimicked the neutral salen lanthanum complex [8].

In conclusion, the salen type imidozalen ligand acts as a unidentate ligand and one of the –NH groups of the ligand binds to one lanthanum ion and the other –NH group is expected to bind to another La ion, thus forming a polymeric chain. Further attempts to obtain the product in crystalline form are in progress, which would help study the complex as a polymeric chain. This complex is also being studied as a catalyst for epoxidation. The basic study of toxicity of this complex raises interesting questions about its mechanism.

Acknowledgement: *We thank the Department of Chemistry Manasagangotri, Mysore for providing the facility for elemental analyses and electronic spectra.*

REFERENCES

1. S. Mizukami, H. Houjou, Y. Nagawa, M. Kanesato, *Chem. Commun.*, **10**, 1148 (2003).
2. N. J. Kerrigan, H. Muller-Bunz, D. G. Gilheany, *J. Mol. Catal. A*, **227**, 163 (2005).
3. H. Hamdan, V. Navijanti, H. Nur, M. N. Mohd Muhid, *Solid State Sci.*, **7,** 239 (2005).
4. J. A. Jegier, M. A. M. Hernandez, D. A. Atwood, *J. Chem. Soc.*, **15**, 2583 (1999).
5. R. D. Archer, H. Chen, L. C .Thompson, *Inorg. Chem*., **37**, 2089 (1998).
6. S. Mangani, A. Takeuchi, S. Yamada, P. Orioli, *Inorg. Chim. Acta*, **155**, 149 (1989).
7. J. I. Bullock, H. A .Tajmir-Riahi, *J. Chem. Soc. Dalton Trans*.**,** 36 (1978).
8. W. Xie, M. J. Heeg, P. G. Wang, *Inorg. Chem*., **38**, 2541 (1999).
9. J. Burgess*,* Metal Ions in Solution, Ellis Horwood, Chichester, 1997.
10. A. R. A. Karaghouli, R. O. Day, J. S. Wood, *Inorg. Chem*., **17**, 3702 (1978).
11. J. Inanaga, H. Furuno, T. Hayano, *Catal. Survey Jpn.*, **5**, 37 (2001).
12. K. Daikai, T. Hayano, R. Kino, H. Furuno, T. Kagawa, J. Inanaga, *Chirality*, **15**, 83 (2002).
13. H. A. Koistinen, D. Galuska, A. V. Chibalin, J. Yang, J. K. Zierath, G. D. Holman, W. H. Hendrikson, *Diabetes,* **52***,* 1066 (2003).
14. H. S. Yathirajan, C. R. Raju, K. M. Lokanatha Rai, K. Jailakshmi, P. Nagaraja, K. Palani, M. N. Ponnuswamy, M. Nethaji, *J. Chem. Cryst.*, **35**, 211 (2005).
15. A. Syamal, M. R. Maurya, *Ind. J. Chem*., **24A**, 836 (1985).
16. K. Nakamoto, Infrared and Raman Spectra of Inorganic and Coordination Compounds, Wiley, New York, 1986**.**
17. N. F. Curtis, Y. M. Curtis, *Inorg. Chem*., **4**, 804 (1965).
18. R. S. Srivastava, *Inorg. Chim. Acta*, **56**, 265 (1981).
19. M. C. Goldsworthy, *Phytopathology*, **32**, 498 (1942).
20. K. Jailakshmi, K. M. Lokanatha Rai, P. Nagaraj, H. D. Revannasiddappa, *Bulg. Chem. Commun.,* **39**, 142 (2007).

СИНТЕЗ, ОХАРАКТЕРИЗИРАНЕ И НЯКОИ СВОЙСТВА НА ЛАНТАНОВ КОМПЛЕКС НА N,N'-БИС-(2-БУТИЛ-5-ХЛОРО-3Н-ИМИДАЗОЛ-4-ИЛМЕТИЛЕН)-ЕТАН-1,2-ДИАМИН, ЕДИН ЛИГАНД ОТ САЛЕНОВ ТИП

К. Джайлакшми, К. М. Локаната Рай*, Х. Д. Реванасидапа

Департамент по химия, Университет на Майсур, Манасаганготри, Майсур, Карнатака, Индия

Постъпила на 17 юли 2007 г.; Преработена на 22 април 2008 г.

(Резюме)

Получен е лантанов комплекс с един саленов тип лиганд – „имидозален“, N,N'-бис-(2-бутил-5-хлоро-3Н-имидазол-4-илметилен)-етан-1,2-диамин. Комплексът е охарактеризиран с елементен анализ, УВ-видима и ИЧ спектроскопия, ЯМР, магнитни, термични и кондуктометрични изследвания. Комплексът има възможно приложение като катализатор при епоксидиране.

Bulgarian Chemical Communications, Volume 41, Number 1 (pp. 50–53) 2009

The attenuation effect through methylene group*

V. Jagannadham

Department of Chemistry, Osmania University, Hyderabad-500 007, India

Received March 26, 2008; Revised April 23, 2008

There are several hundreds of redox, condensation, disproportionation, nucleophilic and electrophilic substitution, and addition reactions with *meta*- and *para*-substituted benzene derivatives in the literature, for which the Hammett reaction constants (ρ) were reported. If benzene can deprotonate behaving like a carboxylic acid, what could be the Hammett ρ value for such kind of equilibrium reaction?

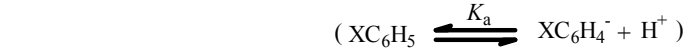

Here the author has tried to evaluate such Hammett ρ value by a simple and new protocol using of attenuation effect of a methylene group on benzoic acid dissociation equilibriums.

Key words: Attenuation effect, methylene group, acid dissociation equilibriums.

The effect of structure on the benzoic acid dissociative equilibria (K_a) and subsequently on chemical reactivity (k) is well explained by the putative Hammett equation (1). Based on the concept of this equation several hundreds of papers have emerged in chemical literature in the last century on the effect of structure on reactivity. It relates acid dissociative equilibria (K_a) or the chemical reactivity (k) in *meta*- and *para*-substituted benzene derivatives in terms of two parameters, the reaction constant (ρ) and the substituent constant (σ). Thus the equation proposed by Hammett for acid dissociative equilibria (K_a) is

$$\log K_a^X = \log K_a^H + \rho\sigma \qquad (1)$$

where K_a^X is the dissociation constant of substituted benzoic acid and K_a^H is that for the unsubstituted benzoic acid in water at 25°C, ρ is the reaction constant and σ is the substituent constant and for chemical reactivity (k), it is:

$$\log k_X = \log k_H + \rho\sigma \qquad (2)$$

where k_X is the rate constant for the substituted benzene derivative and k_H is for unsubstituted benzene derivative. Using equation 1 and a value of unity is chosen arbitrarily for ρ in aqueous solution and at 25°C, the σ values were evaluated. Using such σ values equation 2 is applied to several reactions to explain the effect of structure on reactivity. The value of ρ is a measure of the magnitude of the effect of structure either on acid dissociation equlibria or on the reactivity of *meta*- and *para*-substituted benzene derivatives. First, let us consider the acid dissociation equilibria of different oxygen containing acids in aqueous solution with increasing length of carbon chain between the ionizable proton and the aromatic ring carbon.

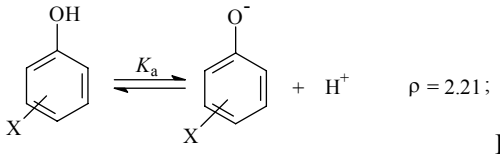

ρ = 2.21 ; Ref. 2 (3)

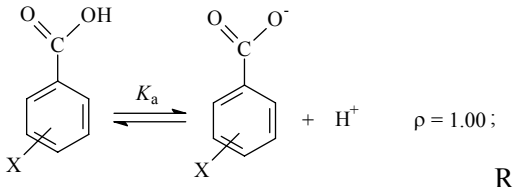

ρ = 1.00 ; Ref. 1 (4)

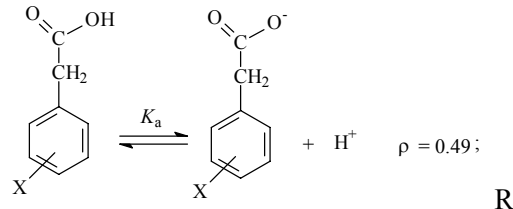

ρ = 0.49 ; Ref. 2 (5)

E-mail: vjchem@osmania.ac.in; jagannadham1950@yahoo.com

* Presented at the Virtual Conference on Chemical Education part of 20th International Conference on Chemical Education held on August 3-8, 2008, in Mauritius. Sponsored by IUPAC. http://vcampus.uom.ac.mu/icce/index.php

© 2009 Bulgarian Academy of Sciences, Union of Chemists in Bulgaria

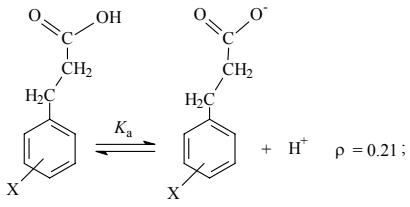

Ref. 2 (6)

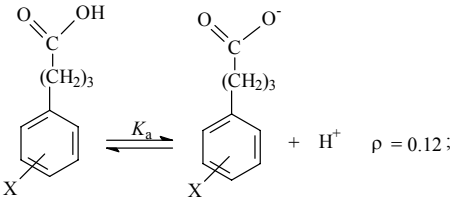

Ref. 3 (7)

The substituent effects can be transmitted in three ways: (i) inductive effects, (ii) steric effects and (iii) resonance effects. The first two kinds of effects naturally diminish very rapidly as the distance between the reaction center and the substituent increases. The third one is very effective due to polarization of the π-electron system conjugated by resonance and it is due to mutual intervening conjugation between substituent and the reaction center. And also the substituent effect through the resonance due to polarization of the conjugated π-electron system will be strongly affected and will decrease rapidly upon introducing an increasing number of methylene groups between the ionizable proton and the ring carbon atom in the dissociation of benzoic acid series. This could be observed in the above acid dissociation equilibriums. The ρ value decreases as the number of methylene groups increases. This effect was explained by Andrew Williams (4) by proposing an empirical equation (Eqn. (8)) and back calculating the Hammett ρ values for the dissociation equilibriums of phenols and phenyl acetic acids, which were found to be close to those determined experimentally.

$$\rho = (2.4)^{2-i} \qquad (8)$$

where '*i*' is the number of atoms between the ionizable proton and the ring carbon atom of benzoic acids. This could be seen as a beautiful exponential decay curve as it is shown in the figure by extending the application of Eqn. (8) further to dissociation equilibriums of benzoic, and other two acid series. From the figure one can always expect the ρ value to be a function of the number of methylene carbons or *vice versa*. But the reduction in the ρ value is by more than 50% comparing phenol dissociation to benzoic acid dissociation. Whereas going from benzoic acid dissociation onwards it is a systematic reduction in the ρ value each time by 50% only. This could be due to introduction of a sp^2 hybridized carbon atom (>C=O), which can probably provide an additional stabilization to the carboxylate anion of the benzoic acid. And from benzoic acid onwards the carbon chain is increased each time with one sp^3 hybridized carbon atom.

Further the large difference in substituent effects between the benzoic acid and the phenol series is well explained by Wiberg (5). It can result from strong field effect due to the decreased distance between the negative charge and the substituents in the phenoxide ions, compared to benzoates. The increased negative charge in the ring of the phenoxides results from π-donation from the anionic site and it enables a direct π-electron interaction between the phenoxide ion and the substituents. This type of interaction is not present in the benzoate ions.

In the study of substituent effects on benzoic acids, a particularly useful comparison was made between benzoic acids and the corresponding phenylacetic acids. Here, a very good linear relationship was found. Since the CH_2 group acts like an insulator, which prevents a direct π-electron interaction. The linear relationship showed that in both series the substituents effects have a common origin and they result from a Coulombic field effect of interaction of the carboxylate group with the charge distribution in the aromatic ring that was caused by the substituents.

Another striking and interesting comparison is between the dissociation equilibria of phenols and the corresponding benzyl alcohols.

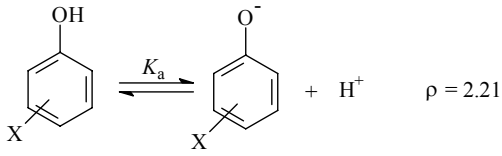

Ref. 2 (3)

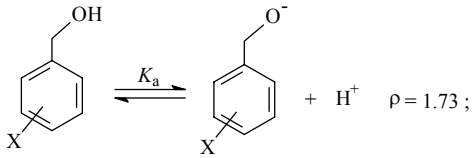

Ref. 6 (9)

One might be concerned about the ability of the CH_2 group in benzyloxide anion to act as a π-insulator (Eqn. 9). Here the Hammett ρ value for benzyl alcohols dissociation equilibria should be simply 1.11, which is half of that of phenoxide ion equilibria, based on the fact that the Hammett ρ value for phenyl acetic acids has become reduced to half of that of benzoic acids again upon the introduction of one CH_2 group between the

carboxylate carbon and the benzene ring carbon. But the actual ρ value was found to be 1.73 (6). One putative explanation of this, offered by Wiberg (5), is: In gas-phase alkoxide ions, the negatively charged oxygen atom polarizes the C–H bonds, placing considerable negative charge at the hydrogen atoms and a positive charge at the carbon atom. The carbon has an attractive Coulombic interaction with the negatively charged oxygen, leading to a shorter C–O bond, which may lead to somewhat larger substituent effect and in turn in aqueous solution even larger. Another explanation may come from the hyperconjugation of the benzyloxide ion, which may be even further stabilized by charge delocalization onto benzene ring as it is shown below (Eqn. (10)) to contribute towards higher Hammett ρ value.

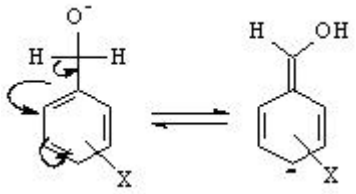

(10)

And this kind of effect is not present in benzoic acid, where the entire negative charge is concentrated on carboxylate group.

In conclusion, the introduction of an sp^2 hybridized carbon (>C=O) reduces the ρ value by a factor of more than 50% (2.21 to 1.00), when we go from phenol dissociation to benzoic acid dissociation, where the introduction of an sp^3 carbon ($–CH_2–$) reduces the ρ value by a factor of only 22% (2.21 to 1.73), which could be interpreted to the effect that the $–CH_2–$ is a good π-interaction insulator.

From Eqn. (8), it is clear that if $i = 0$ i.e. if there are no atoms between the ionizable proton and the benzene ring carbon, the example would be benzene itself, the Hammett ρ value would be 5.76 ($\rho = 2.4^{(2-i)} = 2.4^{(2-0)} = (2.4)^2$) for such system, if anybody determined it (see below the dissociation equilibrium, Eqn. (11)). It can also be seen from the graph by interpolation, the Hammett ρ value turns out to be 5.42, which is close to 5.76. But to the author's knowledge, nobody has determined the Hammett ρ value for such dissociation equilibrium. Also it could be further concluded that the Hammett ρ value should not exceed 5.76 for any kind of reactions, involving *meta*- and *para*-substituted benzene derivatives.

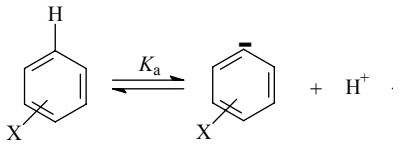

(11)

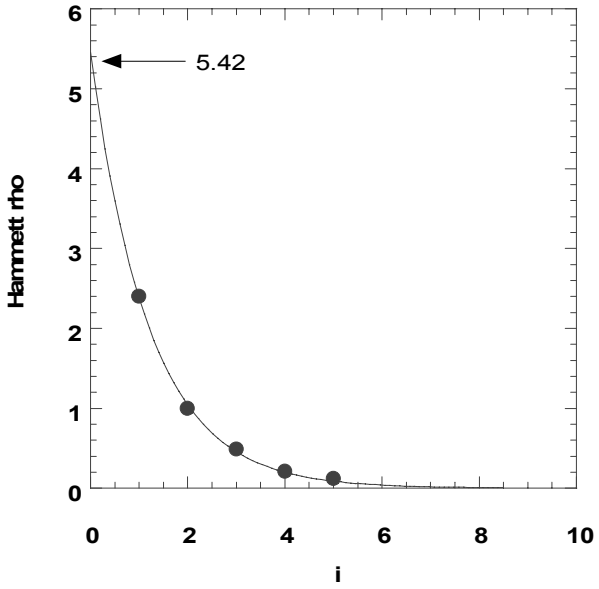

Fig. 1. Plot of Hammett ρ versus the number of atoms between the ionizable proton and ring carbon.

REFERENCES

1. L. P. Hammett, Physical Organic Chemistry, McGraw-Hill, New York, 1940, pp. 184–189.
2. H. H. Jaffe, *Chem. Rev*, **53**, 191 (1953)
3. J. Deles, B. Szechner, *Roczniki Chemii*, **45**, 1243 (1971).
4. A. Williams, Free Energy Relationships in Organic and Bioorganic Chemistry, Royal Society of Chemistry, Cambridge, 2003, p. 75.
5. K. B. Wiberg, *J. Org. Chem.,* **68**, 875 (2003).
6. The ρ value for this equilibrium is an estimate based on the correlation of gas-phase ΔH_{acid} values (5) of different oxygen containing acids and is done as follows: The Hammett ρ value for phenol dissociation equilibriums in aqueous solution is 2.21 (2). The gas-phase ρ value for this same equilibrium is 1.28 (5). Hence the ratio (ρ_{aq}/ρ_{gas}) is 1.73. The Hammett ρ value from the correlation of gas-phase ΔH_{acid} values of benzyl alcohols versus those of phenyl acetic acids is 1.00 (5). Therefore the Hammett ρ value for benzyl alcohols dissociation equilibria in aqueous solution on benzoic acid dissociation scale would be: (ρ of phenyl acetic acids) x (ρ_{aq}/ρ_{gas}) = 1.00 x 1.73 = 1.73.

ЕФЕКТ НА СПРЯГАНЕ ПРЕЗ МЕТИЛЕНОВА ГРУПА

В. Джаганадхам

Департамент по химия, Университет на Османия, Хайдерабад 500 007, Индия

Постъпила на 26 март 2008 г.; Преработена на 23 април 2008 г.

(Резюме)

В литературата има няколкостотин редокс реакции, реакции на кондензация, диспропорциониране, нуклеофилно и електрофилно заместване, на присъединяване с *мета*- и *пара*-заместени бензенови производни, за които са дадени константите на реакцията на Хамет (ρ). Ако бензен може да се депротонира, действайки като карбоксилова киселина, каква трябва да бъде стойността на ρ за тази равновесна реакция:

$$(XC_6H_5 \overset{K_a}{\rightleftharpoons} XC_6H_4^- + H^+)$$

Авторът се е опитал да оцени стойността на константата на реакцията на Хамет чрез нова и лесна за изпълнение процедура, използвайки ефекта на метиленовата група върху дисоциационните равновесия на бензоените киселини.

Bulgarian Chemical Communications, Volume 41, Number 1 (pp. 54–58) 2009

Microwave-assisted reaction in synthesis of tetra- and hexa-cyclic spiro systems

M. I. Marzouk*

Department of Chemistry, Faculty of Science, Ain Shams University, Abassia, Cairo, Egypt

Received June 25, 2008; Revised August 4, 2008

The reaction of 3-(4-chloro-3-methyl)benzoylprop-2-enoic acid and barbituric acid yielded 2,2'-(2,4,6-trioxohexahydropyrimidine-5,5-diyl)bis[3-(4-chloro-3-methyl)benzoylpropionic acid], which was reacted with hydroxylamine hydrochloride and hydrazine hydrate to give the corresponding spiro compounds. The spiro compound, containing a pyridazine moiety, was reacted with $PCl_5/POCl_3$ to give the dichloro derivative, which was reacted with sodium azide, monosaccharide hydrazones and acidhydrazides to give the tetrazolo and the triazolo derivatives respectively. All the reactions were carried out under conventional and microwave reaction conditions.

Key words: spiro compounds, microwave, monosaccharide hydrazones.

INTRODUCTION:

Microwave irradiation has gained popularity as a powerful tool for rapid and efficient synthesis of a variety of organic compounds, because of the selective absorption of microwave energy by polar molecules [1–4]. In this work the author sought to investigate the behaviour of 3-(4-chloro-3-methyl) benzoylprop-2-enoic acid in regard to barbituric acid by using the microwave radiation, with the aim to synthesize tetra- and hexa-cyclic spiro systems with anticipated pharmaceutical action.

RESULTS AND DISCUSSION

It is well known that barbituric acid is added readily to β-aroylacrylic acid as carbon nucleophile generated from the active methylene group under the influence of basic catalysts [5]. Thus, when 3-(4-chloro-3-methyl)benzoylprop-2-enoic acid **1** was reacted with barbituric acid under conventional and microwave irradiation it gave the same product **2**. 3-(4-chloro-3-methyl)benzoylprop-2-enoic acid **1** can be attacked by nucleophiles either at the unsaturated carbon in β position to the aroyl carbonyl group or caboxyl group. As the aroyl carbonyl group is better activated than the carboxyl group, so the attack occurs predominantly at the carbon in β position to the aroyl carbonyl group.

The formation of **2** was supposed to occur through the nucleophilic attack of the anion formed from the barbituric acid on the unsaturated carbon in β position to the aroyl carbonyl, followed by further addition to the unsaturated carbon atom in β position of a second molecule of the 3-(4-chloro-3-methyl) benzoylprop-2-enoic acid **1**.

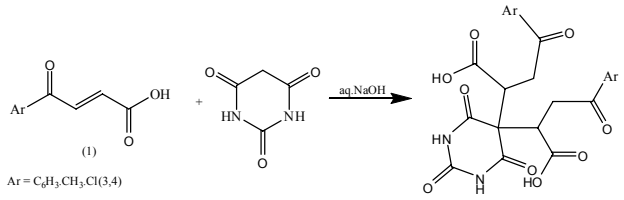

Scheme(1)

Table 1. ^{13}C-NMR data for compound No **2** [8].

Structure	^{13}C-NMR
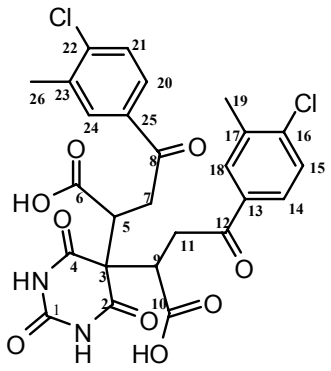	150.7 (C_1), 170.4 (C_2), 48.9 (C_3), 170.4 (C4), 39.0 (C5), 173.8 (C_6), 38.3 (C7), 196.9 (C_8), 39.0 (C_9), 173.8 (C_{10}), 38.3 (C_{11}), 196.9 (C_{12}), 133.8 (C_{13}), 127.1 (C_{14}), 128.0 (C_{15}), 138.4 (C_{16}), 135.2 (C17), 130.5 (C_{18}), 19.5 (C_{19}), 127.1 (C_{20}), 128.0 (C_{21}), 138.4 (C_{22}), 135.2 (C_{23}), 130.5 (C_{24}), 133.8 (C_{25}), 19.5 (C_{26})

Excitation with microwave radiation results in the molecules orientating their dipoles within the external field. The strong agitation, provided by the reorientation of molecules, in phase with the electrical field excitation, causes an intensive internal heating. By comparing the reaction rates of the case, where the reaction is carried out under irradiation and the case of conventional heating, it was found that a reaction that takes several hours under conventional conditions can be completed in the course of minutes under irradiation.

* E-mail: douda56@yahoo.com

© 2009 Bulgarian Academy of Sciences, Union of Chemists in Bulgaria

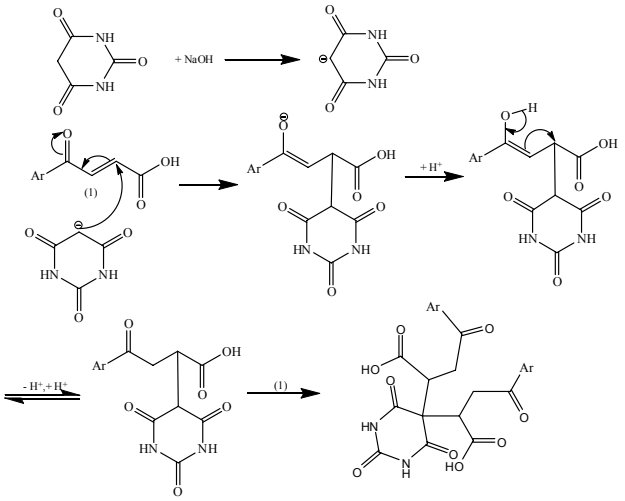

Scheme(2)

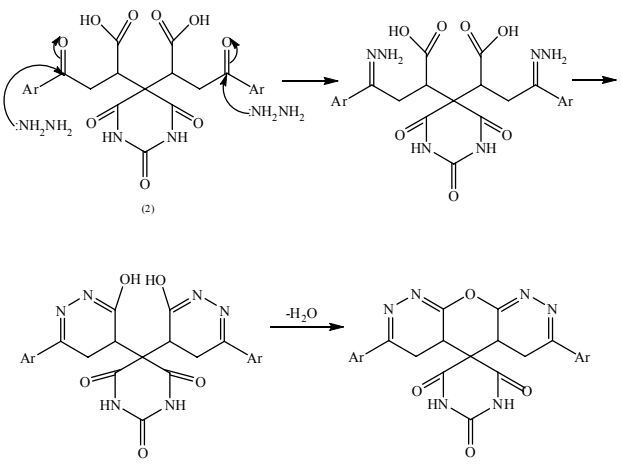

Scheme(3)

The benzoylpropionic acid **2** was reacted under conventional and microwave irradiation conditions with hydroxylamine hydrochloride in pyridine to afford the spiro compound with oxazine moiety **3**, while its reaction with hydrazine hydrate afforded the spiro compound with pyridazine moiety **4**.

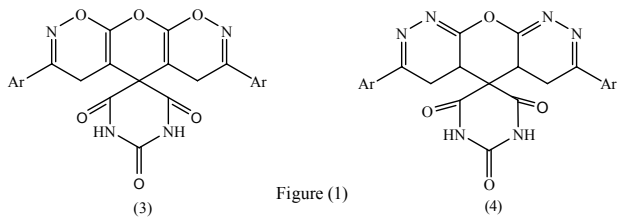

Figure (1)

The formation of compound **4** under microwave irradiation was carried out under solvent-free conditions; the procedure gives the product in excellent yield (98%) within 3 minutes avoiding problems associated with solvent use such as cost, handling and safety precautions, because of fire hazard due to occurrence of sparks in microwave ovens. But the reaction is less effective and it takes 6 hours to be completed, when carried out in ethanol under reflux and the corresponding derivative was obtained in 50% yield.

The formation of the spiro compounds **3** and **4** possibly takes place *via* formation of bis-monohydrazone derivative followed by cyclization. A proposed mechanism for the formation of compound **4** is shown in Scheme 3.

The spiro compound with pyridazine moiety **4** was treated with $PCl_5/POCl_3$ under conventional and microwave irradiation conditions to give the dichloro derivative **5**. The reaction can be performed within minute's time interval and in excellent yield, when carried out in microwave irradiation conditions (Table 2).

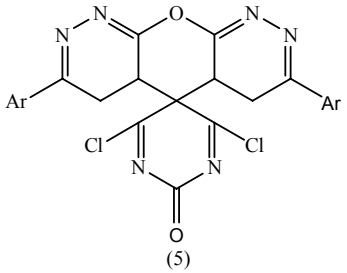

Figure (2)

Treatment of the dichloro compound **5** with sodium azide in DMF afforded the tetrazolo derivative **6**. Each of the two carbons attached to the two chlorine atoms has electron deficiency and can easily be attacked by a strong nucleophile such as the azide ion (N_3^-), followed by ring closure to afford the desired product bis-tetrazole.

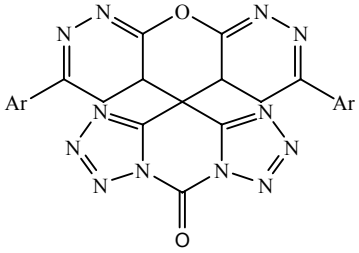

Figure (3)

It was reported [6] that heterocyclic nucleosides show broad-spectrum antiviral activity. In this investigation, the author sought to study the behaviour of the dichloro derivative towards the hydrazones of glucose and mannose with the aim to obtain a nucleus, bearing a nucleoside moiety. Thus, when compound **5** was allowed to react with hydrazones of glucose and mannose in boiling butanol, it afforded **7a, b** respectively. These

products (**7a**, **b**) were also prepared under microwave conditions, which considerably reduced the time of the reaction (Table 2).

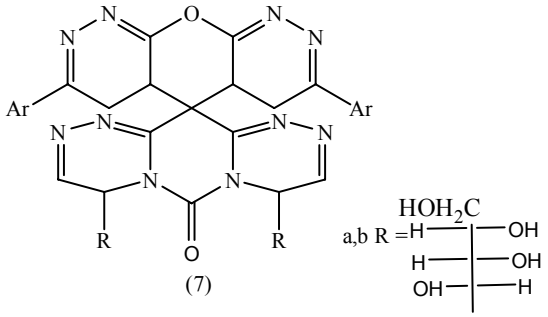

(7)

Figure(4)

It was reported that triazolo-pyridazines showed activity in tests indicative of anxiolytic activity [7]. So, the author sought to improve the yield of the reaction by using the microwave irradiation. The reaction of compound **5** with acylhydrazines, namely benzoylhydrazine, and salicyloylhydrazine in refluxing butanol gave triazolopyridazine **8** and **9**. Although the yield by the conventional method and the microwave irradiation was approximately the same, the microwave irradiation was saving time, whereas the reaction time was reduced from 48 hours for the conventional method down to 8–10 minutes for microwave irradiation (Table 2).

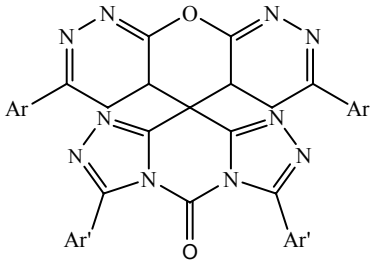

(8) Ar' = C_6H_5
(9) Ar' = C_6H_4.OH(2)

Figure(5)

Table 2. Observed yield and reaction time.

Comp.	Conventional heating	Microwave irradiation		
No.	Yield, %	Time, min	Power, W	Yield, %
2	49.2	20	180	75
		20	270	96.8
3	28.8	4	540	57.6
4	50	3	540	98
5	62	5	540	82.8
6	96.8	–		–
7a	40	8	630	38
7b	52	8	630	47
8	63	10	720	67.4
9	73.2	8	720	75

CONCLUSION

In conclusion, the results demonstrate a simple and efficient synthesis method of spiro derivatives in almost excellent yields. While the conventional thermal methods require considerable reaction time, the microwave irradiation can substitute classical methods allowing easy and rapid access to spiro derivatives, reducing the reaction times from hours to minutes with improved yields.

EXPERIMENTAL

All microwave reactions were carried out in a domestic microwave oven (Galanz WP900AP23-2). All melting points were uncorrected. The IR spectra were recorded in KBr on FTIR Mattson Spectrometers. The ^{1}H NMR and ^{13}C NMR spectra were measured on Varian Gemini 200 MHz instrument with chemical shift (δ) expressed in ppm downfield from TMS. The mass spectra were recorded on Shimadzu GC-MS-QP 1000 Ex and MS_5988 instruments at 70 eV. The TLC analysis was run using TLC aluminium sheets silica gel F_{254} (Merck). The structures of all compounds have been confirmed by spectroscopic studies.

Synthesis of 3-(4-chloro-3-methyl)benzoylprop-2-enoic acid **1**. This compound has been prepared according to reference [9] as yellow crystals, m.p. 130–131°C.

Synthesis of 2,2'-(2,4,6-trioxohexahydropyrimidine-5,5-diyl)bis[3-(4-chloro-3-methyl)benzoylpropionic acid) **2**. *(A) By conventional method.* To a mixture of 3-(4-chloro-3-methyl)benzoylprop-2-enoic acid **1** (2 g) and barbituric acid (1.03 g) in 30 ml ethanol, 2 ml of aqueous NaOH (50%) were added .The mixture was left to stay at room temperature for 4 days. The solvent was evaporated; the solid that separated was dissolved in water and then poured onto ice/HCl, filtered, washed with water and recrystallized from benzene.

(B) By microwave radiation. A mixture of 3-(4-chloro-3-methyl)benzoylprop-2-enoic acid **1** (2 g) and barbituric acid (1.03 g) in 10 ml of aqueous NaOH (50%) was irradiated with microwaves at *P* = 180 and 270 W for 20 min in subsequent intervals (5 min for each interval) (Table 2). The solid phase that separated was dissolved in water and then poured onto ice/HCl, filtered, washed with water and recrystallized from benzene.

The product was yellow crystals, m.p. 200–202°C; IR cm^{-1}: 1756–1683 (C=O),) and 3316 (NH). ^{1}H NMR (DMSO) δ: 2.4 (s, 6H, CH_3), 3.47–3.49 (dd, 2H, 2CH), 3.6–4.0 (2dd, 4H, $2CH_2$), 7.5–7.9 (m, 6ArH), 11.2 (s,2H, 2NH) and 11.3 (s, 2H, 2COOH). MS m/z: 533 (18.75), 224 (8.19), 180

(10.69), 153 (48.47), 128 (14.58), 105 (100), 77 (45.97) and 55 (46.39); Anal. calcd. for $C_{26}H_{22}Cl_2N_2O_9$: C, 54.11; H, 3.81; Cl, 12.28; N, 4.85; Found: C, 54.32; H, 3.72; Cl, 12.36; N, 4.79.

Synthesis of spiro compound with oxazine moiety **3**. *(A) By conventional heating*. A mixture of the acid **2** (0.01mol) and hydroxylamine hydrochloride (0.01mol) in pyridine was refluxed for 3 h. The reaction mixture was poured onto ice/HCl, filtered, washed with water and recrystallized from ethanol.

(B) By microwave radiation. A mixture of the acid **2** (0.01 mol) and hydroxylamine hydrochloride (0.01 mol) in the smallest amount of pyridine was irradiated with microwaves at P = 540 W for 4 min (Table 2). The reaction mixture was poured onto ice/HCl, filtered, washed with water and recrystallized from ethanol.

The product was brown crystals, m.p. 240–242°C; IR cm^{-1}: 1624 (C=C), 1655 (C=N), 1684 (C=O), and 3426 (NH). ^{1}H NMR (DMSO) δ: 2.4 (s, 6H, $2CH_3$), 4.1 (s, 4H, $2CH_2$), 6.7–7.9 (m, 6ArH) and 11.1 (s, 2H, 2NH). MS m/z: 510 (54.29), 386 (45.71), 385 (45.71), 343 (34.29), 309 (37.14), 172 (68.57), 80 (82.86), and 58 (100). Anal. calcd. for $C_{26}H_{18}Cl_2N_4O_6$: C, 56.45; H, 3.25; Cl, 12.81; N, 10.12; Found: C, 55.95; H, 3.19; Cl, 12.67; N, 10.15.

Synthesis of spiro compound with pyridazine moiety **4**. *(A) By conventional heating*. A mixture of the acid **2** (0.01 mol) and hydrazine hydrate (0.01 mol) in ethanol (30 ml) was refluxed for 6 h. The solid phase that separated out after concentrating and cooling down was filtered off and recrystallized from methanol to give **4**.

(B) By microwave radiation. A mixture of the acid **2** (0.01 mol) and hydrazine hydrate (0.01 mole) was irradiated under microwaves at P = 540 W for 3 min (Table 2). The solid phase that separated out, was filtered off and recrystallized from methanol to give **4**.

The product was yellow crystals m.p. 220–222°C, IR cm^{-1}: 1592 (C=N), 1682 (C=O) and 3330 (NH). ^{1}H NMR (DMSO) δ: 1.10–1.80 (m, 4H, $2CH_2$), 2.19–2.39 (m, 2H, 2CH), 2.48, 2.49 (2s, 6H, $2CH_3$), 6.9–8.0 (m, 6H, ArH), and 11.18 (s, 2H, 2NH). MS m/z: 407 (1.4), 398 (10.3), 220 (57.2), 219 (63.8), 162 (31.2), 127 (100), 128 (82.3) and 52 (20.5). Anal. calcd. for $C_{26}H_{20}Cl_2N_6O_4$: C, 56.65; H, 3.26; Cl, 12.86; N, 15.24; Found: C, 56.70; H, 3.73; Cl, 12.83; N, 15.30.

Synthesis of the dichloro derivative **5.** *(A) By conventional heating*. A mixture of the spiro compound with pyridazine moiety **4** (0.01 mol) and PCl_5 (0.5 g) in $POCl_3$ (10 ml) was heated on a water bath for 3 h. The reaction mixture was poured gradually onto crushed ice and the solid phase that separated out was filtered off and recrystallized from methanol.

(B) By microwave radiation. A mixture of the spiro compound with pyridazine moiety **4** (0.01 mol) and PCl_5 (0.5 g) in $POCl_3$ (10 ml) was irradiated under microwaves at P = 540 W for 5 min (Table 2). The reaction mixture was poured gradually onto crushed ice and the solid phase that separated out was filtered off and recrystallized from methanol.

The product was pale brown crystals, m.p. 230–232°C, IR cm^{-1}: 1602 (C=N) and 1687(C=O), ^{1}H NMR (DMSO) δ: 2.10–2.13 (m, 4H, $2CH_2$), 2.40–2.45 (m, 2H, 2CH), 2.45 (s, 6H, $2CH_3$) and 7.2–8.1 (m, 6H, ArH). MS m/z: 564 (43.33), 432 (36.67), 358 (43.33), 324 (33.33), 233 (53.33), 234 (63.33), 78 (36.67), 70 (53.33), 72 (100), and 68 (40.00). Anal. calcd. for $C_{26}H_{18}Cl_4N_6O_2$: C, 53.10; H, 3.06; Cl, 24.11; N, 14.28; Found: C, 53.35; H, 3.03; Cl, 24.23; N, 14.24 .

Synthesis of the spirotetrazolo derivative **6**. A mixture of the dichloro derivative **5** (0.003 mol) and sodium azide (0.5 g/5 ml water) in DMF (30 ml) was refluxed for 3 h, cooled down and 100 ml of water was added. The solid phase that separated out was filtered off and recrystallized from ethanol.

The product was brown crystals, m.p. > 300°C, IR cm^{-1}: 1583 (C=C), 1597 (C=N), and 1685 (C=O). ^{1}H NMR (DMSO) δ: 2.38–2.39 (m, 4H, $2CH_2$), 2.74, 2.88 (dd, 2H, 2CH), 2.49 (s, 6H, $2CH_3$), and 7.5–7.9 (m, 6H, ArH); MS m/z: 438 (13.9), 110 (32.0), 98 (24.3), 96 (54.0), 94 (25.9), 70 (56.0), 57 (91.3), 56 (100), and 54 (64.7). Anal. calcd. for $C_{26}H_{18}Cl_2N_{12}O_2$: C, 51.94; H, 2.99; Cl, 11.79; N, 27.94; Found: C, 51.64; H, 2.97; Cl, 11.84; N, 27.64.

Synthesis of the triazolo derivatives **7**. *(A) By conventional heating.* A solution of the dichloro derivative **5** (0.01 mol) and monosaccharide hydrazones namely glucose hydrazone, and mannose hydrazone (0.15 mol) in *n*-butanol (40 ml) was refluxed for 6 h. The solid phase that separated after concentrating and cooling down was filtered out and recrystallized from acetic acid.

(B) By microwave radiation. The dichloro derivative **5** (0.01 mol) and monosaccharide hydrazones namely glucose hydrazone, and mannose hydrazone (0.15 mol) in the smallest amount of *n*-butanol were irradiated with microwaves at P = 630 W for 8 min (Table 2). The solid phase that separated was recrystallized from acetic acid.

The product was brown crystals, m.p. 260°C (dec.); IR cm^{-1}: 1545 (C=C), 1588 (C=N), 1683 (C=O), and 3061 (OH). ^{1}H NMR (DMSO) δ: 1.30–1.50 (m, 4H, $2CH_2$), 2.34–2.36 (m, 2H, 2CH), 2.40

(s, 6H, $2CH_3$), 3.75 (d, 2H, 2-CHOH–CH–N), 3.78–3.82 (m, 10H, carbohydrate moiety), 4.08 (br.s, 8H, 8OH), and 6.89–7.86 (m, 8H, 6ArH+2N=CH). MS m/z: 841 (36.36), 843 (48.48), 766 (33.33), 658 (36.36), 522 (33.33), 342 (42.42), 313 (51.52), and 170 (100). Anal. calcd. for $C_{38}H_{40}Cl_2N_{10}O_{10}$: C, 52.62; H, 4.61; Cl, 8.17; N, 16.14; Found: C, 52.35; H, 4.59; Cl, 8.20; N, 16.32 .

Synthesis of the spirotriazolopyridazine derivatives **8**, **9**. *(A) By conventional heating.* A solution of the dichloro derivative **5** (0.01 mol) and the acylhydrazines (0.01 mol), namely benzoylhydrazine and salicyloylhydrazine in 30 ml butanol was heated under reflux for 48 h. The solid phase that separated after concentrating and cooling down was filtered out and recrystallized from ethanol.

(B) By microwave radiation. The dichloro derivative **5** (0.01 mol) and the acylhydrazines (0.01 mol), namely benzoylhydrazine and salicyloylhydrazine in the smallest amount of *n*-butanol were irradiated under microwaves at P = 720 W for 8, 10 min (Table 2). The solid phase that separated was recrystallized from ethanol.

Spirotriazolopyridazine derivatives **8**. The products were brown crystals, m.p. > 300°C, IR cm^{-1} 1550 (C=C), 1600 (C=N), and 1660 (C=O). ^{1}H NMR (DMSO) δ: 1.22 (m, 4H, $2CH_2$), 2.3–2.40 (m, 2H, 2CH), 2.49 (s, 6H, $2CH_3$), and 7.62–8.51 (m, 16H, ArH). MS m/z: 740 (32.35), 704 (32.35), 467 (32.35), 327 (55.88), 276 (32.35), 196 (32.35), 168 (100), and 96 (29.41). Anal. calcd. for $C_{40}H_{28}Cl_2N_{10}O_2$: C, 63.94; H, 3.72; Cl, 9.43; N, 18.63; Found: C, 63.65; H, 3.82; Cl, 9.31; N, 18.71.

Spirotriazolopyridazine derivatives **9**. The products were brown crystals, m.p. > 300°C, IR cm^{-1} 1550 (C=C), 1601 (C=N), 1671 (C=O) and 3199 (OH). ^{1}H NMR (DMSO) δ: 1.23 (m, 4H, $2CH_2$), 2.43–2.46 (m, 2H, 2CH), 2.46 (s, 6H, $2CH_3$), 7.1–8.6 (m, 14, ArH), and 11.02 (br.s, 2H, 2OH). MS m/z: 322 (35.58), 320 (100.0), 194 (40.14), 126 (43.89), 96 (51.84), 84 (66.47), 68 (68.11), and 56 (66.35). Anal. calcd. for $C_{40}H_{28}Cl_2N_{10}O_4$: C, 61.33; H, 3.57; Cl, 9.05; N, 17.87; Found: C, 61.17; H, 3.68; Cl, 9.11; N, 17.76.

REFERENCES

1. C. O. Kappe, *Angew. Chem. Int. Ed.,* **43**, 6250 (2004).
2. P. Lidström, J. Tierney, B. Wathey, J. Westman, *Tetrahedron*, **57**, 9225 (2001).
3. R. S. Varma, *Green Chem*., **1**, 43 (2001).
4. C. Gabriel, S. Gabriel, E. H. Grant, B. S. Halstead, D. M. Mingos, *Chem. Soc. Rev*., **27,** 213 (1998).
5. F. G. Baddar, F. H. Al-Hajjar, N. R. El-Rayyes, *J. Heterocycl. Chem*., **13**, 25 (1976).
6. P. A. M. Herdewign, *Antiviral Res*., **19**, 1 (1992).
7. J. D. Albright, D. B. Moran, W. B. Wright, J. B. Collins, B. Beer, A. S. Lippa, E. N. Greenbalt, *J. Med. Chem*., **24**, 592 (1981).
8. G. C. Levy, R. L. Lichter, G. L. Nelson, Carbon-13 Nuclear Magnetic Resonance Spectroscopy, 2nd ed., Wiley-Interscience Publication, New York, 1980.
9. D. Papa, E. Schwenk, F. Villani, E. Klingsberg, *J. Am. Chem. Soc*., **70**, 3356 (1948).

СИНТЕЗ НА ТЕТРА- И ХЕКСАЦИКЛИЧНИ СПИРО СИСТЕМИ ПОД ДЕЙСТВИЕ НА МИКРОВЪЛНИ

М. И. Марзук

Департамент по химия, Факултет по науки, Университет Аин Шамс, Абасия, Кайро, Египет

Постъпила на 25 юни 2008 г.; Преработена на 4 август 2008 г.

При реакцията на 3-(4-хлоро-3-метил)бензоилпроп-2-енова киселина и барбитурова киселина е получена 2,2'-(2,4,6-триоксохексапиримидин-5,5-диил)бис[3-(4-хлоро-3-метил)бензоилпропионова киселина, която реагира с хидроксиламин хидрохлорид и хидразин хидрат до съответните спиро съединения. При реакцията на спиро съединенията, съдържащи пиридазинова част, с $PCl_5/POCl_3$ се получава дихлорно производно, което реагирайки с натриев азид, монозахарид хидразони и ацилхидразиди образува съответни тетразоло- и триазоло-производни. Всички реакции са проведени при обикновени условия и при облъчване с микровълни.

Bulgarian Chemical Communications, Volume 41, Number 1 (pp. 59–64) 2009

Synthesis and antimicrobial activity of 2,4,8,10,13-pentamethyl-6-substituted-13,14-dihydro-12H-6λ^5-dibenzo[d,i] [1,3,7,2]dioxazaphosphecin-6-oxides, sulphides and selenides

A. U. R. Sankar, B. S. Kumar, M. V. N. Reddy, S. S. Reddy, C. S. Reddy, C. N. Raju*,

Department of Chemistry, Sri Venkateswara University, Tirupati-517 502, India

Received January 24, 2008; Revised September 1, 2008

Synthesis of novel 2,4,8,10,13-pentamethyl-6-substituted-13,14-dihydro-12H-6λ^5-dibenzo[d,i][1,3,7,2]dioxazaphosphecin-6-oxides was accomplished by condensation of bis(2,4-dimethyl-2-hydroxybenzyl)methylamine with phosphorus-containing dichlorides in the presence of triethylamine at 40–50°C. Corresponding oxides, sulphides and selenides were prepared in a two-step process. Bis(2,4-dimethyl-2-hydroxybenzyl) methylamine was condensed with phenyldichlorophosphine and ethyldichlorophosphite to obtain the trivalent phosphorus intermediate compounds. In the second step, the latter compounds were treated with hydrogen peroxide, sulphur and selenium to obtain the corresponding oxides, sulphides and selenides, respectively. Their structures were established by elemental analysis, IRS, NMR (^{1}H, ^{13}C and ^{31}P) and mass spectral data. Their antimicrobial activity was also evaluated.

Key words: dioxazaphosphecin-6-oxides, sulphides and selenides, dichlorides, antimicrobial activity.

INTRODUCTION

Organophosphorus compounds containing important pharmacophoric moieties are used in agriculture as pesticides and in medicine as drugs [1]. Phosphorus macrocycles containing P(III) in view of their unique structures (i.e. host molecules) possess complexation abilities [2, 3]. Phosphorus macrocycles have already found numerous industrial [4] and biological [5] applications.

Phosphorus-containing macrocycles are interesting molecules with potential applications in supramolecular and synthetic organic chemistry. They have been synthesized as phosphine oxides, phosphines, phosphonium salts, phosphates, phosphonates and phosphoranes [6]. The importance of these molecules, as phosphorus analogues of crown ethers, is derived from their potential catalytic activity and ion carrying properties. The design of host molecule capable of binding neutral organic molecules as guests is an area of rapidly expanding interest [7]. Cram [8] and Vogtle [9] have made significant advances in the field of host-guest complexation [10]. Phosphorus-containing macrocycles are expected to function as good 'hosts' in the 'host-guest chemistry'. In view of these and several other possible applications, phosphorus macroheterocycles with oxygen and nitrogen as donor atoms, have been synthesized, characterized and their antimicrobial activity has been evaluated.

* To whom all correspondence should be sent:
E-mail: naga_raju04@yahoo.co.in

© 2009 Bulgarian Academy of Sciences, Union of Chemists in Bulgaria

RESULTS AND DISCUSSION

6-Substituted-dioxazaphosphecin-6-oxides (**3a-c**) containing oxygen, nitrogen and phosphorus atoms in the ten-membered heterocycles were synthesized by reacting equimolar quantities of bis(2,4-dimethyl-2-hydroxybenzyl) methylamine (**1**) with 4-nitrophenyl phosphorodichloridate (**2a**), bis(2-chloroethyl)phosphoramidic dichloride (**2b**) and 4-chlorophenyl-phosphorodichloridate (**2c**) in toluene in the presence of triethylamine at 40–50°C. The intermediate trivalent phosphorus compounds (**5a,b**) were prepared by cyclocondensation of **1** with phenyldichlorophosphine and ethyl dichlorophosphite in toluene in the presence of triethylamine at 10–30°C. Compounds **5a** and **5b** were converted into the corresponding oxides, sulphides and selenides (**6a–f**) by reacting with hydrogen peroxide, sulphur and selenium, respectively, in refluxing toluene. Physical data of **3a–c** and **6a–f** are given in Table 1.

The title compounds **3a–c** and **6a–f**, exhibited characteristic bands [11, 12] in their IR spectra, in the regions 1241–1304 cm^{-1}, 954–964 and 1196–1128 cm^{-1} for P=O, P–O–C (Ar), respectively. Characteristic bands were also observed for P=S and P=Se groups in the expected regions 737–774 and 678–687 cm^{-1}, respectively.

Proton NMR spectral data of the title compounds **3a–c** and **6a–f** showed a singlet in the region δ 3.00–3.24 for N–CH_3. The methylene protons (C-12 & C-14) (4H) resonated [13] as a multiplet at δ

3.59–4.48. The aromatic protons showed complex multiplet in the region δ 6.50–8.28. Nitrogen mustard group (**3c**) resonated as two multiplets, one at δ 3.94–4.06 (m, 4H, –N–CH_2–) and the other at δ 3.01–3.04 (m, 4H, –CH_2Cl). The 6-ethoxy group in **6d–f** gave a quartet at δ 4.20–4.25 for –OCH_2– and a triplet at δ 1.31–1.40 for –CH_3.

The ^{13}C NMR chemical shifts of **3a–c** and **6a–f** were interpreted based on additivity rules, computed chemical shifts of starting compound **1,** intensity of signals and carbon coupling with phosphorus. The oxygen bearing carbons in **4a** and **7a** resonated in the region 147.8–151.6 ppm [14]. The methylene carbons (C-12 & C-14) resonated in the region 52.2–57.9 ppm. The N–CH_3 (C-13) resonated in the region 35.20–38.90 ppm as a signlet. The methyl carbons (C-2 & C-10) and (C-4 & C-8) gave signals at δ 20.2–20.6 and at 17.2–17.9, respectively. The two methylene carbons [2C–N(CH_2)$_2$] directly bonded to nitrogen atom of the mustard group in **3c** resonated as a doublet at δ 50.8 [$^2J_{PN–C}$ = 6.3 Hz] due to their coupling with phosphorus atom. A singlet was observed for the chloro-substituted methylene carbons [2C–(CH_2Cl)$_2$] at δ 42.6. Other carbon chemical shifts appeared in the expected region.

^{31}P Resonance signals appeared within the region –3.65 to –10.85 ppm for compounds **3a–c**. ^{31}P NMR resonances of **6b** & **6c** and **6e** & **6f** appeared in the region 79.65, 88.82 and 68.00 & 78.06 ppm due to its attachment to the sulphur and selenium atoms respectively. The compound **6a** and **6d** showed their ^{31}P NMR signals at δ 12.80 and 18.00 respectively [15, 16]. The compounds **3c, 6a** and **6c g**ave $m^{+\bullet}$ ions in their FAB at m/z 420 (19.6), 421 (16.6 M +1) and 484 (98), respectively.

EXPERIMENTAL

Melting points were determined using a Mel-Temp apparatus and were uncorrected. Elemental analyses were performed at the Central Drug Research Institute, Lucknow, India. The IR spectra were recorded as KBr pellets on a Perkin-Elmer 1000 unit. The ^{1}H, ^{13}C and ^{31}P {^{1}H} NMR spectra were recorded on AMX 400 MHz spectrometer operating at 400 MHz for ^{1}H, 100 MHz for ^{13}C and 161.9 MHz for ^{31}P. The compound was dissolved in DMSO-d_6 and the chemical shifts were referenced to TMS (^{1}H & ^{13}C) and 85% H_3PO_4 (^{31}P). Fast atom bombardment (FAB) mass spectra were recorded on JEOL SX 102/DA-6000 system using Argon/Xenon (6 keV, 10 mA) as the FAB gas, at RSIC, Central Drug Research Institute (CDRI), Lucknow, India.

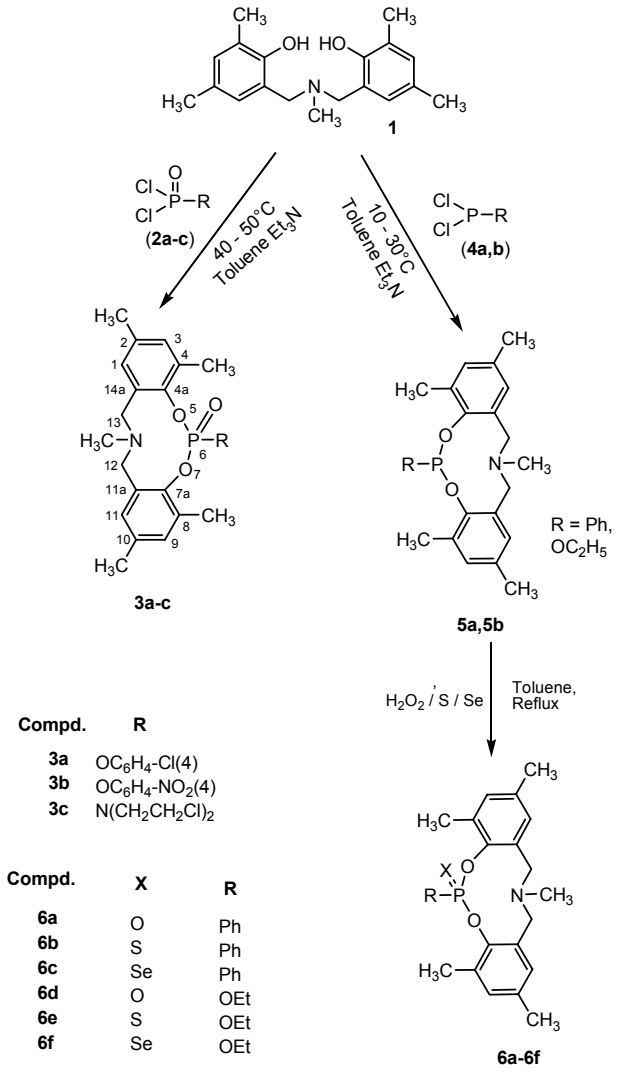

Scheme 1.

GENERAL PROCEDURES

Bis(2,4-dimethyl-2-hydroxybenzyl)-methylamine **(1)** was prepared according to the reported procedure [17].

Synthesis of 2,4,8,10,13-pentamethyl-6-(4-nitro-phenoxy)-13,14-dihydro-12H-6λ^5-dibenzo[d,i][1,3, 7,2]dioxazaphosphecin-6-oxide (**3b**). A solution of 4-nitrophenylphosphorodichloridate (520 mg, 2 mmol) in 25 mL of dry toluene was added dropwise over a period of 20 minutes to a stirred solution of bis(2,4-dimethyl-2-hydroxybenzyl)methylamine (600 mg, 2 mmol) and triethylamine (404 mg, 4 mmol) in 20 mL of dry toluene in the course of 20 minutes at 10°C. After the addition, the temperature of the reaction mixture was raised to room temperature and stirred for 3 h, later the reaction mixture was stirred at 40–50°C for another 3 h. The progress of the reaction was monitored by TLC analysis (ethyl acetate-hexane, 1:2) on silicagel as adsorbent. The precipitated triethylamine hydrochloride was sepa-

rated by filtration and the filtrate was evaporated in a rotary-evaporator. The residue was washed with water and recrystallised from chloroform-hexane (1:3), yield 560 mg (69%); m.p. 132–133°C. Compounds **3a**,**c** were prepared by applying the above procedure.

Preparation of the compounds **6a-c.** A solution of phenyl dichlorophosphine (**4a**, 300 mg, 2 mmol) in 25 mL of dry toluene was added dropwise over a period of 20 minutes to a stirred solution of bis(2,4-dimethyl-2-hydroxybenzyl) methylamine (**1**, 600 mg, 2 mmol) and triethylamine (404 mg, 4 mmol) in 25 mL of dry toluene at 0°C under N_2 atmosphere. After the addition, the temperature of the reaction mixture was raised to room temperature and stirred for 3 h, later the reaction mixture was stirred at 30°C for another 3 h. The triethylamine hydrochloride was removed by filtration. To the filtrate (**5a**) hydrogen peroxide (30%) (200 mg, 2 mmol) was added at 5–10°C and stirred for 3 h at 50–60°C. The progress of the reaction was monitored by TLC analysis (ethyl acetate-hexane, 1:2) on silica gel. The solvent was removed in a rotary-evaporator. The residue was washed with water and recrystallised from 2-propa-nol, yield 860 mg (58%), m.p. 205–207°C. Com-pounds **6b** and **6c** were prepared by reacting with sulphur and selenium respectively by applying the above procedure.

Preparation of the compounds **6d-f.** A solution of ethyl dichlorophosphite (**4b**, 300 mg, 2 mmol) in 20 mL of dry toluene was added dropwise over a period of 20 minutes to a stirred solution of bis(2,4-dimethyl-2-hydroxybenzyl)methylamine (**1**, 600 mg, 2 mmol) and triethylamine (404 mg, 4 mmol) in 25 mL of dry toluene at 0°C under N_2 atmosphere. After the addition, the temperature of the reaction mixture was stirred at 20–30°C for another 2 h. The triethylamine hydrochloride was removed by filtration. To the filtrate (**5b**) selenium (200 mg 2 mmol) was added at 10–20°C and stirred for 3 h at 60–70°C. The progress of the reaction was monitored by TLC analysis (ethyl acetate-hexane, 1:2) on silicagel. The solvent from the reaction mixture was removed in a rotary-evaporator. The residue was washed with water and recrystallised from 2-propanol to obtain **6f**, yield 620 mg (62%); m.p. 156–158°C. Com-pounds **6d** and **6e** were prepared by using hydrogen peroxide and sulphur respectively by adopting the above procedure.

SUMMARY

A new class of substituted 13,14-dihydro-12H-6λ^5-dibenzo[d,i][1,3,7,2]dioxazaphosphecin-6-oxides, sulphides and selenides were conveniently synthesized and shown to have high antimicrobial activity.

ANTIMICROBIAL ACTIVITY

The antibacterial activity of all the title compounds (**3a–c**) and (**6a–f**) was assayed [18] against the growth of *Staphylococcus aureus* (gram +ve) and *Escherichia coli* (gram –ve) at two different concentrations (100, 50 ppm) (Table 1). The majority of the compounds exhibited high activity against both kinds of bacteria. The achievement is that three compounds, **3c**, **6c** and **6f** were more effective than that of the standard penicillin.

The compounds **3a–c** and **6a–f** were screened for their antifungal activity against *Aspergillus niger* and *Helminthosporium oryzae* species along with the standard fungicide *Griseofulvin* (Table 2) by the disc diffusion method [19] at two different concentrations (100, 50 ppm). It is rewarding to observe that the majority of the compounds **3a–c** and **6a–f** exhibited higher antifungal activity when compared with that of the standard *Griseofulvin* .

The great success is the fact that **3b, 6c** and **6f** exhibited higher activity than that of the standard *Griseofulvin* against both kinds of fungi. Thus, new compounds with much higher antimicrobial activity than that of the presently used commercial bactericides/fungicides have been discovered.

Table 1. Antibacterial activity of the compounds (**3a–c**) and (**6a–f**).

Compound	Zone of inhibition, mm			
	Escherichia coli		*Staphylococcus aureus*	
	100	50	100	50
3a	13	7	12	9
3b	12	9	13	6
3c	16	10	18	10
6a	10	8	10	8
6b	12	6	11	6
6c	18	11	16	11
6d	15	5	12	5
6e	13	6	14	7
6f	18	10	16	10
Penicillin	15	8	15	8

Table 2. Antifungal activity of the compounds (**3a–c**) and (**6a–f**).

Compound	Zone of inhibition, mm			
	Aspergillus niger		*Helminthosporium oryzae*	
	100	50	100	50
3a	10	7	12	9
3b	14	10	15	12
3c	11	8	10	8
6a	9	5	11	6
6b	12	6	12	10
6c	15	12	13	6
6d	10	7	10	9
6e	9	8	12	7
6f	14	10	15	10
Griseofulvin	12	8	12	8

2,4,8,10,13-Pentamethyl-6-(4-chlorophenoxy)-13,14-dihydro-12H-6λ^5-dibenzo-[d,i][1,3,7,2]-dioxazaphosphecin-6-oxide (**3a**). Yield 64%; m.p. 164–166°C. IR (KBr) cm^{-1}: 1262 (P=O), 959 (P–O), 1228 (O–C); ^{1}H-NMR (DMSO-d_6) δ: 6.76–7.92 (m, 8H, Ar–H), 3.72–4.35 (m, 4H, CH_2), 3.09 (s, 3H, N–CH_3), 2.21 (s, 12H Ar–CH_3); ^{13}C-NMR(DMSO-d_6) δ: 128.6 (C-1 & C-11), 130.6 (C-2 & C-10), 124.5 (C-3 & C-9), 131.6 (C-4 & C-8), 133.5 (C-11a & C-14a), 52.5 (C-12 & C-14), 148.5 (d, *J* = 8.4 Hz, C-4a & C-7a), 35.5 (N–CH_3), 20.4 (C-2 & C-10, Ar–CH_3), 17.5 (C-4 & C-8, Ar–CH_3), 149.0 (d, *J* = 7.3 Hz, C-1′), 121.2 (C-2′ & C-6′), 125.5 (C-3′ & C-5′), 133.3 (C-4′); ^{31}P-NMR (DMSO-d_6), δ-10.85. Anal.Calcd. for $C_{25}H_{27}ClNO_4P$: C, 63.63; H, 5.77; N, 2.97. Found: C, 63.55; H, 5.72; N, 2.90%.

2,4,8,10,13-Pentamethyl-6-(4-nitro-phenoxy)-13, 14-dihydro-12H-6λ^5-dibenzo-[d,i] [1,3,7,2]-dioxazaphosphecin-6-oxide (**3b**). Yield 62%; m.p. 178–180°C. IR (KBr) cm^{-1}: 1290 (P=O), 954 (P–O), 1218 (O–C); ^{1}H-NMR (DMSO-d_6) δ: 6.70–8.30 (m, 8H, Ar–H), 3.68–4.40 (m, 4H, CH_2), 3.00 (s, 3H, N–CH_3), 2.27 (s, 12H, Ar–CH_3) ^{13}C-NMR (DMSO-d_6) δ: 128.4 (C-1 & C-11), 130.4 (C-2 & C-10), 124.7 (C-3 & C-9), 131.5 (C-4 & C-8), 133.7 (C-11a & C-14a), 52.2 (C-12 & C-14), 148.3 (d, *J* = 8.2 Hz, C-4a & C-7a), 35.2 (N–CH_3), 20.5 (C-2 & C-10, Ar–CH_3), 17.2 (C-4 & C-8, Ar–CH_3), 149.5 (d, *J* = 7.2Hz, C-1′), 120.8 (C-2′ & C-6′), 125.3 (C-3′ & C-5′), 133.4 (C-4′). ^{31}P-NMR (DMSO-d_6) δ: –3.65. Anal. Calcd. for $C_{25}H_{27}N_2O_6P$: C, 62.24; H, 5.64; N, 5.81. Found: C, 62.18; H, 5.60; N, 5.76%.

2,4,8,10,13-Pentamethyl-6-[bis-2-chloroethyl)-amino]-13,14-dihydro-12H-6λ^5-dibenzo-[d,i][1,3,7, 2]dioxazaphosphecin-6-oxide (**3c**). Yield 60%; m.p. 180–182°C. IR (KBr) cm^{-1}: 1292 (P=O), 954 (P–O), 1220 (O–C); (DMSO-d_6) δ: 6.70–7.33 (m, 4H, Ar–H), 3.78–3.87 (m, 4H, CH_2), 3.15 (s, 3H, N–CH_3), 2.21 (s, 12H, Ar–CH_3), 3.94–4.06 (t, 4H, N–CH_2), 3.27–3.24 (t, 4H, CH_2Cl); ^{13}C-NMR (DMSO-d_6) δ: 128.5 (C-1 & C-11), 130.5 (C-2 & C-10), 124.6 (C-3 & C-9),131.4 (C-4 & C-8), 133.6 (C-11a & C-14a), 52.3 (C-12 & C-14), 148.6 (d, *J* = 8.6 Hz, C-4a & C-7a), 35.4 (N–CH_3), 20.6 (C-2 & C-10, Ar–CH_3), 17.4 (C-4 & C-8, Ar–CH_3), 50.8 (d, *J* = 6.3 Hz, N–CH_2), 42.6 (–CH_2Cl). ^{31}P-NMR (DMSO-d_6) δ: –8.20; FAB m/z (%): [420 (19.6) M$^+$], 380 (15), 362 (16), 300 (100), 246 (20), 215 (17), 164 (26), 135 (60), 91(20). Anald. Calcd. for $C_{23}H_{31}Cl_2N_2O_3P$: C, 56.91; H, 6.44; N, 5.77. Found: C, 56.84; H, 6.39; N, 5.71%.

2,4,8,10,13-Pentamethyl-6-phenyl-13,14-dihydro-12H-6λ^5-dibenzo-[d,i][1,3,7,2]-dioxazaphosphecin-6-oxide (**6a**). Yield 58%; m.p. 157–159°C; IR (KBr) cm^{-1}: 1241 (P=O), 748 (P–C aryl); ^{1}H-NMR (DMSO-d_6) δ: 6.82–7.94 (m, 9H, Ar–H), 3.71–4.35 (m 4H, CH_2), 3.20 (s, 3H, N–CH_3), 2.20 (s, 12H, Ar–CH_3); ^{13}C-NMR (DMSO-d_6) δ: 128.7 (C-1 & C-11), 130.7 (C-2 & C-10), 125.3 (C-3 & C-9), 131.7 (C-4 & C-8), 134.1 (C-11a & C-14a), 56.5 (C-12 & C-14), 147.8 (d, *J* = 8.5 Hz, C-4a & C-7a), 38.5 (N–CH_3), 20.6 (C-2 & C-10, Ar–CH_3), 17.4 (C-4 & C-8, Ar–CH_3), 131.1 (C-1^1), 126.6 (C-2^1 & C-6^1), 128.0 (C-3^1 & C-5^1), 124.3 (C-4^1); ^{31}P-NMR (DMSO-d_6) δ: 12.80; FAB m/z (%): [421 (16.6), M+1], 406 (11), 328 (20), 300 (100), 273 (75, 257 (11), 194(10), 164 (17), 154(23), 135 (50), 119(12); Anal. Caled. for $C_{25}H_{28}NO_3P$: C, 71.24; H, 6.70; N, 3.32 Found: C, 71.17; H, 6.65; N, 3.28%.

2,4,8,10,13-Pentamethyl-6-phenyl-13,14-dihydro-12H-6λ^5-dibenzo-[d,i][1,3,7,2]-dioxazaphosphecin-6-sulfide (**6b**). Yield 52%; m.p. 162–164°C; IR (KBr) cm^{-1}: 774 (P=S), 751 (P–C aryl); ^{1}H-NMR (DMSO-d_6) δ: 6.85–8.25 (m, 9H, Ar–H), 3.70–4.26 (m, 4H, CH_2), 3.25 (s, 3H, N–CH_3), 2.20 (s, 12H, Ar–CH_3); ^{13}C-NMR (DMSO-d_6) δ: 131.8 (C-1 & C-11), 130.8 (C-2 & C-10), 126.6 (C-3 & C-9); 133.2 (C-4 & C-8), 134.2 (C-11a & C-14a), 57.0 (C-12 & C-14), 149.0 (d, *J* = 8.2 Hz, C-4a & C-7a), 38.4 (N–CH_3), 20.4 (C-2 & C-10, Ar–CH_3), 17.5 (C-4 & C-8, Ar–CH_3), 131.2 (C-1^1), 127.8 (C-2^1 & C-6^1), 128.0 (C-3^1 & C-5^1), 122.3 (C-4^1); ^{31}P-NMR (DMSO-d_6) δ: 79.65; Anal. Calcd for $C_{25}H_{28}NO_2PS$: C, 68.63; H, 6.45; N, 3.20. Found: C, 68.70; H, 6.40; N, 3.17%.

2,4,8,10,13-Pentamethyl-6-phenyl-13,14-dihydro-12H-6λ^5-dibenzo-[d,i][1,3,7,2]-dioxazaphosphecin-6-selenide (**6c**). Yield 56%; m.p. 216–218°C; IR (KBr) cm^{-1}: 695 (P=Se), 955 (P–O), 1260 (O–C), 753 (P–C aryl); ^{1}H-NMR (DMSO-d_6) δ: 6.96–8.28 (m, 9H, Ar–H), 3.87–4.24 (m, 4H, CH_2) 3.24 (s, 3H, N–CH_3), 2.24 (s, 12H, Ar–CH_3); ^{13}C-NMR (DMSO-d_6) δ: 131.7 (C-1 & C-11), 130.7 (C-2 & C-10), 126.5 (C-3 & C-9), 132.7 (C-4 & C-8), 133.8 (C-11a & C-14a) 56.4 (C-12 & C-14), 149.3 (d, *J* = 8.3 Hz, C-4a & C-7a), 38.3 (N–CH_3), 20.4 (C-2 & C-10, Ar–CH_3), 17.9 (C-4 & C-8, Ar–CH_3), 131.4 (C-1^1), 126.0 (C-2^1 & C-6^1), 128.3 (C-3^1 & C-5^1), 122.3 (C-4^1); ^{31} P-NMR (DMSO-d_6) δ: 88.82; FAB m/z (%): [484 (98), M $^+$•], 483 (22), 482 (21), 422 (35), 441 (20) 440 (100), 407 (19), 406 (13), 241 (15), 164 (30),. 135 (48); Anal. Calcd for $C_{25}H_{28}NO_2PSe$: C, 61.98; H, 5.83; N, 2.89. Found: C, 61.93; H, 5.80; N, 2.85%.

2,4,8,10,13-Pentamethyl-6-ethoxy-13,14-dihydro-12H-6λ^5-dibenzo-[d,i][1,3,7,2]-dioxazaphosphecin-6-oxide (**6d**). Yield 62%; m.p. 156–158°C; IR (KBr) cm^{-1}: 1256 (P=O), 689 (P–O), 1265 (O–C); ^{1}H-NMR (DMSO-d_6) δ: 6.73–7.26 (m, 4H, Ar–H), 3.81–4.20

(m, 4H, CH_2), 3.20 (s, 3H, N–CH_3), 2.22 (s, 12H, Ar–CH_3) 4.20–4.10 (q, 2H OCH_2), 1.31 (t, 3H –CH_3); ^{13}C-NMR (DMSO-d_6) δ: 131.4 (C-1 & C-11), 129.7 (C-2 & C-10), 126.9 (C-3 & C-9), 132.6 (C-4 & C-8), 133.8 (C-11a & C-14a), 56.2 (C-12 & C-14), 151.6 (d, *J* = 8.5 Hz, C-4a & C-7a), 38.4 (N–CH_3), 20.2 (C-2 & C-10, Ar–CH_3), 17.5 (C-4 & C-8, Ar–CH_3), 65.6 (d, *J* = 8.6 Hz, OCH_2), 17.0 (CH_3); ^{31}P-NMR (DMSO-d_6) δ: 18.00; Anal. Calcd. for $C_{21}H_{28}NO_4P$: C, 64.77; H, 7.25; N, 3.60. Found: C, 64.80 H, 7.20; N, 3.56%.

2,4,8,10,13-Pentamethyl-6-ethoxy-13,14-dihydro-12H-6λ^5-dibenzo-[d,i][1,3,7,2]-dioxa zaphosphecin-6-sulfide (**6e**). Yield 60%; m.p. 161–163°C; IR (KBr) cm^{-1}: 737 (P=S), 678 (P–O), 1265 (O–C aryl); ^{1}H-NMR (DMSO-d_6) δ: 6.65–8.10 (m, 4H, Ar–H), 3.59–3.72 (m, 4H, CH_2), 3.17 (s, 3H N–CH_3), 2.21 (s, 12H, Ar–CH_3), 4.23 (q, 2H, OCH_2), 1.36 (t, 3H, CH_3); ^{13}C-NMR (DMSO-d_6) δ: 131.7 (C-1 & C-11), 130.7 (C-2 & C-10), 126.6 (C-3 & C-9), 132.3 (C-4 & C-8), 133.6 (C-11a & C-14a), 57.9 (C-12 & C-14), 149.2 (d, *J* = 8.4 Hz, C-4a & C-7a), 38.9 (N–CH_3), 20.3 (C-2 & C-10, Ar–CH_3), 17.5 (C-4 & C-8, Ar–CH_3), 65.9 (d, *J* = 8.4 Hz, OCH_2), 17.2 (CH_3); ^{31}P-NMR (DMSO-d_6) δ: 68.0; Anal. Calcd. for $C_{21}H_{28}NO_3PS$: C, 62.20; H, 6.96; N, 3.45. Found: C, 62.14; H, 6.90, N, 3.40%.

2,4,8,10,13-Pentamethyl-6-ethoxy-13,14-dihydro-12H-6λ^5-dibenzo-[d,i][1,3,7,2]-dioxazaphosphecin-6-selenide (**6f**). Yield 61%; m.p. 154–156°C; IR (KBr) cm^{-1}: 687 (P=Se), 715 (P–O), 1260 (O–C aryl); ^{1}H-NMR (DMSO-d_6) δ: 6.50–7.23 (m, 4H, Ar–H), 3.75–4.28 (m, 4H, CH_2), 3.18 (s, 3H, N–CH_3), 2.24 (s, 12H, Ar–CH_3), 4.25 (q, 2H, OCH_2), 1.40 (t, 3H, CH_3); ^{31}P-NMR (DMSO-d_6) δ: 78.07; Anal. Calcd. for $C_{21}H_{28}$ NO_3PSe: C, 55.75; H, 6.24; N, 3.10. Found: C, 55.65; H, 6.20; N, 3.04%.

Acknowledgements*: The authors express their thanks to Prof. C. Devendranath Reddy, Department of Chemistry, Sri Venkateswara University, Tirupati for his academic interaction. One of the authors Dr. C. S. R. wishes to thank BRNS, Mumbai, India for providing financial assistance.*

REFERENCES

1. (a) E. K. Gaylis, C. D. Campbell, J. G. Ding Wall, *J. Chem. Soc. Perkin Trans*. **1**, 2845 (1984). (b) A. S. Demir, C. Tannyeli, O. Sesenogle, S. Demic, O. O. Evin, *Tetrahedron Lett.,* **37**, 407 (1996).
2. C. B. Allan, L. B. Spreer, *J. Org. Chem.,* **59**, 7695 (1994).
3. A. M. Caminade, J. P. Majoral, *Chem. Rev.,* **94**, 1183 (1994).
4. J. M. Lehn, *Angew. Chem., Int. Ed. Engl.,* **27**, 89 (1988)**.**
5. D. J. Cram, *Angew. Chem., Int. Ed. Engl*., **27**, 1009 (1988).
6. J. P. Dutasta, P. Simon, *Tetrahedron Lett*., **28**, 3577 (1987).
7. F. Diederich, *Angew. Chem. Int. Ed*. *Engl*., **27**, 362 (1988).
8. A. J. Tucker, C. B. Knobler, K. N. Trueblood, J. D. Cram, *J. Am. Chem. Soc.,* **111**, 8672 (1989).
9. A .Waller, J. Peter-Katinic, W. M. Werher, F. Vogtle, *Chem. Ber*., **123**, 375 (1990)**.**
10. R. Brelow, N. Greenspoon, T. Guo, R. Zarzycki, *J. Am. Chem. Soc.*,**111**, 8296 (1989)**.**
11. L. C. Thomas, The Interpretation of the Infrared Spectra of Organophosphorus Compounds, Heyden and Sons, London, 1974.
12. Y. H. Babu, C. S. Reddy, P. V. G. Reddy, C. D. Reddy,. P. Uma Devi, *J. Heterocycl. Chem.,* **39**, 1039 (2002).
13. R. M. Silverstein, F. X. Webster, Spectrometric Identification of Organic Compounds, 6th ed., John Wiley and Sons, New York, 1998.
14. K. A. Kumar, M. Kasturaiah, C. S. .Reddy, C. D. Reddy, K. D. Berlin, *J. Heterocycl. Chem*., **40**, 345 (2003).
15. P. Haranath, V. Sreedhar Kumar, C. S. Reddy, C. Naga Raju, C. D. Reddy, *Synth. Commun*., **37**, 1697 (2007).
16. L. D. Quin, J. G. Verkade, Phosphorus-31 NMR Spectral Properties in Compound Characterization and Structureal Analysis, VCH, New York, 1994.
17. W. J. Burke, E. L. M. Glennie, C. Weatherbee, *J. Org. Chem***., 29**, 909 (1962).
18. M. V. Narayanareddy, B. Siva Kumar, A. Balakrishna, C. S. Reddy, C. D. Reddy, S. K. Nayak, *ARKIVOC***, XV**, 246 (2007).
19. H. J. Benson, Microbiological Applications, 5th Ed., W. C. Brown Publications, Boston, 1990.

СИНТЕЗ И АНТИМИКРОБНА АКТИВНОСТ НА 2,4,8,10,13-ПЕНТАМЕТИЛ-6-ЗАМЕСТЕНИ-13,14-ДИХИДРО-12Н-6λ^5-ДИБЕНЗО[d,i][1,3,7,2]ДИОКСАЗАФОСФЕЦИН-6-ОКСИДИ, СУЛФИДИ И СЕЛЕНИДИ

А. У. Р. Санкар, Б. С. Кумар, М. В. Н. Реди, С. С. Реди, Ч. С. Реди, Ч. Н. Раджу*,

Департамент по химия, Университет Сри Венкатесвара, Тирупати 517 502, Индия

Постъпила на 24 януари 2008 г.; Преработена на 1 септември 2008 г.

(Резюме)

Проведен е синтез на нови 2,4,8,10,13-пентаметил-6-заместени-13,14-дихидро-12Н-6λ^5-дибензо[d,i][1,3,7,2] диоксазафосфецин-6-оксиди чрез кондензация на бис(2,4-диметил-2-хидроксибензил)метиламин със съдържащи фосфор дихлориди в присъствие на триетиламин при 40–50°С. В двустадиен процес са синтезирани съответните оксиди, сулфиди и селениди. Бис(2,4-диметил-2-хидроксибензил)метиламин кондензира с фенилдихлорфосфин и етилдихлорфосфит до междинни съединения съдържащи тривалентен фосфор. Във втория стадий, тези съединения взаимодействат с хидропероксид, сяра и селен до получаване на съответните оксиди, сулфиди и селениди. Структурата им е установена чрез елементен анализ, ИЧС, ЯМР (^{1}Н, ^{13}С и ^{31}Р) и масспектрометрия. Оценена е също и тяхната антимикробна активност.

Bulgarian Chemical Communications, Volume 41, Number 1 (pp. 65–71) 2009

Inductively coupled plasma atomic emission spectrometry – line selection and accuracy in the determination of platinum, palladium, rhodium, barium and lead in automotive catalytic converters

P. P. Petrova, S. V.Velichkov, I. P. Havezov, N. N. Daskalova*

Institute of General and Inorganic Chemistry, Bulgarian Academy of Sciences, Acad. G. Bonchev St., Block 11, 1113 Sofia, Bulgaria

Received June 27, 2008; Revised October 15, 2008

This work shows that by using ICP-AES and the Q-concept for quantification of spectral interferences in the determination of Pt, Pd, Rh, Pb and Ba in catalytic automotive converters with aluminum as matrix component, the errors in the measurement of net line signals resulting from erroneous background determination can be eliminated. The auto-catalyst certified reference material SRM 2556 for Pt, Pd and Rh was used for experimental demonstration of the accuracy of analytical results. Extraction with *aqua regia* was used as a dissolution procedure. Samples of poisoned automotive catalytic converters were analyzed. The platinum group elements, plus barium and lead were determined. Relatively high concentrations of lead (catalytic poison) were found in the catalyst samples. In this case a non-uniform longitudinal distribution (along the catalyst) of platinum group elements was established.

Key words: ICP-AES, platinum group elements, barium, lead, poisoned automotive catalytic converter.

1. INTRODUCTION

Since 1975 the enforcement of Clean Air Act by the Environmental Protection Agency led to the introduction of catalytic converters for control of the automobile exhaust emission gases. The modifications of catalytic converters include the introduction of "three-way" catalysts, containing platinum group elements (PGEs). Platinum, palladium and rhodium are known as the active components in automotive catalytic converters as well as in catalysts for pharmaceutical industry and petroleum refining. These elements were included in automotive catalytic converters and the converters have been used in all car exhaust systems [1].

The general purpose of the automotive catalytic converter is to oxidize completely carbon monoxide and hydrocarbons to CO_2 and also to convert nitrogen oxides to N_2. The precious metals in different ratios are deposited on a large surface area of γ-alumina (washcoat), which in its turn is dispersed on a honeycomb consisting of aluminum, magnesium and/or calcium aluminum silicates [2–4]. In modern catalysts there is also a barium-containing additive.

The use of expensive platinum group elements in catalyst production fostered the development of accurate methods for their determination in catalytic converters. The A. C. Spark Plug Division of General Motors has extensively investigated various approaches using X-ray fluorescence spectroscopy [5]. Sandell [6], Walsh *et al*. [7] described spectrophotometric methods for determination of platinum. Differential spectrophotometry was used in conjunction with the stannous chloride method for determination of platinum in reforming emission control catalysts [8] The wavelength-dispersive X-ray fluorescence method (WD-XRF) was often used for analysis of catalysts [9]. The most important advantages of this method are the relatively simple sample preparation and the rapid measurement. The basic disadvantages of the method are as follows [10]: (a) Partial conversion of γ-alumina into α-alumina under high-temperature exposure of the catalytic converters. The various forms, in which the alumina may be present, can result in high and fluctuating background signals; (b) The distribution of the PGEs on the support is inhomogeneous; (c) Palladium line interferes with the best rhodium line; (d) The detection limits of the method do not permit trace analysis.

Since the introduction of inductively coupled plasma-atomic emission spectrometry (ICP-AES) and inductively coupled plasma-mass spectrometry (ICP-MS) techniques the trace determination of platinum group elements has achieved a great progress [11, 12]. With these analytical techniques it is important to recognize and document the matrix effects and then, perhaps, to understand on a

* To whom all correspondence should be sent:
E-mail: das15482@svr.igic.bas.bg

© 2009 Bulgarian Academy of Sciences, Union of Chemists in Bulgaria

fundamental level and to control and eliminate them. Matrix effects in ICP-AES and ICP-MS may be divided into two basic categories: matrix induced spectral overlap problems and matrix induced signal intensity changes [13–15].

The analysis of Pt, Pd and Rh by ICP-MS or ICP-AES is complicated by the existence of interferences [16, 17]. Examination of these interferences is critical for selection of most suitable isotopes for isotope dilution mass spectrometry and for assessing whether any additional interference removal measures are required for the analysis. The interferences can potentially be problematic in the determination of PGEs [18–21]. The possibilities for limitation and correction of the interferences in the determination of PGEs by ICP-MS were discussed as follows: Matrix removal by exchange column [22–25], charcoal [26], silica [27–29], plastic foams and polymers [30–31]; Application of high resolution mass spectrometry (HR-ICP-MS) – there is no commercially available HR-ICP-MS, which can separate the oxide interferences on the PGEs [32]; The influence of plasma operating conditions by varying nebulizer gas flow rates, cool plasma techniques and chilled spray chambers [33, 34]; Mathematical corrections [35]; Post-plasma techniques, including the use of collision and reaction cells [36]. These techniques do not influence the plasma parameters and the corresponding operating conditions [36].

The ICP-AES methods also possess the possibilities for simultaneous determination of PGEs [37]. Although the concentrations of PGEs in automotive catalytic converters are relatively high, the use of both techniques ICP-MS and ICP-AES would allow the methods to expand to applications of low concentration level analysis.

Several dissolution procedures of automotive catalyst materials were developed and their possibilities were discussed in [38].

The present paper deals with the ICP-AES determination of platinum, palladium, rhodium, barium and lead in samples taken out of poisoned automotive catalytic converters. All modern converters contain also barium in order to reduce the effect of sulfur poisoning. So in the presence of barium the activity of catalytic converters increases. The general purpose is to ensure the accurate measurement of the net line signals, i.e. the subtraction of the signal, generated by the back-ground at analyte wavelength (λ_a) from the total signal before manipulation of the net signal to derive an analyte concentration. The matrix constituent in this case is aluminium. The question of what it actually is, why it is such severe problem, and what progress has been made in recent years to cope with it, remains. This problem is of primary importance, because the spectral interferences in ICP-AES affect the accuracy of analytical results and the magnitude of the true detection limits. The background under a spectral line cannot be measured directly. An elementary calculation illustrated the importance of correct background subtraction and showed the magnitude of the errors in net signals resulting from erroneous background determination [11].

An interfering line signal, in the presence of a given matrix, has to be considered as a contribution to the background that can be measured only with a far greater uncertainty than continuous background. It was this insight that prompted the introduction of the concepts of "true detection limit" ($C_{L,\,true}$) [13, 39–42] and the "common detection limit" (C_L) for pure solvent [41]. In the case of a single interfering line the true detection limit ($C_{L,\,true}$) is represented by Eqn. (1) [40]:

$$C_{L,\,true} = 0.4\times Q_I(\lambda_a)\times C_I + C_{L,\,conv} \qquad (1)$$

$$C_{L,\,conv} = 2\sqrt{2}\times 0.01\times RSDBL\times[BEC + Q_I(\lambda_a)\times C_I + Q_W(\Delta\lambda_a)\times C_I] \qquad (2)$$

where: C_I is matrix concentration; $C_{L,\,conv}$ – conventional detection limits; $Q_I(\lambda_a)$ – values for line interference [$Q_I(\lambda_a) = S_I(\lambda_a)/S_A$], defined as interferent to analyte sensitivity ratio at the peak wavelength (λ_a) of prominent lines of analytes (Pt, Pd, Rh, Ba, Pb); $Q_W(\Delta\lambda_a)$ – values for wing background interference [$Q_W(\Delta\lambda_a) = S_W(\Delta\lambda_a)/S_A$], defined as wing background to analyte sensitivity ratio in the spectral window ($\Delta\lambda_a$). The use of the symbol ($\Delta\lambda_a$) instead of (λ_a) expresses that [$Q_W(\Delta\lambda_a)$] refers to the overall level in the spectral window ($\Delta\lambda_a$) viewed and not specifically to (λ_a), as happens with the $Q_I(\lambda_a)$ value; RSDBL – relative standard deviation of the total background signal in the presence of matrix; BEC – background equivalent concentration in the pure solvent.

The detection limit of analytes in pure solvent (or dilute acid) is defined by Eqn. (3) [41]:

$$C_L = 2\sqrt{2}\times 0.01\times RSDB\times BEC \qquad (3)$$

where RSDB is the relative standard deviation of the background signal in the presence of pure solvent.

To fulfil the general purpose of the paper the following data have been compiled:

1. Quantification of the spectral interferences by using Q-concept, as proposed by Boumans and Vrakking [40–41] for line interference [$Q_I(\lambda_a)$] and for wing background interference [$Q_W(\Delta\lambda_a)$] for relevant sets of analysis lines and aluminium as interferent;

2. Choice of the "best" analysis lines for determination of PGEs, lead and barium in the presence of aluminium matrix;

3. Measurement of the true detection limits, by using the "true detection limit" criterion [40].

2. EXPERIMENTAL

2.1. Instrumentation

The experiments were performed with Jobin Yvon ULTIMA 2 equipment (Longjumeau, France), whose characteristics are specified in Table 1. The operating conditions are shown in Table 2. The Mg II 280.270 nm/Mg I 285.213 nm line intensities ratio was measured to characterize the robustness of the operating conditions in the plasma [43, 44]. The excitation temperature (T_{exc}) was evaluated by the Boltzmann plot method [45] using titanium lines. Under these experimental conditions higher net line signals and lower detection limits were obtained [46].

Table 1. Specifications of the spectrometer and ICP source.

Monochromator	JY ULTIMA 2 (Jobin Yvon, France)
Mounting	Czerny-Turner, focal length 1 m
Grating	Holographic, 2400 grooves·mm^{-1}
Wavelength range	first and second order
Entrance slit	0.015/0.02 mm
Exit slit	0.02/0.08 mm
Practical spectral bandwidth	5 pm in the 2-nd order from 160 nm to 320 nm; 10 pm in the 1-st order from 320 to 800 nm
Detectors	High Dynamic Detectors based on PMT's
Rf generator	Solid state RF 40.68 MHz
Frequency	40.68 MHz
Power output	0.5–1.55 kW
Nebulizer	Meinhard, concentric glass
Spray chamber	JY Glass cyclonic spray chamber
Plasma torch	fully demountable torch
Pump	Peristaltic, two channels, twelve-roller

Table 2. Operating conditions with the 40.68 MHz ICP JY ULTIMA 2 (Jobin Yvon, France) equipment.

Incident power /(kW)	1.00
Outer argon flow rate, l·min^{-1}	13
Auxiliary gas flow rate, l·min^{-1}	0
Sheath gas flow rate, l·min^{-1}	0.2
Liquid uptake rate, ml·min^{-1}	1.0
Carrier gas flow rate, ·l/min^{-1}	0.4
Nebulizer pressure flow	3.2 bar
Mg II 280.270 nm /Mg I 285.213 nm line intensities ratio	10.4
Excitation temperature	7300 K

Quantitative information about the type of the spectral interferences was derived from wavelength scans around the candidate (prominent) analysis lines of Pt, Pd, Rh, Pb and Ba in the presence of aluminium as interferent. The scans were made in a scanning mode of the spectrometer with step size 3.0 pm and integration time of 1 s.

The total background signal is defined by Eqn. (4) [41]:

$$X_{BL} = X_B + X_W(\Delta\lambda_a) + X_I(\lambda_a) \qquad (4),$$

where:

- X_B is the solvent blank (due to source and solvent);
- $X_W(\Delta\lambda_a)$ – the wing background level with respect to the solvent blank for aluminium as interferent;
- $X_I(\lambda_a)$, – the net interfering signals with respect to the wing background level $X_W(\Delta\lambda_a)$ of aluminium as interferent.

By using analysis and scanning modes of the monochromator the following signals were measured: X_A, X_B, $X_W(\Delta\lambda_a)$, $X_I(\lambda_a)$. The measured signals were reduced to sensitivities: sensitivity of analysis line [S_A] defined as the net line signal [X_A] per unit of analyte concentration [C_A]; interferent sensitivities [$S_W(\Delta\lambda_a)$] and [$S_I(\lambda_a)$], defined as interferent signals [$X_W(\Delta\lambda_a)$] and [$X_I(\lambda_a)$], respectively, per unit interferent concentration [C_I]. The sensitivities were used for calculation of Q-values for wing background interference [$Q_W(\Delta\lambda_a) = S_W(\Delta\lambda_a)/S_A$], Q-values for line interference [$Q_I(\lambda_a) = S_I(\lambda_a)/S_A$], [$BEC_W = Q_W(\Delta\lambda_a)\times C_I$] and [$BEC_I(\lambda_a) = Q_I(\lambda_a)\times C_I$].

2.2. Reagents, test solutions and certified reference material

Reagents of highest purity grade were used: 30% HCl and 65% HNO_3 (Suprapur, Merck) and redistilled water from quartz apparatus. Stock solutions of the analyte (1 mg·ml^{-1} Pt, Pd, Rh, Pb and Ba) were prepared from Merck ICP-AES mono-element standard solutions. Q-values were measured by using the following test solutions: 10 μg·ml^{-1} for each of the analytes in 3% hydrochloric acid and 2 mg·ml^{-1} aluminium in 3% hydrochloric acid as interferent.

The recycled auto-catalyst certified reference material SRM 2556 for Pt, Pd and Rh with mean values and uncertainties at a 95% confidence interval was used for experimental demonstration of the accuracy of analytical results. In the certificate it is indicated that a sample of 0.1 g or a larger one is provided as a representative sub-sample of this material.

2.3. Sampling

Samples taken out of poisoned automotive catalytic converters:

(a) From the front section of the catalyst;
(b) From the rear part of the catalyst;
(c) Soot deposits on the catalyst's front.

2.4. Decomposition procedure

1 g of the catalyst samples was weighed in a 50 ml beaker. 15 ml of freshly prepared mixture of acids (5 ml conc. HNO_3 + 15 ml conc. HCl) was added to the sample and the beaker was covered with a watch glass. The sample was left to stand for 1 h at room temperature in order to prevent vigorous reactions. After that, the sample was heated for 6 h on a water bath and allowed to cool down slowly to room temperature. The content of the beaker was transferred quantitatively into a 100 ml volumetric flask and filled up to the mark with re-distillated water.

The undissolved material (γ-alimina + silicates) has settled down and the supernatant solution was subjected to analysis by ICP-AES. The volume of the solid residue is less than 0.4% of the final volume.

2.5. Calibration procedures

The analytical evaluation function is assumed to be a straight line passing through the origin. Spectral interferences affect the intercept, if the curve is plotted on a linear scale. Multiplicative interferences affect the slope of a calibration curve [12]. The correct calibration from the point of view of the spectral interferences requires a correct background subtraction by using the background signal below the analysis line. The correct calibration from the point of view of multiplicative interferences means a precise matching of the acid and matrix contents both in the reference and in the sample solutions.

ICP-AES is not free from acid matrix interferences [47–49]. The reference solutions for the determination of the analytes were prepared on the basis of a blank containing the acids used for digestion (Section 2.4). The matrix blank contains the acid blank.

3. RESULTS AND DISCUSSION

3.1. Detection limits in pure solvent

The detection limits of the analytes in pure solvent (or diluted acids) were calculated by Eqn. (3) using four prominent lines for Pt, Pd, Pb, Ba and 14 prominent lines for rhodium. The prominent lines in column 1 of Table 3 follow the sensitivity order the analytes in pure solvent in accordance to Boumans ICP-Line Coincidence Tables [50]. The obtained detection limits under our experimental conditions are listed in Table 3, column 2. Table 3 shows that the most prominent lines under our experimental conditions (Table 2): Pt II 203.646 nm, Pd II 229.651 nm and Rh II 233.477 nm. The following detection limits are obtained: 6.4 $ng \cdot ml^{-1}$ (Rh), 7 $ng \cdot ml^{-1}$ (Pt) and 11 $ng \cdot ml^{-1}$ (Pd).

Table 3. Detection limits in pure solvent.

The most prominent lines, nm	Detection limits in solution, $ng \cdot ml^{-1}$
Pt II 214.423 (2)	7.3
Pt II 203.646 (1)	7.0
Pt II 204.937 (4)	24
Pt I 265.945 (3)	14
Pd I 340.458 (2)	13.4
Pd I 363.470 (4)	37.0
Pd II 229.651 (1)	11.0
Pd I 324.270 (3)	25.0
Rh II 250.429 (13)	92.0
Rh I 250.509* (10)	28.0
Rh I 250.384* (13)	45.0
Rh II 233.477 (1)	6.4
Rh II 249.077 (2)	7.7
Rh I 343.489 (4)	12.3
Rh II 252.053 (3)	11.6
Rh I 369.236 (7)	19.7
Rh II 246.104 (5)	14.0
Rh II 251.103 (6)	18.8
Rh II 242.711 (8)	21.0
Rh I 339.682 (11)	30.0
Rh I 352.802 (12)	37.0
Rh I 370.091 (14)	53.0
Rh I 228.857 (9)	22.0
Pb II 220.353 (1)	6.7
Pb I 216.999 (2)	23
Pb II 261.418 (3)	30.0
Pb I 283.306 (4)	36.0
Ba II 455.403 (1)	0.3
Ba II 493.409 (1)	0.3
Ba II 233.527 (1)	0.3
Ba II 230.424 (1)	0.3

* These lines are not listed in Boumans' ICP Tables [50]. They are taken from Harrison's, M.I.T. Wavelength Tables [51].

3.2. Line selection in the presence of aluminium as matrix

The Q-concept was used for quantifying different types of spectral interference [40]. A distinction was made between Q-values for line interference [$Q_I(\lambda_a)$] and Q-values for wing background interferences [$Q_W(\Delta\lambda_a)$] around a relevant set of analysis lines. Table 4 lists $Q_W(\Delta\lambda_a)$ and $Q_I(\lambda_a)$ values for prominent lines of Pt, Pd, Rh, Pb and Ba in the presence of 2 $mg \cdot ml^{-1}$ aluminium as interferent. The optimum line selection for trace analysis requires the choice of prominent lines that are free from line interference and negligibly influenced by wing background interference in the presence of aluminium as matrix.

The results of Table 4 show the following:

(i) The most prominent lines of lead are influenced by line interference in the presence of aluminium as interferent. The "best" analysis line is Pb II 261.418. This line is free of line interference;

(ii) The most prominent lines of Pt, Pd, Rh and Ba are free of line interference and were selected as the "best" analysis lines.

The selected analysis lines are printed in bold.

Table 4. $Q_W(\Delta\lambda_a)$ and $Q_I(\lambda_a)$ for prominent lines of Pt, Pd, Rh, Ba and Pb in the presence of aluminium as matrix element.

Analysis line, nm	Interferents	$Q_W(\Delta\lambda_a)$	$Q_I(\lambda_a)$
Pt II 203.646	**Al**	**7.2×10^{-4}**	**0**
Pt II 214.423	Al	1.0×10^{-4}	2.3×10^{-4}
Pt I 265.945	Al	1.7×10^{-3}	0
Pt II 204.9168	Al	2.2×10^{-3}	0
Pd II 229.651	**Al**	**0**	**0**
Pd I 340.458	Al	0	0
Pd I 324.270	Al	0	0
Pd I 363.470	Al	0	0
Rh II 233.477	**Al**	**0**	**0**
Rh II 249.077	Al	0	0
Rh II 252.053	Al	0	0
Rh I 343.489	Al	0	0
Pb II 220.353	Al	6.5×10^{-5}	2.6×10^{-4}
Pb II 220.353	Al	6.5×10^{-5}	2.6×10^{-4}
Pb II 261.418	**Al**	**4.0×10^{-5}**	**0**
Pb I 283.306	Al	0	0
Ba II 455.403	**Al**	**0**	**0**
Ba II 493.409	Al	0	0
Ba II 233.527	Al	0	0
Ba II 493.409	Al	0	0
Pb II 261.418	Al	4.0×10^{-5}	0
Pb I 283.306	Al	0	0
Ba II 455.403	Al	0	0

3.3. Detection limits in the determination of Pt, Pd, Rh, Pb and Ba in catalytic automotive converters

Table 5 summarizes the selected analysis lines from Table 4 and the true detection limits in [%]. The detection limits, obtained under our experimental conditions, satisfied the requirements of the practice. Therefore, ICP-AES can be used for determination of the Pd, Pt, Rh, Ba and Pb contents in samples of catalytic automotive converters.

Table 5. Selected analysis lines and detection limits (in %) with respect to the dissolved solid sample.

Best analysis lines, nm	Detection limits with respect to the dissolved solid sample, %
Pt II 203.646	7.0×10^{-5}
Pd II 229.651	2.0×10^{-4}
Rh II 233.477	6.4×10^{-4}
Pb II 261.418	3.0×10^{-4}
Ba II 455.403	3.0×10^{-6}

3.4. Analysis of a sample of certified reference material

The certified reference material SRM 2556 (for Pt, Pd and Rh) was dissolved in accordance with the decomposition procedure, described in Section 2.4. The final solution was introduced into the ICP for analysis. The results in the determination of Pt, Pd and Rh contents were compared to the corresponding certified values (Table 6). The selected prominent lines were used as analysis lines (column 1). The confidence intervals of the mean values for five replicates (n = 5) and statistical confidence P = 95% were calculated [52–54]. Using Student's criterion, no statistical differences between the experimental (column 2) and certified values (column 3) were found.

Table 6. Contents of Pt, Pd and Rh (in %) obtained by JY ULTIMA 2 ICP-AES (n = 5 replicates) in the analysis of certified reference material SRM 2656 (column 2) and the corresponding certified values (column 3).

Analysis line, nm	JYULTIMA 2 ICP-AES Concentration, (%) $X \pm \Delta \bar{X}$ (n = 5, P = 95%)	Certified values Concentration, (%) $X \pm \Delta \bar{X}$
Pt II 203.646	0.0692 ± 0.007	0.06974 ± 0.0023
Pd II 229.651	0.0324 ± 0.003	0.0326 ± 0.0016
Rh II 233.477	0.00515 ± 0.001	0.00512 ± 0.0005

3.5. Analysis of samples of damaged catalytic automotive converters

A damaged catalytic automotive converter was submitted to us for analyses from Citroēn Company. The analytical task requires the determination of Pt, Pd, Rh, Ba and Pb contents in the material, sampled from different parts of damaged catalytic automotive converter (Section 2.3). The decomposition method is described in Section 2.4. Table 7 lists the concentration of Pt, Pd, Rh, Ba and Pb in the material, sampled from different pats of catalytic converter. The confidence intervals of the mean values for five replicates (n = 5) and statistical confidence level P = 95% were calculated [52–54].

Table 7. Content of Pt, Pd, Rh, Ba and Pb material sampled from different sections of the damaged catalytic automotive converter.

Type of sample	Content of elements, %				
	Pt	Pd	Rh	Ba	Pb
Catalyst from the deposit of converter	0.07 ± 0.007	0.30 ± 0.007	0.014 ± 0.003	0.16 ± 0.03	0.18 ± 0.003
Catalyst from the inlet of converter	0.20 ± 0.007	0.20 ± 0.007	0.010 ± 0.003	0.60 ± 0.03	0.14 ± 0.003
Catalyst from the outlet of converter	0.34 ± 0.007	0.16 ± 0.007	0.008 ± 0.003	0.73 ± 0.03	0.02 ± 0.003

The results of Table 7 show that relatively high concentrations of lead (catalytic poison) were found in the catalyst samples. The conclusion based on the analytical results was that this automotive catalytic converter was deactivated as a result of utilization of leaded-motor fuel. The catalytic poisoning with lead causes a non-uniform longitudinal distribution (along the catalyst bed) of platinum group elements and barium. This is in accordance with the measurements of the catalytic activity of the analyzed cata-

lytic converters: the higher concentrations of lead correspond to a lower catalytic activity and consequently a greater mass of soot deposits at the converters inlet (up to complete blocking of the catalysts).

4. CONCLUSIONS

This work has shown that, in the analysis of catalytic automotive converter, quantitative information on the spectral interferences is essential. The Q-concept, as proposed by Boumans and Vrakking [40–41], was used for quantification of the spectral interferences in the presence of aluminium as matrix component (Table 4). By using a spectrometer with practical spectral bandwidth of 5 pm (Table 1), it is possible to select the "best" analysis lines for Pt, Pd, Rh, Pb and Ba, which are free from line interference (Table 4). In this case, the detection limits (Table 5) do not significantly deteriorate when compared to the detection limits obtained in pure solvent (Table 3).

Samples of a damaged catalytic automotive converter were analyzed. The results show that relatively high concentrations of lead (catalytic poison) were found in the catalyst samples. Hence, this automotive catalytic converter is deactivated as a result of utilization of leaded-motor fuel. The catalytic poisoning with lead causes a non-uniform longitudinal distribution (along the catalyst bed) of platinum group elements and barium.

5. REFERENCES

1. H. E. Beary, P. J. Paulsen, *Anal. Chem*., **67,** 3193 (1995).
2. A. I. Kindon, R. F. Davis., in: Engineered Materials Handbook, Vol. 4: Ceramic and Glasses, S. J. Schneider (Technical Chairman), ASM International, Metal park, OH, 1991.
3. H. E. Taylor, R. A. Huff, A. Montaser, in: Inductively Coupled Plasma Mass Spectrometry, A. Montaser (Ed.), J. Wiley, New York, 1998.
4. C. J. Jones, D- and F-Block Chemistry, Royal Society of Chemistry, Cambridge, 2001.
5. R. Van Dyne, Summary of Several X-Ray Fluorescence Procedures for Measuring Pt and Pd in Catalyst Materials, Report to ASTM Committee E-32-03 at Philadelphia Meeting, 11 March, 1975.
6. E. B. Sandell, Calorimetric Determination of Traces of Metals, 3rd Edn., Interscience, New York, 1959.
7. T. J. Walsh, A. Hansman, in: Treatise on Analytical Chemistry, Vol. 8, I. M. Kolthoff, P. J. Elving (Eds.), Interscience, New York, 1963.
8. S. Kallmann, *Talanta*, **23,** 579 (1976).
9. S. Kallmann, P. Blumberg, *Talanta*, **27**, 827 (1980).
10. O. G. Borisov. D. M. Coleman, K. A. Oudsema, R. O. Carter, *J. Anal. At. Spectrom*., **12,** 239 (1997).
11. P. W. J. M. Boumans, in: Basic Concepts and Characteristics of ICP-AES, Inductively Coupled Plasma Emission Spectroscopy, Part 1: Methodology, Instrumentation and Performance, P. W. J. M. Boumans (Ed.), Wiley, New York, 1987, Chapter 4, p. 100.
12. D. S. Bollinger, A. J. Schleisman, in: Plasma Source Mass Spectrometry: New Developments and Applications, G. Holland, S. D. Tanner (Eds.), Royal Society of Chemistry, Cambridge, UK, 1999.
13. P. W. J. M. Boumans, *Fresenius Z. Anal. Chem*., **324**, 397 (1986).
14. P. W. J. M. Boumans, in: Line Selection and Spectral Interferences, Inductively Coupled Plasma Emission Spectroscopy, Part 1: Methodology, Instrumentation and Performance, P. W. J. M. Boumans (Ed.), Wiley, New York, 1987, Ch. 7, p. 358.
15. S. H. Tan, G. Horlick*, J. Anal. At. Spectrom*., **2**, 745 (1987).
16. L. A. Simpson, M. Thomsen, B. J. Alloway, A. Parker, *J. Anal. At. Spectrom*., **16,** 1375 (2001).
17. W. Pretorius, D. Chipley, K. Kyser, B. Helmstaedt, *J. Anal. At. Spectrom*., **18,** 302 (2003).
18. H. P. Longerich, G. A., Jenner, B. J Fryer, S. E. Jackson, *Chem. Geol*., **83**, 105 (1990).
19. M. Krachler, A. Alimonte, F. Pettrucci, K. J. Irgolic, F. Forastiere, S. Caroli, *Anal. Chim. Acta,* **363**, 1 (1998).
20. F. Pettrucci, B. Bocca, A. Alimonte, S. Caroli, *J. Anal. At. Spectrom.*, **15**, 525 (2000).
21. L. A Simpson., R. Hearn, T. Catterick, *J. Anal. At. Spectrom.*, **19** 1244 (2004).
22. P. Di, D. E. Davey*, Talanta*, **42**, 685 (1995).
23. M. Grote, A. Kettrup, *Anal. Chim. Acta***, 201,** 95 (1987).
24. I. Jarvis, M. M. Totland, K. E. Jarvis, *Analyst*, **122**, 19 (1997).
25. D. G. Pearson, S. J. Woodland, *Chem. Geol.*, **165**, 87 (2000).
26. G. E. M. Hall, J. C. J. Pelchat, *J. Anal. At. Spectrom*., **8**, 1059 (1993).
27. T. Schilling, P. Schramel, B. Michalke, G. Knapp, *Mikrochim. Acta*, **116**, 83 (1994),
28. M. Schuster, M. Schwarzer, *At. Spectrosc*., **19**, 121 (1998).
29. P. Liu, Q. Pu, Z. Su, *Analyst*, **125**, 147 (2000).
30. L. Jones, N. Iris, K. L Koch, *Anal. Chim. Acta*, **182**, 61 (1986).
31. D. Kundu, S. K. Roy, R. C. Denny, M. J. K. Thomas, Revised Edition of Vogels Textbook of Quantitative Chemical Analysis, 6th edn., Prentice Hall, 2000, p. 76.
32. J. Mendham, J. D. Barnes, R. C. Denny, M. J. K. Thomas, Revised Edition of Vogels Texbook of Quantitative Chemical Analysis, 6-th edn., Prentice Hall, 2000.
33. J. W. H. Lam, J. McLaren, *J. Anal. At. Spectrom*., **5**, 419 (1990).
34. E. R. Denoyer, *At. Spectrosc*., **112**, 215 (1991).
35. G. Hann, K. Kanitsar, K. Korllensperger, G. Stingeder, *J. Anal. At. Spectrom.,* **16**, 1057 (2001).

36. A. Montaser, M. G. Minnich, J. A. McLean, H. Liu, J. A Caruso, C. W. McLeod, in: Inductively Coupled Plasma Mass Spectrometry, A. Montaser (Ed.), Wiley-VCH, 1997.
37. L. Bencs, K. Revindra, R. Van Greken, *Spectrochim. Acta Part B***, 58,** 1723 (2003).
38. J. A. Brown, F. W. Kunz, R. K Belitz*, J. Anal. At. Spectrom.,* **6**, 393 (1991).
39. P. W. J. M. Boumans, *J. Anal. At. Spectrom*., **8**, 767 (1993).
40. P. W. J. M. Boumans, J. J. A. M. Vrakking, *Spectrochim. Acta Part B*, **43**, 69 (1988)
41. P. W. J. M. Boumans, J. A. Tielrooy, F. J. M. J. Maessen, *Spectrochim. Acta Part B*, **43**, 173 (1988).
42. P. W. J. M. Boumans, *Anal Chem.,* **66**, 459A (1994).
43. J. M. Mermet, *Anal. Chim. Acta*, **250**, 85 (1991).
44. J. Dennaud, A. Howes, E. Poussel, J. M. Mermet, *Spectrochim. Acta Part B*, **56,** 101 (2001).
45. J. M. Mermet, in: Spectroscopic Diagnostics: Basic Concepts, Inductively Coupled Plasma Emission Spectroscopy, Part 2: Application and Fundamentals, P. W. J. M. Boumans (Ed.), Wiley, New York, 1987, Ch. 10**,** p. 353.
46. N. Velitchkova, S. Velichkov, N. Daskalova, *Spectrochim. Acta Part B*, (submitted).
47. E. G. Chudinov, I. I. Ostroukhova, G. V. Varvanina, *Z. Anal. Chem*., **335**, 2533 (1989).
48. I. B. Brenner, J. M. Mermet, I. Segal, J. L. Long, *Spectrochim. Acta Part B*, **50**, 323 (1995).
49. J. L. Todolí, J. M. Mermet, *Spectrochim. Acta Part B*, **54,** 895 (1999).
50. P. W. J. M. Boumans, Line Coincidence Tables for Inductively Coupled Plasma Emission Spectrometry, Pergamon, Oxford, 1980.
51. G. R Harrison, M.I.T. Wavelength Tables, M.I.T. Press, Cambridge, MA, 1969.
52. V. V. Nalimov, The Application of Mathematical Statistics to Chemical Analysis, Pergamon, Oxford, 1963.
53. J. Mendel, The Statistical Analysis of Experimental Data, Wiley, New York, 1964.
54. K. Doerffel, Statistic in the Analytical Chemistry, VEB Deutscher Verlag für Grundstoffindustrie, Leipzig, 1984 (in German).

АТОМНА ЕМИСИОННА СПЕКТРОМЕТРИЯ С ИНДУКТИВНО СВЪРЗАНА ПЛАЗМА – ИЗБОР НА АНАЛИТИЧНИ ЛИНИИ И ТОЧНОСТ ПРИ ОПРЕДЕЛЯНЕ НА ПЛАТИНА, ПАЛАДИЙ, РОДИЙ, БАРИЙ И ОЛОВО В АВТОМОБИЛНИ КАТАЛИЗАТОРИ

П. П. Петрова, С. В. Величков, Ив. П. Хавезов, Н. Н. Даскалова*

Институт по обща и неорганична химия, Българска академия на науките, ул. „Акад. Г. Бончев“, блок 11, 1113 София

Постъпила на 27 юни 2008 г.; Преработена на 15 октомври 2008 г.

Атомната емисионна спектрометрия с индуктивно свързана плазма е приложена за определяне на Pt, Pd, Rh, Pb и Ba в автомобилни катализатори. Q-концепцията е използвана за количествена оценка на спектралните пречения, в присъствие на алуминий, като матричен компонент. Определяемите елементи-примеси са извлечени от пробите с царска вода. Точността на аналитичните резултати е доказана експериментално със сертифициран стандартен образец – автомобилен катализатор SRM 2556, за определяне на Pt, Pd и Rh. Анализирани са проби от отровени катализатори. Определени са елементите Pt, Pd, Rh, Pb и Ba. Намерени са относително високи концентрации на олово, като резултат от отравяне на катализатора. Установено е и неравномерно разпределение на Pt, Pd и Rh по дължината на катализатора.

Bulgarian Chemical Communications, Volume 41, Number 1 (pp. 72–79) 2009

Synthesis of amino acid analogues of 10-methoxy dibenz[b,f]azepine and evaluation of their radical scavenging activity

H. V. Kumar, C. R. Gnanendra, D. Ch. Gowda, N. Naik*

Department of Studies in Chemistry, University of Mysore, Manasagangotri, Mysore-570 006, Karnataka, India

Received May 19, 2008; Revised October 6, 2008

A method for the synthesis of L-aminoacid (L-tyrosine, L-phenylalanine, L-hydroxyproline and L-threonine) analogues of 10-methoxy-dibenz[b,f]azepine is proposed. 10-Methoxy-dibenz[b,f]azepine, as a basic molecule was prepared by a known method. The key intermediate 3-chloro-1-(10-methoxy-5H-dibenz[b,f]azepine-5-yl)propan-1-one**,** was obtained by N-acylation of 10-methoxy-dibenz[b,f]azepine with 3-chloro-propionylchloride. Further coupling of the respective L-aminoacids was accomplished to produce 3-(4-hydroxyphenyl)-2-(3-(10-methoxy-5H-dibenz[b,f] azepin-5-yl)-3-oxopropylamino)propanoic acid, 2-(3-(10-methoxy-5H-dibenz[b,f]azepin-5-yl)-3-oxopropylamino)-3-phenyl-propanoic acid, 3-hydroxy-1-(3-(10-methoxy-5H-dibenz[b,f]azepin-5-yl)-3-oxopropyl)pyrrolidine-2-carboxylic acid, and 3-hydroxy-2-(3-(10-methoxy-5H-dibenz[b,f]azepin-5-yl)-3-oxopropylamino)butanoic acid**,** respectively. The synthesized compounds were evaluated in regard to their potential over the 1,1-diphenyl-2-picrylhydrazyl (DPPH) free radical scavenging activity. Butylhydroxy anisole (BHA) and ascorbic acid (AA) were used as reference antioxidant compounds and also a comparative study with the newly synthesized compounds was done. Under the present experimental conditions, the analogues containing L-tyrosine, L-hydroxyproline and L-threonine**,** possess a direct scavenging effect by trapping the stable DPPH free radical. L-Hydroxyproline analogues showed a significant radical scavenging activity among the synthesized analogues. DPPH activity of the pure L-aminoacids was also determined and a comparative study with the newly synthesized products was done. The DPPH activity of products was found to be greater than that of the L-aminoacids.

Key words: 10-methoxy-5H-dibenz[b,f]azepine, 3-chloro-1-(10-methoxy-5H-dibenz[b,f]azepine-5-yl)propan-1-one, L-aminoacids, radical scavenging activity.

INTRODUCTION

Free radicals and active oxygen species have been related to cardiovascular and inflammatory diseases, and even have a role in cancer and ageing [1–2]. Efforts to counteract the damage caused by these species are gaining acceptance as a basis for novel therapeutic approaches and the field of preventive medicines is experiencing an upsurge of interest in medically useful antioxidants [3–4].

A series of compounds that can scavenge radicals by trapping, initiating and/or propagating radicals, are called 'antioxidants' [5]. In biological systems, the definition for antioxidants has been extended to any substance that when it is present in low concentrations, compared to those of an oxidisable substrate, significantly delays or prevents oxidation of that substrate [6]. There is an expanding quest for using antioxidative molecules because they have the capacity to quench free radicals, thereby protecting cells and tissues from oxidative damage. Numerous natural or synthetic antioxidant compounds have been tested with success in various disease models as well as in clinics [7]. Antioxidants are now expected as the drug candidate to combat these diseases. In the literature some tricyclic amines and their chemical structures shows antioxidant neuroprotective activity *in vitro* [8]. Nowadays, the free-radical scavenging mechanism of aromatic amines (Ar_2NHs) has been discussed from the view point of chemical kinetics [9].

10-Methoxy-5H-dibenz[b,f]azepine **1**, is common basic fused tricyclic amine, which belongs to the family of 5H-dibenz[b,f]azepine i.e., iminostilbene. It is used as an intermediate for the synthesis of the registered anticonvulsant drug oxcarbazepine [10], the structure of which has recently been reported [11]. Dibenz[b,f]azepine and its derivatives have been variously reported as having antiallergic activity, specifically antihistaminic activity, spasmolytic, serotonin antagonistic, anticonvulsive, antiemetic, antiepileptic, anti-inflammatory, sedative and fungicidal action [12]. In our earlier studies, the DPPH activity of the basic molecule i.e., 10-methoxy-5H-dibenz[b,f]azepine, was determined and reported [13]. From the studies, the basic molecule possesses significant 1,1-diphenyl-2-picrylhydrazyl (DPPH) activity, so further we plan to synthesize its

* To whom all correspondence should be sent:
E-mail: drnaik_chem@yahoo.co.in

© 2009 Bulgarian Academy of Sciences, Union of Chemists in Bulgaria

new analogues and try to explore the radical scavenging activity by coupling different L-aminoacids.

The research work on free radicals provides theoretical information for the medicinal development, and supplies some *in vitro* methods for quick-optimizing drugs, it attracts more scientific attention of bioorganic and medicinal chemists. In addition to the traditional O–H bond type of antioxidant, tricyclic amines having N–H bond function as antioxidant have attracted much research attention because Ar_2NHs have always been the central structure in many currently used drugs [14]. Usually phenolic compounds were found to have antioxidant and radical scavenging activity; they also inhibit LDL oxidation [15–16]. In the literature aminoacids and some of their derivatives were also found to have antioxidant activity [17].

In the present study we have used a model compound 3-chloro-1-(10-methoxy-5H-dibenz[b,f] azepine-5-yl)propan-1-one to verify the possibility of obtaining the L-aminoacid analogues of 10-methoxy-dibenz[b,f]azepine. Before coupling of different L-aminoacids to the key intermediate, their DPPH activity was evaluated. Since their structure may justify a possible intervention in free radical process we have selected some of the free L-aminoacids to explore better the chemistry and the biological activities. The L-aminoacid analogues of 10-methoxy dibenz[b,f]azepine were synthesized and their structure was established by chemical and spectral analyses. The newly synthesized compounds were investigated in regard to their *in vitro* DPPH free radical scavenging potential and compared to commercially available synthetic antioxidants namely butylated hydroxyanisole (BHA) and ascorbic acid (AA) and also with the L-aminoacids (L-tyrosine, L-phenylalanine, L-hydroxyproline and L-threonine). These studies reflect the possibility for therapeutic uses and application as a source of synthetic antioxidants.

CHEMISTRY

10-Methoxy-5H-dibenz[b,f]azepine **1**, was synthesized applying a known method [10]. The active sites for the coupling of different L-aminoacids to the basic molecule were less and also the methoxy group in the basic molecule is an important group, which can play an important role for the DPPH activity. Hence we select the N-acylation reaction in order to obtain the key intermediate in which the coupling of different L-aminoacids can be done very easily with simple experimental procedure with good yield. Here in the key intermediate $ClCH_2–CH_2–CO–$ plays an important role for the coupling of L-aminoacids. In the present study aminoacids having L-configuration were used for the coupling. The synthesis of L-aminoacid analogues of 10-methoxy-5H-dibenz[b,f]azepine was realized in two steps. In the first step, the key intermediate 3-chloro-1-(10-methoxy-5H-dibenz[b,f]azepine-5-yl)propan-1-one **a**, was prepared in good yield by N-acylation of 10-methoxy-dibenz[b,f]azepine with 3-chloro-propionylchloride in the presence of triethyl amine as base **(**Scheme 1**)**. In the second step, further coupling of respective L-aminoacid to the intermediate were done to obtain the L-aminoacid analogues of 10-methoxy-5H-dibenz[b,f]azepine **b–e**, (Scheme 2).

EXPERIMENTAL

Materials and methods

The following compounds and materials supplied by Sigma Aldrich, were used: L-tyrosine, L-phenylalanine, L-hydroxyproline, L-threonine and 5H-dibenz[b,f]azepine. 3-Chloro-propionylchloride, triethyl amine, benzene, methanol, chloroform, diethyl ether, acetic acid, ethyl acetate, sodium bicarbonate, anhydrous sodium sulphate were all of analytical grade of purity and procured from Merck. TLC aluminium sheets-silica gel 60 F_{254} were also purchased from Merck.

The IR spectra were recorded on a FT-IR021 model in KBr disc. The ^1H NMR spectra were recorded on Jeol GSX 400 MHz spectrophotometer using $CDCl_3$ as a solvent and the chemical shifts (δ) are in ppm relative to the internal standard. The mass spectra were recorded on Waters-Q-TOF Ultima spectrophotometer.

Synthesis of 3-chloro-1-(10-methoxy-5H-dibenz[b,f]azepine-5-yl)propan-1-one

To the well stirred solution of 10-methoxy-dibenz[b,f]azepine (2 mM) and triethyl amine (2.2 mM) in 50 ml benzene, 3-chloro-propionyl chloride (2.2 mM) in 25 ml benzene was added drop by drop for about 30 min. Then the reaction mixture was stirred at room temperature for about 6 h. The progress of the reaction was monitored by TLC using 9:1 hexane:ethyl acetate mixture as mobile phase. After the completion of reaction, the reaction mass was quenched in ice cold water and extracted in diethyl ether. The ether layer was washed twice with 5% $NaHCO_3$ and once with distilled water. Finally the ether layer was dried with anhydrous Na_2SO_4. The pale-brown semi solid product was obtained by desolventation through rotary evaporator at 50°C.

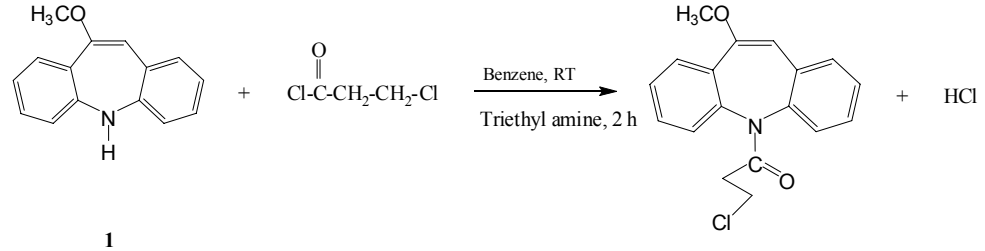

1 **a**

Scheme 1.

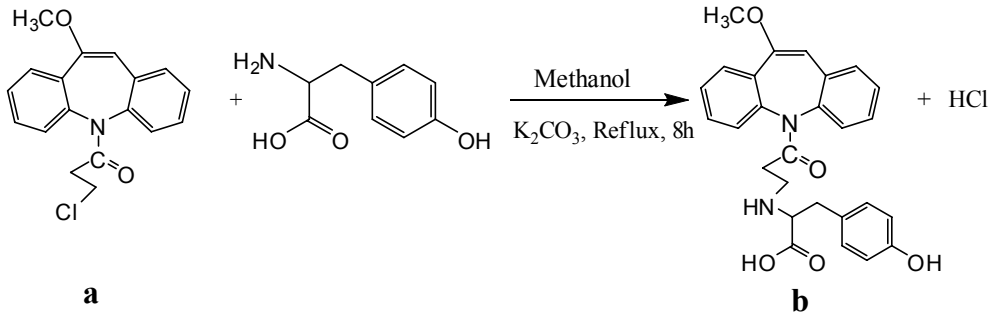

a **b**

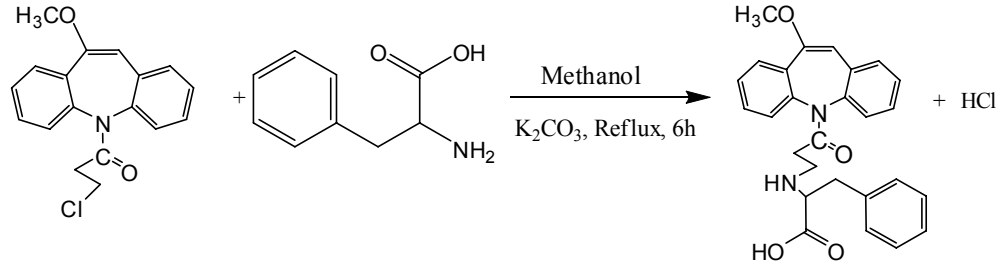

c

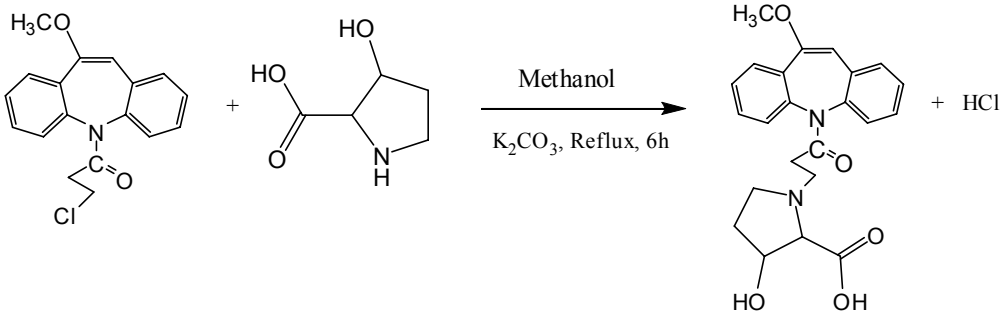

d

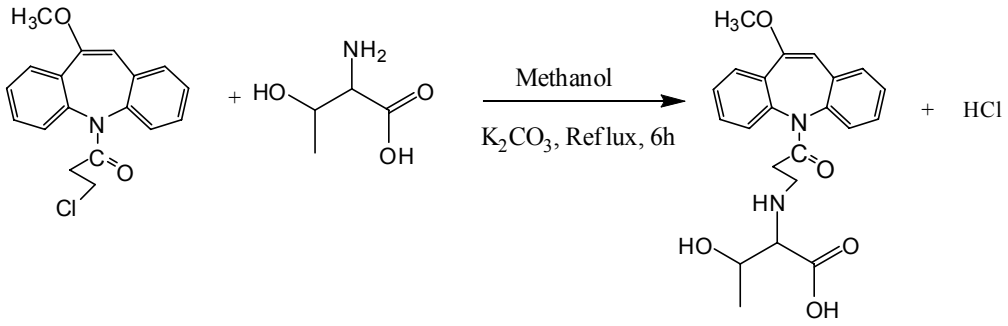

Scheme 2 **e**

3-Chloro-1-(10-Methoxy-5H-dibenz[b,f]azepine-5-yl)propan-1-one, ***a***. Pale brown semi solid, yield 86%. IRS (KBr) 2467.7–3321.6 (OH– carboxylic acid), 1687.1 (C=O), 2835.7 and 2958.4 (CH_2) cm^{-1}; ^1H NMR ($CDCl_3$) δ 2.86 (t, 2, α C=O, 2H), 3.90 (t, 2, β C=O, 2H), 5.92 (s, 1, CH, 1H), 3.71 (s, 3, OCH_3, 3H), 7.19–7.81 (m, 7, Ar–H, 7H), 8.23 (d, 1, Ar–H, 1H). MS (m/z, % abundance): 314 (M^+ 96), 312 (8), 310 (20), 308 (4), 316 (41). Anal. calc. for $C_{18}H_{16}ClNO_2$: C, 68.90; H, 5.14; N, 4.46; O, 10.20; Found: C, 68.12; H, 5.19; N, 4.30; O, 10.36%.

Synthesis of 3-(4-hydroxyphenyl)-2-(3-(10-methoxy-5H-dibenz[b,f]azepin-5-yl)-3-oxopropylamino) propanoic acid

L-Tyrosine (1.2 mM) in methanol (25 mL) was neutralized with triethyl amine (1.2 mM). To this solution K_2CO_3 (600 mg) was added. Later the solution of 3-chloro-1-(10-methoxy-5H-dibenz[b,f] azepine-5-yl)propan-1-one (1 mM) in methanol (50 mL) was added drop by drop for 30 min. The reaction mixture was refluxed for 6–8 h. The progress of the reaction was monitored by TLC. The reaction mixture was then desolventized in a rotary evaporator and the compound was extracted in ethyl acetate. The ethyl acetate layer was washed with water and dried over anhydrous Na_2SO_4. The brown semi-solid was obtained by further desolventation in a rotary evaporator at 50°C.

L-Phenylalanine, L-hydroxyproline and L-threonine aminoacid analogues of 10-methoxy-dibenz [b,f]azepine were obtained by the same procedure. The analogues were separated and purified by column chromatography using mixture of chloroform/methanol/acetic acid 85:15:3. The products were characterized by IRS, Mass spectroscopy, ^1H NMR and elemental analysis.

3-(4-hydroxyphenyl)-2-(3-(10-methoxy-5H-dibenz [b,f]azepin-5-yl)-3-oxopropylamino)propanoic acid, ***b***. Brownish semi-solid, Yield 73%; IRS (KBr): 3321.4 (N–H), 2339.4–3062.8 (OH– carboxylic acid), 1671.8 (C=O), 1599.3 and 1618.5 (CH_2) cm^{-1}; ^1H NMR ($CDCl_3$) δ: 2.36 (d, 2, α C=O, 2H), 2.98 (d, 2, β C=O, 2H), 5.92 (s, 1, CH, 1H), 3.7 (s, 3, OCH_3, 3H), 6.78–8.33 (m, 12, Ar–H, 12H), 9.40 (s, 1, Ar–OH, 1H), 11.5 (s, 1, COOH, 1H), 2.40 (s, 1, NH, 1H), 4.1 (s, 1, CH, 1H), 3.11–3.40 (t, 2, CH_2, 2H). MS (m/z, % abundance): 458.31 (M^+ 97), 468 (11), 457 (47), 456 (41), 455 (40). Anal. calcd. for $C_{27}H_{26}N_2O_5$: C, 70.73; H, 5.72; N, 6.11; O, 17.45: Found: C, 70.92; H, 5.12; N, 6.71; O, 17.25%.

2-(3-(10-methoxy-5H-dibenz[b,f]azepin-5-yl)-3-oxopropylamino)-3-phenylpropanoic acid, ***c***. Brownish semi-solid , Yield 69%; IRS (KBr): 3318.0 (N–H), 2071.0–30628 (OH– carboxylic acid), 1675.9 (C=O), 1566.1 and 1620.3 (CH_2) cm^{-1}; ^1H NMR ($CDCl_3$) δ: 2.36 (d, 2, α C=O, 2H), 2.98 (d, 2, β C=O, 2H), 5.92 (s, 1, CH, 1H), 3.7 (s, 3, OCH_3, 3H), 7.30–8.3 (m, 13, Ar–H, 13H), 11.5 (s, 1, COOH, 1H), 2.40 (s, 1, NH), 4.1 (t, 1, CH, 1H), 3.11–3.40 (t, 2, CH_2, 2H). MS (m/z, % abundance): 458.31 (M^+ 29), 441 (25), 443 (20), 440 (62). Anal. calcd. for $C_{27}H_{26}N_2O_4$ C, 73.28; H, 5.92; N, 6.33; O, 14.46; Found: C, 73.01; H, 5.87; N, 6.78; O, 14.94%.

3-hydroxy-1-(3-(10-methoxy-5H-dibenz[b,f]azepin-5-yl)-3-oxopropyl)pyrrolidine-2-carboxylic acid, ***d***. Brownish semi-solid, yield 68%; IRS (KBr): 2311.4 and 3418.8 (OH– carboxylic acid), 1670.6 (C=O), 1566.3 and 1619.1 (CH_2) cm^{-1}. ^1H NMR ($CDCl_3$) δ: 2.36 (d, 2, α C=O, 2H), 2.98 (d, 2, β C=O, 2H), 5.92 (s, 1, CH, 1H), 3.7 (s, 3, OCH_3, 3H), 7.19–7.81 (m, 7, Ar–H, 7H), 11.5 (s, 1, COOH, 1H), 1.72–1.95 (m, 2, CH_2, 2H), 2.25–2.35 (q, 2, CH_2, 2H), 3.80 (q, 1, CH, 1H), 3.31 (d, 1, CH, 1H). MS (m/z, % abundance): 408 (M^+ 61), 410 (45), 406 (2), 404 (2), 410 (10). Anal. calcd. for $C_{27}H_{26}N_2O_4$: C, 73.28; H, 5.92; N, 6.33; O, 14.46; Found: C, 73.56; H, 5.84; N, 6.28; O, 14.11%.

3-hydroxy-2-(3-(10-methoxy-5H-dibenz[b,f]azepin-5-yl)-3-oxopropylamino)butanoic acid, ***e***. Brownish semi-solid, yield 71%. IRS (KBr): 3308.8 (N–H), 2748.1–3066.4 (OH-carboxylic acid), 1676.8 (C=O), 1566.1and 1619.4 (CH_2) cm^{-1}. ^1H NMR ($CDCl_3$) δ: 2.36 (d, 2, α C=O, 2H), 2.98 (d, 2, β C=O, 2H), 5.92 (s, 1, CH, 1H), 3.7 (s, 3, OCH_3, 3H), 7.19–7.81 (m, 7, Ar–H, 7H), 11.5 (s, 1, COOH, 1H), 5.1 (s, 1, OH, 1H), 4.1 (t, 1, CH, 1H), 1.22 (d, 3, CH_3, 3H), 3.65 (d, 1, CH, 1H). MS (m/z, % abundance): 396 (M^+ 15), 397 (17), 399 (12), 400 (15). Anal. calcd. for $C_{23}H_{24}N_2O_5$: C, 67.63; H, 5.92; N, 6.86; O, 19.59%; Found: C, 67.79: H, 5.89; N, 6.74; O, 19.01%.

Radical scavenging activity

In the present study, the newly synthesized compounds were screened in regard to their DPPH free radical scavenging activity. The DPPH evaluation of different L-aminoacids (L-tyrosine, L-phenylalanine, L-hydroxyproline and L-threonine) was also carried out and a comparative study towards newly synthesized products was also done. The compounds under studies were dissolved in distilled ethanol (50 mL) to prepare 1000 μM solution. Solutions of different concentrations (10, 50, 100, 200 and 500 μM) were prepared by serial dilution and the free radical scavenging activity was studied.

The DPPH radical scavenging effect was evaluated according to the method first employed by Blois [18]. Compounds of different concentrations were prepared in distilled ethanol, 1 mL of each

compound solution having different concentrations (10, 50, 100, 200 and 500 μM). These were taken in different test tubes, 4 mL of a 0.1 mM ethanol solution of DPPH was added and shaken vigorously. The tubes were then incubated in a dark room at room temperature for 20 min. A DPPH blank was prepared without any compound, and ethanol was used for the baseline correction. Changes (decrease) in the absorbance at 517 nm were measured using a UV-visible spectrophotometer and the remaining concentration of DPPH was calculated. The percentage decrease in the absorbance was recorded for each concentration, and the percentage quenching of DPPH was calculated on the basis of the observed decrease in absorbance of the radical. The radical scavenging activity was expressed as the inhibition percentage and was calculated using the formula:

$$\textit{Radical scavenging activity} = [(A_0 - A_1)/A_0] \times 100 ,$$

where A_0 is the absorbance of the control (blank, without compound) and A_1 is the absorbance of the compound. The radical scavenging activities of BHA and ascorbic acid were also measured and compared with that of the newly synthesized compound. The % DPPH activities for all the pure L-aminoacids and newly synthesized compounds were determined and showed in Figures 1 and 2. On the other hand, the half inhibition concentration (IC_{50}) for all the newly synthesized compounds and L-aminoacids including the reference antioxidants was calculated graphically using a linear regression algorithm and showed in the Table 1.

RESULTS AND DISCUSSIONS

The key intermediate 3-chloro-1-(10-methoxy-5H-dibenz[b,f]azepine-5-yl)propan-1-one was prepared with a good yield by N-acylation reaction. In practice, 10-methoxy 5H-dibenz[b,f]azepine and 3-chloro-propionyl chloride were mixed at 1:1.2 ratio. Triethylamine was used to maintain basic conditions. The reaction was carried out for 6 h at room temperature. The final product was separated from the reaction mixture by washing the HCl salt (precipitate) with distilled water and the compound was extracted with diethyl ether. Further, it was washed with 5% $NaHCO_3$ to remove the remaining quantity of acids. Then the organic phase was separated and desolventized by vacuum-distillation and finally the product was isolated through column chromatography by using 9:1 hexane:ethyl acetate mixture as mobile phase.

The direct inclusion of L-aminoacids to 10-methoxy-5H-dibenz[b,f]azepine was unfavourable, because here the active sites for the direct inclusion are less and the experimental procedure was difficult, which leads to the major disadvantages for direct coupling of L-aminoacid. So, to overcome these problems, a key intermediate was needed to couple L-aminoacid. Thus we synthesized 3-chloro-1-(10-methoxy-5H-dibenz[b,f]azepine-5-yl)propan-1-one, where the inclusion of L-aminoacids can be done very easily with simple experimental procedure resulting good yield.

Aminoacid analogues of 10-methoxy-5H-dibenz [b,f]azepine were obtained by reacting respective L-aminoacid:3-chloro-1-(10-methoxy-5H-dibenz[b,f] azepine-5-yl)propan-1-one = 1.2:1 mM. The respective L-aminoacids were obtained dissolved in methanol. 600 mg of anhydrous K_2CO_3 was added and stirred for 30 min. 3-Chloro-1-(10-methoxy-5H-dibenz[b,f]azepine-5-yl)propan-1-one in methanol was added drop by drop and refluxed for 6 h. The reaction was monitored by TLC. The methanol containing the final product was desolventized by vacuum-distillation and the product was extracted with ethyl acetate. Further, the ethyl acetate layer was washed with water to remove K_2CO_3 and dried over anhydrous Na_2SO_4. Desolventation by vacuum-distillation was done and the final product was isolated by column chromatography by using chloroform/methanol/acetic acid = 85: 15: 3 as mobile phase.

The newly synthesized compounds were screened in regard to their DPPH free radical scavenging activity. The DPPH test provided information about the reactivity of the tested compounds with a stable free radical. Because of its odd electron, the DPPH radical showed a strong absorption band at 517 nm in visible light region (a deep purple color). As this electron is paired off in the presence of a free radical scavenger, the absorption band vanishes and the resulting discolouration is stochiometric with respect to the number of electrons taken up. This bleaching of DPPH colouring, which occurs in the odd electron of the radical is paired, thus it is representative of the capacity of the compounds to scavenge free radicals independently. Initially, before coupling the L-aminoacids to the key intermediate the DPPH activity for the respective L-aminoacids was evaluated. Some comparative studies including standard antioxidants and the newly synthesized products were also done. Our study reveals that the L-aminoacids have potential with respect to DPPH activity showing slightly lower activity than the products and standard antioxidants.

Figure 1 illustrates the DPPH activity – L-aminoacids like L-tyrosine and L-hydroxyproline exhibited good activity, L-threonine showed average activity and L-phenylalanine showed negligible

activity. All the L-aminoacids showed lower activity than the standards like ascorbic acid and BHA. Increase in activity was observed after coupling these L-aminoacids to the intermediate. This may be due to the presence of OCH_3, in the basic molecule. Keeping standard antioxidants in mind, comparative studies with the standard antioxidants (Ascorbic acid and **BHA**) and the newly synthesized compound were done. The DPPH free radical scavenging ability of the newly synthesized compounds is showed in Figure 2.

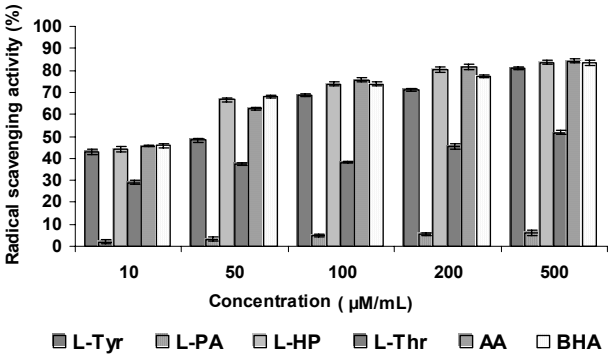

Fig. 1. DPPH free radical scavenging ability of respective L-aminoacids. Values represent arithmetic means ± SD (n = 3). Where: L-Tyr = L-tyrosine, L-PA = L-phenylalanine, L-HP = L-hydroxyproline, L-Thr = L-threonine, AA = Ascorbic acid and BHA = Butylated hydroxyanisole.

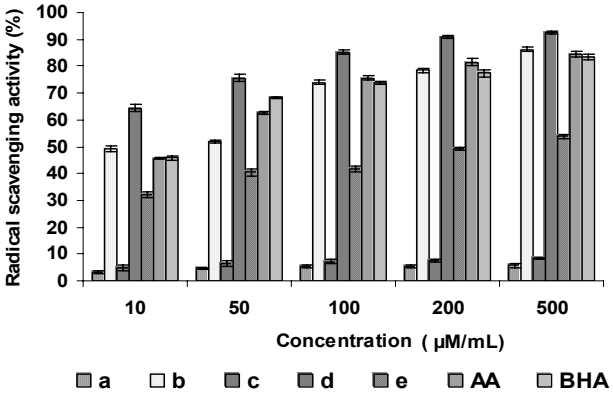

Fig. 2. DPPH free radical scavenging ability of 3-chloro-1-(10-methoxy-5H-dibenz[b,f]azepine-5-yl)propan-1-one and its L-aminoacid analogues.
Values represent arithmetic means ± SD (n = 3).
The notations are: **a**. 3-chloro-1-(10-methoxy-5H-dibenz [b,f]azepine-5-yl) propan-1-one; **b**. 3-(4-hydroxyphenyl)-2-(3-(10-methoxy-5H-dibenz[b,f]azepin-5-yl)-3-oxopropylamino) propanoic acid; **c**. 2-(3-(10-methoxy-5H-dibenz[b,f]azepin-5-yl)-3-oxopropylamino)-3-phenylpropanoic acid; **d**. 3-hydroxyl-1-(3-10-methoxy-5H-dibenz[b,f]azepine-5yl)-3-oxopropyl)pyrrolidine-2-carboxylic acid; **e**. 3-hydroxy-2-(3-(10-methoxy-5H-dibenz[b,f]azepin-5-yl)-3-oxopropyl amino)butanoic acid. AA - ascorbic acid; BHA - butylated hydroxyanisole.

The half inhibition concentration (IC_{50}) for all the L-aminoacids and newly synthesized compounds including standard antioxidants is summarized in the Table 1 and Table 2.

Table 1. 50% Inhibition of DPPH radical by L-aminoacid including standard antioxidants. The sign (–) corresponds to negligible activity. Values represent arithmetic means ± SE (n = 3). AA - ascorbic acid; BHA - butylated hydroxyanisole.

Compound	IC_{50}, µM/mL
L-Tyrosine	47±0.90
L-Phenylalanine	–
L-Hydroxyproline	4.1 ±0.87
L-Threonine	176.0± 1.2
AA	4.94 ± 0.63
BHA	5.26 ± 0.87

Table 2. 50% inhibition of DPPH radical by 3-chloro-1-(10-methoxy-5H-dibenz[b,f]azepine-5-yl)propan-1-one and its L-aminoacid analogues. The sign (–) corresponds to negligible activity. AA - ascorbic acid; BHA - butylated hydroxyanisole.

Compound	IC_{50}, µM/mL
a	–
b	40 ± 1.02
c	–
d	2.9 ± 0.92
e	160.0 ± 1.21
AA	4.94 ± 0.63
BHA	5.26 ± 0.87

IC_{50} - concentration required for 50% reduction of 0.1 mM DPPH radical. Values represent arithmetic means ± SE (n=3). The notations are: **a** - 3-chloro-1-(10-methoxy-5H-dibenz[b,f]azepine-5-yl)propan-1-one; **b** - 3-(4-hydroxyphenyl)-2-(3-(10-methoxy-5H-dibenz[b,f]azepin-5-yl)-3-oxopropylamino)propanoic acid; **c** - 2-(3-(10-methoxy-5H-dibenz[b,f]azepin-5-yl)-3-oxopropylamino)-3-phenylpropanoic acid; **d** - 3-hydroxyl-1-(3-10-methoxy-5H-dibenz[b,f]azepine-5yl)-3-oxopropyl)pyrrolidine-2-carboxylic acid; **e** - 3-hydroxy-2-(3-(10-methoxy-5H-dibenz[b,f]azepin-5-yl)-3oxopropylamino)butanoic acid. AA – Ascorbic acid; BHA - Butylated hydroxyanisole.

Initially the DPPH free radical scavenging capacity of 3-chloro-1-(10-methoxy-5H-dibenz[b,f] azepine-5-yl)propan-1-one **a**, was assessed and found not to be effective. Consequently, molecules with L-aminoacid groups were coupled to enhance the radical scavenging activity effect. Analogues of L-tyrosine **b**, L-hydroxyproline **d**, and L-threonine **e**, aminoacids showed promising radical scavenging activity with a major activity for L-hydroxyproline analogues **d**. When L-tyrosine molecule is coupled to 3-chloro-1-(10-methoxy-5H-dibenz[b,f]azepine-5-yl)propan-1-one **a,** the activity will be enhanced due to the presence of phenolic group. The activity disappears due to the absence of –OH group in L-phenylalanine. When L-hydroxyproline is coupled to the intermediate, the RSA increases with a major activity due to the presence of –OH group, attached to the five member heterocyclic ring. May be the presence of free –OH group in L-threonine showed

the average activity over all the analogues. These results showed the major importance of the L-aminoacid substituent in DPPH free radical effects. An increasing order of DPPH activity for the synthesized compounds can be given as follows:

3-hydroxyl-1-(3-10-methoxy-5H-dibenz[b,f]azepine-5yl)-3-oxopropyl)pyrrolidine-2-carboxylic acid, **d** > 3-(4-hydroxyphenyl)-2-(3-(10-methoxy-5H-dibenz[b,f]azepin-5-yl)-3-oxopropylamino)propanoic acid, **b** > 3-hydroxy-2-(3-(10-methoxy-5H-dibenz[b,f]azepin-5-yl)-3oxopropylamino)butanoic acid, **e** > 2-(3-(10-methoxy-5H-dibenz[b,f]azepin-5-yl)-3-oxopropylamino)-3-phenyl propanoic acid, **c** > 3-chloro-1-(10-methoxy-5H-dibenz[b,f]azepine-5-yl) propan-1-one, **a**. The synthesized compounds were compared to internal standards (AA and BHA). Among the synthesized compounds L-tyrosine analogues **b**, showed almost equal activity compared to standards and L-hydroxyproline analogues **d**, showed more effective DPPH activity than the standards.

CONCLUSION

The method, proposed by us, reproduces the synthesis of L-aminoacid analogues of 10-methoxy-5H-dibenz[b,f]azepine. The synthesized compounds were characterized with the help of spectroscopic technique and were screened in regard to their ability to DPPH radical scavenging activity. Based on the biological assay it was found that the key intermediate 3-chloro-1-(10-methoxy-5H-dibenz[b,f] azepine-5-yl)propan-1-one **a**, showed no effect towards DPPH activity, but the moiety of 3-chloro-1-(10-methoxy-5H-dibenz[b,f]azepine-5-yl)propan-1-one containing L-tyrosine **b**, L-hydroxyproline **d,** and L-threonine **e,** showed promising DPPH radical scavenging activity. However, L-hydroxyproline analogue **d**, was found to have most effective radical scavenging activity compared to the other analogues and also internal standards (AA and BHA). The comparative studies on DPPH activity of L-aminoacids with the newly synthesized products reveal that L-aminoacids possess lower DPPH activity compared to the respective products and the standard antioxidants. Our study provides evidence that several L-aminoacid analogues of 10-methoxy-5H-dibenz[b,f]azepine exhibit interesting direct DPPH free radical activity. These effects may be useful in the treatment of pathologies, in which free radical oxidation plays a fundamental role.

REFERENCE

1. K. B. Beckman, B. N. Ames, *Physiol. Rev.*, **78**, 447 (1998).
2. B. Halliwell, J. M. C. Gutteridge, Free Radicals in Biology and Medicine, Clandon Press, Oxford, 1989, p. 416.
3. G. Block, *Nutr. Rev.s*, **50**, 207 (1992).
4. A. C. Rice evans, N. J. Miller, G. Paganga, *Free Radical Biol. Med.*, **20,** 933 (1996).
5. E. Denisov, I. V. Khudyakov, *Chem. Rev.*, **87**, 1313 (1987).
6. B. Halliwell, *Free Radical Res. Commun*., **9**, 1 (1990).
7. C. A. Rice Evans, A. T. Diplock. *Free Radical Biol. Med.*, **15**, 77 (1993).
8. L. Chirtian Beh, B. Moosmann, *Free Radical Biol. Med.*, **33**, 182 (2000).
9. M. Lucarini, P. Pedrielli, G. F. Pedulli, L. Valgimigli, D. Gigmes, P. Toroda, *J. Am. Oil Chem. Soc.,* **121**, 11546 (1999).
10. L. J. Krichka, A. Ledwith, *Chem. Rev.*, **74**, 101 (1974).
11. A. Hempel, N. Camerman, A. Camerman, D. Mastropaolo, *Acta Crystallogr. E,* **61**, 01313 (2005).
12. J. Fouche, A. Leger, German Pat. 2,031,236 (1971); *Chem. Abstr*. **74**, 76346r (1971).
13. H. Vijay Kumar, C. R. Gnanendra, Nagaraja Naik, D. Channe Gowda, *E-J. Chem.*, **5 (S2)**, 1123 (2008).
14. T. You-Zhi, L. Zai-Qun, *Bioorg. Med. Chem.*, **15**, 1903 (2007).
15. J. A. Vinson, Y. A. Dabbagh, M. M. Serry, J. Jang, *J. Agric. Food Chem*., **43**, 2800 (1995).
16. P. L. Teissedre, A. L. Waterhouse, *J. Agric. Food Chem.*, **48,** 3801 (2000).
17. R. Amarowicz, F. Shahidi, *Food Chem.*, **58,** 355 (1997).
18. M. S. Blois, *Nature,* **26**, 1199 (1958).

СИНТЕЗ НА АМИНОКИСЕЛИННИ АНАЛОЗИ НА 10-МЕТОКСИ-ДИБЕНЗ[b,f]АЗЕПИН И ОЦЕНКА НА ТЯХНАТА АКТИВНОСТ КАТО АНТИОКСИДАНТИ

Х. В. Кумар, К. Р. Гнанендра, Д. Ч. Гоуда, Н. Наик*

Департамент по химични изследвания, Университет на Майсур, Манасаганготри, Майсур 570 006, Карнатака, Индия

Постъпила на 19 май 2008 г.; Преработена на 6 октомври 2008 г.

(Резюме)

Предложен е метод за синтез на L-аминокиселинни (L-тирозинов, L-фенилаланинов, L-хидроксипролинов и L-треонинов) аналози на 10-метокси-дибенз[b,f]азепин. 10-Метокси-дибенз[b,f]азепин като основна молекула е синтезиран по известен метод. Ключовото междинно съединение 3-хлоро-1-(10-метокси-5H-дибенз[b,f]азепин-5-ил)пропан-1-он е получено чрез N-ацилиране на 10-метокси-дибенз[b,f]азепин с 3-хлоро-пропионилхлорид. Проведено е последващо сдвояване на съответните L-аминокиселини до получаване съответно на 3-(4-хидроксифенил)-2-(3-(10-метокси-5H-дибенз[b,f]азепин-5-ил)-3-оксопропиламино)пропанова киселина, 2-(3-(10-метокси-5H-дибенз[b,f]азепин-5-ил)-3-оксопропиламино)-3-фенилпропанова киселина, 3-хидрокси-1-(3-(10-метокси-5H-дибенз[b,f]азепин-5-ил)-3-оксопропил)пиролидин-2-карбоксилна киселина и 3-хидрокси-2-(3-(10-метокси-5H-дибенз[b,f]азепин-5-ил)-3-оксопропиламино)бутанова киселина. Оценена е активността на получените съединения като антиоксиданти по отношение на 1,1-дифенил-2-пикрилхидразил (ДФПХ) свободни радикали. Бутилхидроксианизол (БХА) и аскорбинова киселина са използвани като стандартни антиоксиданти и е направено сравнение с новополучените съединения. При използваните експериментални условия, аналозите съдържащи L-тирозин, L-хидроксипролин и L-треонин имат пряко действие като анти-оксиданти чрез улавяне на стабилния ДФПХ радикал. L-хидроксипролиновите аналози показват значителна активност като анти-оксиданти сред синтезираните аналози. Активността на чистите L-аминокиселини спрямо ДФПХ също е оценена и е сравнена с тази на синтезираните продукти. Установено е, че продуктите проявяват по-висока антиоксидантна активност спрямо тази на L-аминокиселините.

Bulgarian Chemical Communications, Volume 41, Number 1 (pp. 80–83) 2009

One pot synthesis of dihydroisoxazoles *via* 1,3-dipolar cycloaddition of nitrile oxides to allyl chloride

A. S. Paniraj, K. M. Lokanath Rai*

Department of Chemistry, University of Mysore, Manasagangotri-570006, India

Received February 26, 2008; Revised September 23, 2008

Nitrile oxides derived from oxidative dehydrogenation of aldoximes by chloramine-T react with allyl chloride to afford 5-(chloromethyl)-3-aryl-4,5-dihydroisoxazoles in good yields. All compounds were characterized by IR, ^{1}H-NMR, and MS studies.

Key words: chloramine-T, nitrile oxide, dipolar cycloaddition, dihydroisoxazoles.

INTRODUCTION

Isoxazoles, isoxazolines, isoxazolidines and their derivatives have been isolated from natural sources or synthesized and individual compounds or closely related group of compounds have been reported to be active as herbicides, anti-protozoan drugs, hypoglycemic agents, anti-inflammatory agents or antipyretic agents. The 4,5-dihydroisoxazoles are versatile sources of the functional groups present in the natural products and there is renewed interest in the synthesis of these compounds *via* 1,3-dipolar cycloaddition of nitrile oxides to olefins. The 1,3-dipolar cycloaddition reactions are a useful tool for constructing biologically potent five-membered heterocyclic compounds [1]. Cycloaddition of nitrile oxide to olefinic or acetylenic compounds is of synthetic interest, since the obtained products are the versatile intermediates for the synthesis of bifunctional compounds [2]. Apart from the various dipolarophiles known, nitrile oxides have been extensively used.

The synthesis of nitrile oxides usually involves the oxidative dehydrogenation of aldoximes using oxidants such as lead tetraacetate [3], alkalihypohalite [4], *N*-bromosuccinimide in DMF followed by treatment with a base [5], chloramine-T [6], mercuric acetate [7] or 1-chlorobenzotriazole [8] as well as the reactions of nitro-compounds with aryl isocyanate [9] and di-*tert*-butyl-dicarbonate in the presence of *N,N*-dimethylaminopyridine [10].

In continuation of our earlier work on 1,3-dipolar cycloaddition reactions, an attempt was made by using allyl chloride as dienophile for the cycloaddition of preformed nitrile oxides to obtain dihydroisoxazoles. The reactions were successfully carried out at 40°C for 2 h in ethanol and the dihydroisoxazoles were obtained in 50–65% yield.

RESULTS AND DISCUSSION

Various reactions have been reported with isolated nitrile oxides and without isolation of nitrile oxide, in this paper we report intramolecular cycloaddition of *in situ* generated nitrile oxide with ally chloride afforded dihydroisoxazoles. In a typical reaction, aldoxime, excess of allyl chloride, ethanol, and chloramine-T were mixed together (Scheme 1). Exothermic reaction was observed with the formation of a product, though no effort was made to control this exothermic reaction. The reaction mixture was then allowed to cool down to room temperature, which after the usual processing gave the product in 65% yield. The cycloaddition reactions afforded 4,5-dihydroisoxazoles in good yields (Table 1).

The reaction was investigated using alkene/nitrile oxide ratios of 1:1, 2:1, 3:1 respectively, whereupon the reactions at lower ratios gave poor yields and polymerization of the nitrile oxide [11]. The fast reaction of aldoximes with chloramine-T explains why the reaction proceeds in the presence of olefinic double bonds. The role of chloramine-T in these transformations may be chlorination of aldoxime to a hydroxamic acid chloride, followed by base catalyzed HCl elimination. Although no blue colour was detected in the reactions of aldoximes with chloramine-T, we found that the treatment of cyclohexanone oxime with this reagent produced a blue colour suggesting of formation of 1-chloro-1-nitrosocyclohexane [12].

* To whom all correspondence should be sent:
E-mail: kmlrai@yahoo.com

© 2009 Bulgarian Academy of Sciences, Union of Chemists in Bulgaria

Table 1. 5-(chloromethyl)-3-aryl-4,5-dihydroisoxazoles.

Entry	Oxime	Structure	Yield, %
1	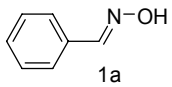 1a	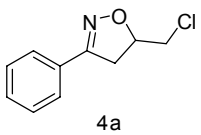 4a	65
2	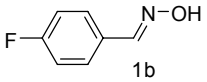 1b	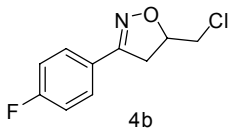 4b	55
3	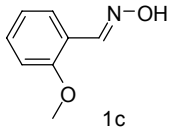 1c	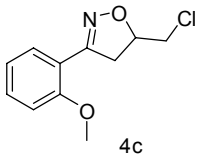 4c	50
4	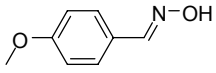 1d	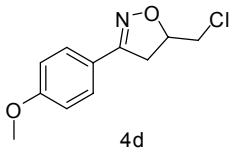 4d	60
5	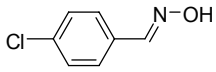 1e	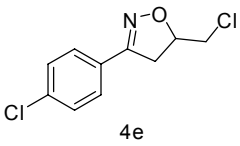 4e	65
6	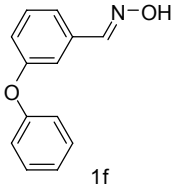 1f	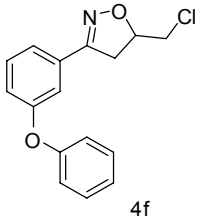 4f	55
7	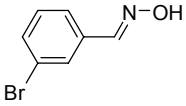 1g	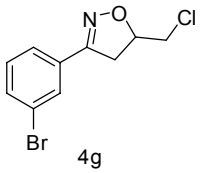 4g	60
8	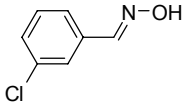 1h	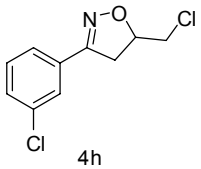 4h	56
9	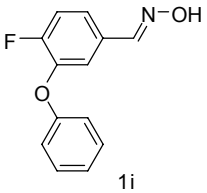 1i	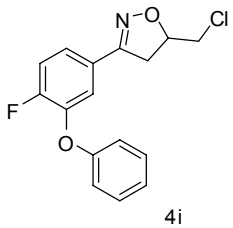 4i	55
10	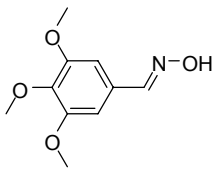 1j	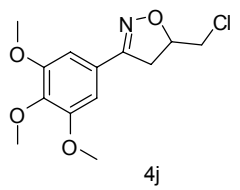 4j	50

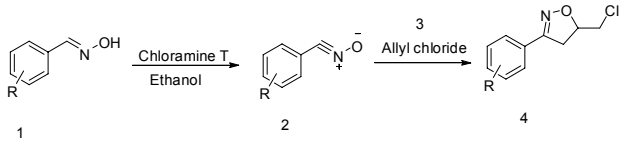

R = H; 4-F; 2-OMe; 4-OMe; 4-Cl; 3-OPh; 3-Br; 3-Cl; 4-F; 3-Oph; 3,4,5 $(OMe)_3$.

Scheme 1.

EXPERIMENTAL SECTION

^{1}H-NMR spectra were recorded on 400 MHz Bruker AVANCE 400 spectrometer and ^{13}C-NMR spectra were recorded on 100 MHz Bruker AVANCE 400 spectrometer, respectively, using TMS as an internal standard. IR spectra were recorded on a Perkin-Elmer FT/IR 100 spectrometer. Mass spectra were recorded on ESI MS mass spectrometer. All the reactions were monitored by thin layer chromatography (TLC). TLC was performed on F_{254}, 0.25 mm silica gel coated plates (Merck). The plates were eluated with appropriate solvent systems prepared in the laboratory. The developed plates were analysed under UV light 254 nm. Column chromatography was performed using silica gel with particle size 100–200 mesh.

General procedures for the synthesis

3-aryl-5-(chloromethyl)-4,5-dihydroisoxazole. A mixture of aldoxime (10 mmol), ethanol (20 mL), chloramine-T (12 mmol) and allyl chloride (10 mL) was stirred at ambient temperature. An exothermic reaction occurred and the temperature rises to 45°C. After 30 min, the temperature was maintained at 40°C by heating in an oil bath for 2 h or till the disappearance of oxime. After the completion of the reaction, the solvent was evaporated in vacuum, and the residual mass was extracted with ether (25 mL), washed with water, 1 N NaOH solution (10 mL), brine solution (10 mL) and dried over anhydrous sodium sulphate. Evaporation of the solvent under reduced pressure afforded a white mass, which was purified by column chromatography over silica gel using chloroform as eluent.

5-(chloromethyl)-3-phenyl-4,5-dihydroisoxazole (**4a**). White solid; m.p. 53–55°C; IRS (KBr): 3060, 2956, 1697, 1598, 1447 cm^{-1}; ^{1}H-NMR ($CDCl_3$) δ: 3.32–3.38 (dd, *J* = 6.4 and 16.8 Hz, 1H), 3.47–3.54 (dd, *J* = 10.4 and 16.8 Hz, 1H), 3.55–3.60 (dd, *J* = 7.6 and 11.2 Hz, 1H), 3.70–3.74 (dd, *J* = 4.4 and 11.2 Hz), 4.95–5.02 (m, 1H), 7.41–7.42 (m, 3H), 7.67–7.69 (m, 2 H); ^{13}C-NMR ($CDCl_3$) 38.1, 51.6, 69.6, 128.2, 128.8, 131, 136, 156.2; ESI-MS *m/z*: 196 $[M+1]^+$.

5-(chloromethyl)-3-(4-fluorophenyl)-4,5-dihydroisoxazole (**4b**). White solid; m.p. 65–67°C; IRS

(KBr): 3074, 2928, 1694, 1602, 1446 cm^{-1}; ^{1}H-NMR ($CDCl_3$) δ: 3.32–3.38 (dd, *J* = 6.4 and 16.8 Hz, 1H), 3.47–3.54 (dd, *J* = 10.4 and 16.8 Hz, 1H), 3.55–3.60 (dd, *J* = 7.6 and 11.2 Hz, 1H), 3.70–3.74 (dd, *J* = 4.4 and 11.2 Hz), 4.95–5.02 (m, 1H), 7.29–7.36 (m, 2H), 7.62–7.81 (m, 2H); ^{13}C-NMR ($CDCl_3$) 38.1, 51.6, 69.6, 115.6, 126, 129.5, 156.2, 165.2; ESI-MS *m/z*: 214 $[M+1]^+$.

5-(chloromethyl)-3-(2-methoxyphenyl)-4,5-dihydroisoxazole (**4c**). White solid; m.p. 80–85°C; IRS (KBr): 3067, 2933, 1689, 1604, 1449 cm^{-1}; ^{1}H-NMR ($CDCl_3$) δ: 3.32–3.38 (dd, *J* = 6.4 and 16.8 Hz, 1H), 3.47–3.54 (dd, *J* = 10.4 and 16.8 Hz, 1H), 3.55–3.60 (dd, *J* = 7.6 and 11.2 Hz, 1H), 3.70–3.74 (dd, *J* = 4.4 and 11.2 Hz), 3.83 (s, 3H), 4.95–5.02 (m, 1H), 6.95–7.01 (m, 1H), 7.22–7.26 (m, 1H), 7.39–7.50 (m, 2H); ^{13}C-NMR ($CDCl_3$) 38.4, 51.6, 55.8, 69.6, 111.2, 117.2, 121.1, 131.7, 132, 156.2; ESI-MS *m/z*: 226 $[M+1]^+$.

5-(chloromethyl)-3-(4-methoxyphenyl)-4,5-dihydroisoxazole (**4d**). White solid; m.p. 75–76°C; IRS (KBr): 3068, 2932, 1690, 1607, 1445 cm^{-1}; ^{1}H-NMR ($CDCl_3$) δ: 3.32–3.38 (dd, *J* = 6.4 and 16.8 Hz, 1H), 3.47–3.54 (dd, *J* = 10.4 and 16.8 Hz, 1H), 3.55–3.60 (dd, *J* = 7.6 and 11.2 Hz, 1H), 3.70–3.74 (dd, *J* = 4.4 and 11.2 Hz), 3.83 (s, 3H), 4.95–5.02 (m, 1H), 7.03–7.08 (m, 2H), 7.89–7.93 (m, 2H); ^{13}C-NMR ($CDCl_3$) 38.1, 51.6, 55.8, 69.6, 114.4, 122.7, 128.7, 156.2, 162.9; ESI-MS *m/z*: 226 $[M+1]^+$.

5-(chloromethyl)-3-(4-chlorophenyl)-4,5-dihydroisoxazole (**4e**). White solid; m.p. 95–97°C; IRS (KBr): 3072, 2937, 1695, 1609, 1447 cm^{-1}; ^{1}H-NMR ($CDCl_3$) δ: 3.32–3.38 (dd, *J* = 6.4 and 16.8 Hz, 1H), 3.47–3.54 (dd, *J* = 10.4 and 16.8 Hz, 1H), 3.55–3.60 (dd, *J* = 7.6 and 11.2 Hz, 1H), 3.70–3.74 (dd, *J* = 4.4 and 11.2 Hz), 4.95–5.02 (m, 1H), 7.50–7.56 (m, 2H), 7.95–7.99 (m, 2H); ^{13}C-NMR ($CDCl_3$) 38.1, 51.6, 69.6, 128.2, 128.5, 136.6, 156.2; ESI-MS *m/z*: 230 $[M+1]^+$.

5-(chloromethyl)-3-(3-phenoxyphenyl)-4,5-dihydroisoxazole (**4f**). White solid; m.p. 85–86°C; IRS (KBr): 3077, 2942, 1698, 1606, 1449 cm^{-1}; ^{1}H-NMR ($CDCl_3$) δ: 3.26–3.32 (dd, *J* = 6.4 and 17.2 Hz, 1H), 3.42–3.49 (dd, *J* = 10.4 and 17.2 Hz, 1H), 3.53–3.58 (dd, *J* = 7.2 and 11.2 Hz, 1H), 3.67–3.71 (dd, *J* = 4.4 and 12 Hz, 1H), 4.93–5.0 (m, 1H), 6.99–7.06 (m, 3H), 7.1–7.14 (m, 1H), 7.32–7.39 (m, 5H); ^{13}C-NMR ($CDCl_3$) 38.1, 51.6, 69.6, 116.5, 118.9, 121.2, 121.3, 128.4, 128.5, 133.7, 156.2, 157, 157.1; ESI-MS *m/z*: 288 $[M+1]^+$.

3-(3-bromophenyl)-5-(chloromethyl)-4,5-dihydroisoxazole (**4g**). White solid; m.p. 80–83°C; IRS (KBr): 3075, 2941, 1695, 1606, 1449 cm^{-1}; ^{1}H-NMR ($CDCl_3$) δ: 3.26–3.32 (dd, *J* = 6.4 and 17.2 Hz, 1H), 3.42–3.49 (dd, *J* = 10.4 and 17.2 Hz, 1H), 3.53–3.58 (dd, *J* = 7.2 and 11.2 Hz, 1H), 3.67–3.71 (dd, *J* = 4.4 and 12 Hz, 1H), 4.93–5.0 (m, 1H), 7.39–7.42 (m, 1H), 7.54–7.59 (m, 1H), 7.97–7.98 (m, 2H); ^{13}C-NMR ($CDCl_3$) 38.1, 51.6, 69.6, 123, 126.6, 127.2, 129.8, 133.9, 136.2, 156.2; ESI-MS *m/z*: 275 $[M+1]^+$.

5-(chloromethyl)-3-(3-chlorophenyl)-4,5-dihydroisoxazole (**4h**). White solid; m.p. 77–79°C; IRS (KBr): 3074, 2940, 1696, 1605, 1445 cm^{-1}; ^{1}H-NMR ($CDCl_3$) δ: 3.26–3.32 (dd, *J* = 6.4 and 17.2 Hz, 1H), 3.42–3.49 (dd, *J* = 10.4 and 17.2 Hz, 1H), 3.53–3.58 (dd, *J* = 7.2 and 11.2 Hz, 1H), 3.67–3.71 (dd, *J* = 4.4 and 12 Hz, 1H), 4.93–5.0 (m, 1H), 7.44–7.54 (m, 2H), 7.8–7.92 (m, 2H); ^{13}C-NMR ($CDCl_3$) 38.1, 51.6, 69.6, 126.3, 129.2, 130.2, 131.1, 134.4, 135.4, 156.2; ESI-MS *m/z*: 231 $[M+1]^+$.

5-(chloromethyl)-3-(4-fluoro-3-phenoxyphenyl)-4,5-dihydroisoxazole (**4i**). White solid; m.p. 85–87°C; IRS (KBr): 3073, 2941, 1698, 1604, 1448 cm^{-1}; ^{1}H-NMR ($CDCl_3$) δ: 3.26–3.32 (dd, *J* = 6.4 and 17.2 Hz, 1H), 3.42–3.49 (dd, *J* = 10.4 and 17.2 Hz, 1H), 3.53–3.58 (dd, *J* = 7.2 and 11.2 Hz, 1H), 3.67–3.71 (dd, *J* = 4.4 and 12 Hz, 1H), 4.93–5.0 (m, 1H), 7.12–7.19 (m, 3H), 7.3–7.42 (m, 3H), 7.51–7.55 (m, 1H), 7.62–7.65 (m, 1H); ^{13}C-NMR ($CDCl_3$) 38.1, 51.6, 69.6, 115.3, 118.1, 118.9, 121.8, 122.6, 128.4, 129.3, 143.2, 156.2, 157, 157.6; ESI-MS *m/z*: 306 $[M+1]^+$.

5-(chloromethyl)-3-(3,4,5-trimethoxyphenyl)-4,5-dihydroisoxazole (**4j**). White solid; m.p. 96–99°C; IRS (KBr): 3078, 2945, 1699, 1610, 1449 cm^{-1}; ^{1}H-NMR ($CDCl_3$) δ: 3.26–3.32 (dd, *J* = 6.4 and 17.2 Hz, 1H), 3.42–3.49 (dd, *J* = 10.4 and 17.2 Hz, 1H), 3.53–3.58 (dd, *J* = 7.2 and 11.2 Hz, 1H), 3.67–3.71 (dd, *J* = 4.4 and 12 Hz, 1H), 3.83 (s, 9H), 4.93–5.0 (m, 1H), 6.95 (dd, 2H); ^{13}C-NMR ($CDCl_3$) 38.1, 51.6, 56.1, 60.8, 69.6, 106.6, 128.3, 141.5, 153.2, 156.2; ESI-MS *m/z*: 286 $[M+1]^+$.

***Acknowledgements**: The authors acknowledge help and support by Department of Chemistry, University of Mysore, Manasagangotri-570006, India.*

REFERENCES

1. P. Caramella, P. Grunanger, in: 1,3-Dipolar Cycloaddition Chemistry, A. Padwa, Ed., Wiley and Sons, New York, 1984.
2. K. M. Lokanath Rai, A. Hassner, *Ind. J. Chem*., **36B**, 242 (1997); C. Grundman, P. Grunanger, in: The Nitrile Oxide, Springer Verlag, New York, 1971.
3. G. Just, L. Dahl, *Tetrahedron,* **24**, 5251 (1968).
4. C. Grundaman, J. M. Dean, *J. Org. Chem.,* **30,** 2809 (1965).
5. C. Grundaman, R. Richter, *J. Org. Chem.,* **33**, 476 (1969).
6. A. Hassner, K. M. L. Rai, *Synthesis,* 57 (1989).

7. K. M. L. Rai, N. Linganna, A. Hassner, C. A. Murthy, *Org. Prep. Proced. Int.,* **24**, 91 (1992).
8. J. N. Kim, E. K. Rui, *Synth. Commun.,* **20**, 1373 (1990).
9. T. Mukaiyama, T. Hoshino, *J. Am. Chem. Soc.,* **82**, 5399 (1960).
10. Y. Basel, A. Hassener, *Synthesis,* 309 (1997).
11. C. J. Easton, S. J. Barrow, *Tetrahedron Lett.,* **38**, 2175 (1997).
12. E. J. Corey, H. Estreicher, *Tetrahedron Lett.,* **21**, 1117 (1980).

ЕДНОСТАДИЕН СИНТЕЗ НА ДИХИДРОИЗОКСАЗОЛИ ЧРЕЗ 1,3-ДИПОЛЯРНО ЦИКЛОПРИСЪЕДИНЯВАНЕ НА НИТРИЛОКСИДИ КЪМ АЛИЛХЛОРИД

А. Ш. Панирадж, К. М. Локанат Рай*

Департамент по химия, Университет на Майсур, Манасаганготри 570006, Индия

Постъпила на 26 февруари 2008 г.; Преработена на 23 септември 2008 г.

(Резюме)

При реакцията на нитрилоксиди, получени чрез окислително дехидрогениране на алдоксими с хлорамин-Т, с алилхлорид са получени 5-(хлорометил)-3-арил-4,5-дихидроизоксазоли с добър добив. Всички съединения са охарактеризирани чрез ИЧ, ^{1}Н ЯМР и масспектрални изследвания.

Bulgarian Chemical Communications, Volume 41, Number 1 (pp. 84–88) 2009

Microwave assisted condensation of hydrazone derivatives with aldehydes

M. I. Marzouk

Chemistry Department, Faculty of Science, Ain Shams University, Abassia, Cairo, Egypt

Received May 12, 2008; Revised November 6, 2008

3-(4-Chloro-3-methyl)benzoylpropionic acid and 3-(4-chloro-3-methyl)benzoylprop-2-enoic acid reacted with hydrazine hydrate under conventional and microwave irradiation conditions in the absence of solvents to afford 6-(4-chloro-3-methyl)phenyl-(2H)-4,5-dihydropyridazine-3-one and 6-(4-chloro-3-methyl)phenyl-(2H)-pyridazine-3-one in good yields. The oxidation of dihydropyridazinone with Br_2/AcOH gave 6-(4-chloro-3-methyl)phenyl-(2H)-pyridazine-3-one. 6-(4-Chloro-3-methyl)phenyl-(2H)-4,5-dihydropyridazine-3-one reacted with ethyl bromoacetate under microwave irradiation in polyethyleneglycol to give 6-(4-chloro-3-methyl)phenyl-2-carbethoxymethyl dihydropyri-dazine-3-one, which further reacted with hydrazine hydrate under microwaves to give the corresponding hydrazide. The hydrazide reacted with certain aldehydes namely benzaldehyde, *p*-nitrobenzaldehyde, 3,4,5-trimethoxybenzaldehyde, piperonal and 2-hydroxynaphthaldehyde in DMF under microwave irradiation to give the corresponding hydrazones.

Key words: pyridazinone, microwave, condensation reaction, hydrazones.

INTRODUCTION:

The present day industrialization has led to immense environmental quality deterioration. The increasing environmental consciousness throughout the world has put a pressing need to develop an alternative synthetic approach for biological and synthetic important compounds. This requires a new approach, which will reduce the material and energy consumption of chemical process and products, minimize or eliminate the emission of harmful chemicals in the environment in a way that improves the environmentally benign approach and meet the challenges of green chemistry [1]. There is a considerable current interest in organic reactions under microwave irradiation [2]; it provides advantage [3–6] with respect to reducing reaction time, and increasing product yields, when compared to conventional heating. Pyridazinones have anti-hypertensive activity [7, 8], analgesic and anti-inflammatory activity [9].

In this work, the author sought to investigate the effect of microwave irradiation on the synthesis of some pyridazinones and some hydrazones.

RESULTS AND DISCUSSION

Microwave irradiation using commercial domestic ovens in the absence of solvent is very efficient to synthesize 6-(4-chloro-3-methyl)phenyl-(2H)-4,5-dihydropyridazin-3-one **3** and 6-(4-chloro-3-methyl)phenyl-(2H)-pyridazin-3-one **4** from 3-(4-chloro-3-methyl)benzoylpropionic acid **1** and 3-(4-chloro-3-methyl)benzoylprop-2-enoic acid **2** and hydrazine hydrate, respectively, giving rise to remarkable rate enhancements (Table 1).

The authentic sample of the pyridazinone derivative **4** was prepared by the oxidation of the dihydropyridazinone **3** with Br_2/AcOH.

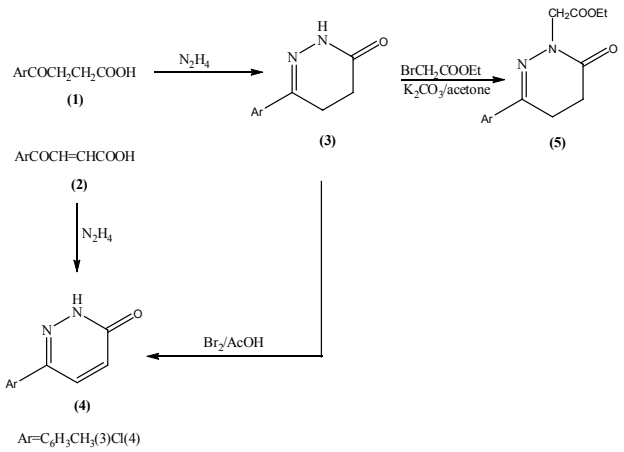

Scheme 1.

The microwave-assisted reaction was also examined in the absence of solvent and using various reaction media such as *n*-butanol and polyethyleneglycol (PEG) [10, 11] to prepare 6-(4-chloro-3-methyl)phenyl-2-carboethoxymethyl-4,5-dihydropyridazin-3-one **5** by the reaction of 6-(4-chloro-3-methyl)phenyl-(2H)-4,5-dihydropyridazine-3-one **3** with ethyl bromoacetate in the presence of K_2CO_3. The reaction in the absence of solvent and in *n*-butanol did not occur. The development of PEG eliminates the need of volatile organic solvents. This reaction [12] was also carried out by the conven-

* E-mail: douda56@yahoo.com

© 2009 Bulgarian Academy of Sciences, Union of Chemists in Bulgaria

tional method in the presence of K_2CO_3 in acetone to yield the same compound **5**.

The reaction of the 6-(4-chloro-3-methyl)phenyl-2-carboethoxymethyl-4,5-dihydropyridazin-3-one **5** with hydrazine hydrate to afford 6-(4-chloro-3-methyl)phenyl hydrazinocarbomethyl-4,5-dihydropyridazin-3-one **6** was achieved under neat reaction conditions (solvent free) and it showed a yield improvement and a time saving with respect to the conventional method (Table 1).

N,N-Dimethylformamide was used as a reaction medium in the synthesis of the aldehyde hydrazones **7(a-e)** by the reaction of 6-(4-chloro-3-methyl)-phenyl hydrazinocarbomethyl-4,5-dihydropyridazin-3-one **6** with several aldehydes namely benzaldehyde, *p*-nitrobenzaldehyde, 3,4,5-trimethoxybenzaldehyde, piperonal and 2-hydroxynaphthaldehyde. Irradiated by microwave, the reactions were completed at 360–630 W in 4–10 minutes, in contrast to the conventional method that needed 3–6 h.

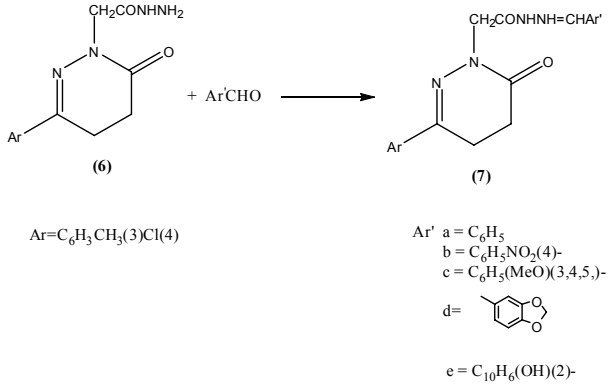

Scheme 2.

The structures of all the compounds have been confirmed by spectroscopic studies.

EXPERIMENTAL

All microwave reactions were carried out in a domestic microwave oven. All melting points were uncorrected. The IR spectra were recorded in KBr on FTIR Matteson Spectrometers. The ^{1}H NMR spectra were measured on Varian Gemini 200 MHz instrument with chemical shift (δ) expressed in ppm downfield from TMS. The mass spectra were recorded on Shimadzu GC-MS-QP 1000 Ex instrument at 70 eV. TLC was run using TLC aluminium sheets silica gel F_{254} (Merck).

*Synthesis of 6-(4-chloro-3-methyl)phenyl-(2H)-4,5-dihydropyridazin-3-one (**3**) and 6-(4-chloro-3-methyl)phenyl-(2H)-pyridazin-3-one (**4**)*

(A) By conventional heating. A mixture of the acids **1** and/or **2** (0.01 mol) and hydrazine hydrate (0.01 mol, 99%) in ethanol (30 ml) was refluxed for 6 h. The solid that separated out after concentration and cooling down was filtered off and recrystallized from ethanol to give the expected pyridazinone **3** and **4,** respectively.

(B) By microwave irradiation. A mixture of the acids **1** and/or **2** (0.01 mol) and hydrazine hydrate (0.01 mol) was irradiated with microwaves at *P* = 540 W and time 2–5 min (Table 1). The solid that was obtained was recrystallized from ethanol to give the expected pyridazinone **3** and **4**, respectively.

(C) By oxidation. A stirred solution of **3** (0.01 mol) in glacial acetic acid was heated up to ~ 60–70°C and then treated portion wise with bromine (0.01 mol) for 15 min. The mixture was stirred further for 3 h and poured into ice water. The separated solid was filtered and recrystallized from ethanol.

Table 1. Yield and reaction time interval in the synthesis of compounds **3**, **4, 5** and **6**.

Comp.	Yield A*	Microwave irradiation (neat conditions)		
No.	%	Time, min	Power, W	Yield B*, %
3	86.0	2	540	86.48
		5	540	99.00
4	95.9	2	540	79.59
		3	540	85.7
		5	540	99.00
5	80	30	360	90.00
6	65	4	450	15
		5	540	30
		10	540	80

* A - Conventional heating; B - Microwave irradiation.

Table 2. Yield and reaction time interval in the synthesis of compounds **7**(**a**–**e**).

Comp.	Yield A*	Microwave irradiation		
No.	%	Time, min	Power, W	Yield B*, %
7a	99	4	360	-
		5	450	-
		8	630	99
7b	83.3	4	360	33
		5	630	99
7c	60	4	360	-
		5	630	99
7d	83	4	360	-
		6	450	70
		10	450	78
7e	16	4	360	-
		8	630	40

* A - Conventional heating; B - Microwave irradiation.

6-(4-Chloro-3-methyl)phenyl-(2H)-4,5-dihydropyridazin-3-one (**3**): M.p. 159–62°C; ethanol. IRS cm^{-1}: 1590 (C=C), 1612 (C=N), 1683 (C=O), 3448 (NH). ^{1}H NMR (DMSO) δ: 2.3 (s, 3H, Me), 2.4–2.5 (t, 2H, CH_2 pyridazinone ring β- to C=O), 2.91–2.99 (t, 2H, CH_2 pyridazinone ring α- to C=O), 7.4–7.7 (m, 3H, Ar–H) and 10.9 (s, 1H, NH).

6-(4-Chloro-3-methyl)phenyl-(2H)-4,5-pyridazin-3-one (**4**): M.p. 228–30°C; ethanol; IRS cm^{-1}: 1590 (C=C), 1615 (C=N), 1664 (C=O), 3217 (NH), 3423 (OH). ^{1}H NMR (DMSO) δ: 2.3 (s, 3H, Me), 6.94–6.96 (d, 1H, CH– β- to C=O), 6.99–7.0 (d, 1H, CH– α- to C=O), 7.4–8.0(m, 3ArH), 12.8 (s, 1H, NH).

*Synthesis of 6-(4-chloro-3-methyl)phenyl-2-carboethoxymethyl-4,5-dihydropyridazin-3-one (**5**).*

(A) By conventional heating. A mixture of the pyridazinone **3** (0.01 mol) ethyl bromoacetate (0.04 mol) anhydrous potassium carbonate (0.04 mol) and acetone (60 ml) was refluxed for 48 h on a water bath. The solvent was then evaporated and the reaction mixture was poured into water. The separated solid was filtered off, dried and recrystallized from petroleum ether (b.p. 40–60°C).

(B) By microwave irradiation. A mixture of the pyridazinone **3** (0.01mol), ethyl bromoacetate (0.04 mol) anhydrous potassium carbonate (0.04 mol) and PEG600 (2 ml) was mixed well and the contents were then heated in a microwave oven at *P* = 360 W for 30 min. After cooling down, the product was extracted with diethyl ether to afford compound **5** after evaporation. The separated solid was recrystallized from petroleum ether (b.p. 40–60°C).

Compound **5**: m.p. 98–100°C; petroleum ether b.p. 40–60°C. IRS cm^{-1}: 1230 (C–O), 1615 (C=C), 1630 (C=N), 1740 (C=O). ^{1}H NMR (DMSO) δ: 1.26–1.31 (t, 3H, $COOCH_2\underline{CH_3}$), 2.4 (s, 3H, CH_3 attached to the ring), 2.65–2.69 (t, 2H, CH_2– β- to C–O), 2.99–3.01(t, 2H, CH_2– α- to C–O), 4.21–4.23 (q, 2H, –COO–$\underline{CH_2}CH_3$), 4.59 (s, 2H, –$O\underline{CH_2}COOCH_2CH_3$) and 7.37–7.83 (m, 3Ar–H).

*Synthesis of 6-(4-chloro-3-methyl)phenyl hydrazinocarbomethyl-4,5-dihydrazin-3-one **6**.*

(A) By conventional heating. 6-(4-Chloro-3-methyl)phenyl-N-carboethoxymethyl-4,5-dihydropyridazin-3-one **5** (0.01 mol) was dissolved in ethanol (30 ml), the hydrazine hydrate (0.01 mol, 99%) was added and then the reaction mixture was refluxed for 5 h. The separated solid after concentration was filtered off and recrystallized from ethanol.

(B) By microwave irradiation. A mixture of the ester **5** (0.01 mol) and hydrazine hydrate (0.01 mol) was irradiated with microwaves at *P* = 450 W, t = 4 min, *P* = 540 W, t = 5 min and t = 10 min (Table 1) to give the hydrazide **6** with different yields. The solid that obtained was crystallized from ethanol.

Compound **6**: m.p. 199–200°C; ethanol. IRS cm^{-1}: 1523 (C=C), 1648 (C=O), 1668 (C=O pyridazinone ring) and 3314 (NH). ^{1}H NMR (DMSO) δ: 2.3 (s, 3H, CH_3), 2.4 (s, 2H, NH_2), 2.50–2.59 (t, 2H, CH_2– β- to C=O), 2.9–3.0 (t, 2H, CH_2– α- to C=O), 4.3 (s, 2H, CH_2CO), 7.3–7.7 (m, 3 Ar–H) and 9.1 (s, 1H, NH). MS m/z: 294 ($M^{+\bullet}$ 16.7), 296 ($M^{+\bullet}$ + 2, 6.4), 263 (36.8), 235 (100), 236 (8.5), 208 (8.7), 206 (7.3), 172 (17.0), 89 (12.8), 82 (6.7), 55 (45.7).

*Synthesis of 6-(4-chloro-3-methyl)phenylarylidene hydrazinocarbomethyl-4,5-dihydropyridazin-3-one **7(a-e)***

(A) By conventional heating. A mixture of 6-(4-chloro-3-methyl)phenyl hydrazinocarbomethyl-4,5-dihydropyridazin-3-one **6** (0.01 mol) and aromatic aldehydes namely benzaldehyde, *p*-nitrobenzaldehyde, 3,4,5-trimethoxybenzaldehyde, piperonal and 2-hydroxynaphthaldehyde (0.01 mol) in DMF or ethanol (30 ml) was refluxed for 3–6 h. The solid that separated out after concentration and cooling down was filtered off and recrystallized from the proper solvent.

(B) By microwave irradiation. A mixture of the hydrazide **6** (0.01 mol) and the aromatic aldehydes namely benzaldehyde, *p*-nitrobenzaldehyde, 3,4,5-trimethoxybenzaldehyde, piperonal and 2-hydroxynaphthaldehyde (0.01 mol) was wetted with DMF and irradiated with microwaves at *P* = 360–630 W, t = 4–10 min (Table 2) to give the corresponding aldehyde hydrazones **7**(**a–e**), which were recrystallized from the proper solvent.

6-(4-Chloro-3-methyl)phenylbenzylidenehydrazinocarbomethyl-4,5-dihydropyridazin-3-one **7a**: m.p. 210–12°C; ethanol. IRS cm^{-1}: 1580 (C=C), 1610 (C=N), 1658 (C=O), 1692 (C=O, pyridazinone ring) and 3447 (NH). ^{1}H NMR (DMSO) δ: 2.3 (s, 3H, CH_3), 2.5–2.6 (t, 2H, CH_2β-to C=O), 2.9–3.0 (t, 2H, CH_2 α-to C=O), 4.8 (s, 2H, CH_2CON), 7.4–8.0 (m, 8Ar–H), 8.2 (s, 1H, N=CH) and 11.5 (s, 1H, NH). MS m/z: 382 ($M^{+\bullet}$, 18.6), 384 ($M^{+\bullet}$ + 2, 10.6), 263 (19.5), 265 (8.3), 264 (3.9), 235 (81.7), 237 (26.3), 236 (24.4), 208 (30.1), 207 (23.8), 206 (3.6), 172 (18.5), 120 (3.0), 89 (26.2), 82 (1.8), 55 (100), 57 (6.3), 56 (22.5), 54 (6.6) and 36 (17.2).

6-(4-Chloro-3-methyl)phenyl-p-nitrobenzylidenecarbomethyl-4,5-dihydropyridazin-3-one **7b**: m.p. 260–62°C; DMF. IRS cm^{-1}: 1586 (C=C), 1615 (C=N), 1660 (C=O), 1693 (C=O, pyridazinone ring) and 3448 (NH). ^{1}H NMR (DMSO) δ: 2.3 (s, 3H, CH_3), 2.5–2.6 (t, 2H, CH_2 β- to C=O), 2.8–3.0 (t, 2H, CH_2 α- to C=O), 4.9 (s, 2H, CH_2CON), 7.4–8.2

(m, 7 Ar–H), 8.3 (s, 1H, N=CH) and 11.9 (s, 1H, NH). MS m/z: 427 ($M^{+\bullet}$ 9.3), 429 ($M^{+\bullet}$ + 2, 4.9), 264 (6.2), 263 (14.9), 235 (70.9), 236 (34.9), 234 (85.9), 208 (25.0), 206 (21.8), 171 (18.1), 172 (15.9), 82 (4.9), 89 (25.6), 63 (25.9), 55 (100), 57 (10.6), 56 (31.9) and 54 (99.4).

6-(4-Chloro-3-methyl)phenyl-2,3,5-trimethoxybenzylidenehydrazinocarbomethyl-4,5-dihydropyridazin-3-one **7c**: m.p. 216–18°C; acetic acid. IRS cm^{-1}: 1581 (C=C), 1615 (C=N), 1661 (C=O), 1687 (C=O, pyridazinone ring) and 3270 (NH). ^{1}H NMR (DMSO) δ: 2.3 (s, 3H, CH_3), 2.4–2.5 (t, 2H, CH_2 β- to C=O), 2.9–3.0 (t, 2H, CH_2 α- to C=O), 3.6 (s, 3H, OCH_3 *p*-), 3.8 (s, 6H, OCH_3 *m*-), 4.9 (s, 2H, CH_2CON), 7.0–7.9 (m, 5Ar–H), 8.1 (s, 1H, N=CH) and 11.5 (s, 1H, NH). MS m/z: 472 ($M^{+\bullet}$ 16.8), 474 ($M^{+\bullet}$ + 2, 7.0), 263 (13.5), 235 (71.4), 236 (20.9), 208 (27.4), 206 (6.2), 172 (17.7), 82 (5.3), 55 (100) and 54 (6.1).

6-(4-Chloro-3-methyl)phenylpiperonylidenehydrazinocarbomethyl-4,5-dihydropyridazin-3-one **7d**: m.p. 228–230°C; acetic acid. IRS cm^{-1}: 1580 (C=O), 1600 (C=N), 1670 (C=C), 1692 (C=O, pyridazinone ring) and 3443 (NH). ^{1}H NMR (DMSO) δ: 2.3 (s, 3H, CH_3), 2.3–2.5 (t, 2H, CH_2– β- to C=O), 2.9–3.1 (t, 2H, CH_2– α- to C=O), 4.8 (s, 2H, CH_2CON), 6.0 (s, 2H, O–CH_2–O), 6.9–7.9 (m, 6 Ar–H), 8.4 (s, 1H, N=CH) and 11.4 (s, 1H, NH). MS m/z: 426 ($M^{+\bullet}$ 16.8), 306 (11.9), 235 (62.7), 236 (29.8), 208 (32.9), 84 (9.6), 55 (100) and 54 (15.9).

6-(4-Chloro-3-methyl)phenyl-2-hydroxynaphthylidenehydrazinocarbomethyl-4,5-dihydropyridazin-3-one **7e**: m.p. 220–22°C; ethanol. IRS cm^{-1}: 1599 (C=C), 1624 (C=N), 1665 (C=O), 1693 (C=O pyridazinone ring) and 3426 (NH). ^{1}H NMR (DMSO) δ: 2.3 (s, 3H, CH_3), 2.4–2.5 (t, 2H, CH_2 β- to C=O), 2.57–2.65 (t, 2H, CH_2 α- to C=O), 4.9 (s, 2H, CH_2CON), 7.1–9.2 (m, 9 Ar–H), 8.0 (s, 1H, N=CH), 11.5 (s, 1H, NH) and 12.4 (s, 1H, OH). MS m/z: 448 ($M^{+\bullet}$ 29.5), 450 ($M^{+\bullet}$ + 2, 13.8), 263 (19.3), 235 (87.9), 236 (17.9), 208 (36.3), 207 (21.2), 172 (21.3), 55 (100), 57 (14.2), 56 (22.2) and 54 (8.9).

CONCLUSION

Microwave irradiation is very efficient energy source and it can be used to reduce significantly the reaction times of numerous organic reactions. Moreover, microwaves can lead to improvement of isolated yields compared to conventional technology.

REFERENCES

1. W. Xie; Y. Jin; P. G. Wang, *Chemtech.,* **29**, 23 (1999).
2. D. Michael, P. Mingos, *Chem. Soc. Rev.,* **20**, 1 (1991).
3. (a) C. O. Kappe, *Angew. Chem., Int. Ed*., **43**, 6250 (2004); (b) B. L. Hayes, *Aldrichim. Acta X*, **37**, 66 (2004).
4. G. Bram, A. Loupy; M. Majdoub; E. Guetierrez, E. Ruiz-Hitzsky, *Tetrahedron,* **46**, 5167 (1990).
5. L. Baozhi, Z. Jinsong, L. Yufeng, *http://www.chemistrymag.org/cji/2003/059074ne.htm*
6. V. A. Monge, I. Aldana, P. Parrado, P. Daries, E. Fernandez-Alvarez, *An. Quim. Ser.*, **C79 (3, Suppl. 1)** 462 (1983); *Chem. Abstr*., **102**, 95598 (1985).
7. V. A. Monge, I. Aldana, M. Font; P. Parrado, E. Fernandez-Alvarez, J. A. Fuentes, *An. Quim. Ser.* **C79(2),** 242(1983), *Chem. Abstr*., **102**, 6363 (1985).
8. G. Nannimi, G. Biasoli, E. Perrone, A. Forgione, A. Buttinoni, M. Ferrari, *Eur. J. Med. Chem. Chim. Ther.,* **4**, 53 (1979).
9. G. H. Tamman, E. A. Soliman; A. M. El-Gendy, A. Y. El-Kady, *J. Chem. Soc. Pak.,* **9,** 1 (1987).
10. V. V.Namboodiri, R. S. Varma, *Green Chem.,* **3**, 146 (2001).
11. Y. Ju, R. S. Varma, *Tetrahedron Lett.*, **46,** 6011 (2005).
12. M. A.Salem, N. S. Harb, M. A. El-Hashash, M. I. Marzouk, *Ain Shams Sci. Bull.*, **29A**, 427 (1991).

КОНДЕНЗАЦИЯ НА ХИДРАЗОНОВИ ПРОИЗВОДНИ С АЛДЕХИДИ ПОД ДЕЙСТВИЕ НА МИКРОВЪЛНИ

М. И. Марзук

Департамент по химия, Факултет по науки, Унишверситет Аин Шамс, Абасия, Кайро, Египет

Постъпила на 12 март 2008 г.; Преработена на 6 ноември 2008 г.

(Резюме)

При реакцията на 3-(4-хлоро-3-метил)бензоилпропионова киселина и 3-(4-хлор-3-метил)бензоилпроп-2-енова киселина с хидразинхидрат в обикновени условия и при микровълново облъчване в отсъствие на разтворители са получени 6-(4-хлоро-3-метил)фенил-(2H)-4,5-дихидропиридазин-3-он и 6-(4-хлор-3-метил)-фенил-(2H)-пиридазин-3-он с добри добиви. Чрез окисление на дихидропиридазинона с Br_2/AcOH е получен 6-(4-хлор-3-метил)фенил-(2H)-пиридазин-3-он. Реакцията на 6-(4-хлоро-3-метил)фенил-(2H)-4,5-дихидропиридазин-3-он с етилбромацетат в среда от полиетиленгликол при облъчване с микровълни води до получаване на 6-(4-хлоро-3-метил)фенил-2-карбетоксиметилдихидропиридазин-3-он, който реагира с хидразинхидрат при облъчване с микровълни до съответния хидразид. В среда от диметилформамид и при микровълново облъчване хидразидът реагира с определени алдехиди, а именно бензалдехид, *p*-нитробензалдехид, 3,4,5-триметоксибензалдехид, пиперонал и 2-хидроксинафталдехид до съответните хидразони.

In Memoriam

Evgeni B. Budevski
(1922–2008)

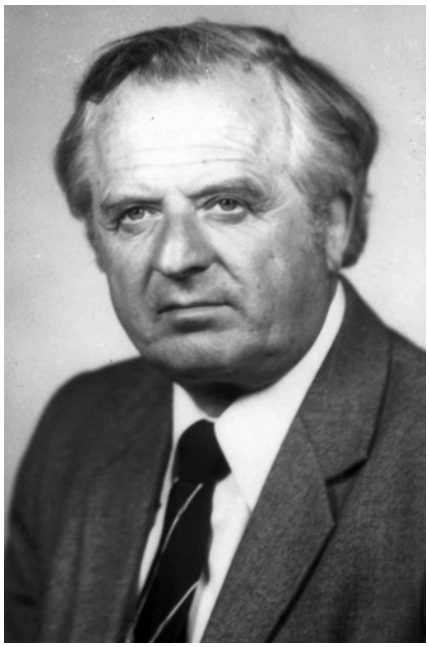

On October 13, 2008 Academician Evgeni Budevski, the founder and pioneer of the Bulgarian Electrochemical School, passed away following a sudden illness.

Acad. Budevski started his research work in the field of electrocrystallization in 1949 immediately after graduation in Chemistry at the University of Sofia "St. Kliment Ohridski". He was well known with the development of the original capillary method for preparation of dislocation-free faces of Ag single crystals. With his co-workers, he succeeded to confirm the 2D theory of crystal growth, introduced by Stranski and Kaischew in the 1930s and supplemented Frank's theory with quantitatively validated theoretical calculations related to the growth of polygonized spirals.

As the first director of the Central Laboratory of Electrochemical Power Sources (CLEPS), today Institute of Electrochemistry and Energy Systems, Prof. Budevski was deeply involved in the research and development of electrochemical power sources. CLEPS electrical car on primary Zn-air batteries made its first 220-km run 6 months before that of General Motors.

In the last part of his carrier, which stopped with his death, Evgeni Budevski was one of the strong supporters (dedicated) of Hydrogen economy and renewable energy and actively worked on PEM.

Prof. Budevski left more than 150 publications and 40 patents with large impact in the scientific world. He was member of the editorial boards of Electrochimica Acta, J. Applied Electrochemistry and J. Power Sources.

During his distinguished carrier, Evgeni Budevski received national and international awards: Dimitrov State Prize (the most prestigious Bulgarian award at that time), the prize of the Electrodeposition Division of the American Electrochemical Society, Marin Drinov Medal on ribbon of the Bulgarian Academy of Sciences. He was Vice-President of the International Society for Electrochemistry (1974–1978), Foreign Member of the Saxonian Academy of Sciences (1974), member of the IUPAC Committee of Electrochemistry (1980–1987), Member of the Advisory Committee of UNESCO-EPS on Energy Saving and Storage, Member of the Advisory Committee of the President of Republic Bulgaria (1997–2001).

Evgeni Budevski will be remembered with the freshness and originality of his scientific and personal philosophy, which did not leave him till his last breath. He loved nature and camping life. A keen skier and yachtsman, he inspired the passion for his hobbies in his co-workers. He loved to spend every weekend together with his wife Lily in their mountain house and to meet there his numerous friends, which he continued to do till his last days.

© 2009 Bulgarian Academy of Sciences, Union of Chemists in Bulgaria

BULGARIAN CHEMICAL COMMUNICATIONS

Instructions about Preparation of Manuscripts

General remarks: Manuscripts are submitted in English by e-mail or by mail (in duplicate). The text must be typed double-spaced, on A4 format paper using Times New Roman font size 12, normal character spacing. The manuscript should not exceed 15 pages (about 3500 words), including photographs, tables, drawings, formulae, etc. Authors are requested to use margins of 3 cm on all sides. For mail submission hard copies, made by a clearly legible duplication process, are requested. Manuscripts should be subdivided into labelled sections, e.g. **Introduction, Experimental, Results and Discussion**, *etc*.

The title page comprises headline, author's names and affiliations, abstract and key words.

Attention is drawn to the following:

a) **The title** of the manuscript should reflect concisely the purpose and findings of the work. Abbreviations, symbols, chemical formulas, references and footnotes should be avoided. If indispensable, abbreviations and formulas should be given in parentheses immediately after the respective full form.

b) **The author**'s first and middle name initials, and family name in full should be given, followed by the address (or addresses) of the contributing laboratory (laboratories). **The affiliation** of the author(s) should be listed in detail (no abbreviations!). The author to whom correspondence and/or inquiries should be sent should be indicated by asterisk (*).

The abstract should be self-explanatory and intelligible without any references to the text and containing not more than 250 words. It should be followed by key words (not more than six).

References should be numbered sequentially in the order, in which they are cited in the text. The numbers in the text should be enclosed in brackets [2], [5, 6], [9–12], etc., set on the text line. References, typed with double spacing, are to be listed in numerical order on a separate sheet. All references are to be given in Latin letters. The names of the authors are given without inversion. Titles of journals must be abbreviated according to Chemical Abstracts and given in italics, the volume is typed in bold, the initial page is given and the year in parentheses. Attention is drawn to the following conventions:

a) The names of all authors of a certain publications should be given. The use of "*et al*." in the list of references is not acceptable.

b) Only the initials of the first and middle names should be given.

In the manuscripts, the reference to author(s) of cited works should be made without giving initials, e.g. "Bush and Smith [7] pioneered...". If the reference carries the names of three or more authors it should be quoted as "Bush *et al*. [7]", if Bush is the first author, or as "Bush and co-workers [7]", if Bush is the senior author.

Footnotes should be reduced to a minimum. Each footnote should be typed double-spaced at the bottom of the page, on which its subject is first mentioned.

Tables are numbered with Arabic numerals on the left-hand top. Each table should be referred to in the text. Column headings should be as short as possible but they must define units unambiguously. The units are to be separated from the preceding symbols by a comma or brackets.

Note: The following format should be used when figures, equations, *etc*. are referred to the text (followed by the respective numbers): Fig., Eqns., Table, Scheme.

Schemes and figures. Each manuscript (hard copy) should contain or be accompanied by the respective illustrative material as well as by the respective figure captions in a separate file (sheet). As far as presentation of units is concerned, SI units are to be used. However, some non-SI units are also acceptable, such as °C, ml, l, etc.

The author(s) name(s), the title of the manuscript, the number of drawings, photographs, diagrams, etc., should be written in black pencil on the back of the illustrative material (hard copies) in accordance with the list enclosed. Avoid using more than 6 (12 for reviews, respectively) figures in the manuscript. Since most of the illustrative materials are to be presented as 8-cm wide pictures, attention should be paid that all axis titles, numerals, legend(s) and texts are legible.

The authors are asked to submit **the final text** (after the manuscript has been accepted for publication) in electronic form either by e-mail or mail on a 3.5'' diskette (CD) using a PC Word-processor. The main text, list of references, tables and figure captions should be saved in separate files (as *.rtf or *.doc) with clearly identifiable file

names. It is essential that the name and version of the word-processing program and the format of the text files is clearly indicated. It is recommended that the pictures are presented in *.tif, *.jpg, *.cdr or *.bmp format, the equations are written using "Equation Editor" and chemical reaction schemes are written using ISIS Draw or ChemDraw programme. The authors are asked to submit the final text with a list of three potential reviewers. The Editorial Board of the journal is not obliged to accept these proposals.

EXAMPLES FOR PRESENTATION OF REFERENCES

REFERENCES

1. D. S. Newsome, *Catal. Rev.–Sci. Eng*., **21**, 275 (1980).
2. C.-H. Lin, C.-Y. Hsu, *J. Chem. Soc. Chem. Commun*., 1479 (1992).
3. R. G. Parr, W. Yang, Density Functional Theory of Atoms and Molecules, Oxford Univ. Press, New York, 1989.
4. V. Ponec, G. C. Bond, Catalysis by Metals and Alloys (Stud. Surf. Sci. Catal., vol. 95), Elsevier, Amsterdam, 1995.
5. G. Kadinov, S. Todorova, A. Palazov, in: New Frontiers in Catalysis (Proc. 10th Int. Congr. Catal., Budapest, 1992), L. Guczi, F. Solymosi, P. Tetenyi (eds.), Akademiai Kiado, Budapest, 1993, Part C, p. 2817.
6. G. L. C. Maire, F. Garin, in: Catalysis. Science and Technology, J. R. Anderson, M. Boudart (eds), vol. 6, Springer-Verlag, Berlin, 1984, p. 161.
7. D. Pocknell, *GB Patent* 2 207 355 (1949).
8. G. Angelov, PhD Thesis, UCTM, Sofia, 2001.
9. JCPDS International Center for Diffraction Data, Power Diffraction File, Swarthmore, PA, 1991.
10. CA **127**, 184 762q (1998).
11. P. Hou, H. Wise, *J. Catal.*, in press.
12. M. Sinev, private communication.
13. http://www.chemweb.com/alchem/articles/1051611477211.html.

CONTENTS

B. D. Koleva, E. H. Ivanova, Flow injection analysis coupled with atomic spectrometry (Review) 3
H. M. F. Madkour, M. E. Azab, M. A. E. Ibraheem, 5,6,7,8-Tetrahydrobenzo[b]thieno[2,3-d]pyrimidine-4(3*H*)-one as a synthon of heterocyclic systems …… 12
S. Loonker, *J. K. Sethia*, Use of newly synthesized guar based chelating ion exchange resin in chromatographic separation of copper from nickel ions …… 19
E. Gorodkiewicz, A. Sankiewicz, I. Sveklo, Z.A. Figaszewski, Atomic force microscopy for the characterization of human platelets before and after interaction with selected anticoagulant drugs ……... 23
V. B. Konsulov, Z. S. Grozeva, J. I. Tacheva, K. D. Tachev, Study of the copolymerization of N-(dichlorophenyl)maleimides with methyl methacrylate ……. 31
L. N. Petkov, K. N. Ignatova, Investigation of the processes and mechanism of electrodeposition of copper from ammonium nitrate electrolyte by the method of cyclic voltamperometry ……. 39
K. Jailakshmi, K. M. Lokanatha Rai, H. D. Revanasiddappa, Synthesis, characterization and some properties of lanthanum complex of bis(2-*n*-butyl-4-chloro-imidazole)-5-iminoethane, a salen type ligand …….. 46
V. Jagannadham, The attenuation effect through methylene group ……... 50
M. I. Marzouk, Microwave-assisted reaction in synthesis of tetra- and hexa-cyclic spiro systems ….. 54
A. U. R. Sankar, B. S. Kumar, M. V. Reddy, S. S. Reddy, C. S. Reddy, C. N. Raju, Synthesis and antimicrobial activity of 2,4,8,10,13-pentamethyl-6-substituted-13,14-dihydro-12H-6λ^5-dibenzo [d,i][1,3,7,2]dioxazaphosphecin-6-ones/sulfides/selenones ……... 59
P. P. Petrova, S. V. Velichkov, I. P. Havezov, N. N. Daskalova, Inductively coupled plasma atomic emission spectrometry – line selection and accuracy in the determination of platinum, palladium, rhodium, barium and lead in automotive catalytic converters …….. 65
H. V. Kumar, C. R. Gnanendra, D. Ch. Gowda, N. Naik, Synthesis of aminoacid analogues of 10-methoxy-dibenz[b,f]azepine and evaluation of their radical scavenging activity ……. 72
A. Sh. Paniraj, K. M. L. Rai, One pot synthesis of dihydroisoxazoles *via* 1,3-dipolar addition of nitrile oxides to allyl chloride ……... 80
M. I. Marzouk, Microwave assisted condensation of hydrazone derivatives with aldehydes …… 84
Evgeni B. Budevski – In Memoriam …….. 89
Instructions about Preparation of Manuscripts ……... 90

СЪДЪРЖАНИЕ

Б. Д. Колева, Ел. Хр. Иванова, Поточно-инжекционен анализ съчетан с атомна спектрометрия (обзор) 11
Х. М. Ф. Мадкур, М. Е. Азаб, М. А. Е. Ибрахим, 5,6,7,8-Тетрахидробензо[b]тиено[2,3-d]пиримидин-4(3H)-он като синтон за хетероциклени системи 18
С. Луункер, Дж. К. Сетия, Използване на новосинтезирана хелатна йонообменна смола на основата на гума гуар за хроматографско разделяне на медни от никелови йони 22
Е. Городкиевич, А. Санкиевич, И. Свекло, З. А. Фигашевски, Атомно силова микроскопия за охарактеризиране на човешки тромбоцити преди и след взаимодействие с определени антикоагулиращи лекарства 30
В. Б. Консулов, З. С. Грозева, Й. И. Тачева, К. Д. Тачев, Изследване на съполимеризацията на N-(дихлорофенил)малеимиди с метилметакрилат 38
Л. Петков, К. Игнатова, Изследване на процесите и механизма на електроотлагане на мед от амониевонитратен електролит с метода на цикличната волтамперометрия 45
К. Джайлакшми, К. М. Локаната Рай, Х. Д. Реванасидапа, Синтез, охарактеризиране и някои свойства на лантанов комплекс на бис(2-*N*-бутил-4-хлоримидазол)-5-иминоетан, един лиганд от саленов тип 49
В. Джаганадхам, Ефект на спрягане през метиленова група 53
М. И. Марзук, Синтез на тетра- и хексациклични спиро системи под действие на микровълни .. 58
А. У. Р. Санкар, Б. С. Кумар, М. В. Н. Реди, С. С. Реди, Ч. С. Реди, Ч. Н. Раджу, Синтез и антимикробна активност на 2,4,8,10,13-пентаметил-6-заместени-13,14-дихидро-12H-6λ^5-дибензо[d,i][1,3,7,2]диоксазафосфецин-6-оксиди, сулфиди и селениди 64
П. П. Петрова, С. В. Величков, Ив. П. Хавезов, Н. Н. Даскалова, Атомна емисионна спектрометрия с индуктивно свързана плазма – избор на аналитични линии и точност при определяне на платина, паладий, родий, барий и олово в автомобилни катализатори 71
Х. В. Кумар, К. Р. Гнанендра, Д. Ч. Гоуда, Н. Наик, Синтез на аминокиселини аналози на 10-метокси-дибенз[b,f]азепин и оценка на тяхната активност като антиоксиданти 79
А. Ш. Панирадж, К. М. Локанат Рай, Едностадиен синтез на дихидроизоксазоли чрез 1,3-диполярно циклоприсъединяване на нитрилоксиди към алилхлорид 83
М. И. Марзук, Кондензация на хидразонови производни с алдехиди под действие на микровълни 88